2-7-2020 1:00 PM

Mushroom body-specific gene regulation by the SWI/SNF chromatin remodeling complex

Kevin CJ Nixon, *The University of Western Ontario*

Supervisor: Kramer, Jamie M., *The University of Western Ontario*
Co-Supervisor: Daley, Mark J., *The University of Western Ontario*
A thesis submitted in partial fulfillment of the requirements for the Doctor of Philosophy degree in Physiology and Pharmacology

Abstract

Over the lifetime of an organism, neurons must establish, remodel, and maintain precise connections in order to form neural circuits that are required for proper nervous system functioning. Disruptions in these processes can lead to neurodevelopmental disorders such as intellectual disability (ID) and autism spectrum disorder. Mutations in genes encoding subunits of the SWI/SNF chromatin remodeling complex have been implicated in ID, yet the role of this complex in neurons is poorly understood. In this project, I established cell-type specific methods to examine the effect of SWI/SNF subunit knockdowns on gene transcription and chromatin structure in the memory-forming neurons of the *Drosophila* mushroom body (MB) during periods of neuronal remodeling and experience-dependent synaptic plasticity. Combining transcriptome and epigenome profiling of MB neurons at the onset of pupation revealed that the SWI/SNF complex is critical for regulating genes that are essential to MB γ neuron axon pruning during pupation. These genes include the steroid hormone receptor *EcR-B1* and members of the ubiquitin proteasome system. Additionally, the SWI/SNF complex was shown to have a stage-specific effect in regulating chromatin accessibility and transcription of genes required during a critical window of experience-dependent synaptic plasticity in juvenile adult flies. Among these were several genes involved in response to stimulus and axon guidance, including: *forked end*, *Calmodulin*, and *Dichaete*, and the gene encoding an actin-binding protein involved in brain development, *Ciboulot*. This study investigates the neuron-specific gene regulatory role of the SWI/SNF complex. These findings reveal specific roles for the SWI/SNF complex in regulating distinct processes in post-mitotic neurons and provide the groundwork in understanding the effect of chromatin regulation in SWI/SNF-related ID.

Keywords

Drosophila melanogaster, SWI/SNF complex, mushroom body, epigenetics, chromatin remodeling, neurodevelopment, synaptic plasticity, learning and memory, RNA-sequencing, transcriptome analysis, ATAC-sequencing, INTACT

Summary for Lay Audience

Throughout the lifetime of an organism, neurons must establish, remodel, and maintain precise connections in order to form neural circuits that are required for proper nervous system functioning. Disruptions in these processes can lead to neurodevelopmental disorders such as intellectual disability (ID) and autism spectrum disorder. Mutations in genes encoding members of the SWI/SNF chromatin remodeling complex have been associated with ID, suggesting a link between DNA organization and brain wiring. The role of the SWI/SNF complex in neurons in neurons, however, is poorly understood. In this project, I examined the effect of SWI/SNF knockdown on gene expression and chromatin structure in the *Drosophila* mushroom body (MB) – the learning and memory centre of the fly brain. During pupation, the MB undergoes neuronal remodeling and also undergoes a period of experience-dependent brain wiring in the early hours of adult life. In this thesis, I find that the SWI/SNF complex is critical in regulating the expression of genes involved in MB neuron remodeling during pupation, and that the SWI/SNF complex targets genes important for MB development in the juvenile adult. These findings reveal new and specific roles for the SWI/SNF complex in regulating distinct processes governing neurodevelopment and provides the groundwork in understanding the effect of chromatin structure in SWI/SNF-related ID.

Co-Authorship Statement

All analyses in this project were conducted by the author. Optimization and implementation of wet lab experiments for establishing mushroom body specific-genes in adult flies was conducted in association with Spencer G. Jones. Andrew Bell assisted with adult fly collections for genetic experiments. All experiments were designed, funded, and supervised by Dr. Jamie M. Kramer.

Acknowledgements

First and foremost, I would like to thank my supervisor, Dr. Jamie Kramer for providing me with the opportunity to work with him. Your mentorship and support throughout my career as a PhD student have helped me to develop my skills as a researcher. I am honoured to be your first PhD student and I wish you all the best in your future endeavors.

I would also like to thank all of the members of the Kramer Lab, past and present. I would especially like to thank Melissa Chubak and Max Stone for performing the initial screens that led to the development of my project. I would also like to thank Spencer Jones and Nicholas Raun for their support and companionship over the last four years. It has been a pleasure working with you to develop new and exciting techniques that will hopefully never stop working again. I would like to thank my volunteer, Andrew Bell, for his dedication and hard work helping me to complete my project. I am grateful for your contributions and wish you well in your promising future in research.

I would like to thank the members of my advisory committee, Dr. Mark Daley, Dr. Amanda Moehring, Dr. Chris Pin, and Dr. Lina Dagnino, for all of their feedback and encouragement throughout my project. A special thank-you to Dr. Amanda Moehring for providing feedback on my thesis.

A special thanks to David Carter and the London Regional Genomics Centre for not only providing their sequencing services, but also their patience and willingness to sequence ATAC-Seq libraries for the first time. I would also like to thank Dale Laird and Kevin Barr for the use of their confocal microscope.

I would like to thank a very special person in my life: my beautiful fiancée, Avery, for her continued love, support, patience, and trust in me throughout our time here in London. You have taught me so much and never stopped believing in me. I cannot thank you enough.

Finally, I would like to thank my parents, John and Heather Nixon, and my sister, Jacqueline Zwambag, for their love and support throughout my life. You are my role models, and everything I accomplish is thanks to the values you instilled in me.

Table of Contents

List of Tables

List of Figures

List of Appendices

List of Abbreviations

ATAC	Assay of transposase accessible chromatin
ATP	Adenosine triphosphate
babo	*Baboon*
BAF	BRG1-associated factor
BAP	Brahma associated protein
Bap60	*Brahma-associated protein 60 kiloDaltons*
BDSC	Bloomington *Drosophila* Stock Center
BMP	Bone morphogenetic protein
bp	Base-pair
bpkm	Bases per kilobase per million reads
BRG1	*Brahma-related gene 1*
brm	*Brahma*
cAMP	Cyclic adenosine monophosphate
cDNA	Complimentary DNA
ChIP	Chromatin immunoprecipitation
CNS	Central nervous system
CREB	cAMP response element binding protein
CRISPR	Clustered regularly interspaced short palindromic repeats
dac	*Dachshund*
Dcr2	*Dicer2*
deGradFP	Degrade GFP
DIG	Dominant ID gene
DIOPT	*Drosophila* RNAi Screening Center Integrative Ortholog Prediction Tool
DN	Dominant negative
DNA	Deoxyribonucleic acid
E(y)3	*enhancer of yellow 3*
EcR	*Ecdysone receptor*
esBAF	Embryonic stem cell BAF
ey	*Eyeless*

FasII	Fasciclin II
FDR	False discovery rate
GAL4	Galactose responsive transcription factor GAL4
GFP	Green fluorescent protein
GO	Gene ontology
Hr38	*Hormone receptor-like 38*
Hr39	*Hormone receptor-like 39*
ID	Intellectual disability
INTACT	Isolation of Nuclei TAgged in a Cell Type
JNK	Jun N-terminal kinase
KC	Kenyon cell
KD	Knockdown
Ldh	*Lactate dehydrogenase*
lhRNA	Long hairpin RNA
LTM	Long-term memory
MAPK	Mitogen-activated protein kinase
MB	Mushroom body
MiMIC	Minos Mediated Integration Cassettes
nBAF	Neuronal BAF
NDD	Neurodevelopmental disorder
npBAF	Neuronal progenitor BAF
oamb	*Octopamine receptor in mushroom bodies*
PBAP	Polybromo associated protein
PCA	Principal component analysis
prom	*Prominin*
put	*Punt*
repo	*Reversed polarity*
RNA	Ribonucleic acid
RNAi	RNA interference
rRNA	Ribosomal RNA
RT-qPCR	Reverse-transcriptase quantitative polymerase chain reaction
rut	*Rutabaga*

SEM	Standard error of the mean
shRNA	Short hairpin RNA
smox	*smad on X*
sNPF	*Short neuropeptide F precursor*
Snr1	*Snf5-related 1*
STM	Short-term memory
SWI/SNF	SWItch/Sucrose Non-Fermenting
TGF-β	Transforming growth factor β
toy	*Twin of eyeless*
Tre1	*Trapped in endoderm 1*
TRiP	Transgenic RNAi project
Trpl	*Transient potential receptor-like*
TSS	Transcription start site
UAS	Upstream activating sequence
UPS	Ubiquitin proteasome system
USP	*Ultraspiracle*
VDRC	Vienna *Drosophila* Resource Centre
WH	Whole head
wit	*Wishful thinking*

Chapter 1

1 Introduction

Over the course of development, neurons must establish, maintain, and remodel precise connections in order to form circuits that are required for proper nervous system functioning. The ability of neurons to make these circuits is highly dependent on processes such as neuron migration, synaptogenesis, axonogenesis, dendrite formation, and axon pruning which are heavily influenced by endogenous and environmental factors (Chaudhury et al., 2016). Epigenetic regulatory complexes play a crucial role in regulating gene transcriptional programs required for the proper formation of neural circuits in response to developmental signals and environmental stimuli (Ronan et al., 2013; Wu et al., 2007). Disruptions in either neurodevelopmental or epigenetic processes can lead to cognitive disorders such as intellectual disability (ID) and autism spectrum disorder (Chaudhury et al., 2016; Minshew & Williams, 2007). In this thesis, I describe novel functions of the SWI/SNF chromatin remodeling complex in gene regulation governing neural circuit formation at important life transitions in the *Drosophila* mushroom body (MB).

1.1 Wiring in the brain and central nervous system

During development, the differentiation of neuroblasts into post-mitotic neurons is guided by transcriptional programs regulated by transcription factors and epigenetic regulators in response to developmental signals (de Graaf & Steensel, 2013; Hargreaves & Crabtree, 2011; Lessard et al., 2007; Vogel-Ciernia et al., 2013). For neurons to survive and function normally, the gene expression programs that are established during differentiation must be maintained throughout the life of the neuron (Deneris & Hobert, 2014; Ninkovic et al., 2010; Tsarovina et al., 2010). These transcriptional programs that dictate the neuronal cell identity must also be plastic so that the neurons can adapt to changing environmental stimuli. The maintenance and plasticity of the neuronal transcriptome is, in part, regulated by epigenetic modifiers.

After differentiation, the neurons in the brain and central nervous system undergo periods of high levels of activity in order to influence the connections and circuitry required for proper functioning (Chaudhury et al., 2016). For these connections to be made, several different events must occur including neurogenesis, neuron migration, synaptogenesis, axonogenesis, and dendrite formation (Kandel et al., 2000) all of which are heavily influenced by spontaneous neuronal activity and stimulation-dependent mechanisms programmed into the neuronal transcriptome upon differentiation (Born & Rubel, 1988; Spitzer et al., 1995; Deneris & Hobert, 2014).

Spontaneous activity during neurodevelopment occurs when action potentials are generated by the developing neurons independent of external or environmental stimuli (Graven & Browne, 2008). These action potentials mediate the formation of synapses by driving neuronal migration and axon branching (Hua et al., 2005; Komuro & Rakic, 1996), and continued activity can even refine synapses by affecting synaptic plasticity through axonal pruning processes (Catsicas et al., 1998). The circuits formed from this spontaneous activity are also thought to affect learning and memory later in life (Emptage et al., 2001). This spontaneous activity has been shown to be facilitated by fluctuations in intracellular calcium between developing neurons (Catsicas et al., 1998) or by release of neurotransmitters (Johnson & Kerschensteiner, 2014). The ability of neurons to generate and respond to spontaneous neural activity requires that the cells are expressing the proper ion channels, neurotransmitters, and neurotransmitter receptors which is dependent on the neuronal transcriptome established upon differentiation (Deneris & Hobert, 2014; Schulz et al., 2006).

The primary mechanisms through which neural circuits are formed, however is through stimulation-dependent processes, which occur when neurons respond to either endogenous or exogenous signals (Chaudhury et al., 2016). For example, neurons must be able to respond to endogenous signals through various cell signaling pathways such as the phosphatidylinositol 3-kinase (PI3K) and transforming growth factor β (TGF-β) signaling pathways (Nakashima et al., 2018; Waite & Eickholt, 2010; Wang et al., 2017). Throughout development, neurons receive many endogenous signals, such as cytokines or extracellular proteins, that activate signaling pathways, driving a variety of cellular responses. These responses include: gene transcriptional activation, cytoskeletal remodeling, and even protein ubiquitination and degradation (Waite & Eickholt, 2010). Cell signaling events can also regulate neuromorphogenesis, ultimately affecting neuronal wiring (Nakashima et al., 2018; Wang et al., 2017). The ability of a neuron to respond to these endogenous signals is programmed in the neuronal transcriptome and is crucial for proper brain wiring (Deneris & Hobert, 2014).

In addition to endogenous signaling mechanisms, stimulation-dependent neuronal processes can be activated by external stimuli (Born & Rubel, 1988; Katz & Shatz, 1996). During development, there are critical windows of sensitivity where brain circuits are formed from experience-dependent mechanisms (Espinosa & Stryker, 2012; Hensch, 2005). In humans, these windows have been shown to arise during the prenatal stage, early infancy, and even adolescence, when the neural circuits in the brain are open to plastic changes and susceptible to environmental stimuli (Marco et al., 2011). During these windows, synaptic connections are formed and strengthened through repeated stimulation of neural circuits, whereas inactive connections are pruned (Chen & Baram, 2016; Espinosa & Stryker, 2012). For example, several studies have shown that experience-dependent synaptic plasticity triggered through environmental stimuli such as auditory signals affects the formation of neural circuits responsible for species-specific maternal calls in chicks (Jain et al., 2004), learning in rodents (Chikahisa et al., 2006; Kim et al., 2006), and even higher brain function in humans (Krumhansl & Jusczyk, 1990; Trehub et al., 1997). The neural activity and synaptic connections generated throughout neurodevelopment by environmental stimuli affects synaptic efficiency and is important for synaptic plasticity later in life (Chaudhury et al., 2016).

Epigenetics, or the regulation of gene expression independent of DNA sequence (Berger et al., 2009), plays a major role in the formation of neural circuits during neurodevelopment (Chen et al., 2013; Feng et al., 2010; Hutnick et al., 2009; Ronan et al., 2013; Wu et al., 2007). Epigenetic mechanisms, primarily those that regulate chromatin structure, have been shown to regulate genes required for the differentiation of neurons and other major events required for proper brain wiring during early development (Ronan et al., 2013). Furthermore, gene transcriptional changes in response to environmental stimuli and experience-dependent neural activity have been shown to be regulated by epigenetic modifications (Chen et al., 2013).

1.2 Disruptions in brain wiring lead to neurodevelopmental disorders

The neural connections formed throughout development, either through endogenous developmental signaling mechanisms or during critical windows of experience-dependent synaptic plasticity, are crucial for cognitive function. Studies have shown that disruptions in endogenous signaling mechanisms such as TGF-β or PI3K signaling pathways in neurons have resulted in developmental abnormalities in neuronal morphology contributing to neurodevelopmental disorders (NDDs) such as epilepsy, autism spectrum disorder, and intellectual disability (ID) (Nakashima et al., 2018; Waite & Eickholt, 2010; Wang et al., 2017). Furthermore, adverse early-life experiences during critical windows of synaptic plasticity affect the maturation of brain circuits, negatively impacting cognitive function (Davis et al., 2019; Davis et al., 2017) and potentially causing neuromorphological abnormalities that can lead to the onset of NDDs (Chaudhury et al., 2016; Ghiani & Faundez, 2017).

Neurodevelopmental disorders are a heterogeneous group of disorders including ID and autism spectrum disorder (Harris, 2005). Within this group, ID affects 1-3% of the world population, and is characterized by limitations in intellectual functioning and adaptive behaviour before the age of 18 (Diagnostic and Statistical Manual of Mental Disorders, 5th edition). Although cases of ID have been attributed to environmental factors, it is primarily a genetic disorder (Chiurazzi & Pirozzi, 2016). With recent advancements in genetic technology, an increasing number of genes have been implicated in ID, and with the identification of these genes, investigators are able to identify common pathways that are disrupted in individuals with ID (Chelly et al., 2006; Kleefstra et al., 2014). To date, over 1200 genes have been implicated in ID with only 428 of these genes exhibiting *de novo* germline mutations inherited in an autosomal dominant pattern (http://sysid.cmbi.umcn.nl; Kochinke et al., 2016), hereafter referred to as dominant ID genes (DIGs). Although DIGs account for only 34% of all ID genes, they are attributed to approximately 60% of all cases of ID (Gilissen et al., 2014).

Gene ontology (GO) enrichment analysis of these DIGs has shown enrichment for terms related to neuronal components (**Figure 1.1** – non bold terms; Chubak et al., 2019). Disruptions in neuronal functions, such as neuronal migration, axonal guidance, synaptogenesis, and synaptic activity can lead to aberrant activity-dependent neural circuit formation and ultimately NDDs (Chaudhury et al., 2016; Kleefstra et al., 2014). In fact, mutations in genes involved in synaptic organization and plasticity, are enriched in NDDs (Hamdan et al., 2009; van Bokhoven, 2011; Kleefstra et al., 2014). Deficiencies in synaptic function would affect the development of brain circuits in early life and negatively impact cognitive function later in life (Chaudhury et al., 2016).

1.3 Intellectual Disability and chromatin

The GO enrichment analysis of DIGs has also shown enrichment of terms related to chromatin regulation (**Figure 1.1** – bold terms; Chubak et al., 2019). Enrichment of factors regulating chromatin in ID genes demonstrates that disruption in chromatin is a major factor in the aetiology of ID. Chromatin regulation plays a major role in the developmental programming of the cell-type specific transcriptome and also in response to environmental stimuli (Lord et al., 2000; Minshew & Williams, 2007; Ronan et al, 2013). Disruptions in brain wiring cause ID and the prevalence of proteins regulating chromatin in DIGs suggests that disruptions in chromatin regulation affect brain wiring. In fact, the most enriched cellular component within the DIGs is that of the SWI/SNF chromatin remodeling complex (**Figure 1.1**). In this thesis, I investigate the role of SWI/SNF-mediated chromatin remodeling in the wiring of neuronal circuits.

Mutations in genes encoding several different SWI/SNF subunits cause syndromic NDDs including Nicolaides-Baraitser syndrome (Mendelian Inheritance of Man gene #601358) and Coffin-Siris syndrome (Mendelian Inheritance of Man gene #135900) (Bramswig et al., 2017; Tsurusaki et al., 2012; Wieczorek et al., 2013). Furthermore, mutations in 11 of the 29 human SWI/SNF subunits have been implicated in NDDs, including ID and psychiatric disorders such as schizophrenia (**Figure 1.2**) (Di Donato et al., 2014; Dias et al., 2016; Hoyer et al., 2012; Johnston et al., 2013; Nixon et al., 2019; Rivière et al., 2012; Santen et al., 2013, 2012; Tsurusaki et al., 2012; Van Houdt et al., 2012; Wieczorek et al., 2013; Wolff et al., 2011), emphasizing the essential role of this complex in neuron development and function.

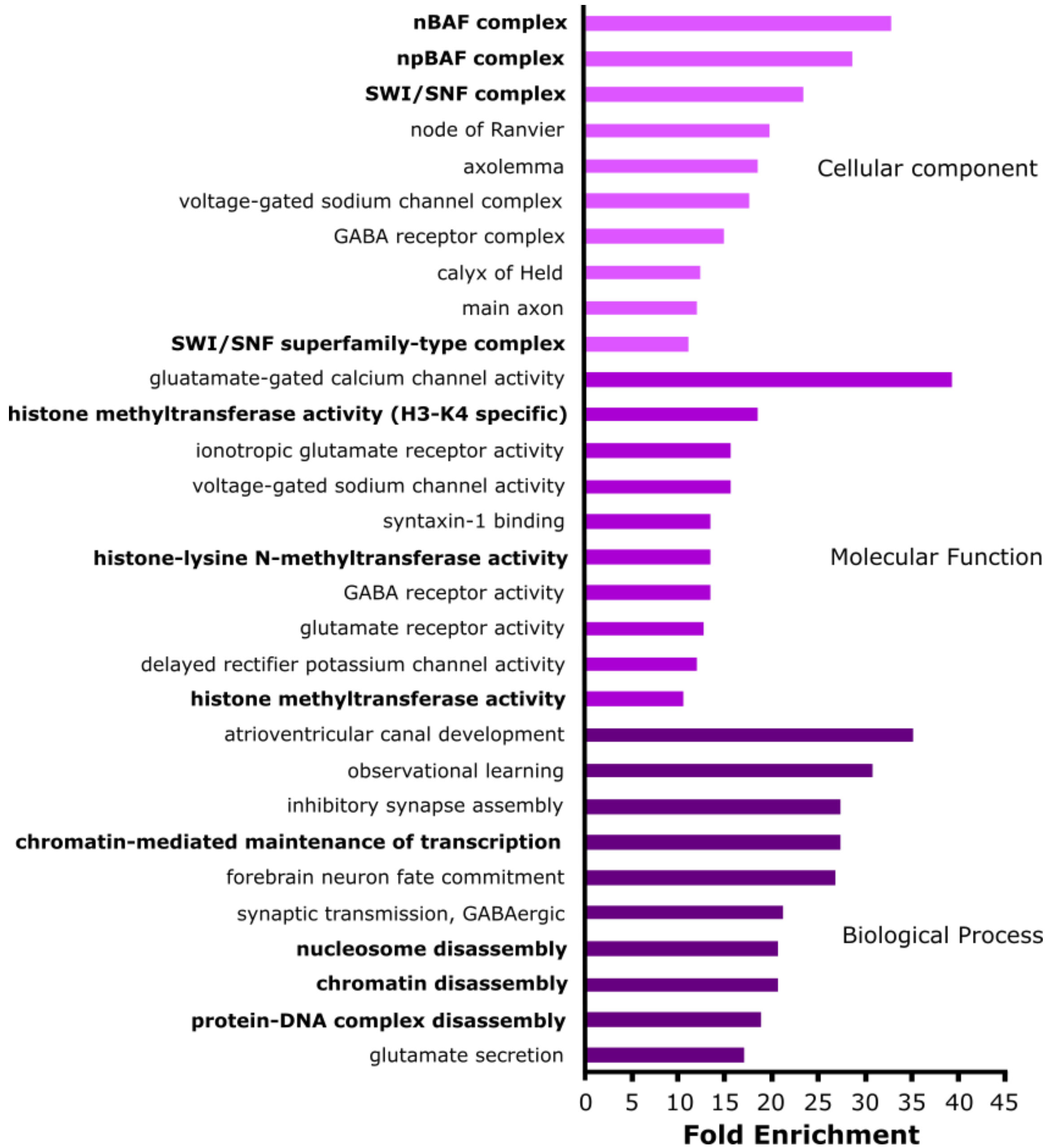

Figure 1.1 Gene ontology enrichment analysis of DIGs.

Gene ontology enrichment analysis of 428 DIGs (http://sysid.cmbi.umcn.nl) reveals the most enriched cellular component terms are related to the SWI/SNF chromatin remodeling complex. Top ten enriched terms with a Bonferroni-corrected P-value <0.05 for each GO category are shown. Terms in bold are related to chromatin regulation.

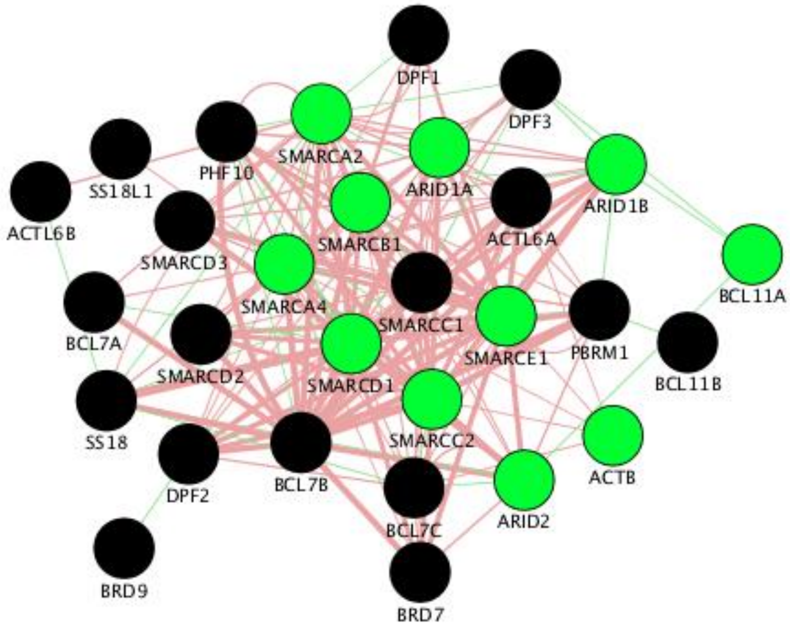

Figure 1.2 SWI/SNF subunits implicated in intellectual disability.

Protein-protein interaction network of the 29 human SWI/SNF subunits. The 11 subunits highlighted in green have been previously implicated in ID (Di Donato et al., 2014; Dias et al., 2016; Hoyer et al., 2012; Johnston et al., 2013; Nixon et al., 2019; Rivière et al., 2012; Santen et al., 2013, 2012; Tsurusaki et al., 2012; Van Houdt et al., 2012; Wieczorek et al., 2013; Wolff et al., 2011). This figure was generated using the geneMania plugin for Cytoscape (v.3.5.0) (Franz et al., 2016).

1.4 Chromatin and the SWI/SNF complex

The DNA found in eukaryotic organisms is organized and compacted into highly ordered chromatin structures. These structures consist of DNA wrapped around a histone octamer, forming the basic unit of chromatin called a nucleosome. Most nuclear DNA is found in a beads-on-a-string structure where the position of nucleosomes (beads) in this structure is critical to controlling processes such as DNA replication, recombination, gene transcription and more (de Graaf & Steensel, 2013; Li & Reinberg, 2011). Generally, chromatin is classified into one of two groups depending on the compaction of nucleosomes: euchromatin and heterochromatin (Li & Reinberg, 2011). Euchromatin is characterized by less compact nucleosome structures, resulting in more accessible DNA and a higher rate of gene transcription. Heterochromatin, however is characterized by more compact nucleosomes, resulting in areas of inactive gene transcription. Most chromatin regulators act on nucleosomes by either physically altering their position, or by chemically modifying the histone proteins (Ronan et al., 2013).

The SWI/SNF complex is an ATP-dependent chromatin remodeling complex. It was first described in yeast for its role in mating type switching and sucrose fermentation, hence its name: SWItch/Sucrose Non-Fermenting (Neigeborn & Carlson, 1984; Stern et al., 1984). The complex is highly conserved in eukaryotic organisms including humans and model organisms such as flies and rodents (Son & Crabtree, 2014). The SWI/SNF complex is recruited to active chromatin marks around the promoters of various genes by binding DNA-bound transcription factors containing activation domains (Clapier & Cairns, 2009; Yudkovsky et al., 1999). The complex then uses ATP hydrolysis to disrupt the interaction between DNA and histones to create a micro-loop in the DNA, allowing it to shift the loop and the nucleosome along a length of DNA (López & Wood, 2015; Vogel-Ciernia et al., 2013). This shift in nucleosome position has been associated with the DNA being more accessible to transcriptional machinery resulting in an increase in gene transcription (Biggar & Crabtree, 1999; Kassabov et al., 2003; Lomvardas & Thanos, 2001; Lorch et al., 2001).

Recently, Mashtalir and colleagues (2018) described the modular organization and assembly of the SWI/SNF complex, in which subunits form three distinct modules which are then incorporated into different configurations of SWI/SNF complexes. Assembly of a core module common to different SWI/SNF configurations occurs first, followed by the association of an ARID module consisting of subunits that distinguish different established configurations of the SWI/SNF complex (Mashtalir et al., 2018). Assembly is finalized with the addition of an ATPase module that is common to the different SWI/SNF complexes (Mashtalir et al., 2018). The order of assembly of each of the SWI/SNF modules is critical to the proper formation of the entire complex. Disruptions in the assembly of any of the modules can completely inhibit the assembly of a functional SWI/SNF complex (Mashtalir et al., 2018). The modular organization of the SWI/SNF complex, and the subunits that comprise each module are highly conserved between mammals, yeast, and *Drosophila* (Mashtalir et al., 2018; Son & Crabtree, 2014).

1.4.1 The mammalian SWI/SNF complex

The SWI/SNF complex is known as the BAF (Brg1-Associated Factor) complex in mammals. In total, 29 genes from 15 gene families encode various subunits of the mammalian BAF complexes (Staahl & Crabtree, 2013). Since the BAF complexes are comprised of only 15 subunits, there exists multiple different subunits available for one position in the complex (Kadoch & Crabtree, 2015) and the incorporation of specific paralogs can distinguish various configurations of the BAF complex (Mashtalir et al., 2018; Son & Crabtree, 2014). For instance, incorporation of the ARID2 subunit in place of the ARID1 A/B subunit leads to the formation of the polybromo-associated BAF (PBAF) complex instead of the BAF complex (Mashtalir et al., 2018). By undergoing combinatorial assembly, there are a number of highly specialized conformations that are formed, resulting in cell-type specific conformations such as: embryonic stem cell (esBAF), neuronal progenitor (npBAF), and neuronal (nBAF) (Son & Crabtree, 2014).

At various stages of cell differentiation and development, these BAF complexes undergo subunit switching resulting in a switch of its cell-specific functions. For example, as neuronal progenitor cells differentiate into post-mitotic neurons, there is a process through which the npBAF-specific subunits, BAF45a and BAF53a, are replaced by their nBAF-specific paralogs, BAF45b/c and BAF53b (Lessard et al., 2007; Yoo et al., 2009). Preventing these replacements results in impaired neuronal differentiation, suggesting a specific requirement of the nBAF complex in post-mitotic neurons (Lessard et al., 2007). In fact, the nBAF complex has been shown to be required for neural development and dendritic morphogenesis in post-mitotic neurons (Parrish et al., 2006; Wu et al., 2007).

Previous research has shown a critical role for the BAF complex in neurodevelopment, particularly the differentiation of neurons and establishing neuron identities (Hargreaves & Crabtree, 2011; Lessard et al., 2007; Narayanan et al., 2015; Narayanan & Tuoc, 2014; Olave et al., 2002; Tuoc et al., 2016). Loss of the core BAF subunits, BAF170 and BAF155, in mice affects neurodevelopment, causes behavioural deficits, and impairs learning (Tuoc et al., 2016). Narayanan and colleagues (2015) have shown that loss of these subunits is associated with a decrease in active chromatin marks, and an increase in repressive chromatin marks, suggesting that the SWI/SNF complex interacts with histone modifying enzymes and is required for gene transcription activation during neurodevelopment. Furthermore, the complex plays an important role in adult cognition (López & Wood, 2015; Tuoc et al., 2016; Vogel-Ciernia et al., 2013; Wu et al., 2007). Mice expressing a mutant nBAF complex in post-mitotic neurons have shown deficiencies in synaptic plasticity and memory formation (Vogel-Ciernia et al., 2013). Taken together, these findings show that not only is the chromatin remodeling complex required for regulating the genes involved in neurodevelopment, it is also required for the post-mitotic regulation of acute neuronal processes such as those involved in learning and memory.

1.4.2 The *Drosophila* SWI/SNF complex

Drosophila also have multiple forms of the SWI/SNF complex, referred to as: BAP (Brahma-associated protein) and PBAP (Polybromo-associated BAP) complexes (Rendina et al., 2010). These different forms are composed of a common protein core module (Bap60, Snr1, mor, and Bap111), an ATPase module (brm, Bap55, and Act5C), and are defined by one of two distinct ARID modules (Mashtalir et al., 2018). In the case of the BAP complex, the ARID module consists of Osa, whereas in order to form the PBAP complex, the ARID module consists of Bap170, Polybromo, and E(y)3 (Mohrmann et al., 2004; Moshkin et al., 2007; Rendina et al., 2010) (**Figure 1.3**).

Although research is beginning to show separate functions for these two complexes, it is known that both are abundant and required for viability (Moshkin et al., 2007). For instance, studies investigating chromatin binding sites of both the BAP and PBAP complexes in polytene chromosomes have shown that they target both distinct and overlapping regions of transcriptionally active chromatin (Chalkley et al., 2008; Mohrmann et al., 2004). Evidence of distinct regions targeted by either the BAP or PBAP version of the complex suggests that certain genes, and possibly distinct processes are regulated by specific conformations of the SWI/SNF complex.

Several studies have been performed investigating the role of the *Drosophila* SWI/SNF complexes in neurons. An RNAi screen knocking down several core SWI/SNF subunits resulted in defective arborization of class I sensory neurons, causing dendrite misrouting, and reduced branching (Parrish et al., 2006). Subunits of the ATPase module, Bap55 and brm, have been shown to be required for dendrite targeting in olfactory projection neurons and dendrite pruning in multidendritic neurons, respectively (Tea & Luo, 2011; Kirilly et al., 2011). Although the SWI/SNF complex has been studied in both *Drosophila* and mammalian neurons, there is little research investigating the impact of the SWI/SNF complex on gene regulation in neurodevelopment or neuronal function. The research presented in this thesis will be focusing on the role of the *Drosophila* SWI/SNF complex on gene regulation in memory forming neurons at two different life stages in the fly.

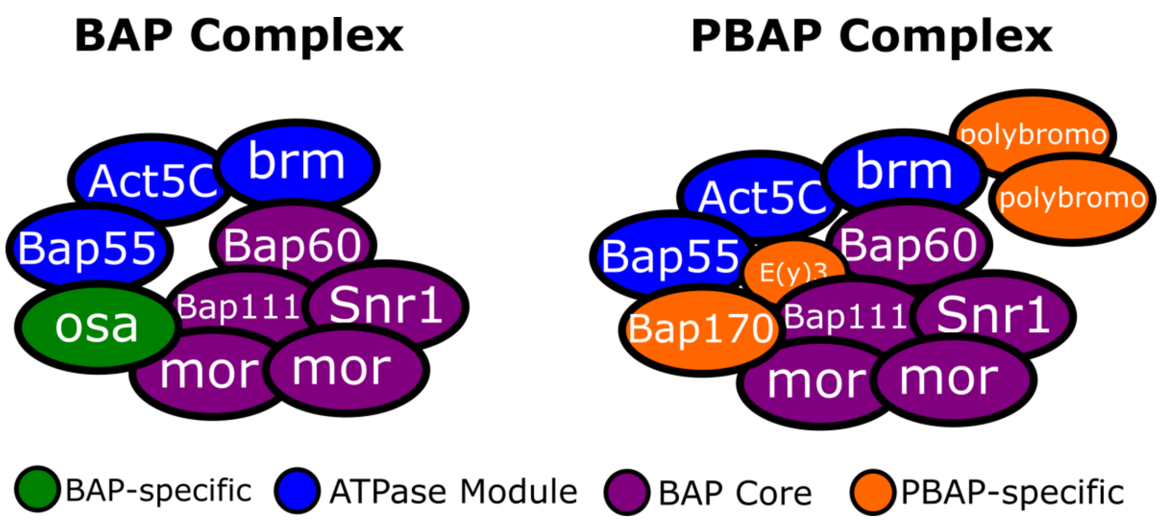

Figure 1.3 The *Drosophila* SWI/SNF complexes.

Simplified visual representation showing both *Drosophila* SWI/SNF complexes: the BAP and PBAP complexes. The complexes are sequentially formed, starting with the assembly of the BAP core module, composed of the mor, Bap111, Snr1, and Bap60 subunits (purple), which then associates with either the BAP-specific osa subunit (green) or PBAP-specific subunits, Bap170, E(y)3, and polybromo subunits (orange). The assembly of both complexes is completed with the addition of the ATPase module made of Bap55, Act5C, and brm (blue).

1.5 *Drosophila* mushroom body as a model for studying brain wiring

One of the main characteristics of ID is a deficit in learning and memory (Detterman, 1987; Vicari, 2004). Many genes implicated in NDDs have been shown to be important for hippocampal development and function, including genes encoding epigenetic regulators (Lagali et al., 2010). To fully understand the aetiology of NDDs, it is necessary to study the roles of NDD genes in relevant brain structures. The *Drosophila* mushroom body (MB) is the olfactory learning and memory centre of the fly brain and, at times, has been argued to be analogous to several mammalian brain structures, including the hippocampus – a key brain centre involved in several forms of learning and memory (Campbell & Turner, 2010; Heisenberg et al., 1985; Coll-Tané et al., 2019).

Each MB is a synaptically dense neuropil composed primarily of ~2000 Kenyon cells (KC) whose axons form five different lobes arising from three classes of KCs (α/β, α'/β', and γ) (Aso et al., 2009; Aso et al., 2014) (**Figure 1.4**). There are two bilaterally symmetrical MB structures in the fly brain that, in total, have ~4000 cells (Krashes et al., 2007). These KCs receive olfactory input from the antennal lobe through projection neurons, which synapse onto KC dendrites within the MB calyx (Aso et al., 2014). Although KCs receive a great deal of olfactory input, their response is very selective, to allow for accurate memory formation and recall (Campbell & Turner, 2010). The lobes of the MB form synapses with MB output neurons, which then project axons to various neuropils outside of the MB (Aso et al., 2014). Dopaminergic neurons are also present which aid in the learning of new behaviours through a proposed reward-punishment system. The dopaminergic neurons act to modify the synapses between KCs and the MB output neurons and are the predominant modulatory neurons in the MB (Aso et al., 2014). Not only is the MB a useful brain structure to study learning and memory, but it is one of the most extensively described brain regions of any organism (Aso et al., 2014). The well-known synaptic connections and neuronal circuits of the MB make it an ideal model to study the mechanisms underlying brain wiring. Additionally, MBs have been studied for their role in several behaviours, such as associative and olfactory learning (Heisenberg et al., 1985), habituation (Acevedo et al., 2007), and even decision making (DasGupta et al., 2014; Groschner et al., 2018). Taken together, these features make the MB an ideal system to study NDD genes in the context of cellular function and behaviour.

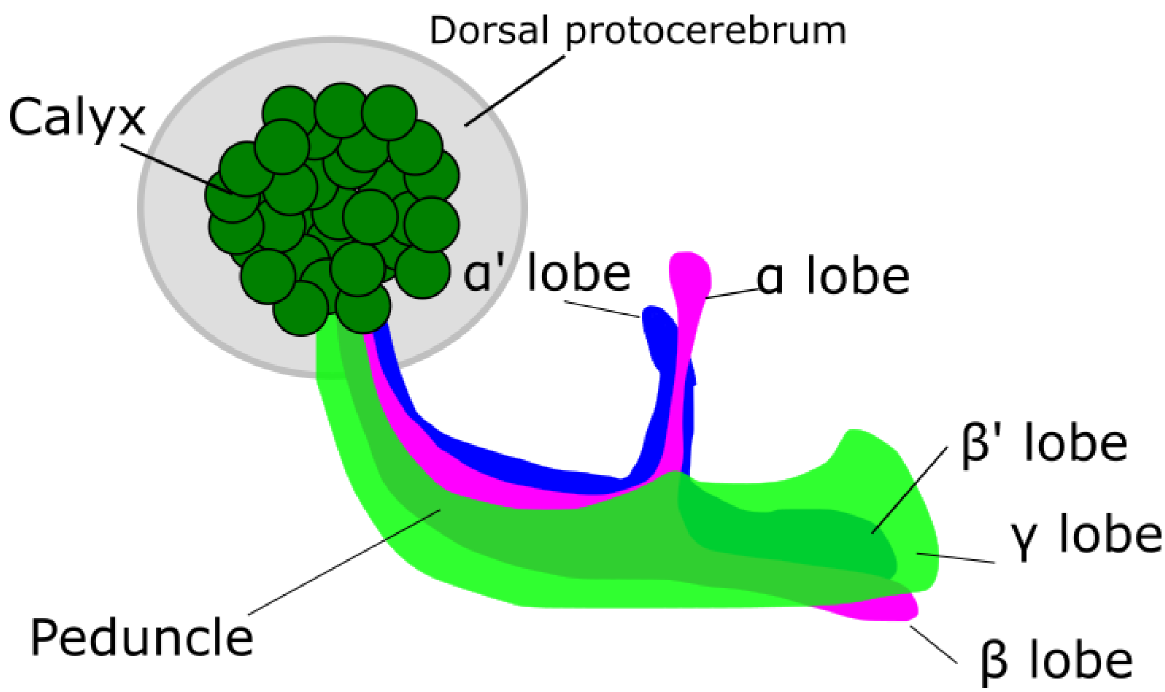

Figure 1.4 Structure of the adult *Drosophila* mushroom body.

The MB is a pair of symmetrical neuropils composed of Kenyon cells (KC), with cell bodies in the dorsal protocerebrum. One set of neuropils is shown, with the centre of the brain to the right side of the figure. Dendrites of the KCs project into the calyx to receive olfactory input where axons from the KCs extend through the peduncle to form five lobes: γ, α, β, α', and β'.

1.5.1 SWI/SNF in Mushroom body development

The MB is comprised of KCs that arise from four MB neuroblasts that are continuously dividing from the embryonic to late pupal stages (Kunz et al., 2012). These MB neuroblasts sequentially give rise to three distinct classes of KCs throughout development forming the five lobes of the MB (Kunz et al., 2012; Lee et al., 1999). The first to develop are the γ lobes, which are the only lobes present during the larval stages of development. During this time, the axons of the γ neurons form both medial and dorsal projections (**Figure 1.5**). Once the larvae reach the late third instar stage, which is the final stage before pupation, the α' and β' lobes begin to extend and from both medial and dorsal projections. Upon pupation, the γ lobes undergo pruning processes where both the medial and dorsal projections are pruned back to the peduncle. These pruning processes occur within the first 18 hours after pupation, followed by re-extension of the γ neurons, but only in the medial direction. During this time, the α and β neurons also project medially and dorsally to form their respective lobes (Lee et al., 1999). By the time the adult fly ecloses from its pupa, the MB is fully formed (**Figure 1.5**).

Although the MB is fully formed in adult flies, it continues to develop after eclosion. Like human brains, the MB has been shown to have a critical window of experience-dependent synaptic plasticity in the juvenile adult brain (Barth & Heisenberg, 1997; Cabirol et al., 2017; Heisenberg et al., 1995; Seugnet et al., 2011). Within the early hours after eclosion, the MB undergoes structural alterations and forms new synaptic connections. These changes are dependent on sensory input and are required for normal memory in later life stages in flies (Barth & Heisenberg, 1997; Doll & Broadie, 2015; Doll et al., 2017; Seugnet et al., 2011).

The development of the *Drosophila* MB has been extensively described and the axonal projections forming the lobes can be easily visualized using publicly available genetic tools for *Drosophila*. Previous studies have shown that the processes regulating γ neuron remodeling are highly dependent on dynamic gene regulation that is, in part. regulated by chromatin (Alyagor et al., 2019; Taniguchi & Moore, 2014).

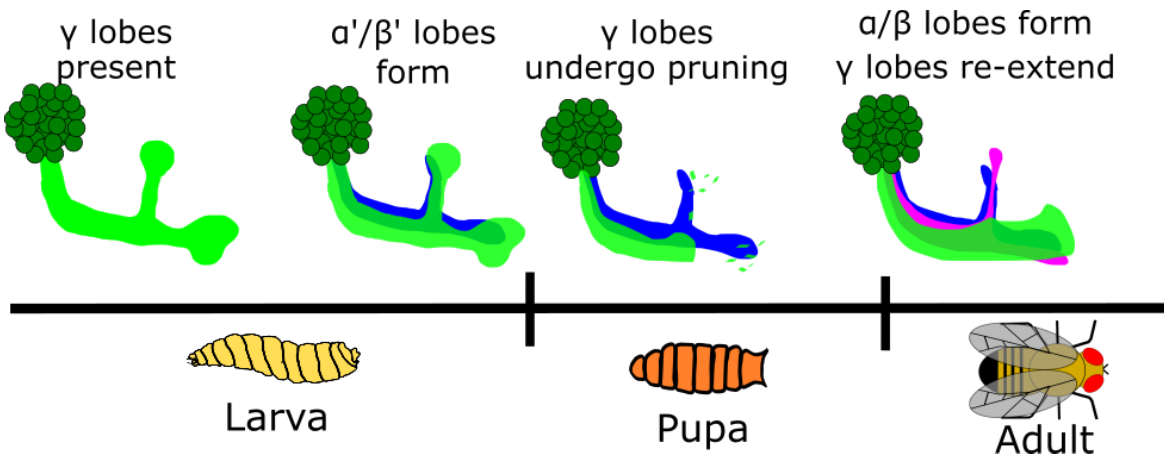

Figure 1.5 Development of the *Drosophila* mushroom body.

The *Drosophila* MB is composed of three different classes of KCs that arise at different points during development. The γ neurons are present upon larval hatching from the egg, forming dorsal and medial lobes which exist throughout the larval phase. The α' and β' lobes are the next to arise, forming dorsal and medial lobes before puparium formation. At the onset of pupation, the γ lobes undergo pruning processes whereby the dorsal and medial projections are both pruned back to the peduncle. Throughout the remainder of pupal development, the α and β lobes extend, forming dorsal and medial projections, and the γ lobes re-extend only in the medial direction. These processes are complete at the time of eclosion, when the adult fly emerges from the pupa.

One well-studied mechanism involved in the pruning and extension processes of the γ lobes is that involving the ecdysone hormone signaling pathway. Ecdysone is a steroid hormone that triggers pupation in flies (Schubiger et al., 1998). One of the three ecdysone receptor isoforms (EcR-A, EcR-B1, or EcR-B2) must associate with ultraspiracle (USP) to form a functional ecdysone nuclear receptor in order to elicit a γ lobe pruning response (Alyagor et al., 2018; Lee et al., 2000; Schubiger et al., 1998; Kirilly et al., 2009). High expression of the EcR isoform, EcR-B1 is induced in γ neurons at the onset of metamorphosis, and loss of function mutations in either *EcR-B1* or *USP* genes result in defective γ neuron pruning phenotypes (Lee et al., 2000). Additionally, Lai et al. (2016) found that the expression of a microRNA 34 (miR-34) against EcR-B1 in the MB γ neurons results in impaired γ pruning (Lai et al., 2016). Interestingly, the ATPase SWI/SNF subunit, brm, functions downstream of EcR in multidendritic neurons during remodeling (Kirilly et al., 2011), suggesting a possible role for the SWI/SNF complex in the ecdysone-mediated γ neuron remodeling pathway. Furthermore, Zraly *et al*., (2006) showed that mutants of the SWI/SNF subunits brm and Snr1 result in strong misregulation of ecdysone-induced genes during pupation.

The expression of EcR-B1 in γ neurons at pupation has been shown to be regulated by two separate pathways: the TGF-β signaling pathway, and the Ftz-f1 hormone receptor. For TGF-β signaling to induce EcR-B1 transcription, TGF-β ligand (dActivin or myoglianin) secreted by glial cells must bind the TGF-β type I receptor, baboon (babo), and either of the TGF-β type II receptors: punt (put) or wishful thinking (wit). Once activated, babo phosphorylates smad on X (smox), which promotes high-level expression of EcR-B1 (Yaniv & Schuldiner, 2016; Zheng et al., 2003). In another, less understood, pathway, the Ftz-f1 orphan hormone receptor can be activated, leading to the upregulation of *EcR-B1* and downregulation of *Hr39*, a hormone receptor known to inhibit MBγ axon pruning (Boulanger et al., 2011). Additionally, the Jun N-terminal kinase (JNK) signaling pathway has also been implicated in MBγ axon pruning by inhibiting cell adhesion (Bornstein et al., 2015). This mechanism has been shown to operate independently of ecdysone signaling. The identification of these independent signaling pathways suggests that there are multiple parallel mechanisms that act to regulate MBγ remodeling.

More recently, the transcriptional program triggered by the ecdysone nuclear receptor in MB γ neurons to induce remodeling has been elucidated (Alyagor et al., 2018). EcR-B1/USP activation by ecdysone has been shown to induce the expression of the transcription factors Sox14 and E75 just before puparium formation (**Figure 1.6**). Upon puparium formation, genes involved in cellular respiration are downregulated and genes that are part of the ubiquitin-proteasome system (UPS) are upregulated (**Figure 1.6**). After puparium formation, Sox14 and E75 continue to act on key genes required to continue the γ neuron pruning and, eventually re-extension processes (Alyagor et al., 2018). For instance, genes regulated by Sox14 consist of autophagy-related genes, and endosome-related genes including the endosomal sorting complexes (ESCRT complex), which are involved in removing unnecessary cellular components during pruning (Alyagor et al., 2018).

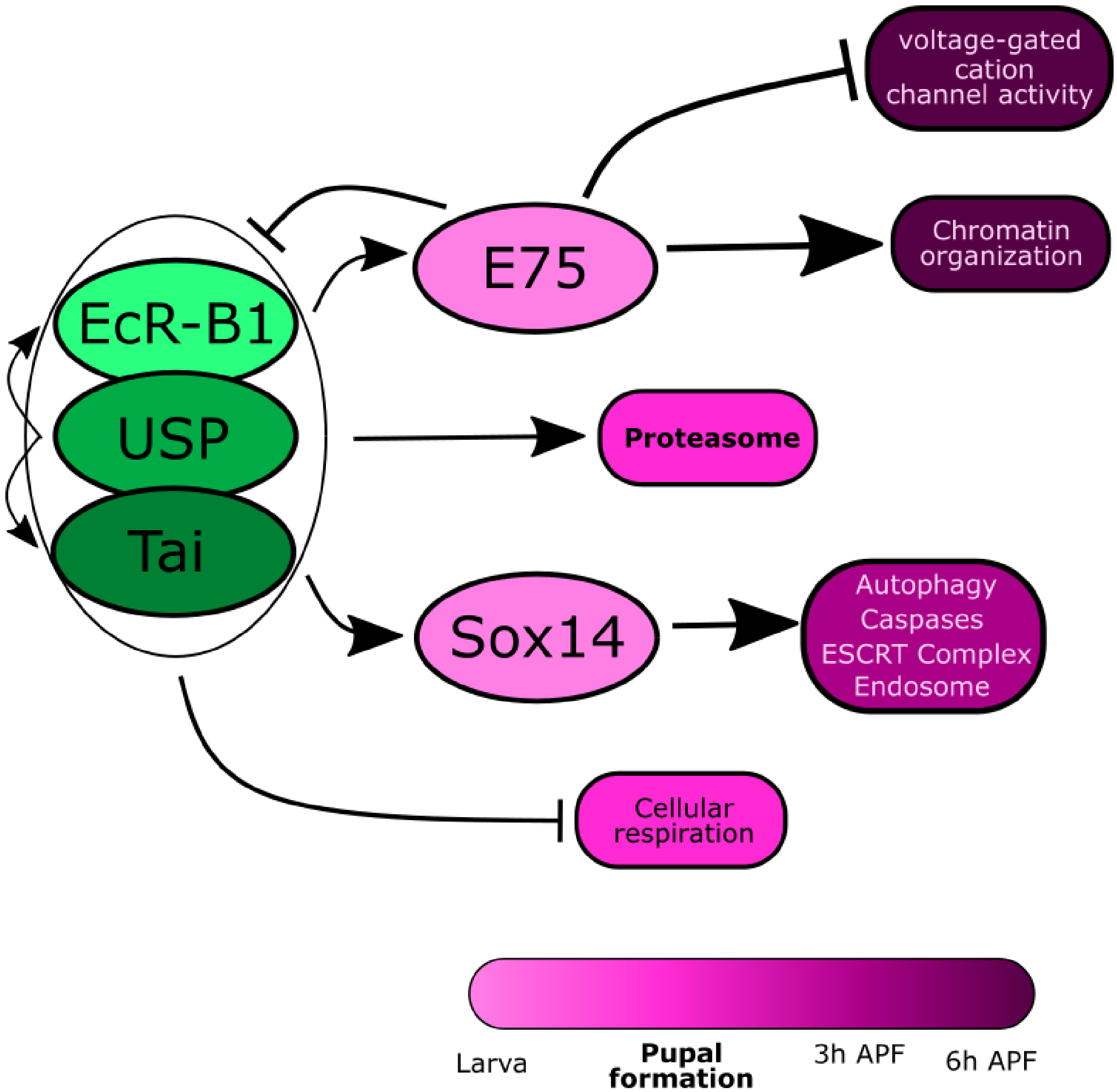

Figure 1.6 Mushroom body neuron remodeling is governed by an ecdysone-mediated transcriptional cascade.

The insect moulting hormone, ecdysone, activates the ecdysone receptor, EcR-B1, in the MB in the late third instar larval stage, signaling pupation and MB neuron remodeling. An EcR-B1 complex regulates the transcription of a series of genes and transcription factors required for neuronal remodeling over the course of pupation. *Adapted from* Alyagor *et al.* (2018).

Our lab performed an RNAi screen targeting MB neurons knocking down different SWI/SNF subunits (Chubak et al., 2019). In this screen, a role for the SWI/SNF complex in MB neuron remodeling was identified. More specifically, the core SWI/SNF subunits Bap60 and Snr1, along with the PBAP-specific subunit E(y)3, were observed to have additional dorsal γ lobe projections in the adult MB (Chubak et al., 2019). The extra dorsal projections that are observed in SWI/SNF knockdown flies could result from defective pruning or aberrant re-extension of the γ neurons.

Both the SWI/SNF complex and EcR-B1 are required for proper MB γ neuron remodeling (Chubak et al., 2019; Lee et al., 2000), and the SWI/SNF complex has been shown to act downstream of the ecdysone receptor in multidendritic neurons (Kirilly et al., 2011). Therefore, there is reason to believe that both the SWI/SNF complex and EcR-B1 act within the same gene regulatory pathways to govern MB γ neuron remodeling. It remains to be determined whether the SWI/SNF complex affects γ neuron pruning or re-extension and which genes are being targeted by the SWI/SNF complex to govern γ neuron remodeling.

1.5.2 SWI/SNF is required in the MB for memory

Chemical ablation of the MB has been shown to affect both short-term memory (STM) – a fast-acting and short-lived process that, in flies lasts for only two to three hours – and long-term memory (LTM) – a process that occurs over a longer period of time to maintain memories, and can last up to nine days in flies (de Belle & Heisenberg, 1994; Mcbride et al., 1999; Koemans, et al., 2017). Further investigation has shown that different lobes of the MB are required for the consolidation of different phases of memory: the γ neurons are required for receiving input and processing STM, whereas the α’/β’ and α/β neurons are more critical in consolidating and recalling LTM information from γ neurons, respectively (Krashes et al., 2007; Montague & Baker, 2016; Trannoy et al., 2011). Studies have shown that although the brain structures responsible for learning and memory in mammals and insects are structurally different, the molecular mechanisms responsible for both STM and LTM are very similar, making the *Drosophila* MB neurons an excellent model to study the cellular and molecular processes of learning and memory (Adroschuk et al., 2015; Coll-Tané et al., 2019).

At a molecular level, the processes governing STM and LTM are different. For STM to occur, neurons must be in a poised state, with all of the required proteins present in the cytoplasm and at the appropriate levels for immediate post-translational modifications upon activation of the neuron (Blum et al., 2009; Dunning & During, 2003). This poised state of the neuron is dependent upon the cell-specific transcriptome, which is determined upon differentiation of the cell during development and maintained through epigenetic regulation (Tsankova et al., 2007). Unlike STM, LTM is a transcription-dependent process that requires the activation and suppression of specific memory genes in order to consolidate memories (Hirano et al., 2016; Zovkic et al., 2016). The cyclic AMP (cAMP) response element binding (CREB) protein is the most well characterized transcription factor in the consolidation of LTM, however it is not the only gene regulatory element that is activated during learning (Adroschuk et al., 2015).

Previous studies in our lab have identified a role for the SWI/SNF complex in the MB for both STM and LTM (Chubak et al., 2019; Nixon et al., 2019). In *Drosophila*, MB remodeling during pupation was required for STM to occur but not LTM (Redt-Clouet et al., 2012). For some SWI/SNF components, loss of STM correlated with a strong defect in MB γ lobe remodeling, however several SWI/SNF subunit knockdowns resulted in memory defects that occurred in the absence of remodeling defects (Chubak et al., 2019). Additionally, adult-specific knockdown of the core SWI/SNF subunit, Bap60, resulted in long-term memory defects (Nixon et al., 2019). Taken together, these results suggest that the SWI/SNF complex has a specific role in memory formation in the adult fly brain, and this requirement is consistent with evidence from mammals suggesting a critical role for the neuron-specific nBAF complex in differentiated neurons (Olave et al., 2002; Vogel-Ciernia et al., 2013; Wu et al., 2007).

1.6 Research hypothesis and rationale

The importance of the SWI/SNF complexes in neurons has been well established. Additionally, analysis of dominant ID genes (DIGs) shows that the SWI/SNF complex is the most enriched cellular component (**Figure 1.1;** Chubak et al., 2019), and mutations in 11 of the 29 human SWI/SNF subunits are associated with ID (**Figure 1.2**). The prevalence of genes encoding chromatin regulators in the DIGs suggests that chromatin plays a key role in brain wiring. Therefore, my governing hypothesis is that the SWI/SNF complex is required for chromatin and gene regulation crucial to proper brain wiring. The main goal of my thesis was to understand how SWI/SNF-mediated gene regulation can affect brain wiring. I study this using an established *in vivo* RNAi knockdown of SWI/SNF subunits in the *Drosophila* MB. Our lab has shown that the SWI/SNF complex is important in the MB during development, and post-development, in adult flies (Chubak et al, 2019; Nixon et al, 2019). My main objectives were to:

1. Establish cell-type specific methods for analyzing the MB transcriptome and chromatin.
2. Determine the effect of the SWI/SNF complex on gene expression and chromatin structure in MB development during γ lobe remodeling.
3. Determine the effect of the SWI/SNF complex on gene expression and chromatin structure in the adult MB.

This study investigates the impact of the SWI/SNF complex on gene expression and chromatin structure in neurons, more specifically in a brain structure relevant to learning and memory. In this project, I find that the SWI/SNF complex plays a critical role in MB γ neuron pruning at the onset of pupation, and that the complex has a profound effect on the expression of neurodevelopmental genes in the MB during a critical time window of juvenile adult brain development.

Chapter 2

2 Methods

2.1 Fly stocks and culture

All fly stocks were maintained at room temperature on standard media (cornmeal-sucrose-yeast-agar) supplemented with the mould inhibitors methyl paraben and propanoic acid. All of the fly strains used in this study were obtained from either the Bloomington *Drosophila* Stock Center (BDSC; Bloomington, USA) or the Vienna *Drosophila* Resource Centre (VDRC; Vienna, Austria), with the exception of *UAS-Unc84::GFP*, which was a gift from Gilbert L. Henry (Henry et al., 2012). Inducible RNAi stocks were obtained from the BDSC's Transgenic RNAi Project (TRiP) library (Perkins et al., 2015) and VDRC's GD and KK libraries (Dietzl et al., 2007). Flies containing the MB-specific *R14H06-GAL4* were generated by the Rubin lab for the Janelia Research Campus FlyLight project (Jenett et al., 2012; Li et al., 2014) and were obtained from BDSC (Stock #48667). See **Appendix A** for a list of stocks used in this thesis.

In addition to any phenotypes identified in prior screens using these lines, RNAi lines used in SWI/SNF knockdown experiments were selected based on an evaluation of RNAi efficacy using either a lethality assay or RT-qPCR (Chubak et al., 2019). For knockdown experiments, controls were generated using the appropriate genetic background stocks. In knockdown experiments using BDSC RNAi lines, a hairpin stock targeting the mCherry fluorophore (genotype: [$y^1 sc^* v^1$; *P{VALIUM20-mCherry}attP2*]), a protein that does not exist in the *Drosophila* genome, was used to account for the genetic background of the third chromosome inserted transgenes as well as the effect of RNAi (Perkins et al., 2015).

All crosses were performed on a 12h-12h light-dark cycle in 70% humidity. For consistency with previously observed phenotypes, crosses from which larval progeny were to be collected were reared at 29°C and crosses from which adult progeny were to be collected were reared at 25°C (Chubak et al., 2019; Nixon et al., 2019).

2.2 GAL4-UAS system

Mushroom body-specific expression of RNAi and transgenes was achieved through the use of the GAL4-UAS binary expression system. In this system, the yeast transcriptional activator, GAL4, is expressed under the control of a tissue-specific promoter. Once expressed, GAL4 binds an upstream activating sequence (UAS) to drive expression of downstream genes of interest (Brand & Perrimon, 1993) (**Figure 2.1**).

The *R14H06-GAL4* driver was developed by Jennett et al. (2012) using a fragment of the *rutabaga* adenylyl cyclase gene enhancer. For visualization of the MB, *R14H06-GAL4* was combined with *UAS-mCD8::GFP* (plasma membrane-bound GFP) using standard genetic techniques. For MB-specific gene expression and chromatin analyses, *R14H06-GAL4* was combined with *UAS-unc84::2XGFP* (nuclear membrane-bound GFP). To perform MB-specific RNAi-mediated gene knockdown, flies containing the *R14H06-GAL4* transgene were crossed to those containing *UAS*-RNAi constructs (**Appendix A**).

Transgenic RNAi in *Drosophila* can be transcribed into short hairpin RNA (shRNA) or long hairpin RNA (lhRNA). The use of either shRNA or lhRNA for RNAi-mediated knockdown requires an endogenous protein, dicer 2 (dcr2), for processing (Dietzl et al., 2007). For shRNA, endogenous dcr2 is sufficient to process the hairpin RNA into single-stranded RNA. In instances where lhRNA transgenes were used for gene knockdown, an additional GAL4-mediated dcr2 is used to make RNAi knockdown more effective.

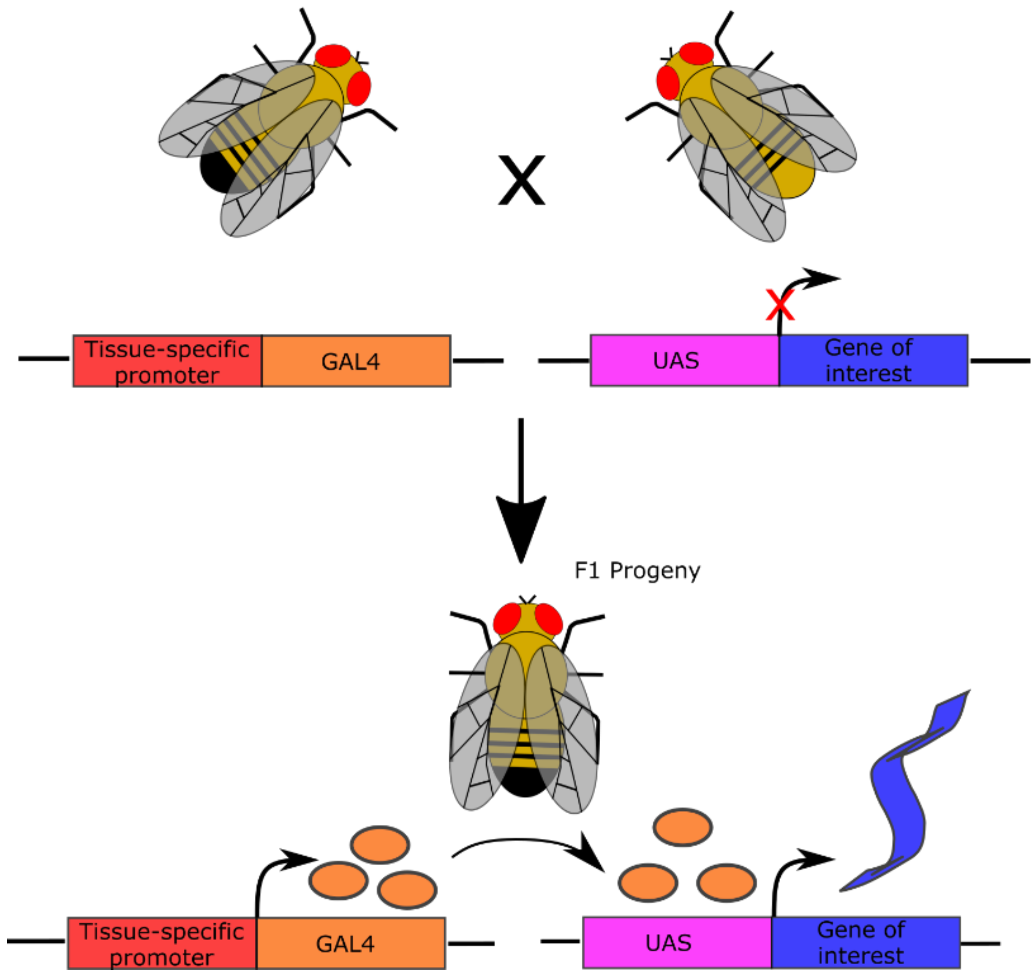

Figure 2.1 The GAL4-UAS system in *Drosophila*.

Flies carrying the GAL4 yeast transcriptional activator under the control of a tissue-specific promoter are crossed with flies carrying a gene of interest under the control of an upstream activating sequence (UAS). The progeny of the cross will contain both elements, allowing GAL4 to activate transcription of the gene of interest in a tissue-specific manner.

2.3 Sample collection for transcriptome and chromatin analyses

2.3.1 Larval CNS collections

The *R14H06-GAL4* driver was used to express UAS-SWI/SNF^{RNAi}, which knocks down a specific component of the SWI/SNF complex, UAS-EcR-B1^{DN}, which expresses a dominant negative form of EcR-B1 which prevents EcR function in affected cells (Cherbas et al, 2003), or UAS-mCherry^{RNAi} as a control for RNAi knockdown (see **Appendix A**). Each genotype also contained UAS-Unc84::GFP for immunoprecipitation of MB neuron nuclei. Male larvae of each genotype were collected within three hours of pupation. The CNS was crudely dissected in ice cold 1X PBS (pH 7.4). Samples were flash-frozen using liquid nitrogen and stored at -80°C.

2.3.2 Adult Head collections

Juvenile (0-3-hour-old) or mature (1-5-day-old) adult male flies expressing UAS-Bap60^{RNAi} or UAS-mCherry^{RNAi} with UAS-Unc-84::GFP under control of the *R14H06-GAL4* driver (see **Appendix A**) were anesthetized with CO_2 and flash-frozen using liquid nitrogen. Fly heads were separated from the body by vortexing followed quickly by separation using ice-cold sieves. Samples were stored at -80°C.

2.4 Isolation of nuclei tagged in a cell type (INTACT)

INTACT was performed as described previously (Jones et al., 2018). In brief, Protein G Dynabeads (Invitrogen) were adsorbed to 5µg of anti-GFP antibody (Invitrogen, G10362) in PBS with 0.1% Tween-20 (PBST) for 10 min at room temperature. The beads were then isolated with a magnet and resuspended in PBST. Fifty fly heads or 25 larval CNS were then added to homogenization buffer (25 mM KCl [pH 7.8], 5 mM $Mgcl_2$, 20 mM Tricine, 150 nM spermine, 500 nM spermidine, 10nM β-glycerophosphate, 250 mM sucrose, 1X Pierce protease inhibitor tablets – EDTA-free [ThermoFisher Scientific] or 1X Halt protease inhibitor cocktail – EDTA-free [ThermoFisher Scientific]), and the suspension was homogenized for approximately 1 min with a standard tissue homogenizer at 30,000 rpm. The suspension was then placed in a Dounce homogenizer with NP-40 (ThermoFisher Scientific) added to an end concentration of 0.3% and homogenized six times with the tight pestle. The homogenate was filtered through a 40 µm strainer where a small fraction of homogenate was removed as an input sample. Nuclei in the input fraction were pelleted by centrifugation for 10 min at 4°C and the supernatant was removed. The remaining homogenate was then pre-cleared with non-antibody bound beads for 10 min at 4°C with rotation. Antibody-bound beads were added to the homogenate for 30 min at 4°C with rotation, and the beads were then washed in homogenization buffer for 10 min at 4°C. Bead-bound nuclei were then processed for RNA-Sequencing or ATAC-Sequencing (**Figure 2.2**).

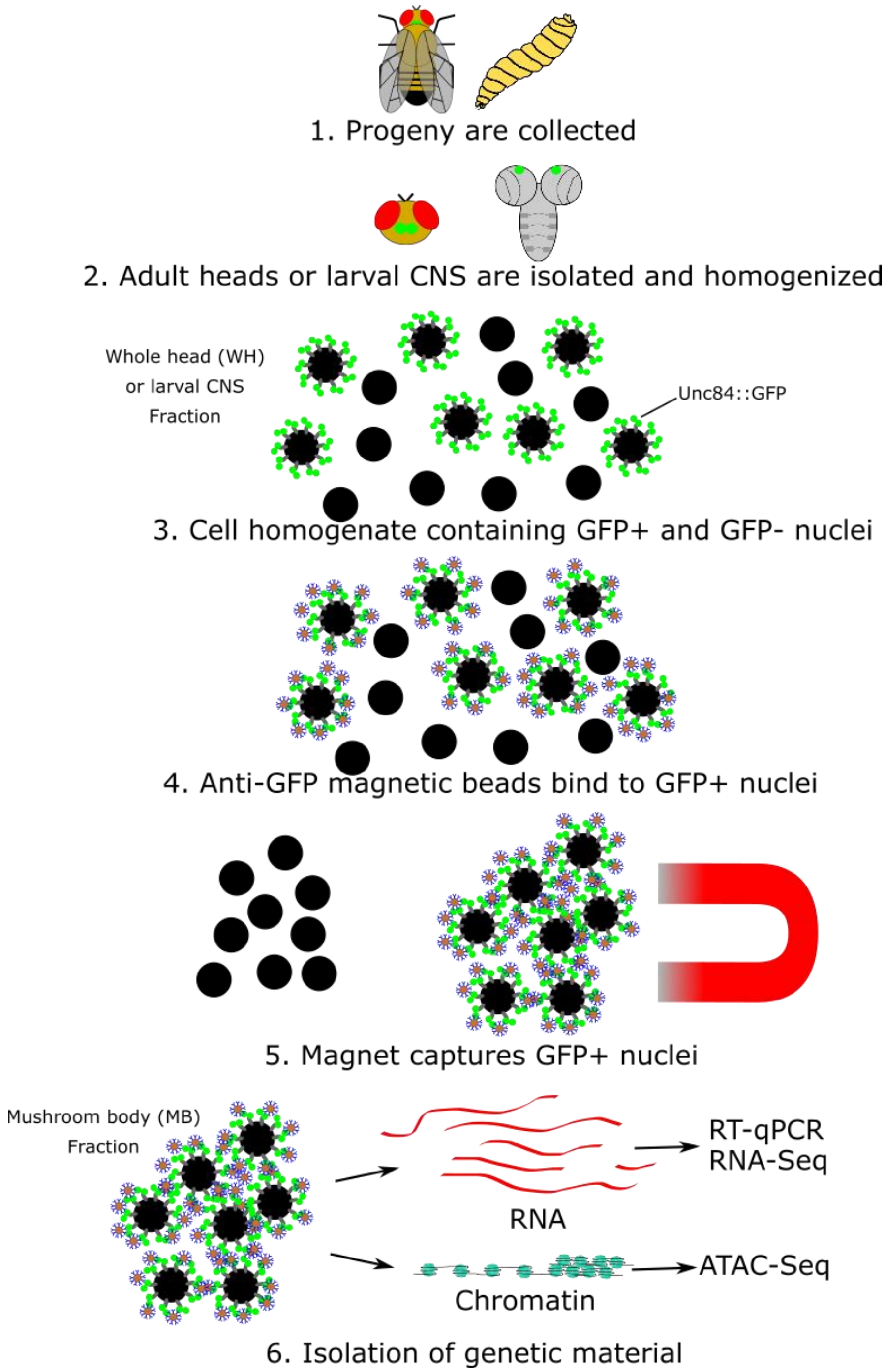

Figure 2.2 Workflow of INTACT.

Progeny expressing Unc84::GFP in the MB are collected and adult heads or larval CNS are isolated. Samples are then homogenized and anti-GFP bound to magnetic beads are used to immunoprecipitate GFP positive MB nuclei. Total RNA or chromatin are isolated from MB nuclei for downstream analyses.

2.5 RNA-Sequencing

Total RNA was isolated from immunoprecipitated nuclei and nuclei from the input fraction, hereafter referred to as the whole-head (WH) sample, using the Arcturus PicoPure RNA isolation kit (ThermoFisher Scientific), and DNase digestion was done with the RNase-free DNase kit (Qiagen) according to the manufacturer's instructions. The quality of the isolated RNA was then assessed with the Bioanalyzer 2100 Pico RNA kit (Agilent) by visual examination of rRNA-peak integrity.

RNA-seq libraries were generated using the NuGEN Ovation *Drosophila* RNA-Seq System (BioLynx), according to the manufacturer's instructions. Size selection with Agencourt SPRIselect beads (Beckman-Coulter) was used for selecting library sized of 200 bp. Library size was assessed with the Bioanalyzer 2100 DNA high-sensitivity kit (Agilent). Sequencing was performed with the Illumina NextSeq500 at the London Regional Genomics Centre (Robarts Research Institute) with the high output v2 75 cycle kit; read length was 75 bp for single-end reads.

2.6 ATAC-Sequencing

ATAC-Seq was performed as previous described (Buenrostro, Wu, Chang, & Greenleaf, 2016) with modifications for nuclei obtained using INTACT. Bead-bound nuclei isolated using INTACT were resuspended in 1XPBS (pH 7.4) and a volume containing ~50,000 permeable nuclei (see Chapter 2.9.1) were transferred to a fresh PCR tube. PCR tubes were placed on a magnet for 5 minutes and the supernatant was removed and discarded. Bead-bound nuclei were then resuspended in 50µl of transposase reaction mix (25µl 2XTD buffer, 2.5µl Tn5 Transposase (Illumina), and 22.5µl of nuclease free water) and incubated for 30 min at 37°C. DNA was then purified and eluted into 10µl of elution buffer using a Qiagen MinElute Kit according to the manufacturer's instructions.

Libraries were then amplified using 1X High-Fidelity PCR Mastermix (NEB) and 1.25µM of custom Nextera PCR Primers (**Appendix B**) using a thermocycler running the following program:

72°C for 5 minutes, 98°C for 30 seconds, (98°C for 10 seconds, 63°C for 30 seconds, 72°C for 1 minute) X 5 + *n* cycles, hold at 4°C.

After the first 5 PCR cycles, libraries were removed from the thermal cycler and 5µl of each library was used in a qPCR guide reaction to determine the number of additional cycles for library amplification (*n*).

The libraries were then purified using a Qiagen PCR Purification Kit eluting to a final volume of 20µl according to the manufacturer's instructions. Size selection with Agencourt SPRIselect beads (Beckman-Coulter) was used to removed primers from the libraries. Library size was assessed with the Bioanalyzer 2100 DNA high-sensitivity kit (Agilent). Sequencing was performed with the Illumina NextSeq500 at the London Regional Genomics Centre (Robarts Research Institute) with the high output v2 75 cycle kit; read length was 45 bp for paired-end reads.

2.7 Reverse transcriptase quantitative polymerase chain reaction (RT-qPCR)

Mushroom body nuclei were isolated from three biological replicates from both mature and juvenile flies expressing RNAi knockdown of Bap60 in the MB (Bap60-KD MB) and control flies in an independent INTACT experiment followed by RNA isolation (see Chapter 2.4). cDNA was synthesized using the SensiFAST cDNA Synthesis Kit (FroggaBio) following manufacturer's instructions. Quantitative PCR was performed on a BioRad CFX 384 using the SensiFAST SYBR No-ROX Kit (FroggaBio) following the manufacturer's instructions using the primers listed in **Appendix B**. Primers were selected from FlyPrimerBank (Hu et al., 2013) and were validated for efficiency using a cDNA dilution series. Relative expression was determined using the ΔΔCt method normalized for the reference genes *eIF2β* and *βCOP*.

2.8 Bioinformatic analysis of sequencing data

2.8.1 RNA-Sequencing Analysis

Raw sequencing reads were trimmed with Prinseq quality trimming (version 0.20.4) (Schmieder & Edwards, 2011) using a minimum base quality score of 30. The read quality was then assessed via FastQC (version 0.11.5). Trimmed reads were aligned to the *Drosophila melanogaster* reference genome (BDGP release 6) (Adams et al., 2000; Consortium Drosophila 12 Genomes, 2007) with the STAR aligner (version 2.5.3a)

(Dobin et al., 2013). To ensure mushroom body specificity of MB samples compared to WH samples, reads were also aligned to the *C. elegans* Unc-84 gene (NC_003284.9). Count tables of reads aligning to genes were generated using reads that aligned to one locus with a maximum of four mismatches and HTSeq-count (version 0.11.2) using the overlap resolution setting 'union' (Anders et al., 2015). Reads mapping to *Drosophila* ribosomal genes were quantified and then removed from count tables prior to normalization. The raw gene counts were normalized using the 'estimateSizeFactors' function in the R package DESeq2 (Anders & Huber, 2010; Love et al., 2014) to account for each sample's library size and RNA composition bias. Differential expression analysis was then performed with DESeq2.

Larval Analysis (Chapter 4)

An average of 23,113,376 high-quality, uniquely aligned single-end reads with a maximum of four mismatches were obtained across all larval samples expressing RNAi knockdown (KD) or a dominant negative (DN) in the MB: E(y)3-KD MBs (n=3), Bap60-KD MBs (n=4), Snr1-KD MBs (n=3), EcR-B1^{DN} MBs (n=2), and controls (n=6). An average of 20,900,603 reads across all samples aligned to genes using HTSeq-count (**Table 2.1**). Y chromosome genes, rRNA genes, and genes with less than an average of 50 counts across all samples were excluded from downstream analysis, leaving 8,242 genes for differential expression analysis. Differentially expressed genes were defined as genes with a Benjamini-Hochberg adjusted *P* value < 0.05.

Adult Analysis (Chapter 5)

An average of 54,803,904 and 46,899,292 high-quality, uniquely aligned single-end reads with a maximum of four mismatches were obtained from juvenile Bap60-KD MBs (n=3) and controls (n=2), respectively, and an average of 26,865,090 and 35,504,102 high-quality, uniquely aligned single-end reads with a maximum of four mismatches were obtained from mature Bap60-KD MBs (n=5) and controls (n=5), respectively. (**Table 2.2**). Y chromosome genes, rRNA genes, and genes with no counts across all samples were excluded, leaving 12,222 and 13,440 genes for downstream analysis for juvenile and mature samples, respectively. Differentially expressed genes were defined as genes with a Benjamini-Hochberg adjusted *P* value <0.05 and with a >1.5 fold or >2-fold change in expression.

Table 2.1 Distribution of RNA-Sequencing data for larval samples

Distribution of reads after processing MB-enriched samples after knockdown of a specific SWI/SNF complex subunit, the dominant negative EcR-B1^{DN} and controls. "Good Reads" are uniquely aligned to the *Drosophila* genome with less than four mismatches. "Genes" column is good reads counted to genes using HTSeq-count.

Sample Name	Total Reads	Unmapped	Multimapped	>4 Mismatch	Good Reads	Genes
E(y)3-1	22,802,236	4,178,624	1,259,536	136,743	17,122,492	15,517,773
E(y)3-2	27,614,969	8,032,577	1,614,670	154,385	17,578,721	15,803,850
E(y)3-3	31,920,086	4,539,607	2,041,741	223,922	24,993,401	22,481,023
Bap60-1	26,693,359	2,288,290	2,053,153	192,144	22,098,382	19,923,727
Bap60-2	24,106,908	3,786,768	1,482,184	154,858	18,593,551	16,887,246
Bap60-3	32,422,751	11,113,243	1,576,543	176,883	19,303,420	17,400,449
Bap60-4	32,777,140	2,904,663	1,707,104	219,735	27,825,672	25,165,644
Snr1-1	27,825,446	3,195,425	1,813,361	200,419	22,601,978	20,498,271
Snr1-2	35,662,371	4,400,316	2,269,689	258,880	28,723,256	25,909,639
Snr1-3	26,836,569	2,257,304	2,342,666	201,261	22,027,964	19,977,512
EcR-B1-1	30,079,226	5,331,958	2,338,991	200,697	22,197,701	20,057,989
EcR-B1-2	28,545,212	8,378,610	1,749,305	169,744	18,233,593	16,493,419
Control-1	28,549,492	1,893,209	2,045,980	196,702	24,359,121	22,036,448
Control-2	26,177,406	1,796,718	1,565,344	187,511	22,563,359	20,429,408
Control-3	29,655,027	2,891,663	1,911,979	205,395	24,553,181	22,190,892
Control-4	31,847,284	2,732,900	2,122,573	216,979	26,682,432	24,160,562
Control-5	35,960,262	2,359,625	3,352,912	269,766	29,970,016	27,187,930
Control-6	33,255,140	3,880,723	2,504,636	238,837	26,612,534	24,089,070

Table 2.2 Distribution of RNA-sequencing data for adult samples

Distribution of reads after processing MB-enriched samples for Bap60 knockdowns and controls in juvenile and mature flies. “Good Reads” are uniquely aligned to the *Drosophila* genome with less than four mismatches. “Genes” column is good reads counted to genes using HTSeq-count.

Sample Name	Total Reads	Unmapped	Multimapped	Uniquely Mapped	>4 Mismatch	Good Reads	Genes
Juvenile-Bap60-1	69,882,637	12,595,968	5,575,417	51,200,942	607,760	50,593,182	45,547,974
Juvenile-Bap60-2	79,689,711	12,900,425	6,696,489	59,606,219	591,594	59,014,625	53,143,845
Juvenile-Control-1	57,253,135	9,773,348	4,114,900	42,521,713	410,427	42,111,286	37,879,789
Juvenile-Control-2	71,255,606	15,179,161	5,939,995	48,981,963	621,782	48,360,181	43,900,119
Juvenile-Control-3	69,291,208	12,733,708	4,822,713	50,737,211	510,803	50,226,408	45,731,087
Mature-Bap60-1	28,008,832	3,668,870	4,341,215	19,490,509	261,373	19,229,136	17,605,227
Mature-Bap60-2	35,693,763	5,786,038	2,334,081	27,274,907	378,554	26,896,353	24,449,371
Mature-Bap60-3	51,440,093	5,897,602	3,014,361	41,871,033	557,810	41,313,223	37,806,307
Mature-Bap60-4	31,597,027	4,454,742	1,968,708	24,954,669	337,963	24,616,706	22,422,814
Mature-Bap60-5	28,292,212	3,845,610	1,632,011	22,574,518	304,486	22,270,032	20,318,570
Mature-Control-1	43,556,931	4,013,821	16,483,563	22,581,077	295,272	22,285,805	20,355,366
Mature-Control-2	47,585,462	6,671,394	3,281,136	36,980,596	513,180	36,467,416	33,065,905
Mature-Control-3	97,781,945	11,400,376	5,894,536	79,239,322	1,038,033	78,201,289	71,462,385
Mature-Control-4	24,988,386	2,827,908	1,619,676	20,285,109	261,018	20,024,091	18,301,658
Mature-Control-5	27,927,228	5,268,679	1,660,518	20,827,018	285,108	20,541,910	18,759,891

2.8.2 ATAC-Sequencing Analysis

Paired-end reads were aligned to the *Drosophila melanogaster* reference genome (BDGP release 6) with the STAR aligner (version 2.5.3a). Reads aligning to multiple loci, the mitochondrial genome, and scaffolds were filtered using samtools view (version 1.4) (Li et al., 2009). Duplicate reads resulting from PCR amplification of the libraries were removed using samtools rmdup. Since the Tn5 transposase has been shown to bind as a dimer and insert two adapters separated by 9bp (Buenrostro et al., 2016), read start sites were adjusted on the forward strand by +4bps, and reads aligning to the reverse strand were adjusted by -5bps. Peaks were called using Macs2 (version 2.1.2) (Zhang et al., 2008) using the –nolambda and –nomodel flags, the –slocal flag set to 10000, and -q flag set to 0.1 to allow for a sensitive detection of peaks. These peaks are regions of the genome where significantly more sequencing reads aligned than compared to the genomic background. In the context of ATAC-Seq, a peak represents a region of accessible chromatin. Peaks were analyzed using the Bioconductor package DiffBind (Stark & Brown, 2011) and regions in which peaks were called in at least two samples were considered to be potentially important for gene regulation and are hereafter referred to as regulatory regions. HTSeq-count (version 0.11.2) was then used to count reads within the regulatory regions using the overlap resolution mode of ‘intersection_nonempty’ to ensure that all bases called within a given region were counted for further analysis. DESeq2 was used to normalize reads aligned within regulatory regions and to determine differentially accessible regions. Differentially accessible regions were defined as having a Benjamini-Hochberg adjusted *P* value <0.05 and were annotated and analyzed using the Bioconductor package ChIPseeker (Yu et al., 2015).

Larval Analysis (Chapter 4)

Sequenced libraries of E(y)3-KD MBs, Bap60-KD MBs, Snr1-KD MBs, and controls (n=2 for all genotypes) resulted in an average of 33,901,552 raw paired-end reads across all samples, with 60% of reads aligning uniquely to the *Drosophila* genome after the removal of mitochondrial reads and duplicates (**Table 2.3**). Peak calling resulted in an average of 13,603 non-stringent peaks called across all samples. A total of 16,056 regulatory regions in 8,272 genes were identified for differential accessibility analysis.

Adult Analysis (Chapter 5)

Sequenced libraries of juvenile and mature Bap60-KD MBs and controls (n=2 for each condition) resulted in an average of 38,842,933 raw paired-end reads across all samples with 43% of reads aligning uniquely to the *Drosophila* genome after the removal of mitochondrial reads and duplicates (**Table 2.4**). Peak calling resulted in an average of 22,070 non-stringent peaks called across all samples and the identification of 26,244 potential regulatory regions in 9,893 genes for differential accessibility analysis.

Table 2.3 Distribution of ATAC-sequencing data in larval samples

Distribution of reads after processing MB-enriched samples for SWI/SNF knockdowns and controls. "Good Reads" are uniquely aligned to the *Drosophila* genome with less than four mismatches after the removal of mitochondrial and duplicate reads. "Peaks called" column is the number of peaks called against the background using MACS2.

Sample Name	Total Reads	Unmapped	Uniquely Mapped	Mitochondrial	Duplicates	Good Reads	Peaks Called
E(y)3-1	31,769,883	6,771,107	22,501,775	1,082,400	1,539,942	19,879,433	14,604
E(y)3-2	47,863,069	10,370,533	33,622,844	1,639,028	6,366,806	25,617,010	16,185
Bap60-1	30,956,339	5,534,422	23,092,352	1,209,307	2,118,419	19,764,626	13,611
Bap60-2	32,041,054	5,988,445	23,477,389	1,248,534	2,109,968	20,118,887	12,904
Snr1-1	32,366,237	6,989,662	22,703,706	1,289,333	1,970,185	19,444,188	12,294
Snr1-2	20,997,613	4,872,687	14,363,220	901,557	1,023,593	12,438,070	8,749
Control-1	39,230,483	7,878,086	28,757,204	2,421,496	1,943,584	24,392,124	16,271
Control-2	35,987,734	7,940,043	25,216,228	1,926,224	2,661,346	20,628,658	14,209

Table 2.4 Distribution of ATAC-sequencing data in adult samples

Distribution of reads after processing MB-enriched samples for Bap60 knockdowns and controls in juvenile and mature flies. "Good Reads" are uniquely aligned to the *Drosophila* genome with less than four mismatches after the removal of mitochondrial and duplicate reads. "Peaks called" column is the number of peaks called against the background using MACS2.

Sample Name	Total Reads	Unmapped	Uniquely Mapped	Mitochondrial	Duplicates	Good reads	Peaks Called
Juvenile-Bap60-1	34,571,046	11,709,403	19,228,525	1,825,230	881,821	16,521,474	26,583
Juvenile-Bap60-2	46,699,910	16,915,209	25,032,093	3,261,465	1,267,148	20,503,480	27,348
Juvenile-Control-1	29,852,119	10,394,970	16,715,037	2,193,225	1,455,365	13,066,447	17,755
Juvenile-Control-2	36,668,218	12,611,420	20,610,720	2,718,923	969,909	16,921,888	21,678
Mature-Bap60-1	34,986,564	14,506,277	18,104,019	3,572,220	1,745,092	12,786,707	16,424
Mature-Bap60-2	42,589,384	17,888,741	21,609,527	3,956,857	1,033,463	16,619,207	21,268
Mature-Control-1	48,456,440	17,387,575	27,175,813	4,574,186	1,456,319	21,145,308	23,322
Mature-Control-2	36,919,781	13,027,742	20,391,581	3,190,432	969,320	16,231,829	22,179

2.8.3 Gene ontology enrichment analysis

Gene ontology (GO) enrichment analysis was performed using Panther (Mi et al., 2017). Gene lists were uploaded to Panther. Gene ontology terms were identified for biological processes, molecular functions, and cellular components and were considered significantly if they had a Benjamini-Hochberg false discovery rate (FDR) corrected *P* value <0.05.

2.8.4 Classification of tissue-specific genes

To generate lists of tissue-specific genes, I used normalized expression values from Brown *et al*. (2014) for several tissues, including adult head (nine samples), adult carcass (three samples), and adult digestive tract (three samples). The relative enrichment in gene expression levels for each of these tissues was calculated by comparing the mean bases per kilobase per million reads (bpkm) for each specific tissue to the mean bpkm across all remaining tissues. Enrichment values for each gene in each tissue type were determine by calculating the $\log_2$ fold-change in expression of that gene in each tissue compared to all other tissues. Tissue-specific and tissue-depleted genes are defined as having an enrichment value outside one standard deviation of the average of all enrichment values. Adult heads were used as a representation of a neuron-enriched tissue and the adult carcass, consisting of tissues remaining after removal of the head, digestive tract, and reproductive organs, as a representation of a muscle-enriched tissue. The statistical significance of over- or under-representation of tissue-specific genes in differentially upregulated and downregulated genes in Bap60-KD MBs was determined with a hypergeometric test.

2.9 Microscopy methods

2.9.1 Quantification of nuclei obtained through INTACT

To investigate the specificity and to estimate the amount of GFP positive nuclei obtained from the INTACT protocol, I calculated the proportion of GFP positive nuclei in both the MB sample (nuclei immunoprecipitated from the whole head cell homogenate) and whole head (WH) sample consisting of nuclei from all cells in the fly head. All permeable nuclei (nuclei that can be used for ATAC-Seq) were labeled with 500nM propidium iodide (ThermoFisher Scientific) at room temperature for five minutes. Nuclei were quantified using a haemocytometer and a Zeiss AxioImager Z1 microscope. The average percentage of GFP nuclei was calculated for each biological replicate by manually counting nuclei.

2.9.2 Immunostaining and confocal microscopy

Adult brains, larval CNS, and pupal CNS were dissected in PBS and fixed with 4% paraformaldehyde for 40 minutes at room temperature, before mounting in Vectashield (Vector Laboratories). For immunohistochemistry, fixed adult brains were blocked in 5% NGS and then incubated overnight with the primary antibody anti-FasII (1:25; DSHB, 1D1) and the secondary antibody goat anti-mouse DyLight 594 (1:300). Images were acquired using a Zeiss LSM800 confocal microscope. Confocal stacks were processed using ImageJ software (Schindelin et al., 2012). Gross MB morphology was assessed and qualitatively quantified by examining confocal stacks. Due to variability in the severity of MBγ pruning phenotypes, the appearance of unpruned γ dorsal projections were classified as ‘normal’, ‘mild’, ‘moderate’, or ‘severe’, as indicated in **Figure 4.4**.

Chapter 3

3 Analysis of mushroom body-specific gene expression

Parts of this chapter are published in Jones et al, 2018.

This study aims to profile the effect of the SWI/SNF complex on gene expression and chromatin availability in the MB. In order to accomplish this, I had to establish a protocol to isolate and analyze genetic material specifically from MB neurons in both late 3rd instar larvae and adult flies. To do this, I adapted a previously described protocol called INTACT (Isolation of Nuclei TAgged in a Cell Type) (Henry et al., 2012) in which a nuclear envelope fusion protein, Unc84::GFP, is expressed in specific cell types under control of the GAL4-UAS system. Tagged nuclei can then be immunoprecipitated from a cell homogenate and genetic material can be isolated and used for downstream analyses (**Figure 2.2**). In this chapter, I use INTACT to isolate nuclei from MB neurons and analyze the MB-specific transcriptome of both late 3rd instar larvae and adult flies.

3.1 Mushroom body specific GAL4 driver

To isolate MB nuclei using INTACT, I first needed to find a GAL4 driver with a MB-specific expression domain in both 3rd instar larvae and adult flies. I used the *R14H06-GAL4* driver line from the Janelia FlyLight collection (Jenett et al., 2012) – a driver line that has been used previously in our lab due to MB-specific expression in adult flies (Chubak et al., 2019; Jones et al., 2018). The expression domain of *R14H06-GAL4* has been documented by the FlyLight project and is publicly available online (http://flweb.janelia.org). The driver shows a lack of expression in embryos and specific labelling of the MB in the larval and adult brain. To confirm the specificity of the *R14H06-GAL4* driver, I crossed it with a *UAS-mCD8::GFP* responder line, dissected and stained late 3rd instar larvae CNS and adult brains, and performed fluorescent confocal microscopy (**Figure 3.1A**). Indeed, the expression domain of the *R14H06-GAL4* driver showed specific and high expression in the larval MBγ neurons (**Figure 3.1B**). Additionally, high expression of GFP was observed in the adult α/β and γ neurons in the MB (**Figure 3.1C**) with higher specificity than many of the classic MB GAL4 lines, which often show some non-specific expression in other regions of the brain (Aso et al., 2009). Given these results, a fly line containing both *R14H06-GAL4* and *UAS-Unc84::GFP*, hereafter referred to as MB-Unc84, was generated to perform MB-specific INTACT.

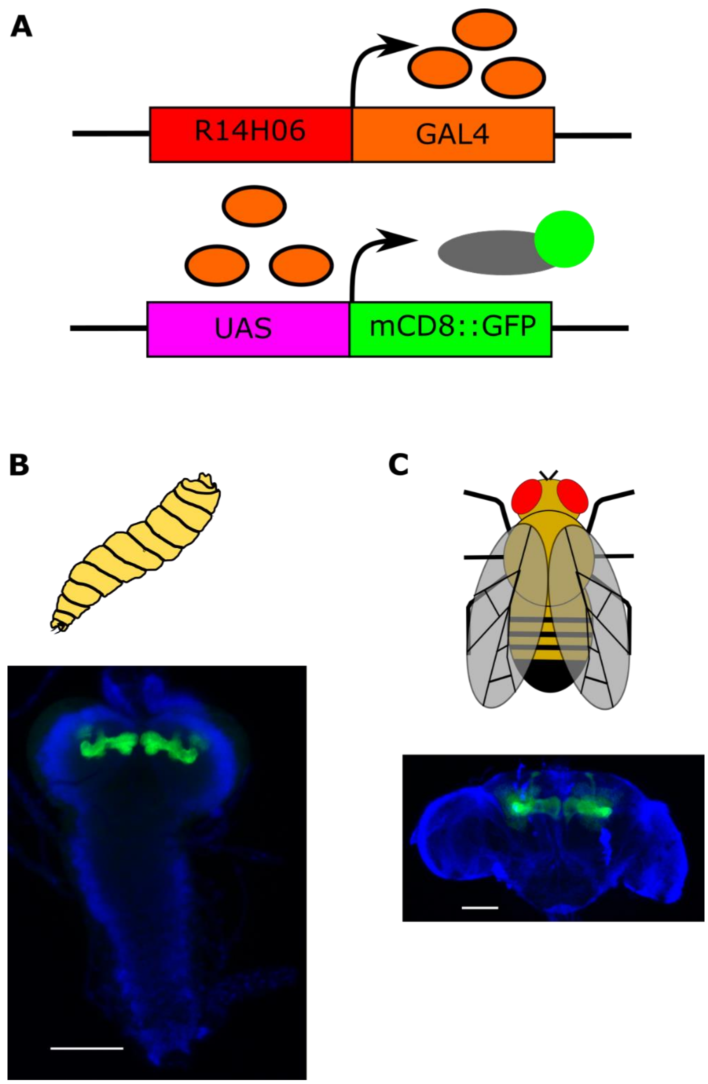

Figure 3.1 The *R14H06-GAL4* driver is MB specific.

(**A**) *R14H06-GAL4* is used to drive the expression of *UAS-mCD8::GFP* for fluorescent confocal microscopy. (**B-C**) Fluorescent confocal microscopy reveals the expression domain of the *R14H06-GAL4* driver in (**B**) the 3rd instar larval CNS and (**C**) the adult brain. Scale bars represent 100 µm.

3.2 INTACT effectively isolates MB nuclei

To validate that the INTACT method was capable of enriching for MB nuclei and to determine the efficiency and yield of the protocol, I stained nuclei obtained from both the whole head (WH) and MB nuclei isolated using INTACT (MB) (see **Chapter 2.9.1**) with propidium iodide. Using a haemocytometer and fluorescent microscopy, the total number of nuclei and the proportion of GFP positive nuclei in the WH sample and MB sample was quantified (**Figure 3.2A**). Overall, a 61% yield of immunoprecipitated GFP positive nuclei was calculated by comparing the total number of GFP positive nuclei in the MB sample to the total number of GFP positive nuclei in the WH sample. Nuclei obtained from the WH of MB-Unc84 flies contained 7% GFP positive nuclei (**Figure 3.2B**). This is likely an overestimation as propidium iodide labels only nuclei that have been permeabilized during homogenization, and therefore not all nuclei in the WH sample would be visible as permeabilization is not 100% efficient. After immunoprecipitation of nuclei from the WH using anti-GFP bound beads, approximately 90% of nuclei in the MB enriched sample were GFP positive, indicating a high level of specificity of the INTACT protocol (**Figure 3.2B**).

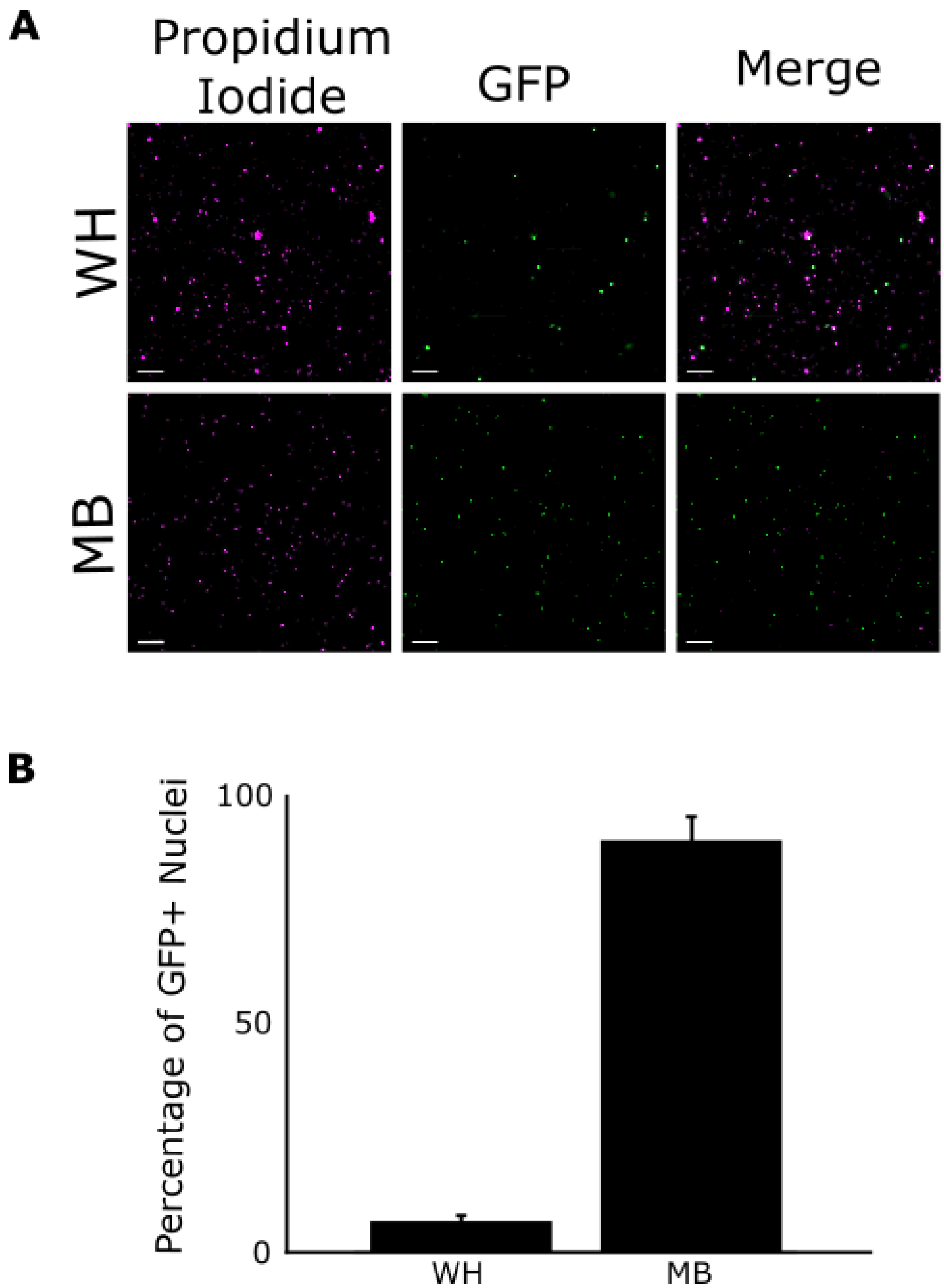

Figure 3.2 INTACT has high specificity for MB nuclei.

(**A**) Fluorescent microscopy images of nuclei from WH and MB samples of the INTACT protocol. All permeable nuclei were stained with propidium iodide. Scale bars represent 100 µm. (**B**) Graph showing the average percentage (±SEM) of GFP positive nuclei in WH and MB samples obtained using INTACT (n=3).

3.3 INTACT yields high-quality MB-enriched RNA

Next, INTACT was performed on adult heads and the larval CNS of male MB-Unc84 flies. Total RNA was isolated from both the WH and MB-specific samples of nuclei for sequencing resulting in an average of 54,424,823 raw single-end reads from the WH sample (n=12) and 54,053,253 raw reads from the MB sample (n=12) in adults. In larval samples, 46,773,817 raw reads were sequenced in the WH sample (n=8) and 30,213,639 reads in the MB samples (n=8). On average, 69% of reads from adult samples and 81% of reads from larval samples aligned uniquely to the *Drosophila* genome with less than four mismatches. Of these reads, an average of 88% were mapped to genes in the genome in adult samples, and an average of 89% mapped to genes in larval samples (**Tables 3.1 and 3.2**). The high percentage of reads aligning to genes suggests that RNA libraries prepared from INTACT-isolated nuclei are high-quality and capable of achieving sufficient read depth for transcriptome analysis (Liu et al., 2014).

Table 3.1 Read distribution for RNA-sequencing data of adult INTACT samples

Distribution of reads after processing for whole head (WH) and mushroom body (MB) samples. "Good Reads" are uniquely aligned to the *Drosophila* genome with less than four mismatches. "Genes" column is good reads counted to genes using HTSeq-count.

Sample Name	Total Reads	Unmapped	Multi-mapped	Uniquely mapped	>4 Mismatch	Good Reads	Genes
WH-1	59,615,982	12,867,699	5,882,020	40,386,876	641,615	39,745,261	35,046,902
WH-2	92,124,257	27,692,010	6,362,175	56,936,702	1,045,540	55,891,162	49,754,003
WH-3	67,716,260	20,744,862	4,614,165	41,548,647	980,893	40,567,754	35,110,614
WH-4	34,623,161	6,339,988	2,238,694	25,930,458	405,540	25,524,918	22,894,808
WH-5	56,439,737	17,079,415	3,236,117	35,779,107	602,289	35,176,818	31,458,214
WH-6	59,437,475	7,905,687	3,853,969	47,244,867	661,102	46,583,765	41,900,320
WH-7	28,122,960	7,055,012	2,201,184	18,563,349	372,709	18,190,640	15,828,523
WH-8	34,733,970	8,061,044	2,863,128	23,541,355	458,851	23,082,504	20,184,796
WH-9	69,100,790	15,371,421	6,895,852	45,989,899	748,658	45,241,241	40,007,496
WH-10	43,284,973	8,197,477	3,318,755	30,925,835	589,260	30,336,575	27,047,844
WH-11	44,443,009	9,453,333	3,513,201	30,713,947	613,771	30,100,176	26,695,827
WH-12	63,455,297	16,614,779	4,616,847	41,094,712	850,959	40,243,753	35,588,831
MB-1	74,926,256	7,823,721	6,568,424	60,305,060	679,332	59,625,728	54,067,796
MB-2	100,449,698	10,271,767	7,624,890	82,314,861	887,236	81,427,625	74,198,583
MB-3	28,945,627	3,539,860	2,191,455	22,931,501	315,102	22,616,399	20,292,244
MB-4	32,910,822	3,884,481	2,569,420	26,225,235	377,020	25,848,215	23,470,908
MB-5	79,221,516	9,567,431	5,150,954	64,190,495	849,253	63,341,242	57,978,480
MB-6	50,296,863	11,022,371	3,515,007	34,205,107	582,705	33,622,402	30,335,987
MB-7	31,385,559	12,353,650	2,740,538	15,809,134	511,569	15,297,565	12,461,996
MB-8	66,128,463	36,288,012	6,753,870	19,975,211	1,212,859	18,762,352	13,041,769
MB-9	45,759,703	7,933,439	3,444,988	33,934,506	489,040	33,445,466	30,169,876
MB-10	43,690,820	4,507,291	3,309,297	35,699,474	503,384	35,196,090	31,998,626

MB-11	38,126,838	2,891,616	2,211,708	32,911,040	419,656	32,491,384	29,573,912
MB-12	56,796,866	7,815,008	3,452,190	45,146,038	609,577	44,536,461	40,438,625

Table 3.2 Read distribution of RNA-sequencing data from larval INTACT samples

Distribution of reads after processing for CNS – termed “whole head” (WH) – and mushroom body (MB) samples. “Good Reads” are uniquely aligned to the *Drosophila* genome with less than four mismatches. “Genes” column is good reads counted to genes using HTSeq-count.

Sample Name	Total Reads	Unmapped	Multimapped	>4 Mismatch	Good Reads	Genic
WH-1	39,005,189	3,316,091	2,947,891	304,453	32,415,865	28,981,311
WH-2	39,027,904	4,232,389	2,798,186	278,749	31,701,301	28,445,946
WH-3	36,857,989	4,681,004	2,456,298	265,930	29,434,848	26,325,784
WH-4	54,950,648	5,717,959	5,403,899	592,797	43,211,088	29,313,479
WH-5	26,485,232	2,875,191	1,778,986	180,424	21,594,389	19,223,822
WH-6	111,079,414	10,311,862	6,956,796	823,466	92,510,147	82,822,207
WH-7	22,267,957	3,091,965	1,459,891	178,093	17,337,066	15,349,890
WH-8	44,516,203	6,516,231	4,644,073	314,707	32,688,485	28,999,116
MB-1	35,960,262	2,359,625	3,352,912	269,766	29,970,016	27,187,930
MB-2	33,255,140	3,880,723	2,504,636	238,837	26,612,534	24,089,070
MB-3	31,052,948	3,777,463	2,178,867	227,147	24,782,907	22,461,399
MB-4	25,211,556	2,008,169	1,963,246	201,919	21,024,787	18,973,243
MB-5	28,549,492	1,893,209	2,045,980	196,702	24,359,121	22,036,448
MB-6	26,177,406	1,796,718	1,565,344	187,511	22,563,359	20,429,408
MB-7	29,655,027	2,891,663	1,911,979	205,395	24,553,181	22,190,892
MB-8	31,847,284	2,732,900	2,122,573	216,979	26,682,432	24,160,562

To assess the quality of the sequencing results and confirm that the variability between samples corresponds to biological variance and not poor sequencing quality, a principal component analysis (PCA) was conducted on variance-stabilized genic reads using DESeq2 (Anders & Huber, 2010). Principal component analysis assesses the variance between samples and uses values called principal components to represent variance, with the first principal component accounting for as much as the variability as possible. Results of the PCA show clustering and separation of WH samples from MB samples in both adult and larval samples (**Figure 3.3 A** and **B**) along the first principal component (x-axes), indicating that the majority of variance between the samples is due to the biological variance between the WH and MB samples (39% in adults and 40% in larvae).

To further validate the MB-specificity of INTACT-isolated nuclei, normalized gene expression of selected genes was compared between MB samples and WH samples. Genes selected for this analysis were either genes known to be specifically enriched in MB neurons (*toy, oamb, sNPF, rut, ey, EcR-B1,* and *dac*), or genes known to be enriched in other brain tissues, such as the eyes or glial cells (*prom, repo, Tre1* and *trpl*). Indeed, in both the adult and larval samples, there is enrichment of MB-enriched gene expression and depletion of other genes in the MB samples when compared to the WH samples (**Figure 3.3 C** and **D**). Additionally, the most highly expressed and enriched gene in the MB samples in both adult and larval samples is the Unc84 transgene, which is expressed exclusively in the MB neurons mediated by *R14H06-GAL4* expression. Taken together, these results show that RNA isolated from the MB samples of nuclei obtained using the INTACT protocol can generate high-quality reads that reflect the known biology of the MB.

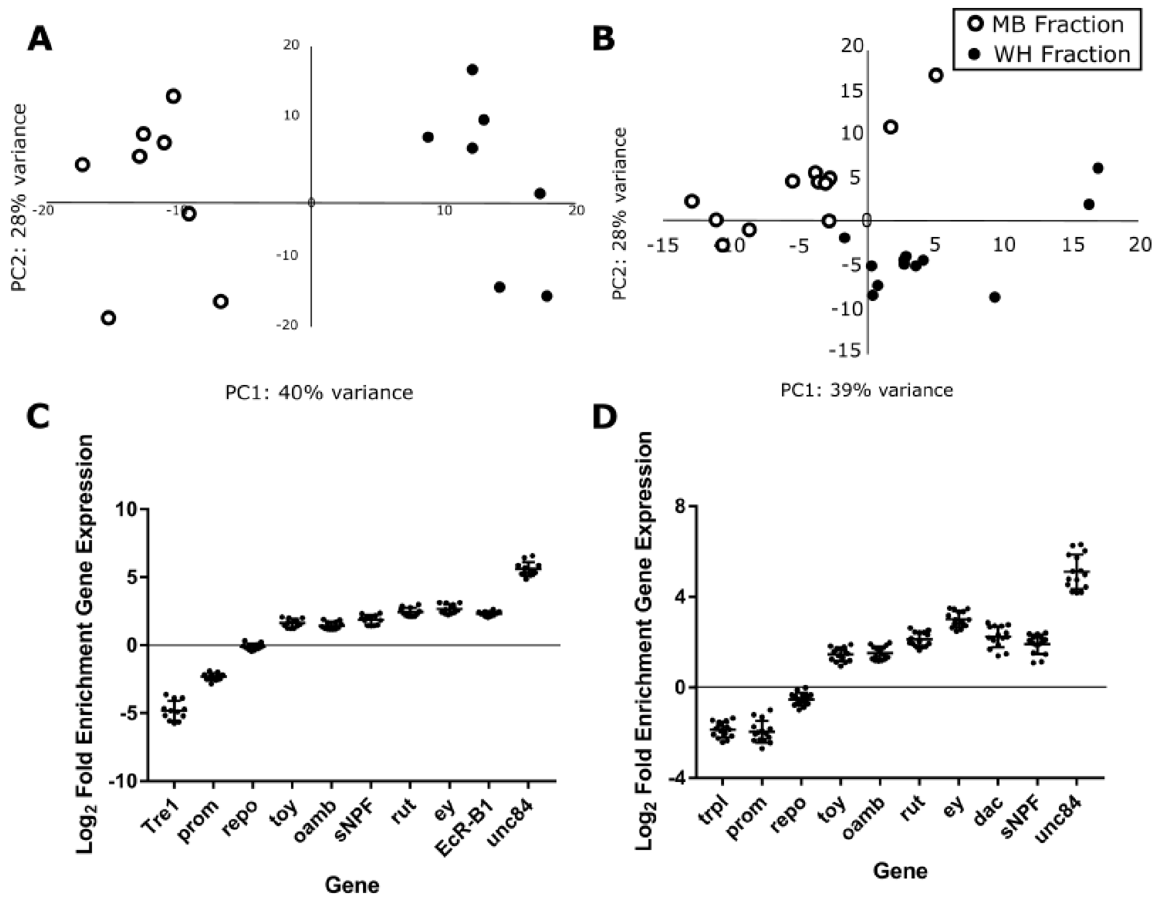

Figure 3.3 RNA obtained from INTACT-isolated nuclei is MB-specific.

(**A-B**) Principal component analysis of the top 150 variable genes in larval (**A**) and adult (**B**) samples. (**C-D**) Log_2 fold enrichment of expression of select genes expressed outside of the MB (larval: *Tre1*, *prom*, and *repo*; adult: *trpl*, *prom*, and *repo*), genes known to be specifically expressed in the MB (larval: *toy*, *oamb*, *sNPF*, *rut*, *ey*, and *EcR-B1*; adult: *toy*, *oamb*, *rut*, *ey*, *dac*, and *sNPF*) , and the *Unc84* transgene in larval (**C**) and adult (**D**) samples. Enrichment was calculated by comparing normalized expression in the MB samples to those in the WH samples.

3.4 Differential expression analysis identifies MB-enriched genes

Next, the transcriptome of the MB was analyzed by performing a differential gene expression analysis between WH and MB samples in both larvae and adults. A total of 470 genes and 85 were found to be significantly enriched in the larval MB and WH samples, respectively (P_{adj}<0.05 and fold-difference>2; **Figure 3.4 A**). In adult samples, 118 genes and 127 genes were found to be significantly enriched in the MB and WH samples, respectively (**Figure 3.4 B**). Comparing the genes enriched in the MB samples (hereafter referred to as MB-specific genes; **Appendix C**) in both the larval and adult samples showed a significant overlap (P= 1.63 x 10^{-76}, hypergeometric test) between the two groups (**Figure 3.4 C**). Indeed, genes that are known to be highly expressed in the MB were identified in both larval and adult MB-specific genes including *Oamb, ey, rut, sNPF,* and *prt* (Brooks et al., 2011; Kurusu et al., 2000; Livingstone et al., 1984; Noveen et al., 2000). Additionally, enrichment of genes encoding dopamine receptors, *Dop1R1, Dop1R2,* and *Dop2R* was identified in both larval and adult MBs. Enrichment of MB-enriched genes *SLC22A*, *Hr3*, and several glutamate receptor subunits (GluRs) was identified in the larval MB (**Figure 3.4 C**) as well as enrichment of *dac*, *toy,* and the gene encoding the serotonin receptor, 5-HT1B in the adult MB (Gai et al., 2016; Johnson et al., 2011; Sinakevitch et al., 2010).

Furthermore, gene ontology (GO) enrichment analysis was performed on genes found to be enriched in only larval or adult samples as well as genes enriched in both (**Figure 3.4D**). Terms that were enriched in both larval and adult MB genes included anesthesia-resistant memory, olfactory learning, and terms involved in cyclic-AMP mediated signaling – all processes that have been previously shown to be enriched specifically in the MB (Aso et al., 2014; Blum et al., 2009; Keleman et al., 2012; Zhang et al., 2015). Additionally, GO molecular function terms show high enrichment of dopamine neurotransmitter receptor activity. Dopaminergic neurons are known to innervate the MB to provide reward or punishment signals to help with learning (Aso et al., 2014).

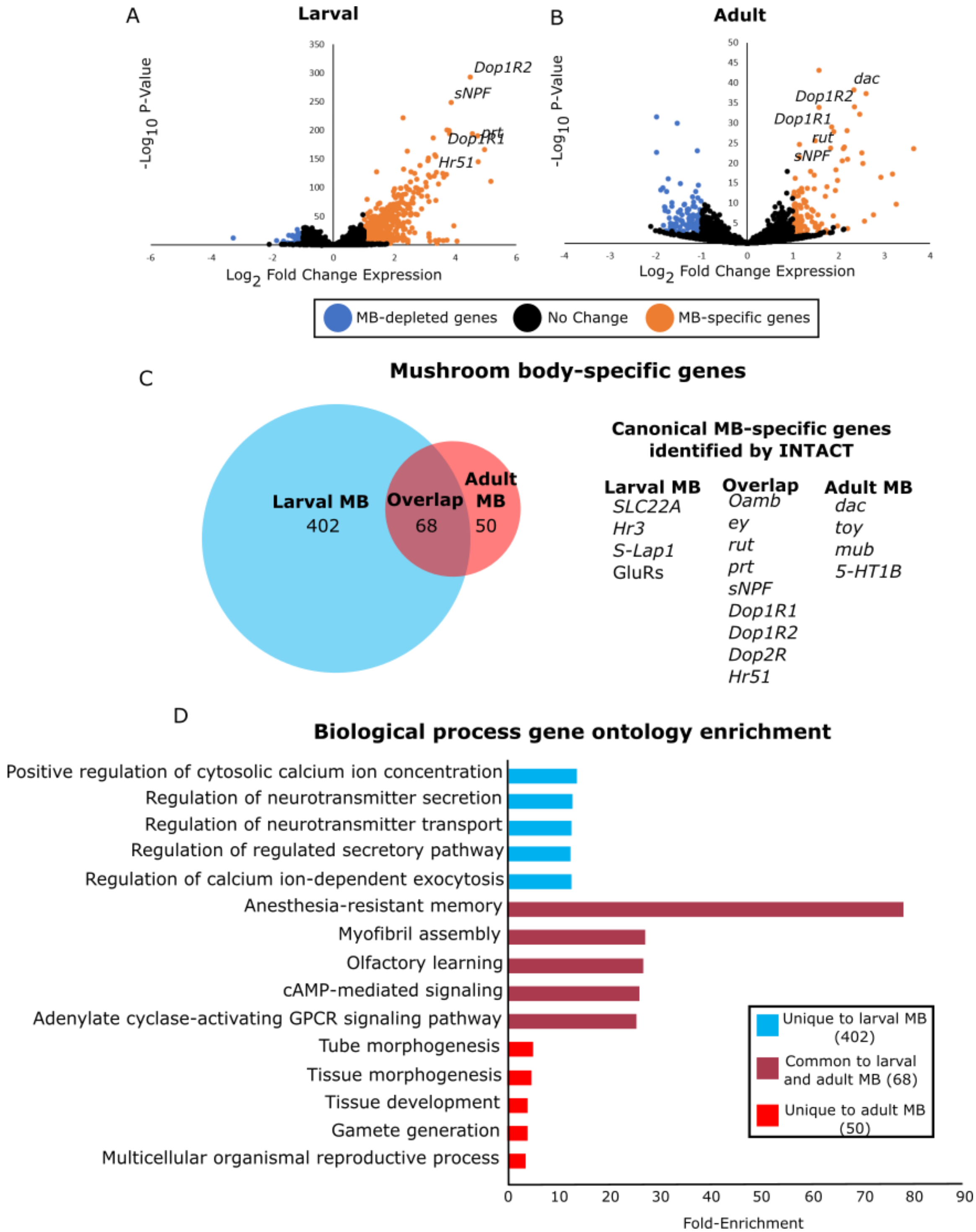
A
Larval
-Log10 P-Value
Log2 Fold Change Expression
Dop1R2
sNPF
prt
Dop1R1
Hr51
B
Adult
dac
Dop1R2
Dop1R1
rut
sNPF
MB-depleted genes
No Change
MB-specific genes
C
Mushroom body-specific genes
Larval MB
402
Overlap
68
Adult MB
50
Canonical MB-specific genes identified by INTACT
Larval MB
SLC22A
Hr3
S-Lap1
GluRs
Overlap
Oamb
ey
rut
prt
sNPF
Dop1R1
Dop1R2
Dop2R
Hr51
Adult MB
dac
toy
mub
5-HT1B
D
Biological process gene ontology enrichment
Positive regulation of cytosolic calcium ion concentration
Regulation of neurotransmitter secretion
Regulation of neurotransmitter transport
Regulation of regulated secretory pathway
Regulation of calcium ion-dependent exocytosis
Anesthesia-resistant memory
Myofibril assembly
Olfactory learning
cAMP-mediated signaling
Adenylate cyclase-activating GPCR signaling pathway
Tube morphogenesis
Tissue morphogenesis
Tissue development
Gamete generation
Multicellular organismal reproductive process
Unique to larval MB (402)
Common to larval and adult MB (68)
Unique to adult MB (50)
0 10 20 30 40 50 60 70 80 90
Fold-Enrichment

Figure 3.4 Differential gene expression analysis comparing MB samples to WH samples in larvae and adults.

(**A-B**) Volcano plots showing differentially expressed genes (P_{adj}<0.05 and >2 fold-change) represented in blue (downregulated) or orange (upregulated) in the larval MB (**A**) or the adult MB (**B**). (**C**) Comparison of MB-specific genes identified in the larval and adult samples. A significant proportion of genes overlap between larval and adult ($P=1.63 \times 10^{-76}$, hypergeometric test) and canonical MB-specific genes can be found in both samples. (**D**) Gene ontology enrichment for biological processes of the MB-specific genes identified in larval, adult, or both samples. Top five enriched terms with at least five genes and an FDR corrected *P* <0.05 are displayed.

When looking at MB-specific genes found only in the adult samples there was very little GO enrichment whereas, MB-specific genes found only in the larval samples, revealed strong enrichment for GO terms related neuronal activity such as to "regulation of neurotransmitter secretion", "regulation of neurotransmitter transport", "intracellular cyclic nucleotide activated cation channel complex", and "delayed rectifier potassium channel activity" (**Figure 3.4D)**.

Taken together, these results show that using RNA isolated from MB nuclei obtained through INTACT can be used to analyze the MB transcriptome. This transcriptome analysis was able to identify known MB-enriched genes in both larvae and adults, as well as show enrichment of biological processes known to occur in the MB.

3.4.1 MB transcriptome analysis identifies potential novel MB genes

In addition to identifying canonical MB genes, this analysis led to the identification of new candidate MB genes that may be important in MB function. One of these genes is *Major Facilitatory Superfamily Transporter 3* (*MFS3*) which is enriched in both the larval and adult MB when compared to their respective WH samples (fold change= 2.73 and 3.32 in larval and adult, respectively). *MFS3* encodes a predicted transmembrane transporter of amino acids, nucleotides, and organic anions. Although its function in *Drosophila* is unknown, MFS3 is orthologous to the mammalian solute carrier family 17 member 5 (SLC17A5; via DIOPT v7.1), a membrane transporter that exports acidic sugars, including sialic acid (Verheijen et al., 1999).

Another candidate MB gene is *Hormone receptor-like 38* (*Hr38*) which is highly enriched in both the larval and adult MB when compared to their respective WH samples (fold change= 8.75 and 2.64 larval and adult, respectively). *Hr38* has been identified as an activity regulated gene (Chen et al., 2016; Croset et al., 2018) – a gene that is upregulated following neuronal stimulation. Recently, a single cell RNA-seq experiment of the *Drosophila* brain performed by Croset et al. (2018) found that activity regulated genes, including *Hr38* experience higher transcription levels in the MBγ neurons. The identification of this activity regulated gene as MB-specific supports the observation that

MB neurons have a high level of activity compared to other neurons in the fly brain (Croset et al., 2018).

A promising MB gene is *lactate dehydrogenase* (*Ldh*), which shows one of the highest enrichments in both the larval and adult MB when compared to their respective WH samples (fold change= 9.85 and 7.57 larval and adult, respectively). Lactate dehydrogenase is an enzyme responsible for metabolizing lactate into pyruvate. This is interesting because it has been previously shown that the *Drosophila* MB undergoes increased pyruvate metabolism during learning (Plaçais et al., 2017) and because a previous study in mammals identified a role for lactate in LTM formation (Suzuki et al., 2011). Given these observations and its particularly high expression in the MB, Ldh may play a critical role in MB function.

Taken together, these results show that the INTACT protocol is capable of enriching MB nuclei for transcriptome analyses that reflect a MB-specific transcriptome. This protocol has been used to identify novel MB-specific genes that may be required for specific processes in the MB. Moving forward in this project, I use this protocol to isolate MB nuclei in SWI/SNF knockdown larvae and adults to investigate the role of the SWI/SNF complex in the MB at the late 3rd instar larval and adult stages in *Drosophila*.

Chapter 4

4 Investigating the role of the SWI/SNF complex in mushroom body remodeling

Parts of this chapter are published in Chubak et al, 2019.

Neuronal remodeling is a crucial part of brain wiring (Chen & Baram, 2016; Espinosa & Stryker, 2012). During pupation, the γ neurons in the *Drosophila* MB undergo neuronal remodeling. This begins by pruning the dorsal and medial projections of the γ lobes to the peduncle within the first 18 hours of pupation followed by re-extension of the γ lobes in only the medial direction. This process is initiated by a spike in the ecdysone moulting hormone at the late 3rd instar larval stage (**Figure 1.6**). Expression of the ecdysone receptor EcR-B1 in Kenyon cells in the late 3rd instar larvae is tightly regulated by the TGF-β signaling pathway and the Ftz-f1 hormone receptor (Boulanger et al., 2011; Zheng et al., 2003). Binding of ecdysone to an ecdysone nuclear receptor complex consisting of EcR-B1 and either Tai or USP, triggers a transcriptional cascade activating genes necessary for γ neuron pruning (Alyagor et al., 2018).

Recently, our lab found a role for the SWI/SNF subunits Bap60, Snr1, and E(y)3 in γ neuron remodeling, where dorsal projections of the γ neurons were found to exist in the adult MB (Chubak et al., 2019). These extra dorsal projections could be due to either defective pruning processes or aberrant re-extension processes. The specific processes, whether neuronal pruning or re-extension, for which the SWI/SNF complex is required, and the genes upon which it acts to regulate these processes remain unknown. The goal of this chapter is to determine whether the SWI/SNF complex is required for γ pruning or re-extension, and to identify the genes it regulates to do so.

4.1 SWI/SNF complex is required for MB γ lobe pruning

To determine whether the extra-dorsal projections of the γ neurons in SWI/SNF knockdowns are due to defective γ neuron pruning process or aberrant re-extension of the γ neurons, each of the subunits with observed dorsal γ projections in adults were knocked down in the MB using transgenic *UAS-RNAi* lines, and brains were dissected and imaged at three different time points: 3rd instar larvae, 19-22 hours after puparium formation, and adult. Knockdown of Bap60, Snr1, and E(y)3 caused no notable defects in larval MB morphology, suggesting that axon pathfinding can occur normally in knockdown flies (**Figure 4.1B**). In pupae, MBγ neuron pruning was observed at 19-22 hours after puparium formation in controls, as expected (**Figure 4.1C**). In contrast, pupae with knockdown of Ba60, Snr1, and E(y)3 did not show MBγ axon pruning (**Figure 4.1C**). This defect was 100% penetrant for all three SWI/SNF subunits and was specific for axons, as pruning of MB dendrites was not affected (**Figure 4.1C**). This verified that SWI/SNF knockdown causes defects in MBγ neuron pruning during pupal morphogenesis, rather than re-extension.

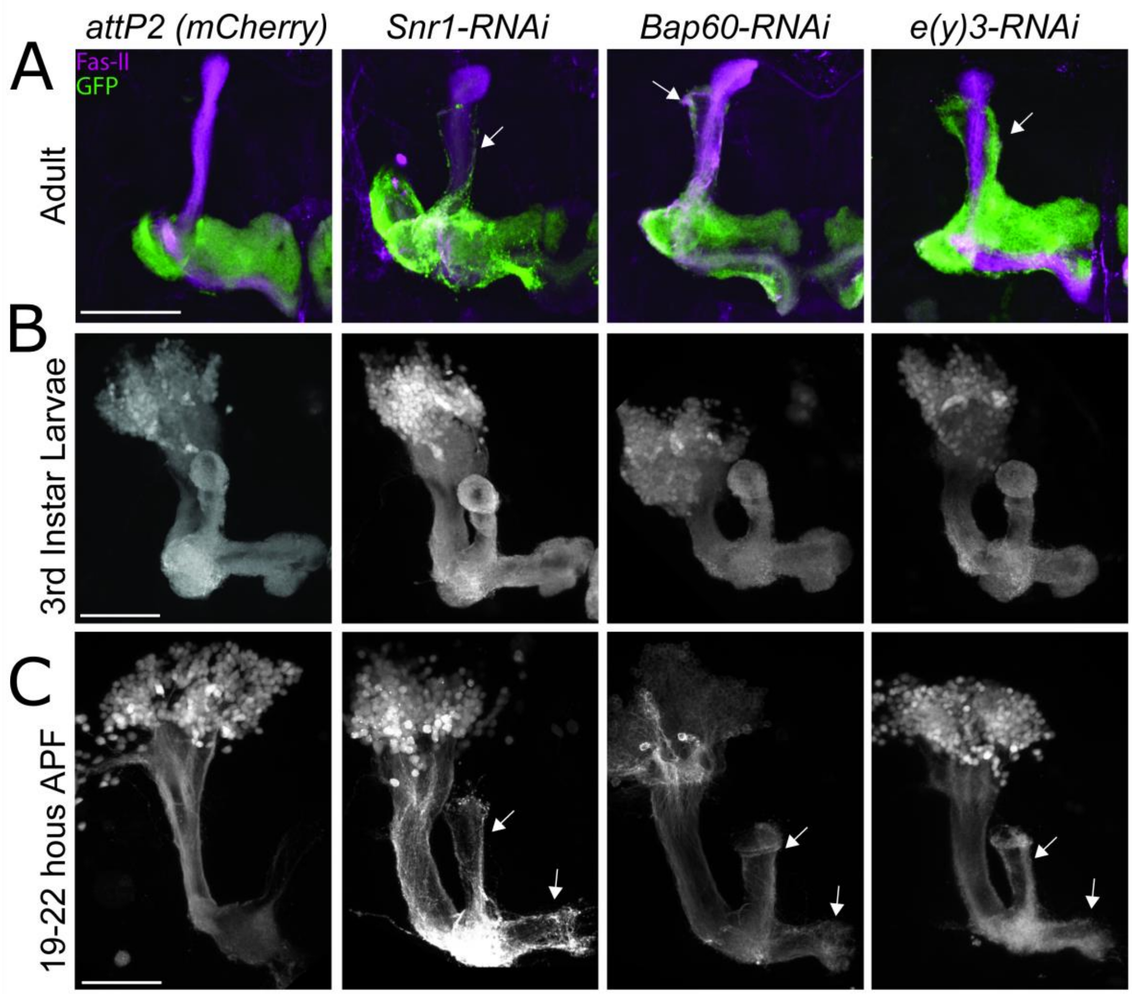

Figure 4.1 SWI/SNF subunits Snr1, Bap60, and E(y)3 are required for MBγ pruning.

Confocal projections showing MB neurons labelled with *R14H06-GAL4* and *UAS-mCD8::GFP*. Controls expressing an RNAi against mCherry were compared to SWI/SNF knockdown RNAi lines for Snr1, Bap60, and E(y)3. Images were obtained for adults (**A**), third-instar larvae (**B**), and early pupae (**C**). FasII was labelled by immunohistochemistry. Scale bars: 50 µm. Arrows indicate the location of unpruned MBγ axons.

4.2 SWI/SNF complex is required for the expression of genes involved in the ecdysone transcriptional cascade

After identifying the requirement of the SWI/SNF complex in MBγ pruning, the remainder of this chapter will focus on the mechanisms of neuron pruning regulated by the SWI/SNF complex. It is well established that ecdysone signaling is critical for MBγ neuron remodeling (Lee et al., 2000). Ecdysone receptor B1 (EcR-B1; also known as EcR) expression is induced in the MB in the late third instar, initiating the expression of downstream transcription factors that are thought to control gene expression programs required for pruning (**Figure 1.7**). Kirilly et al. (2011) showed that the ATPase SWI/SNF subunit brm functions downstream of EcR-B1 and that it may regulate pruning by inducing expression of the ecdysone-responsive transcription factor, Sox14. Furthermore, Zraly et al. (2006) showed that the SWI/SNF mutants display misregulation of ecdysone-induced genes during pupation, suggesting a role for the SWI/SNF complex in ecdysone-mediated transcription. Therefore, I hypothesized that the SWI/SNF complex is required for MBγ pruning by regulating the transcription of genes in the EcR-B1 transcriptional cascade. To identify the role of the SWI/SNF complex in MBγ neuron pruning and whether it is involved in EcR-B1-mediated gene transcription, I performed RNA-sequencing in late 3rd instar larvae within three hours of pupation, at a time point when γ neuron pruning is initiated.

Using INTACT (see **Chapter 2.4**) to isolate MB nuclei from the CNS of late third instar larvae hours before pupation, RNA-sequencing was performed to identify the effect of SWI/SNF knockdowns on gene expression. The MB-specific transcriptomes of Bap60, Snr1, and E(y)3 knockdown larvae were analyzed and compared to those of control larvae. Additionally, the MB transcriptome of larvae with a UAS-mediated dominant negative form of EcR-B1 (EcR-B1^{DN}) was analyzed. Differentially expressed genes were identified by comparing SWI/SNF-KD or EcR-B1^{DN} to control using DESeq2 (**Figure 4.2**; **Appendix D**) and were defined as having a Benjamini-Hochberg adjusted *P* value <0.05.

Knockdown of the SWI/SNF subunits E(y)3 and Snr1 had a major effect on gene expression in the larval MB (**Figure 4.2A and B**) with a total of 510 and 523 differentially expressed genes, respectively. Similarly, EcR-B1^{DN} MB samples had 588 differentially expressed genes (**Figure 4.2D**). In contrast, knockdown of Bap60 did not have much of an effect on gene expression in the larval MB with only 10 differentially expressed genes (**Figure 4.2C**).

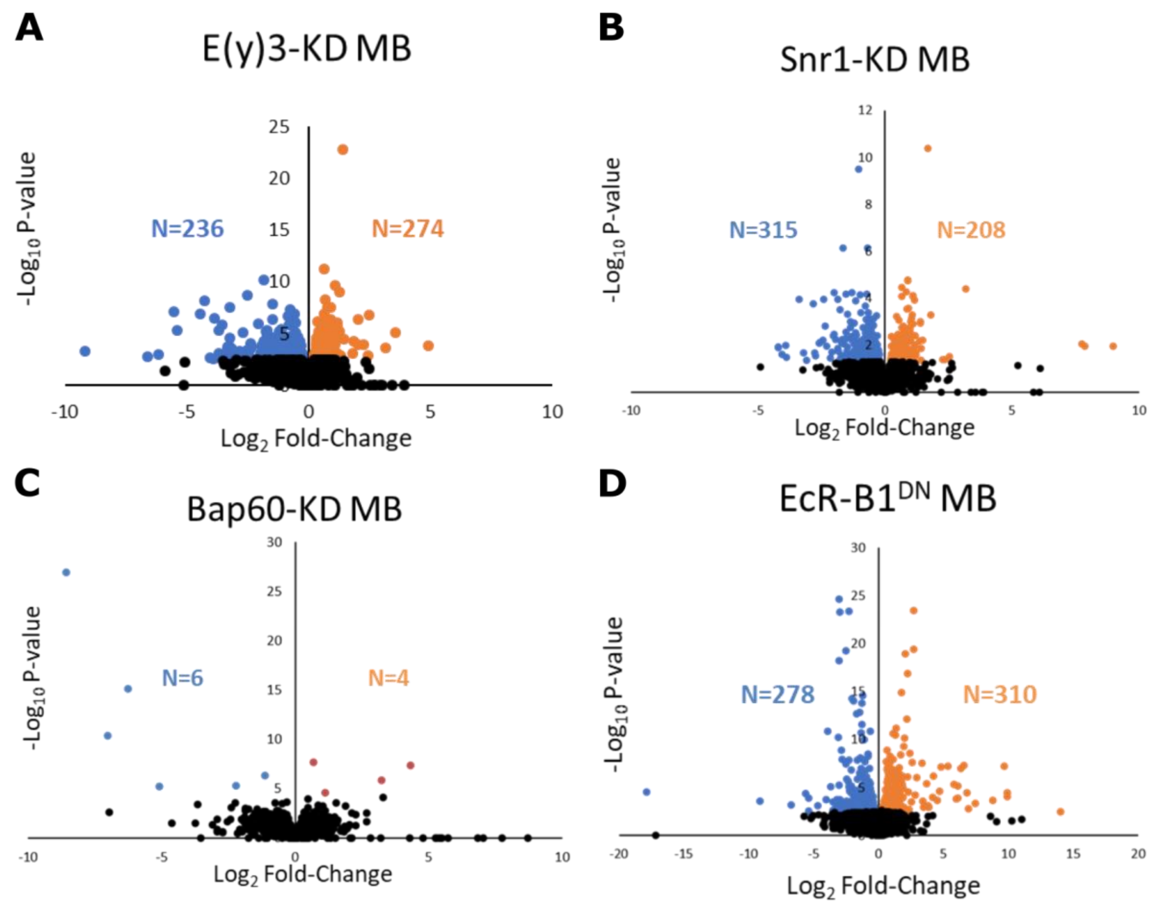

Figure 4.2 Visualization of differentially expressed genes in SWI/SNF-KD MB and EcR-B1^{DN} MB larvae.

Volcano plots showing differentially expressed genes between (**A**) E(y)3-KD MB and control, (**B**) Snr1-KD MB and control, (**C**) Bap60-KD MB and control, and (**D**) EcR-B1^{DN} MB and control. 8242 genes were used for differential expression analysis with differentially expressed genes (P_{adj}<0.05) represented in blue (downregulated) or orange (upregulated).

To investigate whether the SWI/SNF complex is involved in EcR-B1-mediated gene transcription and given that SWI/SNF has been shown to open chromatin to increase gene transcription (Kassabov et al., 2003), I compared genes that were downregulated in SWI-SNF-KD MB, and EcR-B1^{DN} MB samples (**Figure 4.3A**). In total, 165 genes were commonly downregulated between two or more of the three genotypes Snr1-KD, E(y)3-KD, and EcR-B1^{DN} (**Figure 4.3A**). Gene ontology (GO) enrichment analysis on these commonly regulated genes revealed enrichment of biological processes related to Toll signaling, circadian rhythm, proteasome-mediated catabolic process, and actomyosin structure organization (**Figure 4.3B**). The most highly enriched cellular component was the proteasome (**Figure 4.3C**). More specifically, 20 of the 60 proteasomal genes, a significant proportion, were found in the overlapping genes ($P = 2.67 \times 10^{-26}$; hypergeometric test), suggesting that both the SWI/SNF complex and EcR-B1 act upon proteasomal genes at the onset of pupation.

A

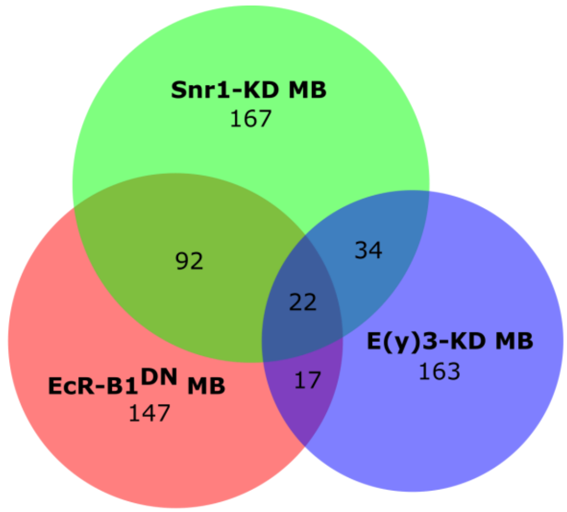

B

GO Biological Process	Fold Enrichment
Toll signaling pathway	25.10
Circadial rhythm	9.35
Proteasome-mediated ubiquitin-dependent protein catabolic process	8.99
Actomyosin structure organization	7.17
Anatomical structure development	1.66

C

GO Cellular Component	Fold Enrichment
Proteasome storage granule	86.04
Proteasome regulatory particle, base subcomplex	43.02
Proteasome regulatory particle, lid subcomplex	35.85
Proteasome core complex, alpha-subunit complex	23.47
Actin filament	10.43

Figure 4.3 Snr1, E(y)3, and EcR-B1 are required to activate proteasome gene transcription.

(**A**) Venn diagram showing overlap of genes downregulated in Snr1-KD MB, E(y)3-KD MB, and EcR-B1^{DN} MB. (**B-C**) Gene ontology enrichment analysis of the 165 genes overlapping in at least two conditions. Top five enriched hierarchical terms displayed for biological process (**B**) and cellular component (**C**).

4.3 The ubiquitin proteasome system is required for MBγ neuron pruning

Alyagor *et al*. (2018) found that the transcription of proteasome subunits is specifically activated in the MB at the onset of pupation. The average relative transcription of proteasome genes is downregulated in the MB when the dominant negative EcR-B1^{DN} is expressed, and when the RNAi knockdowns E(y)3-KD and Snr1-KD are expressed (**Figure 4.3**). To functionally validate the role of the proteasome subunits, I obtained fly lines with *UAS*-mediated RNAi against members of the ubiquitin proteasome system (UPS) that were downregulated in EcR-B1^{DN} MB and E(y)3-KD MB and Snr1-KD MB samples (**Appendix A**). I then imaged adult brains and analyzed confocal stacks to observe for γ-lobe pruning phenotypes, which were classified into four categories of pruning severity: normal, mild, moderate, and severe (**Figure 4.4A-D**).

Mushroom body-specific knockdown of several UPS genes resulted in defective γ-lobe pruning, leading to dorsal MBγ projections remaining present in the adult brain. Knockdown of *prosα2* (44560), *Rpn1* (34348), and *Rpt2* (34795) resulted in very strong and highly penetrant MBγ pruning phenotypes (*UAS-prosα2*^{44560}; P_{adj}=4.10x10^{-5}, *UAS-Rpn1*^{34348}; P_{adj}=1.51x10^{-3}, and *UAS-Rpt2*^{34795}; P_{adj}=2.81x10^{-4}) using only a single RNAi construct per gene (**Figure 4.4E**). Three UPS subunits exhibited a significant proportion of MBs with γ pruning phenotypes in one RNAi construct with the second RNAi construct exhibiting a trend. These included: *Uba1* (*UAS-Uba1*^{76066}; P_{adj}=1.51x10^{-3}, *UAS-Uba1*^{25857}; *P*=0.009), *Usp14* (*UAS-Usp14*^{66956}; P_{adj}=0.03, *UAS-Usp14*^{53262}; *P*=0.003), and *prosα3* (*UAS-prosα3*^{77145}; P_{adj}=4.99x10^{-2}, *UAS-prosα3*^{55217}; *P*=0.005). Several genes with two different RNAi constructs showed MBγ pruning phenotypes with only one of the two constructs. These included: *prosα4* (*UAS-prosα4*^{36063}; no significance, *UAS-prosα4*^{65161}; P_{adj}=3.05x10^{-3}), *prosα6* (*UAS-prosα6*^{34811}; no significance, *UAS-prosα6*^{53974}; P_{adj}=2.80x10^{-3}), *Rpn8* (*UAS-Rpn8*^{31567}; no significance, *UAS-Rpn8*^{35411}; P_{adj}=8.88x10^{-3}), *Rpn10* (*UAS-Rpn10*^{330448}; no significance, *UAS-Rpn10*^{34566}; P_{adj}=1.51x10^{-3}), *Rpt6R* (*UAS-Rpt6R*$^{105002\text{-}KK}$; no significance, *UAS-Rpt6R*^{34342}; P_{adj}=5.14x10^{-3}), and *Plap* (*UAS-Plap*^{31136}; no significance, *UAS-Plap*^{67871}; P_{adj}=1.15x10^{-3}) (**Figure 4.4E**). The discrepancy in MBγ pruning phenotypes between the two RNAi constructs may be due to differences in gene knockdown strength and it is worth noting that the knockdown efficiencies of the RNAi constructs used in this section have not yet been assessed. However, the high penetrance and severity of MBγ pruning phenotypes observed in UPS gene knockdowns demonstrate the requirement of UPS gene expression in the MB for γ neuron pruning processes.

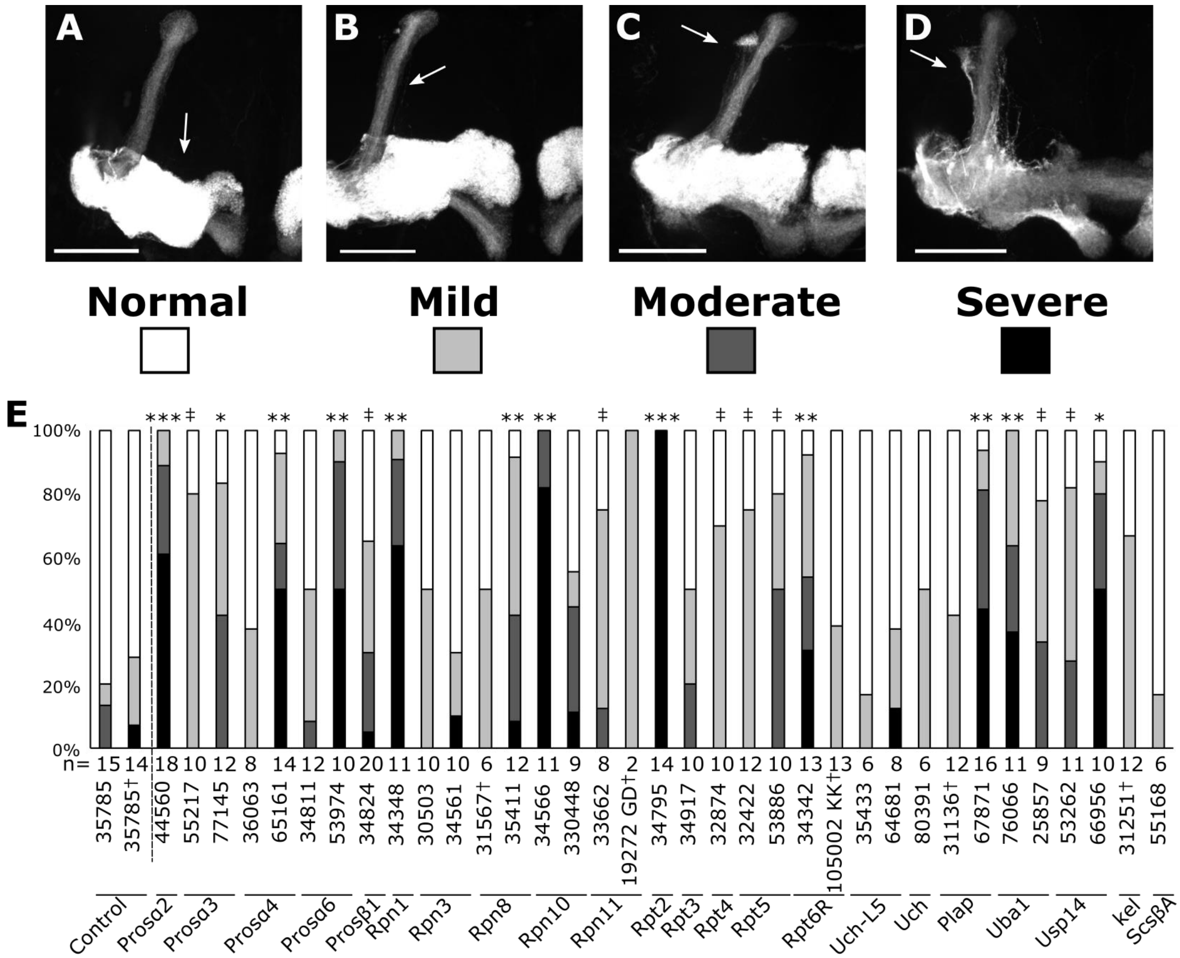

Figure 4.4 UPS components are required for MBγ neuron pruning

The MBγ neuron pruning phenotype was qualitatively classified into four categories: (**A**) normal MB morphology, as well as (**B**) mild, (**C**) moderate, and (**D**) severe forms of MBγ pruning phenotype. (**E**) Bar plot shows the total percentage of MBs exhibiting normal MB morphology (white), in addition to the mild (light grey), moderate (dark grey), and severe (black) forms of MBγ neuron pruning phenotype. The total number of MBs analyzed for each genotype is indicated below the bar plot in the row labeled "n". A Fisher's exact test (one-tailed) was used to compare the proportion of MBs exhibiting MBγ pruning phenotypes between each knockdown and the appropriate control (Bonferroni test for multiple comparisons). †Denotes RNAi lines that were co-expressed with *UAS-dcr2*. Asterisks indicate significance (*P_{adj}<0.05, **P_{adj}<0.01,***P_{adj}<0.001, ‡$P_{unadjusted}$<0.05).

4.4 The SWI/SNF complex is required for promoter accessibility in the MB at the onset of pupation

The SWI/SNF complex acts to shift the position of nucleosomes in chromatin, making DNA more accessible to facilitate transcriptional activation (Kassabov et al., 2003). Therefore, after observing that the SWI/SNF complex is required for transcription of genes critical for γ neuron pruning, I then assessed how chromatin accessibility was directly affected in the MB upon SWI/SNF subunit knockdown. To do this, I isolated MB nuclei from larval CNS using the INTACT protocol (see **Chapter 3**), followed by ATAC-sequencing (Buenrostro et al., 2016). I analyzed the MB-specific chromatin profiles in Bap60, Snr1, and E(y)3 knockdown larvae and compared them to those of control larvae. A total of 16,056 peaks representing regions of accessible chromatin (see **Chapter 2.8.2**) in 8,272 genes were found to be present in at least two of the eight samples analyzed. These peaks are potentially important for the regulation of gene transcription and are hereafter referred to as regulatory regions. Approximately 49% of all regulatory regions that were identified were annotated to promoter regions within 1kb of the transcriptional start site (TSS) of genes (**Figure 4.5**). The TSS regions are where transcription factor complexes must bind in order for gene transcription to be initiated, and therefore must be accessible in active genes. Additionally, approximately 13% and 11% were annotated to intronic and distal intergenic regions, respectively (**Figure 4.5**). These regions could potentially be gene enhancers – regions that act to regulate gene transcription over a great distance. The remainder of the regulatory regions that did not align to promoters or potential enhancer regions were annotated to exons and untranslated regions at a rate of less than two percent each (**Figure 4.5**).

To look for changes in accessibility between SWI/SNF knockdowns and controls, ATAC-Seq reads that aligned to the defined regulatory regions were analyzed using DESeq2 (Anders, 2014). Differentially accessible regions were defined as having an adjusted P value of <0.05 and were annotated using the ChIPseeker *annotatePeak* function with the *Drosophila* dm6 annotation package (BC & BP, 2019; Yu et al., 2015) (**Figure 4.5**; **Appendix E**).

Knockdown of E(y)3 resulted in 281 less accessible regions and 626 more accessible regions within 255 and 551 genes, respectively. Knockdown of Snr1 resulted in 803 less accessible and 619 more accessible regions within 690 and 619 genes, respectively. Finally, Bap60 knockdown resulted in 92 less accessible regions and 31 more accessible regions within 91 and 28 genes, respectively. In all SWI/SNF-KD MB samples, more than 75% of the regions that became less accessible were annotated within 1kb of the TSS (**Figure 4.5**) which is significantly greater than what would be expected by chance ($P<10^{-11}$; hypergeometric test). Conversely, less than 30% of the regions that became more accessible were annotated within those regions (**Figure 4.5**), which is significantly less than what would be expected by chance ($P<10^{-3}$; hypergeometric test). Given that less than nine percent of the regulatory regions analyzed were affected in any given SWI/SNF subunit knockdown, these results suggest that under normal conditions, the SWI/SNF complex preferentially targets TSS regions of a small subset of genes to open them up, making them more accessible to transcriptional machinery.

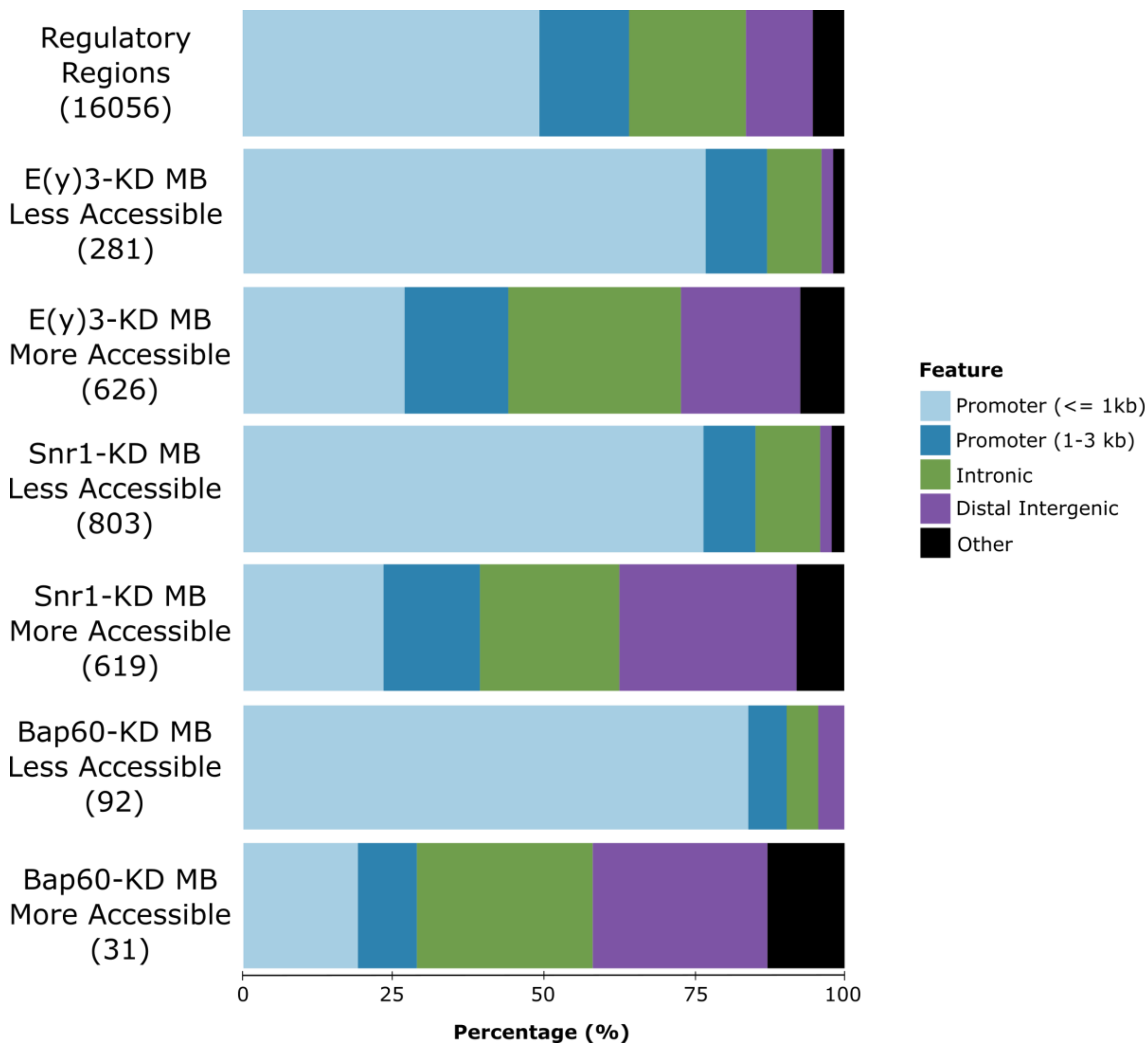

Figure 4.5 Annotation of differentially accessible regions in MB-specific SWI/SNF knockdown larvae.

Regulatory regions of chromatin that become more or less accessible upon the knockdown of SWI/SNF subunits compared to control. Top bar represents annotations of all regulatory regions analyzed. Over 75% of regions that are less accessible in SWI/SNF knockdowns are annotated to promoter regions within 1 kb of the TSS (light blue) whereas less than 30% of regions that become more accessible in SWI/SNF knockdowns are annotated to those regions.

After observing that TSS regions preferentially become less accessible in SWI/SNF knockdowns, I compared the genes that are less accessible in all SWI/SNF knockdowns. In total, 112 genes were found to be less accessible between two or more of the three SWI/SNF-KD MBs (**Figure 4.6A**). Gene ontology enrichment analysis was performed on these commonly regulated genes and although only 112 genes were analyzed, there was strong enrichment of biological process terms related to neuronal remodeling including "larval central nervous system remodeling", "axon target recognition", "induction of programmed cell death by ecdysone", and "regulation of neuron apoptotic process" (**Figure 4.6B**). These biological processes are relevant to processes governing MBγ neuron remodeling known to occur at the onset of metamorphosis. Additionally, 17 of the 23 significantly enriched molecular function terms were directly related to DNA binding and transcription factor activity (**Figure 4.6C**). These results suggest that the gene regulatory regions that become less accessible in SWI/SNF knockdowns regulate the expression of DNA binding proteins and transcription factors involved in neuronal remodeling.

A

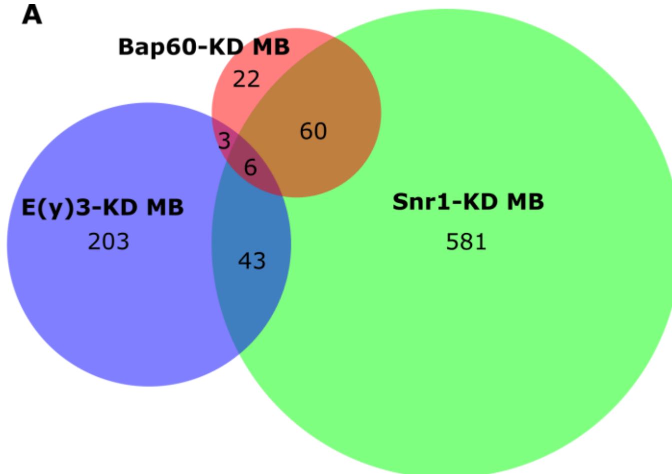

B

GO Biological Process	Fold Enrichment
Larval central nervous system remodeling	70.96
Cell dedifferentiation	42.58
Dedifferentiation	42.58
Negative regulation of DNA-binding transcription factory activity	38.71
Axon target recognition	32.75

C

GO Molecular Function	Fold Enrichment
Protein domain specific binding	10.78
DNA-binding transcription repressor activity, RNA polymerase II-specific	10.44
DNA-binding transcription repressor activity	10.44
Kinase regulator activity	10.14
Transcription factor binding	8.39

Figure 4.6 Comparison of genes that become less accessible in SWI/SNF knockdown.

(**A**) Venn diagram showing overlapping genes that are significantly less accessible in SWI/SNF knockdowns compared to controls. (**B**-**C**) Gene ontology enrichment of the 112 overlapping genes for biological process (**B**) and molecular function (**C**). Top five terms with at least three genes and an FDR corrected *P* value < 0.05 are displayed.

4.5 Identifying potential SWI/SNF targets

To identify the potential target genes regulated by the SWI/SNF complex for MBγ pruning, I compared genes that were less accessible in SWI/SNF-KDs to genes that were downregulated in SWI/SNF-KDs. Although there were few genes that were both less accessible and downregulated in respective SWI/SNF-KDs, there were still relevant candidate direct target genes of SWI/SNF subunits identified (**Appendix F**). No candidate target genes were identified for Bap60. A total of nine candidate target genes were identified in E(y)3-KD MBs (**Figure 4.8A**). These genes include *arouser* (*aru*), which encodes a protein that is involved in synapse regulation (Eddison et al., 2011), *Shroom* (*Shrm*) which is a MB-specific gene involved in actin cytoskeleton organization (Bolinger et al., 2010), and *CG6163*, an uncharacterized transcription factor which could have downstream effects on gene transcription related to MBγ pruning (**Figure 4.8C**). A total of 21 candidate target genes were identified in Snr1-KD MBs (**Figure 4.8B**). Gene ontology enrichment analysis of these genes revealed enrichment of biological process terms related to larval CNS remodeling, brain development, and ubiquitin-dependent protein catabolic process (**Figure 4.8D**). Candidate genes that are associated with larval CNS and brain development are *EcR-B1*, actin binding proteins encoded by *Ciboulot* (*Cib*) and *chickadee* (*chic*), and *homothorax* (*hth*), a gene encoding a homeobox transcription factor involved in neurodevelopment (Nagao et al., 2000). Furthermore, genes that are required for ubiquitination of proteins – a process that signals proteins for degradation by the proteasome – were identified as potential target genes of Snr1 (**Figure 4.8D**). Taken together, these results suggest that the SWI/SNF complex is directly required to increase the accessibility and therefore transcription of genes crucial to MBγ pruning, including *EcR-B1*, at the onset of pupation. Transcriptional activation of these genes is required for downstream activation of proteasome gene transcription, which is required for MBγ pruning.

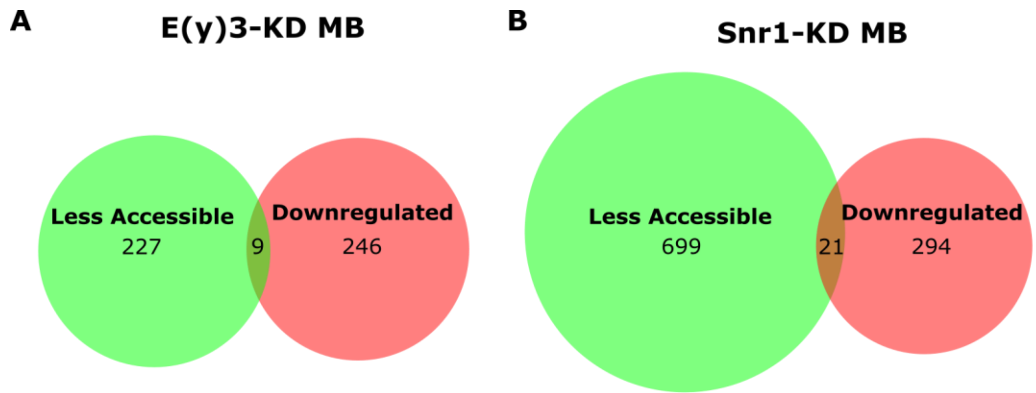

Candidate Target Genes

C

Gene	Associated GO Term
aru	Regulation of synapse structure or activity
Shrm	Actin cytoskeleton organization
CG6163	Transcription factor complex
ckd *CG6175* *CG9747* *Lmpt* *magu* *Fhos*	Other

D

Gene	Associated GO Term
EcR-B1 *Cib* *chic*	Larval CNS/Brain Development
hth	Brain Development
Ube3a *UbcE2H* *Ubr1* *CG11658* *TER94 orthologue*	Ubiquitin-dependent protein catabolic process
MESR6 *lncRNA:CR43857* *AMPdream* *CG2865* *CG5953* *CG9663* *Awh* *chm* *NAT1* *CG45050* *Svil* *lncRNA:CR43334*	Other

Figure 4.7 Identification of potential direct target genes of the SWI/SNF complex. (**A-B**) Venn diagrams showing overlapping genes between genes found to be less accessible and downregulated genes in E(y)3-KD MBs (**A**) and Snr1-KD MBs (**B**). (**C-D**) Candidate target genes and their associated GO terms from (**C**) E(y)3-KD MBs and (**D**) Snr1-KD MBs. No potential target genes were identified for Bap60-KD MBs.

Chapter 5

5 Investigating the role of the core SWI/SNF subunit, Bap60, in the adult mushroom body

Parts of this chapter are published in Nixon et al, 2019.

In Chapter 4, I established a role for the SWI/SNF complex in mushroom body (MB) development. Knockdown of SWI/SNF subunits resulted in aberrant expression of genes critical to MBγ neuron pruning. Previous studies have shown that MBγ remodeling is important for short-term memory (STM) to occur, but not long-term memory (LTM) (Redt-Clouet et al., 2012). An RNAi screen on SWI/SNF subunits was recently performed in our lab (Chubak et al., 2019) and a role for the SWI/SNF complex was seen in both STM and LTM, with the knockdown of the core SWI/SNF subunit, Bap60, demonstrating the greatest relative deficits in memory. Additionally, a temperature sensitive GAL80-mediated adult-specific knockdown of Bap60 resulted in deficiencies in courtship memory (Nixon et al., 2019), suggesting a role for the SWI/SNF complex in adult MB neurons.

Long-term memory is a transcription-dependent process that requires *de novo* gene transcription and translation in order to form lasting changes in synaptic strength (Hirano et al., 2016; Zovkic et al., 2016). Short-term memory, on the other hand, requires that all necessary proteins are present in the cytoplasm and at the appropriate levels for immediate post-translational modifications upon activation of the neuron (Blum et al., 2009; Dunning & During, 2003). In both cases, the neurons must be ready for activation – a state that is determined by the current or past gene expression profile of the cell. Given that SWI/SNF complex subunits have been shown to be required for both STM and LTM, I hypothesized that the SWI/SNF complex is required for the maintenance of neuronal cell identity in the adult MB. To test this hypothesis, the transcriptomes of MB neurons in flies expressing an RNAi knockdown of Bap60 in the MB (Bap60-KD MBs) and control flies expressing an RNAi targeting mCherry, which is not in the *Drosophila* genome, were analyzed at two different time points: juvenile adult (0-3 hours after eclosion) and mature adult (1-5 days after eclosion) to observe for changes in cell type-specific gene transcription.

5.1 Bap60 is required for the expression of neuron-specific genes during a critical period of juvenile adult MB development

The nuclei from MB neurons in juvenile and mature adult flies were isolated using INTACT, RNA was extracted from these MB nuclei, and the effect of Bap60 knockdown on gene expression was determined. In juvenile adult insects, the MB undergoes a period of development and synaptogenesis in the first hours after eclosion (Barth & Heisenberg, 1997; Barth et al., 1997; Doll & Broadie, 2015; Doll & Broadie, 2014; Doll et al., 2017; Jones et al., 2013; Seugnet et al., 2011). During this time, neuronal connections that are critical for normal learning and memory later in life are formed (Doll & Broadie, 2014; Seugnet et al., 2011). The MB-specific transcriptome in Bap60-knockdown flies was compared to controls in early juvenile adults (0-3 hours after eclosion), and mature adults (1-5 days after eclosion).

There was a greater effect of Bap60 on gene expression at the juvenile stage than in the mature adult MB (**Figure 5.1 A and B**). Comparing the transcriptomes of juvenile Bap60-KD MBs and controls yielded 416 differentially expressed genes (P_{adj} <0.05 and a >1.5 fold-change), of which 156 were upregulated and 260 were downregulated (**Figure 5.1 A**; **Appendix G**). In contrast, only 68 differentially expressed genes (29 upregulated and 39 downregulated) were observed in mature Bap60-KD MBs (**Figure 5.1 B**; **Appendix G**). The differential expression of several genes was confirmed by RT-qPCR in independent biological replicates (**Appendix K**, *Ldh, sls, dysf,* and *tmod*). I performed GO enrichment analysis to investigate the functions of the differentially expressed genes. Differentially expressed genes from the mature MB showed very little GO enrichment. GO enrichment analysis of the upregulated genes from the juvenile MB revealed many terms related to muscle, such as “myofibril assembly” and “sarcomere organization”. GO enrichment analysis of downregulated genes in the juvenile MB revealed neuron-related terms such as “neurotransmitter metabolic process”, “synaptic vesicle”, and “regulation of synaptic plasticity”, as well as developmental terms, such as “nervous system development” and “anatomical structure development”. This suggested an important role for Bap60 in the regulation of neurodevelopmental genes in the early juvenile adult MB.

Having observed a downregulation of neuron-related genes and an upregulation of muscle-related genes in juvenile Bap60-KD MBs, I reasoned that Bap60 might be required at this stage to activate the expression of genes that contribute to MB cell identity. To test this, I used existing tissue-specific RNA-seq data to establish a list of 904 “neuron-specific genes” that are enriched in heads compared to other tissues (Brown et al., 2014), and 118 “MB-specific genes” that are enriched in MB-specific INTACT samples compared to whole-head samples (**Figure 3.4**) (**Appendix C**). Of the 260 genes that are downregulated in juvenile Bap60-KD MBs, 78 are neuron-specific and 31 are MB-specific; these numbers are significantly greater than those expected by chance ($P < 10^{-25}$, hypergeometric test) (**Figure 5.1 C**). In contrast, muscle-specific genes (enriched in carcass compared to other tissues) were not significantly over-represented among genes that were downregulated in Bap60-KD MBs. On average, MB and neuron-specific genes are expressed at a consistent level in juvenile and mature control MBs. But in Bap60-KD MBs at the juvenile stage, they have reduced expression that recovers to normal levels in mature adults (**Figure 5.1 D**). These trends were validated by RT-qPCR for a selection of genes in an independent experiment (**Appendix K**, *prt* and *jdp*). These results suggest that Bap60 plays a stage-dependent role in activating the expression of neuron-specific genes in the juvenile MB.

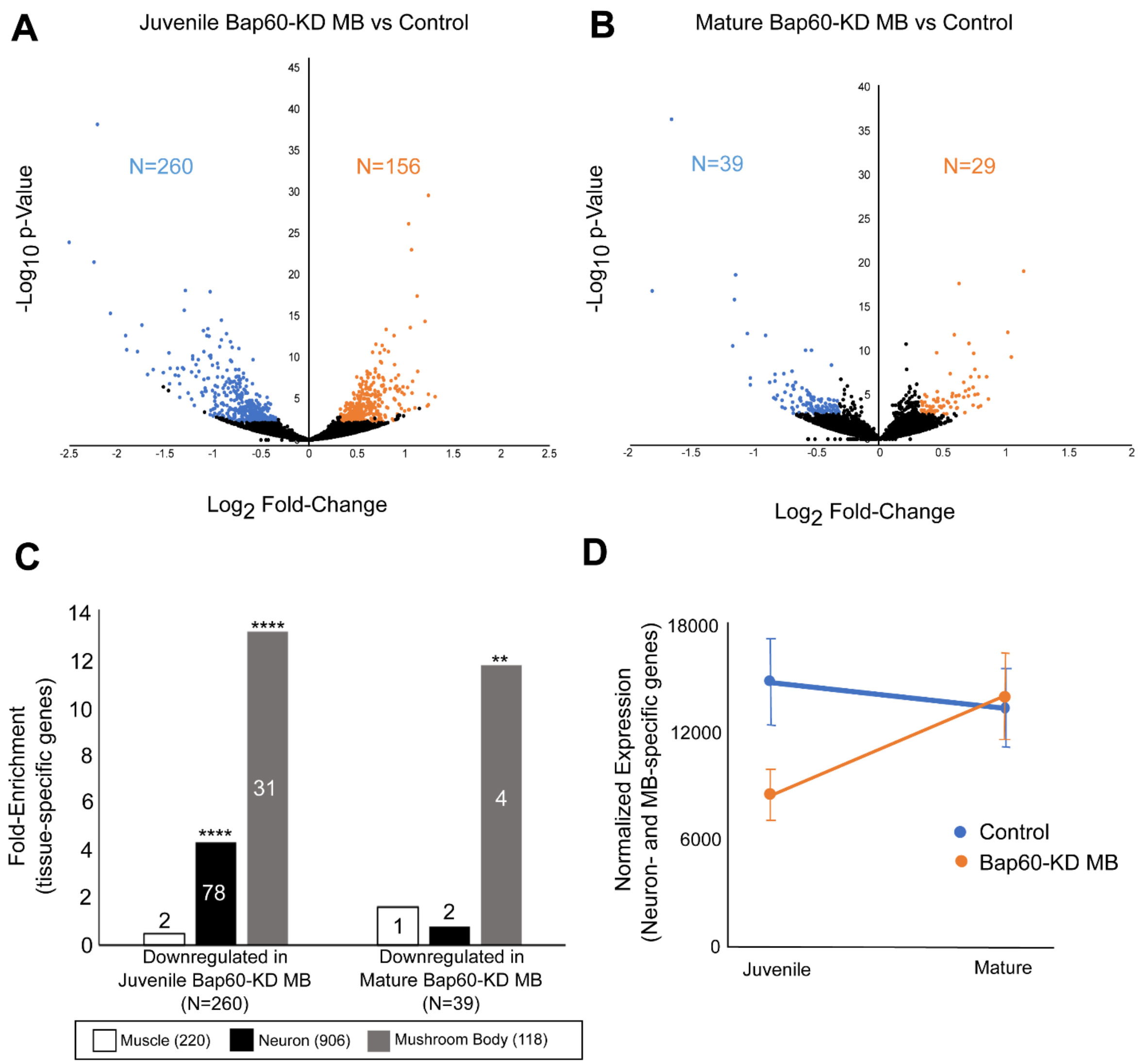

Figure 5.1 Bap60 is required for the expression of neuron-specific genes in the juvenile MB.

(**A** and **B**) Volcano plots showing differentially expressed genes (P_{adj}<0.05 and >1.5 fold-change) represented in blue (downregulated) or orange (upregulated) in (**A**) juvenile Bap60-KD MBs and (**B**) mature Bap60-KD MBs compared to controls of the same age. (**C**) Fold enrichment of muscle-, neuron-, and mushroom body-specific genes (Brown *et al.*, 2014, and Chapter 3) among downregulated genes in juvenile and mature Bap60-KD MBs (** *P*<0.01; **** *P*<0.0001; hypergeometric test). The number of genes in each category is indicated. (**D**) Average normalized expression (±SEM) of neuron- and mushroom body-specific genes in control (blue) and Bap60-KD MB (orange) flies at the juvenile and mature stages.

5.2 Bap60 is required for the expression of developmental genes that are preferentially activated in the juvenile MB

The GO enrichment analysis of genes that are downregulated in Bap60 knockdowns revealed many terms related to neuronal processes and development. I reasoned that Bap60 might be required for the activation of key genes that are involved in experience-dependent MB-development in juvenile adults (Doll & Broadie, 2014; Tessier & Broadie, 2008). To test this, I performed differential expression analysis comparing the MB-specific transcriptome in early juvenile adults to that in mature adults (**Figure 5.2 A**; **Appendix H**). In controls, 549 genes were significantly increased by 2-fold or more in the juvenile adult MB compared to in that of mature adults. Of these 549 juvenile enriched MB genes, 385 genes were also >2-fold enriched in Bap60-KD MBs, but 164 were not (**Figure 5.2 A**). On average, these 164 genes showed significantly lower expression in juvenile Bap60-KD MBs compared to in controls (P=0.047; t-test), suggesting that the extent to which these genes are induced in juvenile Bap60-KD MBs is not as efficient as controls (**Figure 5.2 B**). These expression trends were validated for a selection of genes in an independent RT-qPCR experiment (**Appendix K**). Interestingly, the 164 juvenile induced genes that are not induced in Bap60-KD MBs show a strong GO enrichment for terms related to development and immune response (**Figure 5.2 C**). In contrast, the 385 genes that show juvenile enrichment in both Bap60-KD and control MBs show very little GO enrichment. This suggests that Bap60 is required for the activation of developmental genes during a critical period when the juvenile adult MB needs to establish experience-dependent synaptic connections that are required for normal learning and memory throughout life (Barth & Heisenberg, 1997; Barth et al., 1997; Doll & Broadie, 2015; Doll & Broadie, 2014; Doll et al., 2017; Jones et al., 2013; Seugnet et al., 2011).

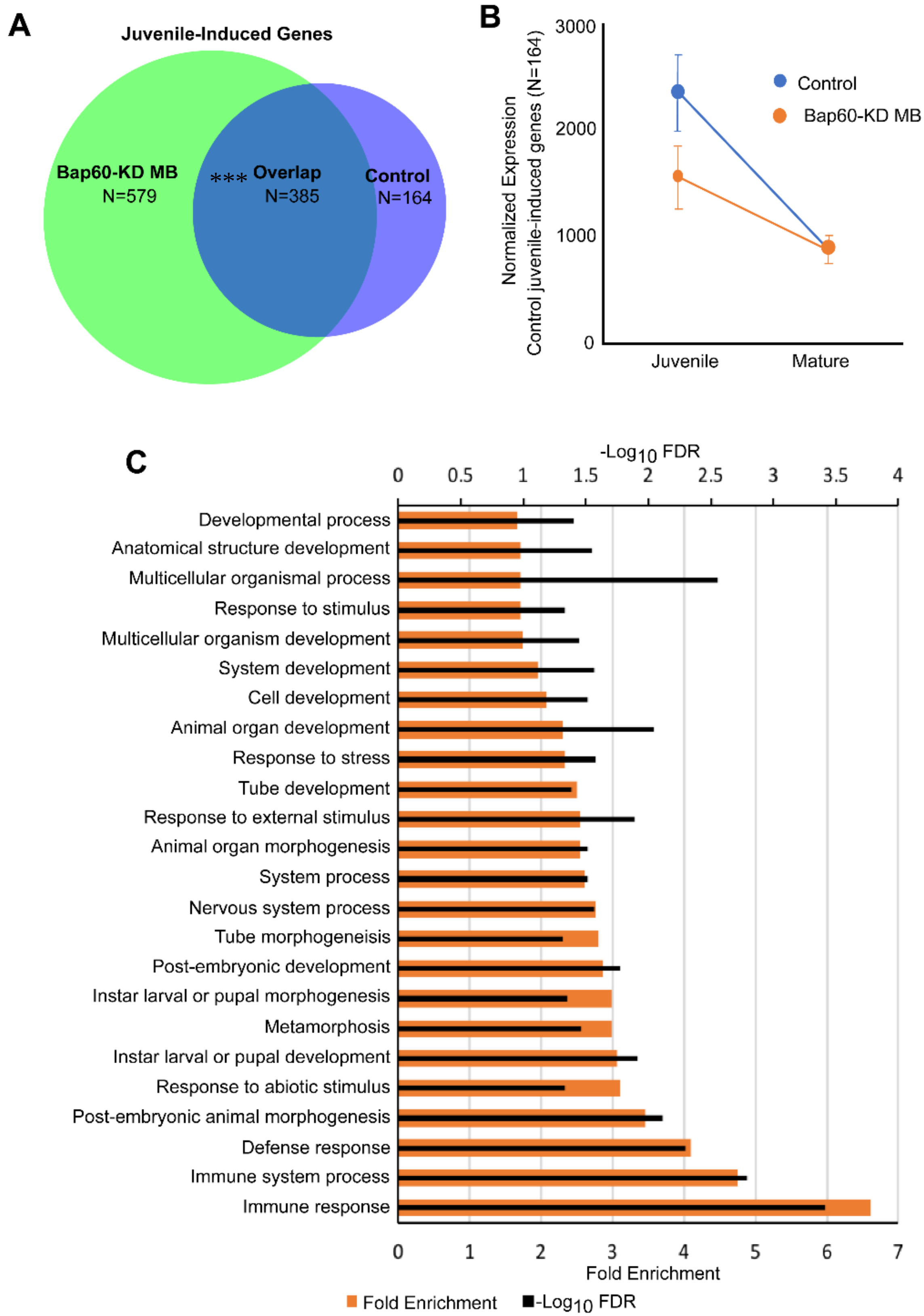
A
Juvenile-Induced Genes
Bap60-KD MB
N=579
*** Overlap
N=385
Control
N=164
B
Normalized Expression
Control juvenile-induced genes (N=164)
3000
2000
1000
0
Control
Bap60-KD MB
Juvenile
Mature
C
-Log10 FDR
0
0.5
1
1.5
2
2.5
3
3.5
4
Developmental process
Anatomical structure development
Multicellular organismal process
Response to stimulus
Multicellular organism development
System development
Cell development
Animal organ development
Response to stress
Tube development
Response to external stimulus
Animal organ morphogenesis
System process
Nervous system process
Tube morphogeneisis
Post-embryonic development
Instar larval or pupal morphogenesis
Metamorphosis
Instar larval or pupal development
Response to abiotic stimulus
Post-embryonic animal morphogenesis
Defense response
Immune system process
Immune response
0
1
2
3
4
5
6
7
Fold Enrichment
Fold Enrichment
-Log10 FDR

Figure 5.2 Bap60 is required for the increased expression of developmental genes in the juvenile MB.

(**A**) Venn diagram showing overlapping genes that are significantly increased in expression in the juvenile MB compared to in the mature MB (juvenile-induced genes) in control and Bap60-KD MB flies. ***$P<10^{-336}$, hypergeometric test. (**B**) Average normalized expression (±SEM) of the 164 genes that are induced in the juvenile MB in controls only. (**C**) Gene ontology enrichment for biological processes of the 164 juvenile-induced genes identified in controls only. Terms with at least ten genes and an FDR corrected $P<0.05$ are displayed.

5.3 Bap60 is required for TSS accessibility in the Juvenile MB

After observing a stage-specific role for Bap60 in the expression of developmental genes in the juvenile MB, I then wanted to assess how chromatin structure was affected in Bap60-KD MBs in both juvenile and mature flies. To do this, MB nuclei were isolated from adult brains using INTACT, followed by ATAC-sequencing in juvenile and mature flies in both Bao60-KD MBs and controls (n=2 for each). A total of 26,244 ATAC-Seq peaks were identified in at least two samples and these were defined as candidate regulatory regions (see **Chapter 2.8.2**). Approximately 42% of all regulatory regions that were identified were annotated to promoter regions within 1kb of the TSS of genes (**Figure 5.3A**). Additionally, approximately 18% and 14% were annotated to intronic and distal intergenic regions, respectively (**Figure 5.3A**). These regions could potentially be gene enhancers that regulate the transcription of genes over a great distance. The remainder of regulatory regions that did not align to promoters or potential enhancer regions were annotated to exons and untranslated regions at a rate of less than 7% each (**Figure 5.3A**).

To look for changes in accessibility between juvenile and mature Bap60-KD MBs and controls, ATAC-seq reads that aligned to the defined regulatory regions were analyzed using DESeq2. Differentially accessible regions were defined as having an adjusted p-value of <0.05 and were annotated using the ChIPseeker *annotatePeak* function with the *Drosophila* dm6 annotation package (BC & BP, 2019; Yu et al., 2015) (**Figure 5.3A**; **Appendix I**). By comparing changes in chromatin accessibility at two different time points in both Bap60-KD MBs and controls, the plasticity of chromatin accessibility can be assessed in each of the genotypes.

In controls, 2,324 regulatory regions in 1,884 genes were found to be more accessible in the juvenile MB when compared to mature and approximately 76 % of these regions were annotated within 1kb of the TSS. Conversely, only 203 regions were found to be more accessible in the mature MB in controls, and only about 30% of these regions were annotated within 1kb of the transcription start site (TSS) (**Figure 5.3A**). These results suggest that in wild-type flies, chromatin near the TSS is more accessible during the juvenile period of experience-dependent synaptic plasticity in the juvenile MB.

Of the 1,884 genes that were more accessible in juvenile controls MBs compared to mature, only 90 were also more accessible in juvenile Bap60-KD MBs (**Figure 5.3B**). In controls, these genes become less accessible in mature flies compared to juvenile, however in Bap60-KD MBs, these regions maintain a constant accessibility (**Figure 5.3C**). This suggests that Bap60 is required for plasticity of TSS accessibility in the adult MB.

Gene ontology enrichment analysis of the juvenile accessible genes revealed enrichment of biological processes related to neuroplasticity, such as “neuron projection regeneration”, “regulation of axon extension involved in axon guidance”, “axon extension”, and “neuron remodeling”. Additionally, there was enrichment of MB-related terms such as “mushroom body development”, “cellular response to dopamine”, and “long-term memory”. Molecular function GO enrichment analysis gave strong enrichment of terms related to DNA binding and gene transcription, such as “transcription cofactor binding”, “RNA polymerase II transcription factor binding”, and “nuclear receptor activity”. Additionally, molecular function terms related to MB activity such as “3’,5’-cyclic-nucleotide phosphodiesterase activity” and “voltage-gated cation channel activity” were also found to be enriched. Taken together, these results suggest that Bap60 is required for the plasticity of TSS accessibility of genes regulating MB and neuroplasticity functions during a critical period of synaptic plasticity (Barth & Heisenberg, 1997; Barth et al., 1997; Doll & Broadie, 2015; Doll & Broadie, 2014; Doll et al., 2017; Jones et al., 2013; Seugnet et al., 2011).

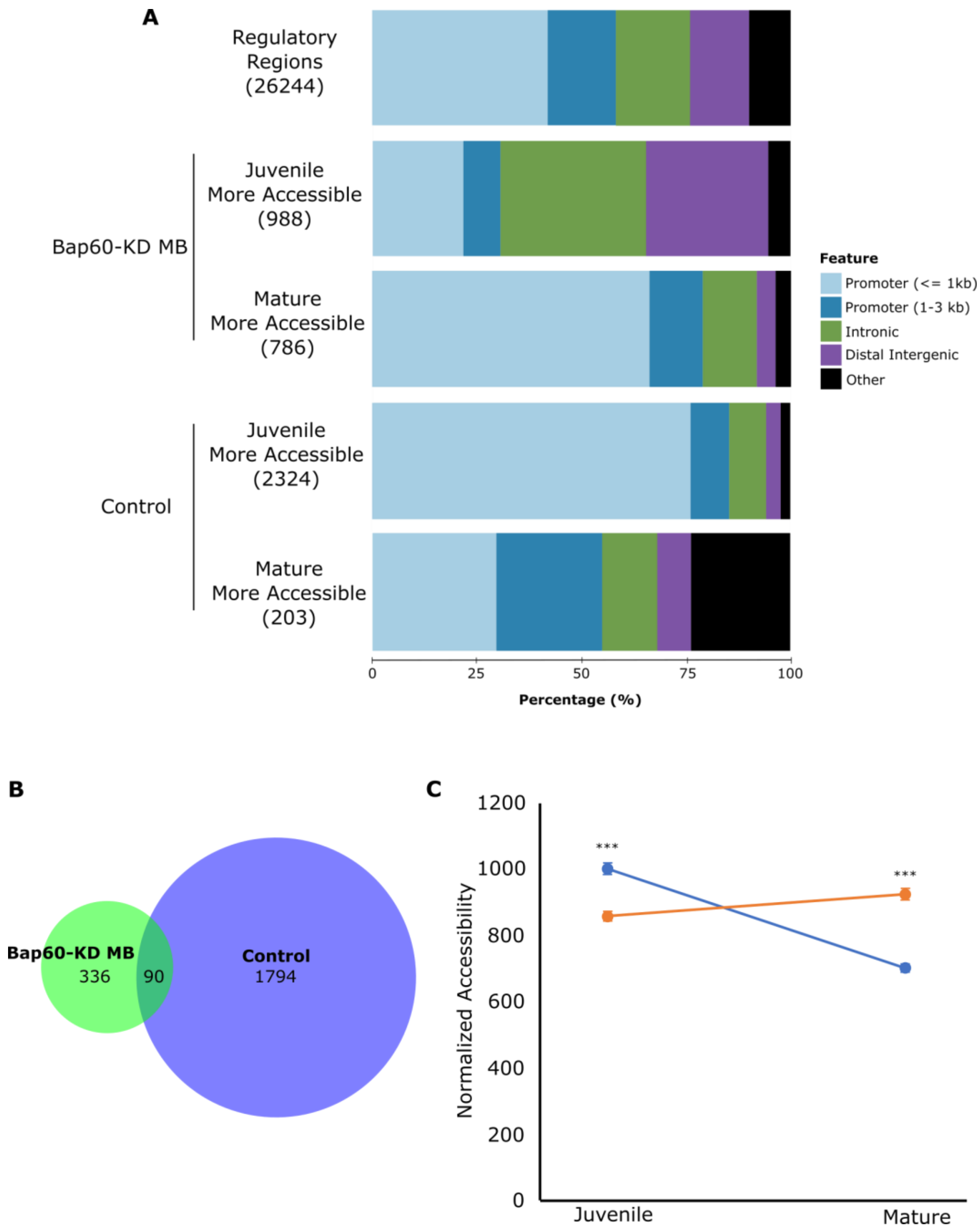

Figure 5.3 Bap60 is required for TSS accessibility in the juvenile MB.

(**A**) Annotations of all regulatory regions that were analyzed (top bar) and differentially accessible regulatory regions between juvenile and mature Bap60-KD MB and control flies. (**B**) Venn diagram showing overlapping genes that are significantly increased in accessibility in the juvenile MB compared to in the mature MB in control and Bap60-KD MB flies. (**C**) Average normalized accessibility (±SEM) of the 1,794 genes that are more accessible in the juvenile controls only. ***$P<10^{-8}$ t-test.

5.4 Identifying potential direct gene targets of Bap60 in the juvenile MB

Using transcriptome analysis, I identified a stage-specific role for Bap60 in the juvenile MB. In these analyses, I identified genes that were downregulated in juvenile Bap60-KD MBs compared to juvenile controls that showed enrichment of neuron- and MB-specific genes (**Figure 5.1C**), hereafter referred to as cell-identity genes. Furthermore, I identified developmental genes that were not efficiently induced in juvenile Bap60-KD MBs (**Figure 5.2**), hereafter referred to as juvenile-induced genes. Using ATAC-seq analyses, I also identified genes that demonstrated reduced plasticity in TSS accessibility in the adult MB in Bap60-KD MBs (**Figure 5.3**). I compared these three groups to identify genes that demonstrated both reduced transcription and plasticity in TSS accessibility and are therefore potential direct target genes of Bap60 (**Figure 5.4A**). In total, 70 genes were identified as potential Bap60 targets (**Appendix J**). Gene ontology enrichment analysis of these genes revealed enrichment of biological processes related to development, neurogenesis, and response to stimuli (**Figure 5.4B**). These results suggest that Bap60 is required for the expression of genes involved in neurodevelopment and stimulus response during the window of experience-dependent synaptic plasticity in the juvenile MB.

Candidate genes that are associated with both development and stimulus response include *forked end* (*fend*), a gene encoding a transmembrane protein involved in axon guidance (Umemiya et al., 2002), *calmodulin* (*Cam*), a gene encoding a calcium binding protein essential for calcium-mediated signaling in neurons and axon guidance (Gaudet et al, 2011; Marrone et al., 2014), and *Dichaete* (*D*), a gene encoding a transcription factor involved in brain development and axon guidance (Melnattur et al., 2013; Sánchez-Soriano & Russell, 2000). Other promising candidates that are involved in stimulus response include *Dopamine 1-like receptor 1* (*Dop1R1*), a MB-specific gene required for olfactory learning and memory (Seugnet et al., 2008; Selcho et al., 2009), and *Dopa decarboxylase* (*Ddc*), a gene whose product has been shown to be involved in memory processes (Chen et al, 2012; Lee et al., 2011). Other developmental genes that are candidate Bap60 targets include *Distal-less* (*Dll*), a gene encoding a homeodomain transcription factor involved in MB development (Plavicki et al., 2012) and *klumpfuss* (*klu*), a gene encoding a transcription factor involved in neurogenesis (Xiao et al., 2012). Interestingly, the MB-specific gene Hr38 was identified as a candidate Bap60 target gene, suggesting that Bap60 is required for the accessibility and transcription of this activity-induced gene during periods of neuronal plasticity. Finally, the gene encoding the actin-binding protein, Ciboulot (Cib), involved in neurodevelopment (Boquet et al., 2000a), was identified as a potential direct target of Bap60. *Cib* was also identified as a potential direct target gene of the core SWI/SNF subunit, Snr1, in the MB of late 3rd instar larvae (**Chapter 4.5**). Previous research has shown that *Cib* mutants have morphological defects in the MB (Boquet et al., 2000a; Boquet et al., 2000b), and taken together with these results suggests that SWI/SNF-mediated transcription of *Cib* may be important for proper neuronal wiring. Here, I have shown that knockdown of Bap60 in the MB results in both reduced TSS plastcitiy and reduced transcription of genes involved in neurodevelopment and stimulus response. These results suggest that the SWI/SNF chromatin remodeling complex directly targets these genes during a critical time window of neuronal wiring in the juvenile adult brain, when synaptic connections that are required for learning and memory are formed.

A

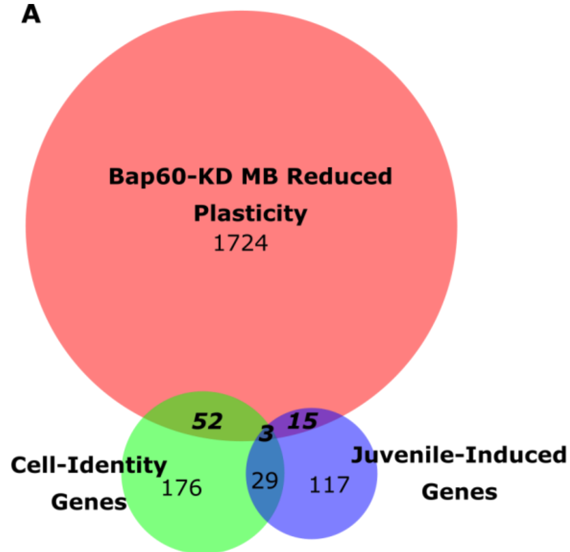

B

GO Biological Process	Fold-Enrichment
Response to abiotic stimulus	4.73
Post-embryonic animal morphogenesis	4.70
Instar larval or pupal development	4.27
Post-embryonic development	3.81
Neuron differentiation	3.40
Response to external stimulus	3.18
Generation of neurons	3.17
Nervous system development	3.12
Anatomical structure morphogenesis	3.06
Neurogenesis	3.03

C

Selected Candidates

Gene	Associated GO term
fend *Cam* *D*	Response to stimulus/ Nervous system development
Dop1R1 *Ddc* *Hr38*	Response to stimulus
Dll *klu* *Cib*	Nervous system development

Figure 5.4 Identification of potential direct gene targets of Bap60.

(**A**) Venn diagram showing overlapping genes between genes that show reduced plasticity in accessibility in Bap60-KD MBs, genes that are downregulated in the juvenile Bap60-KD MB compared to juvenile control (cell-identity genes), and genes that are induced in the juvenile control MB only when compared to mature. (**B**) Gene ontology enrichment analysis of the 70 overlapping genes. Top ten enriched biological process terms with more than 10 genes per term. (**C**) Selected candidate target genes of Bap60. and their associated GO term.

Chapter 6

6 Discussion

In this study, I have established and used cell-type specific methods to identify genes regulated by the SWI/SNF chromatin remodeling complex in the memory forming neurons of the *Drosophila* MB. Results revealed that the SWI/SNF complex is critical for regulating genes that are essential to processes occurring at the important life transitions from larvae to pupae, and from pupae to adults. Using MB-specific RNA-Seq and ATAC-Seq, I have identified key genes regulated by the SWI/SNF complex that are required for MBγ axon pruning during the early hours of pupation, and that are required for a critical window of experience-dependent synaptic plasticity in juvenile adult flies.

6.1 INTACT provides novel insight into the MB-specific transcriptome

In this project, I established and used the INTACT method to isolate MB nuclei from both the larval CNS and adult heads and analyzed the MB-specific transcriptomes. Using this method, I was able to identify a number of genes in both the larval and adult MB that are known to be highly expressed, including *Oamb, ey, rut, toy,* and *prt* (Brooks et al., 2011; Kurusu et al., 2000; Livingstone et al., 1984; Noveen et al., 2000) and enrichment of processes known to occur in the MB. These processes include anesthesia-resistant memory, olfactory learning, and cAMP-mediated signaling (**Figure 3.4D**; Aso et al., 2014; Blum et al., 2009; Keleman et al., 2012; Zhang et al., 2015). Interestingly, there were more than three times the number of MB-specific expressed genes in the larval MB than in the adult MB (**Figure 3.4C**), and more than half of the MB-specific genes in the adults were also enriched in the larval MB. These results are consistent with previous studies that demonstrate that the MBγ neurons play a much larger role in the larval MB than in the adult (Lee et al., 1999; Pauls et al., 2010). During the larval stages, the γ neurons are the only neurons present in the MB, and are therefore responsible for all of the MB-related processes occuring at that time (Lee et al., 1999; Pauls et al., 2010). During pupation, the MBγ neurons undergo extensive remodeling, and adult-specific lobes are formed (Lee et al., 1999), suggesting a switch in roles of the MBγ neurons. Furthermore, the newly formed α/β and α’/β’ lobes are required for LTM and memory consolidation, respectively, wherease the adult γ lobes are required for STM (Krashes et al., 2007; Montague & Baker, 2016; Trannoy et al., 2011). This switch in function to more specialized role in the adult MB could explain the differences in MB transcriptomes between larvae and adults (**Figure 3.4**). In addition to terms related to learning and memory and cAMP-mediated signaling, there is enrichment of terms related to neurotransmitter secretion and transport as well as calcium ion regulation in larval MB genes (**Figure 3.4D**). These terms are related to active neurons forming and strengthening synaptic connections (Bliim et al., 2016).

The transcriptome analyses I performed not only identified enrichment of canonical MB-specific genes, but it also identified several potential novel MB-specific genes. Among these novel MB-specific genes are *Ldh, MFS3* and *Hr38*. Ldh is a metabolic enzyme that converts lactate into pyruvate and is required to shift metabolic programming from aerobic glycolysis in neuroblasts to oxidative phosphorylation in post-mitotic neurons (Magistretti & Allaman, 2015; Zheng et al., 2016). Adult neurons almost exclusively use oxidative phorphosrylation to meet their high energy demands, and it has been hypothesized that lactate can be used for pyruvate production in neurons instead of glucose (Duka et al., 2014; Magistretti & Allaman, 2015). Several studies have shown that astrocyte-derived lactate is important in memory formation in chickens and rodents (Gibbs et al., 2006; Newman et al., 2011). Furthermore, in response to training, the *Drosophila* MB neurons experience increased energy metabolism relying on oxidative phosphorylation (Plaçais et al., 2017). Given that *Ldh* is a highly enriched gene in the MB, and that lactate can be used as a neuronal energy source, Ldh is likely crucial for proper MB functioning. Lactate metabolism may be important in LTM formation, not only to meet the high energy demands of the neuron, but also because the switch from glucose to lactate as an energy source could spare glucose for other purposes such as synapse formation and strengthening during long-term potentiation (Segarra-Mondejar et al., 2018; Goyal & Raichle, 2013).

MFS3 is a predicted transmembrane transporter of amino acids, nucleotides, and organic anions and is orthologous to the mammalian SLC17A5 transporter of acidic sugars and organic anions (Verheijen et al., 1999). Although its function in *Drosophila* remains unknown, its high enrichment in the MB suggests it may be important in shuttling molecules crucial to MB functions, such as sialic acid – an acidic sugar important for proper brain development (Schnaar et al., 2014) and even lactate.

Another novel MB-specific gene, *Hr38*, encodes a transcription factor whose transcription has been shown to be induced in activated neurons (Chen et al., 2016; Crocker et al., 2016; Croset et al., 2018). Recently, Croset et al. (2018) showed that neuron activity regulated genes, including *Hr38*, have higher levels of transcription in the MBγ neurons compared to the rest of the *Drosophila* brain. Furthermore, *Hr38* expression in males has been shown to be induced specifically in the MB in response to exposure to females and ethanol, where it is believed that genes regulated by Hr38 affect behavioural responses (Adhikari et al., 2018; Crocker et al., 2016; Jones et al., 2018).

Although the expression of these novel MB genes was not affected in the SWI/SNF subunit knockdowns in the late 3rd instar larvae, they were affected in the adult Bap60-KD MB. For instance, both *Ldh* and *MFS3* were downregulated in Bap60-KD MBs at both the juvenile and mature stages when compared to their respective controls. Additionally, *Hr38* was identified as a candidate Bap60 target gene in the juvenile MB, suggesting that these genes may be important in proper adult MB function. Some members of our lab have begun investigating the role of both Ldh and Hr38 in the MB. Preliminary results have indicated that both genes may be required for long-term memory using a courtship conditioning assay (*unpublished data*). Although promising, further investigation into the functions of these genes is required to make stronger conclusions as to their specific roles in the MB.

6.2 SWI/SNF complex is required for γ lobe pruning

During pupation, *Drosophila* MBγ neurons undergo remodeling processes whereby the larval γ lobes are pruned to the peduncle and re-extend in only the medial direction to form adult γ lobes (**Figure 1.5**). Previously, the SWI/SNF complex was implicated in γ neuron remodeling, yet whether SWI/SNF was required for pruning or re-extension processes was unknown. In this project, I have demonstrated that the SWI/SNF complex is required specifically for MBγ pruning (**Figure 4.1**) by activating transcription of genes involved in the ubiquitin proteasome system (UPS) (**Figure 4.3**). Using MB-specific RNAi, I have shown that affected members of the UPS are, indeed, required for MBγ pruning (**Figure 4.4**). Ubiquitin proteasome system expression is activated by a transcriptional cascade mediated by EcR-B1 (Alyagor et al., 2018; **Figure 1.6**), and, as expected, transcriptome analysis on MB neurons expressing a dominant negative form of EcR-B1 revealed downregulation of UPS genes. These findings were consistent with other studies that indicated that SWI/SNF operated in regulating genes downstream of EcR-B1 in the transcriptional cascade (Kirilly et al., 2011; Zraly et al., 2006). I then used ATAC-seq to investigate the effect of SWI/SNF knockdowns on chromatin accessibility and identified potential direct target genes of the SWI/SNF complex by finding genes that had both less accessibility and less expression in SWI/SNF knockdowns. Although promising, this analysis yielded only a small number of potential direct target candidates and little indication of the SWI/SNF complex affecting the accessibility of genes downstream of EcR-B1.

Included in these candidate targets were the actin binding proteins such as Shrm, aru, svil, Cib, and chic. During neuronal remodeling, the actin cytoskeleton is highly dynamic (Yaniv & Schuldiner, 2016) and dynamic transcriptional regulation of actin binding proteins may be critical to regulating actin stability throughout remodeling processes. Additionally, *EcR-B1* itself has reduced transcription and accessibility in Snr1-KD MBs, suggesting that the core SWI/SNF subunit Snr1 may directly target and regulate transcription of *EcR-B1* in the MB. Other potential targets of Snr1 included *ubiquitin conjugating enzyme E2H* (*UbcE2H*), and the ubiquitin ligases *Ube3A* and *Ubr1*. Proteins encoded by these genes regulate proteasome-mediated protein degradation. Although these UPS members were not functionally validated in Chapter 4.4 as they were not found to be commonly regulated by either E(y)3 or EcR-B1, they are promising genes for further investigation. Interestingly, the human ortholog of *Ube3A* has been implicated in Angelman syndrome – a NDD characterized by severe ID (Wu et al., 2008; Lu et al., 2009; Lee et al., 2014). Studies in *Drosophila* have shown that Ube3A directly interacts with Rpn10 (Lee et al., 2014). Rpn10 is a proteasome subunit that was downregulated in both Snr1-KD MBs and E(y)3-KD MBs and RNAi knockdown of *Rpn10* resulted in a MBγ pruning phenotype (**Figure 4.4**). Furthermore, Ube3A has been shown to be enriched in neurons, including the MB, and is required for learning and memory (Crocker et al., 2016; Wu et al., 2008; Chakraborty et al., 2015), suggesting an important role for this ubiquitin ligase in the MB. Of course, future studies should investigate these putative targets in MBγ pruning in order to gain further understanding of the molecular mechanisms underlying neuronal pruning. For instance, if antibodies targeting SWI/SNF subunits become more readily available, chromatin immunoprecipitation sequencing (ChIP-seq) could be used to validate regions of the genome that are directly targeted by the SWI/SNF complex.

Alyagor et al (2018) showed that the expression of genes involved in MBγ pruning is extremely dynamic and requires that gene transcription occurs within very specific time windows. Disruptions or delays in this transcriptional program result in defective MBγ pruning. This study examined only one time point during the late 3rd instar larval stage, within three hours of pupation, when a spike in the ecdysone moulting hormone activates EcR-B1. Recently, it was shown that some core and ATPase module subunits of the SWI/SNF complex demonstrate dynamic expression in the MB throughout the remodeling process, including *brm*, *mor*, *Bap55*, *Bap111*, and *Bap60* (Alyagor et al., 2018). The expression of these subunits continues to increase up to 18 hours after pupation, suggesting a requirement of the SWI/SNF complex later in neuronal remodeling. I have shown that Bap60 is required during a specific period of development in the adult MB (**Chapter 5**) and, like the adult MB, the SWI/SNF complex may be required during a specific window of neuronal remodeling after pupation. This may explain why few genes were found to be differentially expressed in the Bap60-KD MBs in the late 3rd instar larvae and why few candidate target genes were identified for the SWI/SNF subunits. In future studies, it would be interesting to look at the effect of SWI/SNF knockdown on transcription and chromatin accessibility at a later time point, when SWI/SNF expression is greater during the remodeling process to gain further insight and identify more candidate direct target genes.

6.3 SWI/SNF complex is required for juvenile expression of genes in the MB

Previous studies from our lab have shown that knockdown of the core SWI/SNF subunit, Bap60, results in deficiencies in both short- and long-term courtship memory (Chubak et al., 2019; Nixon et al., 2019). MBγ remodeling is important for STM, but not

LTM (Redt-Clouet et al., 2012), and the requirement of Bap60 for LTM suggests an acute role for the SWI/SNF complex in adult MB neurons. Using MB-specific transcriptome analysis, I found that Bap60 has a greater effect on gene regulation in the MB of juvenile adult flies than on that of mature flies. In particular, Bap60 seems to be important for activating the expression of neuronal genes (**Figure 5.1**) and developmental genes that normally show increased expression in juvenile MBs (**Figure 5.2**). Additionally, using ATAC-Seq to investigate the effect of Bap60 on chromatin accessibility in juvenile and mature MBs showed that Bap60 had a stage-specific effect on the accessibility of TSS regions in the juvenile MB (**Figure 5.3**).

Using both RNA-Seq and ATAC-Seq to identify potential direct target genes of Bap60, I found enrichment of genes involved in neurodevelopment and response to stimuli (**Figure 5.5**). This is interesting because the MB is known to undergo structure alterations and form new synaptic connections during the early stages of juvenile adult life (Barth & Heisenberg, 1997; Cabirol et al., 2017; Heisenberg et al., 1995; Seugnet et al., 2011). These changes are dependent on sensory input, suggesting that some of the brain's circuitry is developed in response to early life experience (Barth & Heisenberg, 1997; Barth et al., 1997; Cabirol et al., 2017). This early experience-dependent plasticity in the MB is required for normal memory at later life stages in flies (Barth & Heisenberg, 1997; Doll & Broadie, 2015; Doll et al., 2017; Seugnet et al., 2011) and bees (Cabirol et al., 2017; Jones et al., 2013).

By comparing transcriptome and chromatin accessibility data, I was able to identify 70 potential target genes of Bap60 that display both a reduction in transcription and TSS plasticity in the juvenile adult Bap60-KD MBs (**Figure 5.4**). These candidate genes showed enrichment of biological processes related to neurodevelopment and response to stimulus. Included in these were genes important in axon guidance, such as *fend*, *Cam*, and *D* (Umemiya et al., 2002; Gaudet et al., 2011; Marrone et al., 2014; Melnattur et al., 2013; Sánchez-Soriano & Russell, 2000), as well as genes involved in learning and memory such as the MB-specific gene *Dop1R1* and *Ddc* (Seugnet et al., 2008; Selcho et al., 2009; Chen et al., 2012; Lee et al., 2011). Misregulation of the genes in that Bap60-KD MBs in the juvenile brain may affect the formation of critical connections required for learning and memory later in life. Interestingly, the novel MB-specific gene, *Hr38*, was identified as a potential direct target gene of Bap60. Expression of this transcription factor is induced during periods of high neuronal activity (Chen et al., 2016; Crocker et al., 2016; Croset et al., 2018) and its induction may be critical in activating transcription of genes required for forming neuronal connections in the juvenile MB. Another promising direct target gene of Bap60 is *Cib*, a gene encoding an actin-binding protein involved in neurodevelopment (Boquet et al., 2000a). *Cib* is a promising candidate gene for MB wiring not only because *Cib* was identified as a potential target of the Snr1 subunit in the larval MB (**Chapter 4.5**), but also because *Cib* has been previously shown to play a role in MB development (Boquet et al., 2000a; Boquet et al., 2000b). Expression of Cib is induced in the MB Kenyon cells during pupation, and flies mutant for *Cib* have demonstrated defective MB β lobe morphology (Boquet et al., 2000a; Boquet et al., 2000b), suggesting a crucial role for this gene in MB wiring.

Although the candidate target genes identified in this study are promising, they have not yet been technically or functionally validated. Future studies should aim to validate these genes as direct targets of Bap60 using ChIP-Seq, and to functionally validate their requirement in brain wiring in the juvenile MB. One way to do this would be to specifically perturb expression of these genes in the juvenile MB and assess memory as an indicator of proper neuronal wiring. Investigating the roles of these candidate target genes during a window of experience-dependent synaptic plasticity may provide further insight into the role of SWI/SNF-mediated chromatin regulation in brain wiring.

6.4 The *Drosophila* MB as a model for NDD gene functionalization

In this study, I used genetic tools to investigate the role of the SWI/SNF chromatin remodeling complex, which has been implicated in NDDs, in the *Drosophila* MB. The SWI/SNF complex is highly conserved between humans and *Drosophila* (Son & Crabtree, 2014), and until recently, the role of the SWI/SNF complex in post-mitotic neurons had not been extensively investigated (Chubak et al., 2019). However, by combining my research with previous studies from our lab, we have been able to elucidate new stage-specific roles for the SWI/SNF complex in neurons. By showing that the SWI/SNF complex is required for neuronal remodeling by regulating the transcription of specific genes critical to MBγ pruning, and that SWI/SNF is required in adult neurons to govern brain wiring by regulating the expression of genes required during a critical window of neurodevelopment, we now have a greater understanding of the link between chromatin regulation and brain wiring. The data generated in this project may lead to future translational research investigating SWI/SNF-related ID.

There are many other genes that have been implicated in NDDs, and for most of these genes, we have no understanding of their role in neurons. Given that approximately 75% of human disease genes are conserved in *Drosophila* (Reiter et al., 2001), the *Drosophila* MB provides a powerful system to investigate the roles of genes in behaviour and cellular function to better understand the aetiology of NDDs.

6.5 Research limitations

Although the efficiency of the SWI/SNF RNAi lines used in this thesis was validated in previous studies using a ubiquitous *Actin5C-GAL4* driver (Chubak et al., 2019), it is difficult to assay the extent to which the target genes are knocked down in the MB when using the R14H06-GAL4 driver. Since the mechanisms of RNAi primarily occur in the cytoplasm (Giordano, 2002), efficiency of the SWI/SNF knockdowns in the MB cannot be detected using the RNA from INTACT-derived nuclei. One way to test MB knockdown efficiency would be to perform fluorescence-activated cell sorting to isolate whole MB cells expressing a membrane bound GFP. From there, polyadenylated mRNA can be isolated for RT-qPCR and knockdown validation (Mainland et al., 2017). One alternative to RNAi is the use of tissue-specific CRISPR (clustered regularly interspaced short palindromic repeats) (Meltzer et al., 2019). This tool uses a ubiquitously expressed gene-specific guide RNA (gRNA) transgene designed to target a gene of interest and a Cas9 (CRISPR-association protein 9) enzyme under *UAS*-mediated expression to induce a null mutation in the gene of interest, effectively knocking out gene expression. Using a tissue-specific *GAL4* driver to restrict Cas9 expression in only specific cells ensures that the gene of interest is modified in only target cells. This tool was only recently used to successfully knockout gene expression specifically in the MB (Meltzer et al., 2019), and it is currently being implemented in our lab.

Another limitation of this study was that the effect of SWI/SNF knockdown on gene transcription and chromatin accessibility during MBγ pruning was only tested at a single time point: the late 3rd instar larval stage. This time point was chosen to investigate whether the SWI/SNF complex was involved in the EcR-B1 transcriptional cascade upon activation of EcR-B1 by ecdysone. Gene expression in the MB during γ neuron pruning is highly dynamic and requires transcription of specific genes within several specific time windows (Alyagor et al., 2018). By only investigating one of these windows, changes in dynamically expressed genes and changes in chromatin plasticity over time were not observed. This limitation may have resulted in the limited number of candidate SWI/SNF target genes. The identification of candidate Bap60 target genes in the adult MB (**Chapter 5.4**) used transcriptome and accessibility data from two time points to observe for dynamic changes in gene expression and chromatin plasticity. Performing a similar analysis using data from multiple time points during MBγ remodeling may lead to the identification of more potential SWI/SNF targets. Another way to identify SWI/SNF target genes would be to perform ChIP-seq, where antibodies against SWI/SNF subunits are used to immunoprecipitate both the protein, and the DNA with which it is associated. The availability of antibodies targeting *Drosophila* SWI/SNF subunits is currently limited; however should they become more available, MB-specific ChIP-seq in combination with RNA-seq and ATAC-seq would provide further insight regarding SWI/SNF regulation during remodeling.

Candidate targets genes of Bap60 in the juvenile MB were not functionally validated in this study. Validation of these genes during the critical window of juvenile experience-dependent synaptic plasticity in the juvenile MB, will require an elaborate solution: one where gene expression can be perturbed only within the first few hours after eclosion. One potential tool to investigate the roles of these genes within a short window of time is to use the temperature sensitive GAL80 system in conjunction with the tissue-specific GAL4-UAS system. In this model, GAL80 represses activity of GAL4 at restrictive temperatures, but allows for GAL4-mediated transcription at permissive temperatures (Rodrìguez et al., 2013). Use of this system would temporally restrict GAL4-mediated RNAi knockdown of candidate genes to a desired time period, however several considerations must be made, including: the rate at which gene expression is knocked down once GAL4-mediated transcription is activated, the rate at which the existing target protein is degraded, and the rate at which gene expression is rescued once GAL4-mediated transcription is repressed by GAL80. Another potential solution is to use the deGradFP (degrade GFP) (Caussinus et al., 2012). In this system, proteins tagged with GFP are targeted by an engineered F-box protein that will recognize GFP and promote ubiquitination of the protein for rapid degradation. Nagarkar-Jaiswal et al. (2015) describe the generation of GFP-tagged lines using Minos Mediated Integration Cassettes (MiMIC) that can be used with deGradFP technology. By using deGradFP to degrade candidate gene products during the early juvenile adult stage, we will be able to effectively evaluated their specific roles during the period of experience-depedent synaptic plasticity.

6.6 Conclusions, future directions, and research implications

In this study, I have identified a role for the SWI/SNF complex at important life transitions in the *Drosophila* MB (**Figure 6.1**). During the transition from larvae to pupae, I have shown that the SWI/SNF complex regulates genes involved in neuronal remodeling and affects the transcription of genes in the UPS, ultimately affecting MBγ axon pruning (**Figure 6.1A**). I have identified candidate target genes of E(y)3 and Snr1 that are likely involved in MB remodeling, including the actin binding proteins: aru, Shrm, chic, and Cib. Potential targets of the core Snr1 subunit also include the ubiquitin ligase Ube3A, whose human ortholog has been implicated in Angelman syndrome (Wu et al., 2008; Lu et al., 2009; Lee et al., 2014), is enriched in neurons in *Drosophila* and is required for learning and memory (Wu et al., 2008; Chakraborty et al., 2015). Furthermore, I have demonstrated that the SWI/SNF complex regulates genes that are required for neurodevelopment and stimulus response in the juvenile adult MB during a window of experience-dependent synaptic plasticity (**Figure 6.1B**). I have identified potential target genes of Bap60 during this window that are associated with stimulus response and development, including *Cam*, *fend*, and *Cib*, the last of which is involved in MB development (Boquet et al., 2000a; Boquet et al., 2000b). Biological validation and further study of these potential SWI/SNF target genes is required to better understand their roles in neuronal pruning and synaptic plasticity.

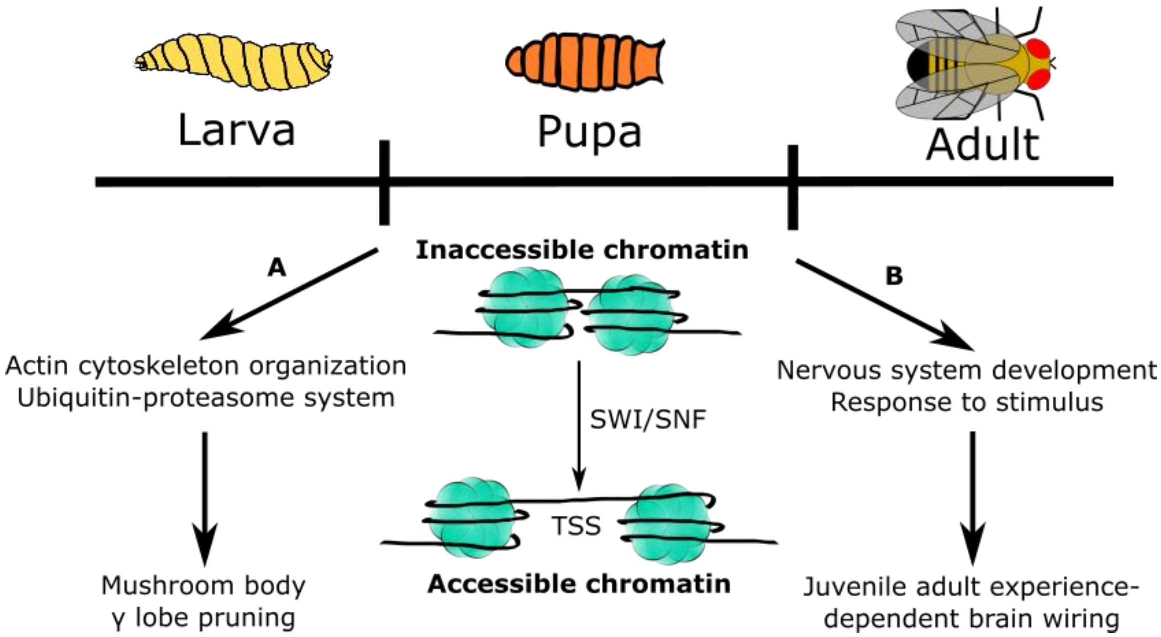

Figure 6.1 The SWI/SNF complex is required in MB neurons at important life transitions.

The SWI/SNF complex is required to make chromatin around the TSS more accessible at (**A**) the transition from larva to pupa, where it targets genes involved in actin cytoskeleton organization and genes in the ubiquitin proteasome system, which are required for MBγ pruning and at (**B**) the transition from pupa to adult where it targets genes involved in nervous system development and stimulus response that are important for experience-dependent brain wiring that is critical for normal memory.

Here, I have provided a link between chromatin and brain wiring by showing that the SWI/SNF chromatin remodeling complex is required for neuronal pruning and experience-dependent synaptic plasticity in the *Drosophila* brain. Although more complex than *Drosophila*, human brains also undergo neuronal pruning processes during development (Chen & Baram, 2016) and show periods of experience-dependent plasticity, especially during adolescence (Ismail et al., 2017). These processes are crucial to the formation of brain circuits required for proper learning and memory later in life (Emptage et al., 2001). So-called “environmental enrichment” therapy for autism is based on the idea that defects in neural wiring might be corrected by providing increased sensorimotor experience (Ismail et al., 2017; Simpson & Kelly, 2011). It will be interesting to further investigate the mechanisms of SWI/SNF-mediated gene regulation in neurodevelopment and experience-dependent brain plasticity. Understanding the role of chromatin structure in neuronal wiring in the postnatal brain could open possibilities for therapy, whereas prenatal developmental intervention seems unlikely.

References

Acevedo, S. F., Froudarakis, E. I., Kanellopoulos, A., & Skoulakis, E. M. C. (2007). Protection from premature habituation requires functional mushroom bodies in *Drosophila*. *Learning & Memory*, *14*, 376–384.

Adams, M. D., Celniker, S. E., Holt, R. A., Evans, C. A., Gocayne, J. D., Amanatides, P. G., … Venter, J. C. (2000). The genome sequence of *Drosophila melanogaster*. *Science*, *287*, 2185–2195.

Adhikari, P., Orozco, D., Randhawa, H., & Wolf, F. (2018). Mef2 induction of the immediate early gene *Hr38* / *Nr4a* is terminated by Sirt1 to promote ethanol tolerance. *Genes, Brain and Behavior*, *18*, e12486.

Adroschuk, A., Al-Jabri, B., & Bolduc, F. V. (2015). From learning to memory : what flies can tell us about intellectual disability. *Frontiers in Psychiatry*, *6*, 1–16.

Alyagor, I., Berkun, V., Keren-Shaul, H., Marmor-Kollet, N., David, E., Mayseless, O., … Schuldiner, O. (2018). Combining developmental and perturbation-seq uncovers transcriptional modules orchestrating neuronal remodeling. *Developmental Cell*, *47*, 38-52.e6.

Anders, S., & Huber, W. (2010). Differential expression analysis for sequence count data. *Genome Biology*, *11*, R106.

Anders, S., Pyl, P. T., & Huber, W. (2015). HTSeq — a Python framework to work with high-throughput sequencing data. *Bioinformatics*, *31*, 166–169.

Aso, Y., Grübel, K., Busch, S., Friedrich, A. B., Tanimoto, H., Aso, Y., … Tanimoto, H. (2009). The mushroom body of adult *Drosophila* characterized by GAL4 drivers. *Journal of Neurogenetics*, *23*, 156–172.

Aso, Y., Hattori, D., Yu, Y., Johnston, R. M., Iyer, N. A., Ngo, T. T. B., … Rubin, G. M. (2014). The neuronal architecture of the mushroom body provides a logic for associative learning. *ELife*, *3*, e04577.

Barth, M., & Heisenberg, M. (1997). Vision affects mushroom bodies and central complex in *Drosophila melanogaster*. *Learning & Memory*, *4*, 219–229.

Barth, M., Hirsch, H. V, Meinertzhagen, I. A., & Heisenberg, M. (1997). Experience-dependent developmental plasticity in the optic lobe of *Drosophila melanogaster*. *The Journal of Neuroscience*, *17*, 1493–1504.

BC, T., & BP, M. (2019). TxDb.Dmelanogaster.UCSC.dm6.ensGene: Annotation package for TxDb object(s). R package version 3.4.6.

Berger, S. L., Kouzarides, T., Shiekhattar, R., & Shilatifard, A. (2009). An operational definition of epigenetics. *Genes and Development*, *23*, 781–783.

Biggar, S. R., & Crabtree, G. R. (1999). Continuous and widespread roles for the Swi – Snf complex in transcription. *The EMBO Journal*, *18*, 2254–2264.

Bliim, N., Leshchyns, I., Sytnyk, V., & Janitz, M. (2016). Transcriptional regulation of long-term potentiation. *Neurogenetics*, *17*, 201–210.

Blum, A. L., Li, W., Cressy, M., & Dubnau, J. (2009). Short- and long-term memory in *Drosophila* require cAMP signaling in distinct neuron types. *Current Biology*, *19*, 1341–1350.

Bolinger, C., Zasadil, L., Rizaldy, R., & Hildebrand, J. D. (2010). Specific isoforms of *Drosophila Shroom* define spatial requirements for the induction of apcial constriction. *Developmental Dynamics*, *239*, 2078–2093.

Boquet, I., Boujemaa, R., Carlier, M., & Préat, T. (2000a). Ciboulot regulates actin assembly during *Drosophila* brain metamorphosis. *Cell*, *102*, 797–808.

Boquet, I., Hitier, R., Dumas, M., Chaminade, M., & Préat, T. (2000b). Central brain postembryonic development in *Drosophila*: Implication of genes expressed at the interhemispheric junction. *Developmental Neurobiology, 42,* 33-48.

Born, D. E., & Rubel, E. W. (1988). Afferent influences on brain stem auditory nuclei of the chicken : Presynaptic action potentials regulate protein synthesis in nucleus magnocellularis neurons. *The Journal of Neuroscience*, *8*, 901–919.

Bornstein, B., Zahavi, E. E., Gelley, S., Zoosman, M., Yaniv, S. P., Fuchs, O., … Schuldiner, O. (2015). Developmental axon pruning requires destabilization of cell adhesion by JNK signaling. *Neuron*, *88*, 926–940.

Boulanger, A., Clouet-Redt, C., Farge, M., Flandre, A., Guignard, T., Fernando, C., … Dura, J.-M. (2011). ftz-f1 and Hr39 opposing roles on *EcR* expression during *Drosophila* mushroom body neuron remodeling. *Nature Neuroscience*, *14*, 37–44.

Bramswig, N. C., Caluseriu, O., Lüdecke, H.-J., Bolduc, F. V., Noel, N. C. L., Wieland, T., … Wieczorek, D. (2017). Heterozygosity for *ARID2* loss-of-function mutations in individuals with a Coffin–Siris syndrome-like phenotype. *Human Genetics*, *136*, 297–305.

Brand, A. H., & Perrimon, N. (1993). Targeted gene expression as a means of altering cell fates and generating dominant phenotypes. *Development*, *118,* 401–415.

Brooks, E. S., Greer, C. L., Romero-Caldéron, R., Serway, C. N., Grygoruk, A., Haimovitz, J. M., … Krantz, D. E. (2011). A putative vesicular transporter expressed in *Drosophila* mushroom bodies that mediates sexual behavior may define a neurotransmitter system. *Neuron*, *72*, 316–329.

Brown, J. B., Boley, N., Eisman, R., May, G. E., Stoiber, M. H., Duff, M. O., … Celniker, S. E. (2014). Diversity and dynamics of the *Drosophila* transcriptome. *Nature*, *512*, 393–399.

Buenrostro, J., Wu, B., Chang, H., & Greenleaf, W. (2016). ATAC-seq: A method for assaying chromatin accessibility genome-wide. *Current Protocols in Molecular Biology*, *109*, 21.29.1-21.29.9.

Cabirol, A., Brooks, R., Groh, C., Barron, A. B., & Devaud, J. M. (2017). Experience during early adulthood shapes the learning capacities and the number of synaptic boutons in the mushroom bodies of honey bees (*Apis mellifera*). *Learning and Memory*, *24*, 557–562.

Campbell, R. A., & Turner, G. C. (2010). The mushroom body. *Current Biology*, *20*, R11–R12.

Catsicas, M., Bonness, V., Becker, D., & Mobbs, P. (1998). Spontaneous Ca2+ transients and their transmission in the developing chick retina. *Current Biology, 8,* 283–286.

Caussinus, E., Kanca, O., & Affolter, M. (2012). Fluorescent fusion protein knockout mediated by anti-GFP nanobody. *Nature Structural & Molecular Biology*, *19*, 117–122.

Chakraborty, M., Paul, B.K., Nayak, T., Das, A., Jana, N.R., & Bhutani, S. (2015). The E3 ligase ube3a is required for learning in *Drosophila melanogaster*. *Biochemical and Biophysical Research Communications, 462,* 71-77.

Chalkley, G. E., Moshkin, Y. M., Langenberg, K., Bezstarosti, K., Blastyak, A., Gyurkovics, H., … Verrijzer, C. P. (2008). The transcriptional coactivator SAYP is a trithorax group signature subunit of the PBAP chromatin remodeling complex. *Molecular and Cellular Biology*, *28*, 2920–2929.

Chaudhury, S., Sharma, V., Kumar, V., & Nag, T. C. (2016). Activity-dependent synaptic plasticity modulates the critical phase of brain development. *Brain and Development*, *38*, 355–363.

Chelly, J., Khelfaoui, M., Francis, F., Chérif, B., & Bienvenu, T. (2006). Genetics and pathophysiology of mental retardation. *European Journal of Human Genetics*, *14*, 701–713.

Chen, C.-C., Wu, J.-K., Lin, H.-W., Pai, T.-P., Fu, T.-F., Wu, C.-L., … Chiang, A.-S. (2012). Visualizing long-term memory formation in two neurons of the *Drosophila* brain. *Science*, *335*, 678–686.

Chen, X., Rahman, R., Guo, F., & Rosbash, M. (2016). Genome-wide identification of neuronal activity-regulated genes in *Drosophila*. *ELife*, *5*, e19942.

Chen, Yuanyuan, Ozturk, N. C., & Zhou, F. C. (2013). DNA methylation program in developing hippocampus and its alteration by alcohol. *PLoS One*, *8*, e60503.

Chen, Yuncai, & Baram, T. Z. (2016). Toward understanding how early-life stress reprograms cognitive and emotional brain networks. *Neuropsychopharmacology2*, *41*, 197–206.

Cherbas, L., Hu, X., Zhimulev, I., Belyaeva, E., & Cherbas, P. (2003). EcR isoforms in *Drosophila*: Testing tissue-specific requirements by targeted blockade and rescue. *Development*, *130*, 271-284.

Chikahisa, S., Sei, H., Morishima, M., Sano, A., Kitaoka, K., Nakaya, Y., & Morita, Y. (2006). Exposure to music in the perinatal period enhances learning performance and alters BDNF/TrkB signaling in mice as adults. *Behavioural Brain Research*, *169*, 312–319.

Ching, T., Huang, S., & Garmire, L. X. (2014). Power analysis and sample size estimation for RNA-Seq differential expression. *RNA*, *20*, 1684–1696.

Chiurazzi, P., & Pirozzi, F. (2016). Advances in understanding – genetic basis of intellectual disability. *F1000Research*, *5*, 1–16.

Choi, Y., Lee, G., & Park, J. H. (2006). Programmed cell death mechanisms of identifiable peptidergic neurons in *Drosophila melanogaster*. *Development*, *133*, 2223–2232.

Chubak, M. C., Nixon, K. C. J., Stone, M. H., Raun, N., Rice, S. L., Sarikahya, M., … Kramer, J. M. (2019). Individual components of the SWI / SNF chromatin remodelling complex have distinct roles in memory neurons of the *Drosophila* mushroom body. *Disease Models & Mechanisms*, *12*, dmm037325.

Clapier, C.R. & Cairns, B.R. (2009). The biology of chromatin remodeling complexes. *Annual Review of Biochemistry*, *78*, 273-304.

Coll-Tané, M., Krebbers, A., Castells-Nobau, A., Zweier, C., & Schenck, A. (2019). Intellectual disability and autism spectrum disorders 'on the fly' : insights from *Drosophila*. *Disease Models & Mechanisms*, *12*, dmm039180.

Conesa, A., Madrigal, P., Tarazona, S., Gomez-cabrero, D., Cervera, A., Mcpherson, A., … Mortazavi, A. (2016). A survey of best practices for RNA-seq data analysis. *Genome Biology*, *17*, 13.

Consortium Drosophila 12 Genomes. (2007). Evolution of genes and genomes on the *Drosophila* phylogeny. *Nature*, *450*, 203–218.

Crocker, A., Guan, X., Murphy, C. T., & Murthy, M. (2016). Cell-type-specific transcriptome analysis in the *Drosophila* mushroom body reveals memory- related changes in gene expression. *Cell Reports*, *15*, 1–17.

Croset, V., Treiber, C. D., & Waddell, S. (2018). Cellular diversity in the *Drosophila* midbrain revealed by single-cell transcriptomics. *ELife*, *7*, e34550.

Daish, T. J., Cakouros, D., & Kumar, S. (2003). Distinct promoter regions regulate spatial and temporal expression of the *Drosophila* caspase *dronc*. *Cell Death and Differentiation*, *10*, 1348–1356.

DasGupta, S., Ferreira, C. H., & Miesenböck, G. (2014). FoxP influences the speed and accuracy of a perceptual decision in *Drosophila*. *Science*, *344*, 901–904.

Davis, E. P., Korja, R., Karlsson, L., Glynn, L. M., Sandman, C. A., Vegetabile, B., … Baram, T. Z. (2019). Across continents and demographics, unpredictable maternal signals are associated with children's cognitive function. *EBioMedicine*, *46*, 256–263.

Davis, E. P., Stout, S. A., Molet, J., Vegetabile, B., Glynn, L. M., Sandman, C. A., … Baram, T. Z. (2017). Exposure to unpredictable maternal sensory signals influences cognitive development across species. *Proceedings of the National Academy of Sciences*, *114*, 10390–10395.

de Belle, J. S., & Heisenberg, M. (1994). Associative odor learning in *Drosophila* abolished by chemical ablation of mushroom bodies. *Science*, *263*, 692–695.

de Graaf, C. A., & Steensel, B. Van. (2013). Chromatin organization : form to function. *Current Opinion in Genetics & Development*, *23*, 185–190.

del Valle Rodrìguez, A., Didiano, D., & Desplan, C. (2013). Power tools for gene expression and clonal analysis in *Drosophila*. *Nature Methods*, *9*, 47–55.

Deneris, E. S., & Hobert, O. (2014). Maintenance of postmitotic neuronal cell identity. *Nature Neuroscience*, *17*, 899–907.

Detterman, D. (1987). Theoretical notions of intelligence and mental retardation. *American Journal of Mental Deficiency*, *92*, 2–11.

Di Donato, N., Rump, A., Koenig, R., Der Kaloustian, V. M., Halal, F., Sonntag, K., … Verloes, A. (2014). Severe forms of Baraitser – Winter syndrome are caused by *ACTB* mutations rather than *ACTG1* mutations. *European Journal of Human Genetics*, *22*, 179–183.

Dias, C., Estruch, S. B., Graham, S. A., Mcrae, J., Sawiak, S. J., Hurst, J. A., … Logan, D. W. (2016). *BCL11A* haploinsufficiency causes an intellectual disability syndrome and dysregulates transcription. *American Journal of Human Genetics*, *99*, 253–274.

Dietzl, G., Chen, D., Schnorrer, F., Su, K., Barinova, Y., Fellner, M., … Dickson, B. J. (2007). A genome-wide transgenic RNAi library for conditional gene inactivation in *Drosophila*. *Nature*, *448*, 151–157.

Dobin, A., Davis, C. A., Schlesinger, F., Drenkow, J., Zaleski, C., Jha, S., … Gingeras, T. R. (2013). STAR: ultrafast universal RNA-seq aligner. *Bioinformatics*, *29*, 15–21.

Doll, C. A., & Broadie, K. (2015). Activity-dependent FMRP requirements in development of the neural circuitry of learning and memory. *Development*, *142*, 1346–1356.

Doll, Caleb A., & Broadie, K. (2014). Impaired activity-dependent neural circuit assembly and refinement in autism spectrum disorder genetic models. *Frontiers in Cellular Neuroscience*, *8*, 1–26.

Doll, Caleb A., Vita, D. J., & Broadie, K. (2017). Fragile X Mental Retardation Protein requirements in activity-dependent critical period neural circuit refinement. *Current Biology*, *27*, 2318-2330.e3.

Duka, T., Anderson, S. M., Collins, Z., Raghanti, M. A., Ely, J. J., Hof, P. R., … Sherwood, C. C. (2014). Synaptosomal lactate dehydrogenase isozyme composition is shifted toward aerobic forms in primate brain evolution. *Brain, Behavior and Evolution*, *83*, 216–230.

Dunning, J., & During, M. J. (2003). Molecular mechanisms of learning and memory. *Expert Reviews in Molecular Medicine*, *5*, 1–11.

Eddison, M., Guarnieri, D. J., Cheng, L., Liu, C., Moffat, K. G., Davis, G., & Heberlein, U. (2011). *arouser* reveals a role for synapse number in the regulation of ethanol sensitivity. *Neuron*, *70*, 979–990.

Emptage, N. J., Reid, C. A., & Fine, A. (2001). Calcium stores in hippocampal synaptic boutons mediate short-term plasticity , store-operated Ca2+ entry , and spontaneous transmitter release. *Neuron*, *29*, 197–208.

Espinosa, J. S., & Stryker, M. P. (2012). Development and plasticity of the primary visual cortex. *Neuron*, *75*, 230–249.

Feng, J., Zhou, Y., Campbell, S. L., Le, T., Li, E., Sweatt, J. D., … Fan, G. (2010). Dnmt1 and Dnmt3a maintain DNA methylation and regulate synaptic function in adult forebrain neurons. *Nature Neuroscience*, *13*, 423–430.

Feng, Y., Li, Z., Lv, L., Du, A., Lin, Z., Ye, X., … Lin, Z. (2018). Tankyrase regulates apoptosis by activating JNK signaling in *Drosophila*. *Biochemical and Biophysical Research Communications*, *503*, 2234–2239.

Franz, M., Lopes, C. T., Huck, G., Dong, Y., Sumer, O., & Bader, G. D. (2016). Cytoscape.js: a graph theory library for visualisation and analysis. *Bioinformatics*, *32*, 309–311.

Gai, Y., Liu, Z., Cervantes-Sandoval, I., & Davis, R. L. (2016). *Drosophila SLC22A* transporter is a memory suppressor gene that influences cholinergic neurotransmission to the mushroom bodies. *Neuron*, *90*, 581–595.

Gaudet, P., Livstone, M.S., Lewis, S.E., & Thomas, P.D. (2011). Phylogenetic-based projection of functional annotations within the Gene Ontology consortium. *Briefings in Bioinformatics*, *12*, 449-462.

Ghiani, C. A., & Faundez, V. (2017). Cellular and molecular mechanisms of neurodevelopmental disorders. *Journal of Neuroscience Research*, *95*, 1093–1096.

Gibbs, M.E., Anderson, D.G., & Hertz, L. (2006). Inhibition of glycogenolysis in astrocytes iterrupts memory consolidation in young chickens. *Glia*, *54*, 214-22.

Gilissen, C., Hehir-kwa, J. Y., Thung, D. T., Vorst, M. Van De, Bon, B. W. M. Van, Willemsen, M. H., … Veltman, J. A. (2014). Genome sequencing identifies major causes of severe intellectual disability. *Nature*, *511*, 344–347.

Giordano, E., Rendina, R., Peluso, I., & Furia, M. (2002). RNAi triggered by symmetrically transcribed transgenes in *Drosophila melanogaster*. *Genetics*, *160*, 637-648.

Goyal, M.S. & Raichle, M.E. (2013). Gene expression-based modeling of human cortical synaptic density. *Proceedings of the National Academy of Sciences*, *110*, 6571-6576.

Graven, S. N., & Browne, J. V. (2008). Auditory development in the fetus and infant. *Newborn and Infant Nursing Reviews*, *8*, 187–193.

Groschner, L. N., Hak, L. C. W., Bogacz, R., & Miesenböck, G. (2018). Dendritic integration of sensory evidence in article dendritic integration of sensory evidence in perceptual decision-making. *Cell*, *173*, 894–905.

Hamdan, F. F., Gauthier, J., Spiegelman, D., Noreau, A., Yang, Y., Pellerin, S., … Michaud, J. L. (2009). Mutations in *SYNGAP1* in autosomal nonsyndromic mental retardation. *The New England Journal of Medicine*, *360*, 599–605.

Hargreaves, D. C., & Crabtree, G. R. (2011). ATP-dependent chromatin remodeling: genetics, genomics and mechanisms. *Cell Research*, *21*, 396–420.

Harris, J. C. (2005). *Intellectual disability: Understanding its development, causes, classification, evaluation, and treatment*. Oxford University Press.

Heinz, S., Benner, C., Spann, N., Bertolino, E., Lin, Y. C., Laslo, P., … Glass, C. K. (2010). Simple combinations of lineage-determining transcription factors prime cis-regulatory elements required for macrophage and B cell identities. *Molecular Cell*, *38*, 576–589.

Heisenberg, M., Heusipp, M., & Wanke, C. (1995). Structural plasticity in the *Drosophila* brain. *The Journal of Neuroscience*, *15*, 1951–1960.

Heisenberg, Martin, Borst, A., Wagner, S., & Byers, D. (1985). *Drosophila* mushroom body mutants are deficient in olfactory learning. *Journal of Neurogenetics*, *2*, 1–30.

Henry, G. L., Davis, F. P., Picard, S., & Eddy, S. R. (2012). Cell type-specific genomics of *Drosophila* neurons. *Nucleic Acids Research*, *40*, 9691–9704.

Hensch, T. (2005). Critical period mechanisms in developing visual cortex. *Current Topics in Developmental Biology*, *69*, 215–237.

Hirano, Y., Ihara, K., Masuda, T., Yamamoto, T., Iwata, I., Takahashi, A., … Yin, J. C. (2016). Shifting transcriptional machinery is required for long-term memory maintenance and modification in *Drosophila* mushroom bodies. *Nature Communications*, *7*, 13471.

Holstege, F. C. P., Jennings, E. G., Wyrick, J. J., Lee, T. I., Hengartner, C. J., Green, M. R., … Young, R. A. (1998). Dissecting the regulatory circuitry of a eukaryotic genome. *Cell*, *95*, 717–728.

Hoyer, J., Ekici, A. B., Endele, S., Popp, B., Zweier, C., Wiesener, A., … Reis, A. (2012). Haploinsufficiency of *ARID1B*, a member of the SWI/SNF-A chromatin-remodeling complex, is a frequent cause of intellectual disability. *The American Journal of Human Genetics*, *90*, 565–572.

Hu, Y., Sopko, R., Foos, M., Kelley, C., Flockhart, I., Ammeux, N., … Mohr, S.E. (2013). FlyPrimerBank: An online database for *Drosophila melanogaster* gene expression analysis and knockdown evaluation of RNAi reagents. *G3*, *3*, 1607-1616.

Hua, J. Y., Smear, M. C., Baier, H., & Smith, S. J. (2005). Regulation of axon growth in vivo by activity-based competition. *Nature*, *434*, 1022–1026.

Hutnick, L. K., Golshani, P., Namihira, M., Xue, Z., Matynia, A., Yang, X. W., … Fan, G. (2009). DNA hypomethylation restricted to the murine forebrain induces cortical degeneration and impairs postnatal neuronal maturation. *Human Molecular Genetics*, *18*, 2875–2888.

Ismail, F. Y., Fatemi, A., & Johnston, M. V. (2017). Cerebral plasticity: Windows of opportunity in the developing brain. *European Journal of Paediatric Neurology*, *21*, 23–48.

Jain, S., Sharma, R., & Wadhwa, S. (2004). Effect of prenatal species-specific and music stimulation on the postanatal auditory preference of domestic chick. *Indian Journal of Physiology and Pharmacology*, *48*, 174–183.

Jenett, A., Rubin, G. M., Ngo, T. T. B., Shepherd, D., Murphy, C., Dionne, H., … Zugates, C. T. (2012). A GAL4-driver line resource for *Drosophila* neurobiology. *Cell Reports*, *2*, 991–1001.

Johnson, O., Becnel, J., & Nichols, C. D. (2011). Serotonin receptor activity is necessary for olfactory learning and memory in *Drosophila melanogaster*. *Neuroscience*, *192*, 372–381.

Johnson, R. E., & Kerschensteiner, D. (2014). Retrograde plasticity and differential competition of bipolar cell dendrites and axons in the developing retina. *Current Biology*, *24*, 2301–2306.

Johnston, J. J., Wen, K.-K., Keppler-Noreuil, K., McKane, M., Maiers, J. L., Grenier, A., … Biesecker, L. G. (2013). Functional analysis of a *de novo ACTB* mutation in a patient with atypcial Baraitser-Winter syndrome. *Human Mutation*, *34*, 1242–1249.

Jones, B. M., Leonard, A. S., Papaj, D. R., & Gronenberg, W. (2013). Plasticity of the worker bumblebee brain in relation to age and rearing environment. *Brain, Behavior and Evolution*, *82*, 250–261.

Jones, S. G., Nixon, K. C. J., Chubak, M. C., & Kramer, J. M. (2018). Mushroom body specific transcriptome analysis reveals dynamic regulation of learning and memory genes after acquisition of long-term courtship memory in *Drosophila*. *G3*, *8*, 3433–3446.

Kadoch, C., & Crabtree, G. R. (2015). Mammalian SWI/SNF chromatin remodeling complexes and cancer: Mechanistic insights gained from human genomics. *Scientific Advances*, *1*, e1500447.

Kandel, E. R., Schwartz, J. H., & Jessell, T. M. (2000). *Principles of neural science* (4th ed.). New York: McGraw-Hill Medical.

Kassabov, S. R., Zhang, B., Persinger, J., & Bartholomew, B. (2003). SWI / SNF unwraps, slides, and rewraps the nucleosome. *Molecular Cell*, *11*, 391–403.

Katz, A. L. C., & Shatz, C. J. (1996). Synaptic activity and the construction of cortical circuits. *Science*, *274*, 1133–1138.

Keleman, K., Vrontou, E., Krüttner, S., Yu, J. Y., Kurtovic-Kozaric, A., & Dickson, B. J. (2012). Dopamine neurons modulate pheromone responses in *Drosophila* courthsip learning. *Nature*, *489*, 145–150.

Kim, H., Lee, M., Chang, H., Lee, T., Lee, H., Shin, M., … Kim, C. (2006). Influence of prenatal noise and music on the spatial memory and neurogenesis in the hippocampus of developing rats. *Brain and Development*, *28*, 109–114.

Kirilly, D., Gu, Y., Huang, Y., Wu, Z., Bashirullah, A., Low, B. C., … Yu, F. (2009). A genetic pathway composed of Sox14 and Mical governs severing of dendrites during pruning. *Nature Neuroscience*, *12*, 1497–2415.

Kirilly, D., Wong, J. J. L., Lim, E. K. H., Wang, Y., Zhang, H., Wang, C., … Yu, F. (2011). Intrinsic epigenetic factors cooperate with the steroid hormone ecdysone to govern dendrite pruning in *Drosophila*. *Neuron*, *72*, 86–100.

Kleefstra, T., Schenck, A., Kramer, J. M., & van Bokhoven, H. (2014). The genetics of cognitive epigenetics. *Neuropharmacology*, *80*, 83–94.

Kochinke, K., Zweier, C., Nijhof, B., Fenckova, M., Cizek, P., Honti, F., … Schenck, A. (2016). Systematic phenomics analysis deconvolutes genes mutated in intellectual disability into biologically coherent modules. *American Journal of Human Genetics, 98*, 149-164.

Koemans, T.S., Oppitz, C., Donders, R.A.T., van Bokhoven, H., Schenck, A., Keleman, K., & Kramer, J.M. (2017). *Drosophila* courtship conditioning as a measure of learning and memory. *Journal of Visualized Experiments, 124,* e55808.

Komuro, H., & Rakic, P. (1996). Intracellular Ca2+ fluctuations modulate the rate of neuronal migration. *Neuron*, *17*, 275–285.

Krashes, M. J., Keene, A. C., Leung, B., Armstrong, J. D., & Waddell, S. (2007). Sequential use of mushroom body neuron subsets during *Drosophila* odor memory processing. *Neuron*, *53*, 103–115.

Krumhansl, C. L., & Jusczyk, P. W. (1990). Infants' perception of phrase structure in music. *Psychological Science*, *1*, 70–73.

Kunz, T., Kraft, K. F., Technau, G. M., & Urbach, R. (2012). Origin of *Drosophila* mushroom body neuroblasts and generation of divergent embryonic lineages. *Development*, *139*, 2510–2522.

Kuo, C. T., Jan, L. Y., & Jan, Y. N. (2005). Dendrite-specific remodeling of *Drosophila* sensory neurons requires matrix metalloproteases, ubiquitin-proteasome, and ecdysone signaling. *Proceedings of the National Academy of Sciences*, *102*, 15230–15235.

Kurusu, M., Nagao, T., Walldorf, U., Flister, S., Gehring, W. J., & Furukubo-tokunaga, K. (2000). Genetic control of development of the mushroom bodies, the associative learning centers in the *Drosophila* brain, by the *eyeless, twin of eyeless*, and *dachshund* genes. *Proceedings of the National Academy of Sciences, 97,* 2140–2144.

Kwon, C. S., & Wagner, D. (2007). Unwinding chromatin for development and growth: a few genes at a time. *Trends in Genetics*, *23*, 403–412.

Lagali, P., Corcoran, C., & Picketts, D. (2010). Hippocampus development and function: role of epigenetic factors and implications for cognitive disease. *Clinical Genetics, 78*, 321–333.

Lai, Y.-W., Chu, S.-Y., Wei, J.-Y., Cheng, C.-Y., Li, J.-C., Chen, P.-L., … Ting, C. Y. (2016). *Drosophila* microRNA-34 impairs axon pruning of mushroom body γ neurons by downregulating the expression of ecdysone receptor. *Scientific Reports, 6*, 39141.

Lee, P., Lin, H., Chang, Y., Fu, T., Dubnau, J., Hirsh, J., … Chiang, A.-S. (2011). Serotonin – mushroom body circuit modulating the formation of anesthesia-resistant memory in *Drosophila*. *Proceedings of the National Academy of Sciences*, *108,* 13794–13799.

Lee, S.Y., Ramirez, J., Franco, M., Lectez, B., Gonzalez, M., Barrio, R., & Mayor, U. (2014). Ube3a, the E3 ubiquitin ligase causing Angelman syndrome and linked to autism, regulates protein homeostasis through the proteasomal shuttle Rpn10. *Cellular and Molecular Life Sciences, 71*, 2747-2758.

Lee, T., Lee, A., & Luo, L. (1999). Development of the *Drosophila* mushroom bodies : sequential generation of three distinct types of neurons from a neuroblast. *Development, 126*, 4065–4076.

Lee, T., Marticke, S., Sung, C., Robinow, S., & Luo, L. (2000). Cell-autonomous requirement of the USP/EcR-B1 ecdysone receptor for mushroom body neuronal remodeling in *Drosophila*. *Neuron*, *28,* 807–818.

Lessard, J., Wu, J. I., Ranish, J. A., Wan, M., Winslow, M. M., Staahl, T., … Crabtree, G. R. (2007). An essential switch in subunit composition of a chromatin remodeling complex during neural development. *Neuron*, *55*, 201–215.

Li, G., & Reinberg, D. (2011). Chromatin higher-order structures and gene regulation. *Current Opinion in Genetics & Development*, *21*, 175–186.

Li, H. H., Kroll, J. R., Lennox, S. M., Ogundeyi, O., Jeter, J., Depasquale, G., & Truman, J. W. (2014). A GAL4 driver resource for developmental and behavioral studies on the larval CNS of *Drosophila*. *Cell Reports*, *8*, 897–908.

Li, H., Handsaker, B., Wysoker, A., Fennell, T., Ruan, J., Homer, N., … Subgroup, 1000 Genome Project Data Processing. (2009). The Sequence Alignment/Map format and SAMtools. *Bioinformatics*, *25*, 2078–2079.

Liu, Y., Zhou, J., & White, K. P. (2014). Gene expression RNA-seq differential expression studies: More sequence or more replication? *Bioinformatics*, *30*, 301–304.

Livingstone, M. S., Sziber, P. P., & Quinrq, W. G. (1984). Loss of calcium/calmodulin responsiveness in adenylate cyclase of *rutabaga*, a *Drosophila* learning mutant. *Cell*, *37*, 205–215.

Lomvardas, S., & Thanos, D. (2001). Nucleosome sliding via TBP DNA binding *in vivo*. *Cell*, *106*, 685–696.

López, A. J., & Wood, M. A. (2015). Role of nucleosome remodeling in neurodevelopmental and intellectual disability disorders. *Frontiers in Behavioral Neuroscience*, *9*, 1–10.

Lorch, Y., Zhang, M., & Kornberg, R. D. (2001). RSC unravels the nucleosome. *Molecular Cell*, *7*, 89–95.

Lord, C., Cook, E. H., Leventhal, B. L., & Amaral, D. G. (2000). Autism spectrum disorders. *Neuron*, *28*, 355–363.

Love, M. I., Huber, W., & Anders, S. (2014). Moderated estimation of fold change and dispersion for RNA-seq data with DESeq2. *Genome Biology*, *15*, 1–21.

Lu, Y., Wang, F., Li, Y., Ferris, J., Lee, J.A., & Gao, F.B. (2009). The *Drosophila* homologue of the Angelman syndrome ubiquitin ligase regulates the formation of terminal dendritic branches. *Human Molecular Genetics*, *18*, 454-462.

Magistretti, P. J., & Allaman, I. (2015). A cellular perspective on brain energy metabolism and functional imaging. *Neuron*, *86*, 883–901.

Mainland, R. L., Lyons, T. A., Ruth, M. M., & Kramer, J. M. (2017). Optimal RNA isolation method and primer design to detect gene knockdown by qPCR when validating Drosophila transgenic RNAi lines. *BMC Research Notes*, *10*, 647.

Marrone, A.K., Kucherenko, M.M., Rishko, V.M., & Shcherbata H.R. (2011). New dystrophin/dystroglycan interactors control neuron behaviour in *Drosophila* eye. *BMC Neuroscience*, *12*, 93.

Mashtalir, N., D'Avino, A. R., Michel, B. C., Luo, J., Pan, J., Otto, J. E., … Kadoch, C. (2018). Modular organization and assembly of SWI/SNF Family Chromatin Remodeling Complexes. *Cell*, *175*, 1–17.

Mcbride, S. M. J., Giuliani, G., Choi, C., Krause, P., Correale, D., Watson, K., … Siwicki, K. K. (1999). Mushroom body ablation impairs short-term memory and long-term memory of courtship conditioning in *Drosophila melanogaster*. *Neuron*, *24*, 967–977.

Melnattur, K. V, Berdnik, D., Rusan, Z., Ferreira, C. J., & Nambu, J. R. (2013). The Sox gene *Dichaete* is expressed in local interneurons and functions in development of the *Drosophila* adult olfactory circuit. *Developmental Neurobiology*, *73*, 107–126.

Meltzer, H., Marom, E., Alyagor, I., Mayseless, O., Berkun, V., Segal-Gilboa, N., … Schuldiner, O. (2019). Tissue-specific (ts)CRISPR as an efficient strategy for in vivo screening in *Drosophila*. *Nature Communications*, *10*, 2113.

Mi, H., Huang, X., Muruganujan, A., Tang, H., Mills, C., Kang, D., & Thomas, P. D. (2017). PANTHER version 11: Expanded annotation data from Gene Ontology and Reactome pathways, and data analysis tool enhancements. *Nucleic Acids Research*, *45*, D183–D189.

Minshew, N. J., & Williams, D. L. (2007). The new neurobiology of autism: Cortex, connectivity, and neuronal organization. *Arch Neurol*, *64*, 945–950.

Mohrmann, L., Langenberg, K., Krijgsveld, J., Kal, A. J., Heck, A. J. R., & Verrijzer, C. P. (2004). Differential targeting of two distinct SWI/SNF-related *Drosophila* chromatin-remodeling complexes. *Molecular and Cellular Biology*, *24*, 3077–3088.

Montague, S. A., & Baker, B. S. (2016). Memory elicited by courtship conditioning requires mushroom body neuronal subsets similar to those utilized in appetitive memory. *PLOS One*, *11*, 1–24.

Moshkin, Y. M., Mohrmann, L., van Ijcken, W. F. J., & Verrijzer, C. P. (2007). Functional differentiation of SWI/SNF remodelers in transcription and cell cycle control. *Molecular and Cellular Biology*, *27*, 651–661.

Nagao, T., Endo, K., Kawauchi, H., Walldorf, U., & Furukubo-Tokunaga, K. (2000). Patterning defects in the primary axonal scaffolds caused by the mutations of the extradenticle and homothorax genes in the embryonic *Drosophila* brain. *Development Genes and Evolution*, *210*, 289–299.

Nagarkar-Jaiswal, S., Lee, P.-T., Campbell, M. E., Chen, K., Anguiano-Zarate, S., Gutierrez, M. C., … Bellen, H. J. (2015). A library of MiMICs allows tagging of genes and reversible, spatial and temporal knockdown of proteins in *Drosophila*. *ELife*, *4*, e05338.

Nakashima, X. H., Tsujimura, K., Irie, K., Ishizu, M., Pan, M., Kameda, T., & Nakashima, K. (2018). Canonical TGF-ß signaling negatively regulates neuronal morphogenesis through TGIF / Smad complex-mediated CRMP2 suppression. *The Journal of Neuroscience*, *38*, 4791–4810.

Narayanan, R., Pirouz, M., Kerimoglu, C., Pham, L., Wagener, R. J., Kiszka, K. A., … Tuoc, T. (2015). Loss of BAF (mSWI/SNF) complexes causes global transcriptional and chromatin state changes in forebrain development. *Cell Reports*, *13*, 1842–1854.

Narayanan, R., & Tuoc, T. C. (2014). Roles of chromatin remodeling BAF complex in neural differentiation and reprogramming. *Cell and Tissue Research*, *356*, 575–584.

Neigeborn, L., & Carlson, M. (1984). Genes affecting the regulation of *SUC2* gene expression by glucose repression in *Saccharomyces cerevisiae*. *Genetics*, *108*, 845–858.

Newman, L.A., Korol, D.L., & Gold, P.E. (2011). Lactate produced by glycogenolysis is astrocytes regulates memory processing. *PLoS One, 6*, e28427.

Ninkovic, J., Pinto, L., Petricca, S., Lepier, A., Sun, J., Rieger, M. A., … Götz, M. (2010). The transcription factor Pax6 regulates the survival of dopaminergic olfactory bulb neurons via crystallin αA. *Neuron*, *68*, 682–694.

Nixon, K. C. J., Rousseau, J., Stone, M. H., Sarikahya, M., Ehresmann, S., Mizuno, S., … Kramer, J. M. (2019). A syndromic neurodevelopmental disorder caused by mutations in *SMARCD1* , a core SWI/SNF subunit needed for context-dependent neuronal gene regulation in flies. *American Journal of Human Genetics*, *104*, 596–610.

Noveen, A., Daniel, A., & Hartenstein, V. (2000). Early development of the *Drosophila* mushroom body: the roles of *eyeless* and *dachshund*. *Development*, *127*, 3475–3488.

Olave, I., Wang, W., Xue, Y., Kuo, A., & Crabtree, G. R. (2002). Identification of a polymorphic, neuron-specific chromatin remodeling complex. *Genes and Development*, *16*, 2509–2517.

Parrish, J. Z., Kim, M. D., Jan, L. Y., & Jan, Y. N. (2006). Genome-wide analyses identify transcription factors required for proper morphogenesis of *Drosophila* sensory neuron dendrites. *Genes and Development*, *20*, 820–835.

Pauls, D., Selcho, M., Gendre, N., Stocker, R. F., & Thum, A. S. (2010). *Drosophila* larvae establish appetitive olfactory memories via mushroom body neurons of embryonic origin. *The Journal of Neuroscience*, *30*, 10655–10666.

Perkins, L. A., Holderbaum, L., Tao, R., Hu, Y., Sopko, R., McCall, K., … Perrimon, N. (2015). The transgenic RNAi project at Harvard medical school: Resources and validation. *Genetics*, *201*, 843–852.

Plaçais, P.-Y., de Tredern, É., Scheunemann, L., Trannoy, S., Goguel, V., Han, K.-A., … Preat, T. (2017). Upregulated energy metabolism in the *Drosophila* mushroom body is the trigger for long-term memory. *Nature Communications*, *8*, 15510.

Plavicki, J., Mader, S., Pueschel, E., Peebles, P., & Boekhoff-Falk, G. (2012). Homeobox gene *distal-less* is required for neuronal differentiation and neurite outgrowth in the *Drosophila* olfactory system. *Proceedings of the National Academy of Sciences*, *109*, 1578–1583.

Redt-Clouet, C., Trannoy, S., Boulanger, A., Tokmatcheva, E., Savvateeva-Popova, E., Parmentier, M.-L., … Dura, J.-M. (2012). Mushroom body neuronal remodelling is necessary for short-term but not for long-term courtship memory in *Drosophila*. *European Journal of Neuroscience*, *35*, 1684–1691.

Reiter, L.T., Potocki, L., Chien, S., Gribskov, M., & Bier, E. (2001). A systematic analysis of human disease-associated gene sequences in *Drosophila melanogaster*. *Genome Research*, *11*, 1114-1125.

Rendina, R., Strangi, A., Avallone, B., & Giordano, E. (2010). Bap170, a subunit of the *Drosophila* PBAP chromatin remodeling complex, negatively regulates the EGFR signaling. *Genetics*, *186*, 167–181.

Rivière, J., Bon, B. W. M. Van, Hoischen, A., Kholmanskikh, S. S., Roak, B. J. O., Gilissen, C., … Dobyns, W. B. (2012). *De novo* mutations in the actin genes *ACTB* and *ACTG1* cause Baraitser-Winter syndrome. *Nature Genetics*, *44*, 440–444.

Ronan, J. L., Wu, W., & Crabtree, G. R. (2013). From neural development to cognition: Unexpected roles for chromatin. *Nature Reviews Genetics*, *14*, 347–359.

Sánchez-Soriano, & Russell, S. (2000). Regulatory mutations of the *Drosophila* sox gene *Dichaete* reveal new functions in embryonic brain and hindgut development. *Developmental Biology*, *220*, 307–321.

Santen, G. W. E., Aten, E., Silfhout, A. T. V., Pottinger, C., Bon, B. W. M. Van, Minderhout, I. J. H. M. Van, … Belzen, M. J. Van. (2013). Coffin–Siris Syndrome and the BAF complex : Genotype–phenotype study in 63 patients. *Human Mutation*, *34*, 1519–1528.

Santen, G. W. E., Aten, E., Sun, Y., Almomani, R., Gilissen, C., Nielsen, M., … Kriek, M. (2012). Mutations in SWI/SNF chromatin remodeling complex gene *ARID1B* cause Coffin-Siris syndrome. *Nature Genetics*, *44*, 379–380.

Schindelin, J., Arganda-carreras, I., Frise, E., Kaynig, V., Longair, M., Pietzsch, T., … Cardona, A. (2012). Fiji: an open-source platform for biological-image analysis. *Nature Methods*, *9*, 676–682.

Schmieder, R., & Edwards, R. (2011). Quality control and preprocessing of metagenomic datasets. *Bioinformatics*, *27*, 863–864.

Schnaar, R.L., Gerardy-Schahn, R., & Hildebrandt, H. (2014). Sialic acids in the brain: Gangliosides and polysialic acid in nervous system development, stability, disease, and regeneration. *Physiological Reviews*, *94*, 461-518.

Schubiger, M., Wade, a a, Carney, G. E., Truman, J. W., & Bender, M. (1998). *Drosophila* EcR-B ecdysone receptor isoforms are required for larval molting and for neuron remodeling during metamorphosis. *Development*, *125*, 2053–2062.

Schulz, D. J., Baines, R. A., Hempel, C. M., Li, L., Liss, B., & Misonou, H. (2006). Cellular excitability and the regulation of functional neuronal identity : From gene expression to neuromodulation. *The Journal of Neuroscience*, *26*, 10362–10367.

Segarra-Mondejar, M., Casellas-Díaz, S., Ramiro-Pareta, M., Müller-Sánchez, C., Martorell-Riera, A., Hermelo, I., … Soriano, F. X. (2018). Synaptic activity-induced glycolysis facilitates membrane lipid provision and neurite outgrowth. *The EMBO Journal*, *37*, e97368.

Selcho, M., Pauls, D., Han, K.A., Stocker, P.F., & Thum, A.S. (2009). The role of dopamine in *Drosophila* larval classical olfactory conditioning. *PLoS One*, *4*, e5897.

Seugnet, L., Suzuki, Y., Donlea, J. M., Gottschalk, L., & Shaw, P. J. (2011). Sleep deprivation during early-adult development results in long-lasting learning deficits in adult *Drosophila*. *Sleep*, *34*, 137–146.

Seugnet, L., Suzuki, Y., Vine, L., Gottschalk, L., & Shaw, P.J. (2008). D1 receptor activation in the mushroom bodies rescues sleep-loss-induced learning impairments in *Drosophila*. *Current Biology*, *18*, 1110-1117.

Simpson, J., & Kelly, J. P. (2011). The impact of environmental enrichment in laboratory rats-Behavioural and neurochemical aspects. *Behavioural Brain Research*, *222*, 246–264.

Sinakevitch, I., Grau, Y., Strausfeld, N. J., & Birman, S. (2010). Dynamics of glutamatergic signaling in the mushroom body of young adult *Drosophila*. *Neural Development*, *5*, 10.

Son, E. Y., & Crabtree, G. R. (2014). The role of BAF (mSWI/SNF) complexes in mammalian neural development. *Am J Med Genet C Semin Med Genet*, *0*, 333–349.

Spitzer, N., Olson, E., & Gu, X. (1995). Spontaneous calcium transients regulate neuronal plasticity in developing neurons. *Journal of Neurobiology*, *26*, 316–324.

Staahl, B. T., & Crabtree, G. R. (2013). Creating a neural specific chromatin landscape by npBAF and nBAF complexes. *Current Opinion in Neurobiology*, *23*, 903–913.

Stark, R., & Brown, G. (2011). DiffBind: differential binding analysis of ChIP-Seq peak data.

Stern, M., Jensen, R., & Herskowitz, I. (1984). Five SWI genes are required for expression of the *HO* gene in yeast. *Journal of Molecular Biology*, *178*, 853–868.

Sudarsanam, P., Iyer, V. R., Brown, P. O., & Winston, F. (2000). Whole-genome expression analysis of snf/swi mutants of *Saccharomyces cerevisiae*. *Proceedings of the National Academy of Sciences*, *97*, 3364–3369.

Suzuki, A., Stern, S. A., Bozdagi, O., Huntley, G. W., Ruth, H., Magistretti, P. J., & Alberini, C. M. (2011). Astrocyte-neuron lactate transport is required for long-term memory formation. *Cell*, *144*, 810–823.

Taniguchi, H. & Moore, A.W. (2014). Chromatin regulators in neurodevelopment and disease: Analysis of fly neural circuits provides insights. *Bioessays*, *36*, 872-883.

Tea, J. S., & Luo, L. (2011). The chromatin remodeling factor Bap55 functions through the TIP60 complex to regulate olfactory projection neuron dendrite targeting. *Neural Development*, *6*, 5.

Tessier, C. R., & Broadie, K. (2008). *Drosophila* fragile X mental retardation protein developmentally regulates activity-dependent axon pruning. *Development*, *135*, 1547–1557.

Trannoy, S., Redt-Clouet, C., Dura, J.-M., & Preat, T. (2011). Parallel processing of appetitive short- and long-term memories in *Drosophila*. *Current Biology*, *21*, 1647–1653.

Trehub, S. E., Unyk, A. M., Kamenetsky, S. B., Hill, D. S., Trainor, L. J., Henderson, J. L., & Saraza, M. (1997). Mothers' and fathers' singing to infants. *Developmental Psychology*, *33*, 500–507.

Tsankova, N., Renthal, W., Kumar, A., & Nestler, E. J. (2007). Epigenetic regulation in psychiatric disorders. *Nature Reviews*, *8*, 355–367.

Tsarovina, K., Reiff, T., Stubbusch, J., Kurek, D., Grosveld, F. G., Parlato, R., … Rohrer, H. (2010). The Gata3 transcription factor is required for the survival of embryonic and adult sympathetic neurons. *The Journal of Neuroscience*, *30*, 10833–10843.

Tsurusaki, Y., Okamoto, N., Ohashi, H., Kosho, T., Imai, Y., Hibi-Ko, Y., … Matsumoto, N. (2012). Mutations affecting components of the SWI/SNF complex cause Coffin-Siris syndrome. *Nature Genetics*, *44*, 376–378.

Tuoc, T., Dere, E., Radyushkin, K., Pham, L., Nguyen, H., Tonchev, A. B., … Stoykova, A. (2016). Ablation of *BAF170* in developing and postnatal dentate gyrus affects neural stem cell proliferation, differentiation, and learning. *Molecular Neurobiology*, *54*, 4618–4635.

Turner, G. C., Bazhenov, M., & Laurent, G. (2008). Olfactory representations by *Drosophila* mushroom body neurons. *Journal of Neurophysiology*, *99*, 734–746.

Umemiya, T., Takasu, E., Takeichi, M., Aigaki, T., & Nose, A. (2002). Forked end: A novel transmembrane protein involved in neuromuscular specificity in *Drosophila* identified by gain-of-function screening. *Journal of Neurobiology*, *51*, 205-214.

van Bokhoven, H. (2011). Genetic and epigenetic networks in intellectual disability. *Annual Review of Genetics*, *45*, 81–104.

van Houdt, J. K., Nowakowska, B. A., Sousa, S. B., van Schaik, B. D., Seuntjens, E., Avonce, N., … Vermeesch, J. R. (2012). Heterozygous missense mutations in *SMARCA2* cause Nicolaides-Baraitser syndrome. *Nature Genetics*, *44*, 445–450.

Verheijen, F. W., Verbeek, E., Aula, N., Beerens, C. E. M. T., Havelaar, A. C., Joosse, M., … Mancini, G. M. S. (1999). A new gene, encoding an anion transporter, is mutated in sialic acid storage diseases. *Nature Genetics*, *23*, 462–465.

Vicari, S. (2004). Memory development and intellectual disabilities. *Acta Paediatrica Supplemental, 93,* 60–63.

Vogel-Ciernia, A., Matheos, D. P., Barrett, R. M., Kramár, E. a, Azzawi, S., Chen, Y., … Wood, M. a. (2013). The neuron-specific chromatin regulatory subunit BAF53b is necessary for synaptic plasticity and memory. *Nature Neuroscience*, *16*, 552–561.

Waite, K., & Eickholt, B. (2010). The neurodevelopmental implications of PI3K signaling. In C. Rommel, B. Vanhaesebroeck, & P. Vogt (Eds.), *Current Topics in Microbiology and Immunology, vol 346*. Springer Berlin Heidelberg.

Wang, L., Zhou, K., Fu, Z., Yu, D., Huang, H., Zang, X., & Mo, X. (2017). Brain development and Akt signaling: The crossroads of signaling pathway and neurodevelopmental diseases. *Journal of Molecular Neuroscience*, *61*, 379–384.

Wieczorek, D., Bögershausen, N., Beleggia, F., Steiner-Haldenstätt, S., Pohl, E., Li, Y., … Wollnik, B. (2013). A comprehensive molecular study on Coffin-Siris and Nicolaides-Baraitser syndromes identifies a broad molecular and clinical spectrum converging on altered chromatin remodeling. *Human Molecular Genetics*, *22*, 5121–5135.

Wolff, D., Endele, S., Azzarello-Burri, S., Hoyer, J., Zweier, M., Schanze, I., … Zweier, C. (2011). In-frame deletion and missense mutations of the C-terminal helicase domain of *SMARCA2* in three patients with Nicolaides-Baraitser Syndrome. *Molecular Syndromology, 2,* 237–244.

Wu, J. I., Lessard, J., Olave, I. A., Qiu, Z., Ghosh, A., Graef, I. A., & Crabtree, G. R. (2007). Regulation of dendritic development by neuron-specific chromatin remodeling complexes. *Neuron*, *56*, 94–108.

Wu, Y., Bolduc, F.V., Bell, K., Tully, T., Fang, Y., Sehgal, A., & Fischer, J.A. (2008). A *Drosophila* model for Angelman syndrome. *Proceedings of the National Academy of Sciences, 105,* 12399-12404.

Xiao, Q., Komori, H., & Lee, C. (2012). *klumpfuss* distinguishes stem cells from progenitor cells during asymmetric neuroblast division. *Development*, *139*, 2670–2680.

Yaniv, S. P., & Schuldiner, O. (2016). A fly's view of neuronal remodeling. *Developmental Biology*, *5*, 618–635.

Yin, J. C. P., & Tully, T. (1996). CREB and the formation of long-term memory. *Current Opinion in Neurobiology*, *6*, 264–268.

Yoo, A. S., Staahl, B. T., Chen, L., & Crabtree, G. R. (2009). MicroRNA-mediated switching of chromatin-remodelling complexes in neural development. *Nature*, *460*, 642–646.

Yoo, S. J., Huh, J. R., Muro, I., Yu, H., Wang, L., Wang, S. L., … Hay, B. A. (2002). Hid, Rpr and Grim negatively regulate DIAP1 levels through distinct mechanisms. *Nature Cell Biology*, *4*, 416–424.

Yu, G., Wang, L., & He, Q. (2015). ChIPseeker : an R / Bioconductor package for ChIP peak annotation, comparison and visualization. *Bioinformatics*, *31*, 2382–2383.

Yudkovsky, N., Logie, C., Hahn, S., & Peterson, C.L. (1999). Recruitment of the SWI/SNF chromatin remodeling complex by transcriptional activators. *Genes and Development, 13,* 2369-2374.

Zhang, J., Tanenhaus, A. K., Davis, J. C., Hanlon, B. M., & Yin, J. C. P. (2015). Spatio-temporal *in vivo* recording of dCREB2 dynamics in *Drosophila* long-term memory processing. *Neurobiology of Learning and Memory*, *0*, 80–88.

Zhang, Y., Liu, T., Meyer, C. A., Eeckhoute, J., Johnson, D. S., Bernstein, B. E., … Liu, X. S. (2008). Model-based Analysis of ChIP-Seq (MACS). *Genome Biology*, (9), R137. https://doi.org/10.1186/gb-2008-9-9-r137

Zheng, Xiaoyan, Wang, J., Haerry, T. E., Wu, A. Y.-H., Martin, J., O'Connor, M. B., … Lee, T. (2003). TGF-beta signaling activates steroid hormone receptor expression during neuronal remodeling in the Drosophila brain. *Cell*, *112*, 303–315.

Zheng, Xinde, Boyer, L., Jin, M., Mertens, J., Kim, Y., Ma, L., … Hunter, T. (2016). Metabolic reprogramming during neuronal differentiation from aerobic glycolysis to neuronal oxidative phosphorylation. *ELife*, *5*, e13374.

Zovkic, I. B., Paulukaitis, B. S., Day, J. J., Etikala, D. M., & Sweatt, D. J. (2016). Histone H2A.Z subunit exchange controls consolidation of recent and remote memory. *Nature*, *515*, 582–586.

Zraly, C. B., Middleton, F. A., & Dingwall, A. K. (2006). Hormone-response genes are direct in vivo regulatory targets of Brahma (SWI/SNF) Complex function. *The Journal of Biological Chemistry*, *281*, 35305–35315.

Appendices

Appendix A List of fly stocks used in this project

Stock #	Genotype	Source	Description
Genetic Tools			
48667	*w^{1118} P{$y^{+t7.7}$ w^{+mC}=GMR14H06-GAL4}attP2*	BDSC	*R14H06-GAL4*: Expresses GAL4 under the control of a rut (FBgn0003301) enhancer
5137	*y^1 w*; P{w w^{+mC}=UAS-mCD8::GFP.L}LL5,P{UASmCD8::GFP.L}2*	BDSC	*UAS-mCD8::GFP*: Expressed mCD8::GFP under UAS control
N/A	*y^1 v^1; P{UAS-Unc84::2XGFP}attP2*	G.L. Henry (2012)	*UAS-Unc84::GFP*: Expresses Unc84::GFP under UAS control
24650	*w^{1118}; P{w^{+mC}=UAS-Dcr2-D}2*	BDSC	*UAS-Dicer2*: Expresses Dicer2 under UAS control
Control			
35785	*y^1 sc* v^1; P{$y^{+7.7}$ $v^{+1.8}$=VALIUM20-mCherry}attP2*	BDSC	*UAS-mCherry^{RNAi}*: RNAi targeting mCherry (not in *Drosophila* genome) under UAS control. Used as control.
SWI/SNF RNAi			
32503	*y^1 sc* v^1; P{TRiP.HMS00507}attP2*	BDSC	*UAS-Bap60^{RNAi}*: RNAi targeting Bap60 under UAS control
32346	*y^1 sc* v^1; P{TRiP.HMS00337}attP2*	BDSC	*UAS-E(y)3^{RNAi}*: RNAi targeting E(y)3 under UAS control
32372	*y^1 sc* v^1; P{TRiP.HMS00363}attP2*	BDSC	*UAS-Snr1^{RNAi}*: RNAi targeting Snr1 under UAS control
EcR-B1 Dominant Negative			

6872	*w^{1118}; P{w^{+mC}=UAS-EcR.B1-DeltaC655.W650A}TP1-9*	BDSC	*UAS-EcR-B1^{DN}*: Dominant negative form of EcR-B1 under UAS control
UPS RNAi			
44560	*y^1 v^1; P{$y^{+t7.7}$ $v^{+t1.8}$=TRiP.HMS02856}attP40*	BDSC	*UAS-Prosα2^{RNAi}*: RNAi targeting Prosα2 under UAS control
34342	*y^1 sc* v^1 sev^{21}; P{$y^{+t7.7}$ $v^{+t1.8}$=TRiP.HMS01330}attP2*	BDSC	*UAS-Rpt6R^{RNAi}*: RNAi targeting Rpt6R under UAS control
105002 KK	*P{KK112643}VIE-260B*	VDRC	*UAS-Rpt6R^{RNAi}*: RNAi targeting Rpt6R under UAS control
34566	*y^1 sc* v^1 sev^{21}; P{$y^{+t7.7}$ $v^{+t1.8}$=TRiP.HMS01039}attP2*	BDSC	*UAS-Rpn10^{RNAi}*: RNAi targeting Rpn10 under UAS control
330448	*P{VSH330448}attP40*	VDRC	*UAS-Rpn10^{RNAi}*: RNAi targeting Rpn10 under UAS control
33662	*y^1 sc* v^1 sev^{21}; P{$y^{+t7.7}$ $v^{+t1.8}$=TRiP.HMS00071}attP2*	BDSC	*UAS-Rpn11^{RNAi}*: RNAi targeting Rpn11 under UAS control
19272 GD	*w^{1118}; P{GD8888}v19272*	VDRC	*UAS-Rpn11^{RNAi}*: RNAi targeting Rpn11 under UAS control
35433	*y^1 sc* v^1 sev^{21}; P{$y^{+t7.7}$ $v^{+t1.8}$=TRiP.GL00357}attP2*	BDSC	*UAS-Uch-L5^{RNAi}*: RNAi targeting Uch-L5 under UAS control
64681	*y^1 sc* v^1 sev^{21}; P{$y^{+t7.7}$ $v^{+t1.8}$=TRiP.HMC05716}attP2*	BDSC	*UAS-Uch-L5^{RNAi}*: RNAi targeting Uch-L5 under UAS control
80391	*y^1 v^1; P{$y^{+t7.7}$ $v^{+t1.8}$=TRiP.HMC06627}attP40*	BDSC	*UAS-Uch^{RNAi}*: RNAi targeting Uch under UAS control
55955	*y^1 sc* v^1 sev^{21}; P{$y^{+t7.7}$ $v^{+t1.8}$=TRiP.HMC04244}attP2*	BDSC	*UAS-Urm1^{RNAi}*: RNAi targeting Urm1 under UAS control

63997	*y^1 v^1; P{$y^{+t7.7}$ $v^{+t1.8}$=TRiP.HMJ30310}attP40/CyO*	BDSC	*UAS-Uba4^{RNAi}*: RNAi targeting Uba4 under UAS control
76066	*y^1 v^1; P{$y^{+t7.7}$ $v^{+t1.8}$=TRiP.HMS05878}attP40*	BDSC	*UAS-Uba1^{RNAi}*: RNAi targeting Uba1 under UAS control
25957	*y^1 v^1; P{$y^{+t7.7}$ $v^{+t1.8}$=TRiP.JF01977}attP40*	BDSC	*UAS-Uba1^{RNAi}*: RNAi targeting Uba1 under UAS control
31136	*y^1 v^1; P{$y^{+t7.7}$ $v^{+t1.8}$=TRiP.JF01611}attP40*	BDSC	*UAS-Plap^{RNAi}*: RNAi targeting Plap under UAS control
67871	*y^1 sc* v^1 sev^{21}; P{$y^{+t7.7}$ $v^{+t1.8}$=TRiP.HMS05685}attP2*	BDSC	*UAS-Plap^{RNAi}*: RNAi targeting Plap under UAS control
55217	*y^1 v^1; P{$y^{+t7.7}$ $v^{+t1.8}$=TRiP.GLC01834}attP40*	BDSC	*UAS-Prosα3^{RNAi}*: RNAi targeting Prosα3 under UAS control
77145	*y^1 sc* v^1 sev^{21}; P{$y^{+t7.7}$ $v^{+t1.8}$=TRiP.HMS05889}attP2*	BDSC	*UAS-Prosα3^{RNAi}*: RNAi targeting Prosα3 under UAS control
30503	*y^1 sc* v^1 sev^{21}; P{$y^{+t7.7}$ $v^{+t1.8}$=TRiP.HM05247}attP2/TM3,Sb^1*	BDSC	*UAS-Rpn3^{RNAi}*: RNAi targeting Rpn3 under UAS control
34561	*y^1 sc* v^1 sev^{21}; P{$y^{+t7.7}$ $v^{+t1.8}$=TRiP.HMS01033}attP2*	BDSC	*UAS-Rpn3^{RNAi}*: RNAi targeting Rpn3 under UAS control
34824	*y^1 sc* v^1 sev^{21}; P{$y^{+t7.7}$ $v^{+t1.8}$=TRiP.HMS00139}attP2/TM3,Sb^1*	BDSC	*UAS-Prosβ1^{RNAi}*: RNAi targeting Prosβ1 under UAS control
34795	*y^1 sc* v^1 sev^{21}; P{$y^{+t7.7}$ $v^{+t1.8}$=TRiP.HMS00104}attP2*	BDSC	*UAS-Rpt2^{RNAi}*: RNAi targeting Rpt2 under UAS control
36063	*y^1 sc* v^1 sev^{21}; P{$y^{+t7.7}$ $v^{+t1.8}$=TRiP.GL00341}attP2*	BDSC	*UAS-Prosα4^{RNAi}*: RNAi targeting Prosα4 under UAS control
65161	*y^1 sc* v^1 sev^{21}; P{$y^{+t7.7}$ $v^{+t1.8}$=TRiP.HMC06039}attP2*	BDSC	*UAS-Prosα4^{RNAi}*: RNAi targeting Prosα4 under UAS control

34348	*y^1 sc* v^1 sev^{21}; P{$y^{+t7.7}$ $v^{+t1.8}$=TRiP.HMS01337}attP2*	BDSC	*UAS-Rpn1^{RNAi}*: RNAi targeting Rpn1 under UAS control
31567	*y^1 v^1; P{$y^{+t7.7}$ $v^{+t1.8}$=TRiP.JF01140}attP40*	BDSC	*UAS-Rpn8^{RNAi}*: RNAi targeting Rpn8 under UAS control
35411	*y^1 sc* v^1 sev^{21}; P{$y^{+t7.7}$ $v^{+t1.8}$=TRiP.GL00333}attP2*	BDSC	*UAS-Rpn8^{RNAi}*: RNAi targeting Rpn8 under UAS control
32422	*y^1 sc* v^1 sev^{21}; P{$y^{+t7.7}$ $v^{+t1.8}$=TRiP.HMS00417}attP2/TM3,Sb^1*	BDSC	*UAS-Rpt5^{RNAi}*: RNAi targeting Rpt5 under UAS control
53886	*y^1 v^1; P{$y^{+t7.7}$ $v^{+t1.8}$=TRiP.HMJ21204}attP40*	BDSC	*UAS-Rpt5^{RNAi}*: RNAi targeting Rpt5 under UAS control
32874	*y^1 sc* v^1 sev^{21}; P{$y^{+t7.7}$ $v^{+t1.8}$=TRiP.HMS00661}attP2*	BDSC	*UAS-Rpt4^{RNAi}*: RNAi targeting Rpt4 under UAS control
34811	*y^1 sc* v^1 sev^{21}; P{$y^{+t7.7}$ $v^{+t1.8}$=TRiP.HMS00120}attP2*	BDSC	*UAS-Prosα6^{RNAi}*: RNAi targeting Prosα6 under UAS control
53974	*y^1 v^1; P{$y^{+t7.7}$ $v^{+t1.8}$=TRiP.HMJ21359}attP40*	BDSC	*UAS-Prosα6^{RNAi}*: RNAi targeting Prosα6 under UAS control
34917	*y^1 sc* v^1 sev^{21}; P{$y^{+t7.7}$ $v^{+t1.8}$=TRiP.HMS01265}attP2*	BDSC	*UAS-Rpt3^{RNAi}*: RNAi targeting Rpt3 under UAS control
53262	*y^1 v^1; P{$y^{+t7.7}$ $v^{+t1.8}$=TRiP.GLC01823}attP40*	BDSC	*UAS-Usp14^{RNAi}*: RNAi targeting Usp14 under UAS control
66956	*y^1 v^1; P{$y^{+t7.7}$ $v^{+t1.8}$=TRiP.HMS05422}attP40*	BDSC	*UAS-Usp14^{RNAi}*: RNAi targeting Usp14 under UAS control
31251	*y^1 v^1; P{$y^{+t7.7}$ $v^{+t1.8}$=TRiP.JF01768}attP40*	BDSC	*UAS-kel^{RNAi}*: RNAi targeting kel under UAS control
55168	*y^1 sc* v^1 sev^{21}; P{$y^{+t7.7}$ $v^{+t1.8}$=TRiP.HMC03847}attP2*	BDSC	*UAS-ScsβA^{RNAi}*: RNAi targeting ScsβA under UAS control

Appendix B List of primers used in this study

Custom PCR primers for ATAC-Seq. Sequences in red are unique sample indices.

Sample Barcode	Primer
Ad1_noMX *	AATGATACGGCGACCACCGAGATCTACACTCGTCGGCAGCGTCAGATGTG
Ad2.1_TAAGGCGA	CAAGCAGAAGACGGCATACGAGAT**TCGCCTTA**GTCTCGTGGGCTCGGAGATGT
Ad2.2_CGTACTAG	CAAGCAGAAGACGGCATACGAGAT**CTAGTACG**GTCTCGTGGGCTCGGAGATGT
Ad2.3_AGGCAGAA	CAAGCAGAAGACGGCATACGAGAT**TTCTGCCT**GTCTCGTGGGCTCGGAGATGT
Ad2.4_TCCTGAGC	CAAGCAGAAGACGGCATACGAGAT**GCTCAGGA**GTCTCGTGGGCTCGGAGATGT
Ad2.5_GGACTCCT	CAAGCAGAAGACGGCATACGAGAT**AGGAGTCC**GTCTCGTGGGCTCGGAGATGT
Ad2.6_TAGGCATG	CAAGCAGAAGACGGCATACGAGAT**CATGCCTA**GTCTCGTGGGCTCGGAGATGT
Ad2.7_CTCTCTAC	CAAGCAGAAGACGGCATACGAGAT**GTAGAGAG**GTCTCGTGGGCTCGGAGATGT
Ad2.8_CAGAGAGG	CAAGCAGAAGACGGCATACGAGAT**CCTCTCTG**GTCTCGTGGGCTCGGAGATGT
Ad2.9_GCTACGCT	CAAGCAGAAGACGGCATACGAGAT**AGCGTAGC**GTCTCGTGGGCTCGGAGATGT
Ad2.10_CGAGGCTG	CAAGCAGAAGACGGCATACGAGAT**CAGCCTCG**GTCTCGTGGGCTCGGAGATGT
Ad2.11_AAGAGGCA	CAAGCAGAAGACGGCATACGAGAT**TGCCTCTT**GTCTCGTGGGCTCGGAGATGT
Ad2.12_GTAGAGGA	CAAGCAGAAGACGGCATACGAGAT**TCCTCTAC**GTCTCGTGGGCTCGGAGATGT
Ad2.13_GTCGTGAT	CAAGCAGAAGACGGCATACGAGAT**ATCACGAC**GTCTCGTGGGCTCGGAGATGT
Ad2.14_ACCACTGT	CAAGCAGAAGACGGCATACGAGAT**ACAGTGGT**GTCTCGTGGGCTCGGAGATGT
Ad2.15_TGGATCTG	CAAGCAGAAGACGGCATACGAGAT**CAGATCCA**GTCTCGTGGGCTCGGAGATGT
Ad2.16_CCGTTTGT	CAAGCAGAAGACGGCATACGAGAT**ACAAACGG**GTCTCGTGGGCTCGGAGATGT
Ad2.17_TGCTGGGT	CAAGCAGAAGACGGCATACGAGAT**ACCCAGCA**GTCTCGTGGGCTCGGAGATGT
Ad2.18_GAGGGGTT	CAAGCAGAAGACGGCATACGAGAT**AACCCCTC**GTCTCGTGGGCTCGGAGATGT

Ad2.19_AGGTTGGG	CAAGCAGAAGACGGCATACGAGAT**CCCAACCT**GTCTCGTGGGCT CGGAGATGT
Ad2.20_GTGTGGTG	CAAGCAGAAGACGGCATACGAGAT**CACCACAC**GTCTCGTGGGCT CGGAGATGT
Ad2.21_TGGGTTTC	CAAGCAGAAGACGGCATACGAGAT**GAAACCCA**GTCTCGTGGGC TCGGAGATGT
Ad2.22_TGGTCACA	CAAGCAGAAGACGGCATACGAGAT**TGTGACCA**GTCTCGTGGGCT CGGAGATGT
Ad2.23_TTGACCCT	CAAGCAGAAGACGGCATACGAGAT**AGGGTCAA**GTCTCGTGGGC TCGGAGATGT
Ad2.24_CCACTCCT	CAAGCAGAAGACGGCATACGAGAT**AGGAGTGG**GTCTCGTGGGC TCGGAGATGT

RT-qPCR primers

Gene	Forward Primer	Reverse Primer
Ldh	AGATCCTGACTCCCACCGAA	GCCTGGACATCGGACATGAT
MFS3	GCCTCCAATGTGACGGCTAA	GTAGCAGCTCAGCAGGGTTC
sls	ATCTCCTATTCGAGTGGAGTGG	CCCTGCAAATTCTCGGCAAG
dysf	CGGAGATAGCCAATCTGAGG	GCTTTCCGCACATAGACACA
tmod	GCAAGGATCTGAGTGAGTACGA	GCCAGTATGGTTATCTCCTCGG
Obp56d	TCCAGCCCGATGTCGTTCT	CCCTTGGTGGCATCACACT
prt	ATGTCGGAGAAATCGAACCGT	GGGGCATTCAGTTGAACAGC
jdp	GGAAACCTTGTGCGATCCC	AGCCACTGTTTGTAGCTCATC
sNPF	CGATCTGGGTGCCGACTAC	CCTCGAACTGAGGAACACTGC
Est-6	TGGGACTGGGACTTATCATTGT	CTGCACCAACAGAGGGTCATC
Salm	GAGCAAAGCACACCAGACCA	ATCGCCACTCTGTTGTTGTTAT
Sosie	ATGGTGTGCCAGTACGAGAAC	TCGCAGAGACACAGCTTGG
kn	CGCGCCCACTTTGAAAAGC	GTTGTCCAGCCCGATCATATAAG
Pvf1	CTGTCCGTGTCCGCTGAG	CTCGCCGGACACATCGTAG
eIF2β	CAGACCCTTAACTTTAGCTCCG	GATGGTCAAATCTGAGACCTGG
βCOP	AGCGGGTAATCAAGTTGCTG	GGCAGGACGAAGCGTATGA

Appendix C MB-specific genes identified using INTACT in larvae and adults

MB-enriched genes Larval					
Gene Symbol	**Flybase ID**	**Gene Symbol**	**Flybase ID**	**Gene Symbol**	**Flybase ID**
a	FBgn0000008	CG14274	FBgn0032023	CG7582	FBgn0039681
mAChR-A	FBgn0000037	jp	FBgn0032129	AdoR	FBgn0039747
nAChRbeta1	FBgn0000038	TBC1D16	FBgn0032249	Rpt6R	FBgn0039788
Act57B	FBgn0000044	CG17108	FBgn0032285	CG15546	FBgn0039807
Act87E	FBgn0000046	CG16854	FBgn0032338	CG11317	FBgn0039816
Ald	FBgn0000064	kek4	FBgn0032484	CG1674	FBgn0039897
b	FBgn0000153	Trpgamma	FBgn0032593	CG1909	FBgn0039911
Pka-C1	FBgn0000273	CG13284	FBgn0032614	c11.1	FBgn0040236
Ddc	FBgn0000422	CG17350	FBgn0032772	Ugt86Dh	FBgn0040252
Hr3	FBgn0000448	Hasp	FBgn0032797	CG17193	FBgn0040571
dnc	FBgn0000479	CG10132	FBgn0032798	CG8012	FBgn0040832
Eip74EF	FBgn0000567	sNPF	FBgn0032840	CG12994	FBgn0040877
ImpL3	FBgn0001258	CG16798	FBgn0032856	hoe1	FBgn0041150
Ca-alpha1D	FBgn0001991	CG10947	FBgn0032857	7B2	FBgn0041707
l(3)mbt	FBgn0002441	CG9338	FBgn0032899	yellow-e	FBgn0041711
Lcp1	FBgn0002531	CG14401	FBgn0032900	yellow-c	FBgn0041713
Mp20	FBgn0002789	tadr	FBgn0032911	prt	FBgn0043005
Pgi	FBgn0003074	CG8245	FBgn0033031	Proc	FBgn0045038
Pkc53E	FBgn0003091	Tsp42Ei	FBgn0033130	GluRIIC	FBgn0046113
Prm	FBgn0003149	Gadd45	FBgn0033153	CG30158	FBgn0050158
rdgB	FBgn0003218	Corin	FBgn0033192	mtt	FBgn0050361
rib	FBgn0003254	CG11191	FBgn0033249	CG30419	FBgn0050419
rut	FBgn0003301	CG14762	FBgn0033250	CG31030	FBgn0051030
Sgs1	FBgn0003372	CG12769	FBgn0033252	Nlg1	FBgn0051146
Sgs3	FBgn0003373	sand	FBgn0033257	CG31191	FBgn0051191
Sgs5	FBgn0003375	CG8248	FBgn0033347	GluRIIE	FBgn0051201
Sgs7	FBgn0003377	CG13954	FBgn0033405	CG31221	FBgn0051221
Sgs8	FBgn0003378	CG1648	FBgn0033446	dpr17	FBgn0051361
Sh	FBgn0003380	KCNQ	FBgn0033494	NKCC	FBgn0051547
Shaw	FBgn0003386	CG12910	FBgn0033502	wry	FBgn0051665
slo	FBgn0003429	CAP	FBgn0033504	RluA-1	FBgn0051719
spir	FBgn0003475	CG13227	FBgn0033589	NA	FBgn0051728
sr	FBgn0003499	Cpr47Eb	FBgn0033598	CG31760	FBgn0051760
betaTub85D	FBgn0003889	Sln	FBgn0033657	dpr10	FBgn0052057
NA	FBgn0004028	CG8888	FBgn0033679	CG32085	FBgn0052085
Tm2	FBgn0004117	CG8850	FBgn0033708	Ptip	FBgn0052133
up	FBgn0004169	Cpr49Ag	FBgn0033730	Ccn	FBgn0052183

Rdl	FBgn0004244	CG3955	FBgn0033793	CG32206	FBgn0052206
Mdr65	FBgn0004513	CG4676	FBgn0033815	CG32248	FBgn0052248
Akh	FBgn0004552	mip120	FBgn0033846	CG32333	FBgn0052333
Edg91	FBgn0004554	Syngr	FBgn0033876	CG32392	FBgn0052392
Syn	FBgn0004575	DJ-1alpha	FBgn0033885	PVRAP	FBgn0052406
Eig71Ee	FBgn0004592	Dh44-R1	FBgn0033932	CG32432	FBgn0052432
Plc21C	FBgn0004611	CG12866	FBgn0033955	CG32506	FBgn0052506
GluRIIA	FBgn0004620	jef	FBgn0033958	CG32547	FBgn0052547
RYa-R	FBgn0004842	Hr51	FBgn0034012	CG32557	FBgn0052557
Ac76E	FBgn0004852	Cyp4aa1	FBgn0034053	dpr8	FBgn0052600
ey	FBgn0005558	Asph	FBgn0034075	Muc12Ea	FBgn0052602
Rab3	FBgn0005586	Mctp	FBgn0034389	CG32647	FBgn0052647
Sox14	FBgn0005612	CG9313	FBgn0034566	CG32683	FBgn0052683
trpl	FBgn0005614	CG15651	FBgn0034567	Hs3st-A	FBgn0053147
bt	FBgn0005666	Swim	FBgn0034709	CG33203	FBgn0053203
CanB	FBgn0010014	PIP5K59B	FBgn0034789	Dop2R	FBgn0053517
CanA1	FBgn0010015	GlyT	FBgn0034911	Unc-89	FBgn0053519
Nmdar1	FBgn0010399	CG5597	FBgn0034920	CG33543	FBgn0053543
TpnC73F	FBgn0010424	CG13575	FBgn0034996	Rim	FBgn0053547
l(2)01289	FBgn0010482	CG13594	FBgn0035041	CG33985	FBgn0053985
Dif	FBgn0011274	ST6Gal	FBgn0035050	Mid1	FBgn0053988
RyR	FBgn0011286	Kah	FBgn0035144	CG34114	FBgn0083950
Dop1R1	FBgn0011582	CG12502	FBgn0035171	Nlg3	FBgn0083963
Elk	FBgn0011589	CG1139	FBgn0035300	CG34219	FBgn0085248
Mef2	FBgn0011656	FMRFaR	FBgn0035385	Vml	FBgn0085362
NA	FBgn0012042	CG14964	FBgn0035410	bma	FBgn0085385
Hsp70Ba	FBgn0013278	CG14982	FBgn0035477	CG34357	FBgn0085386
nSyb	FBgn0013342	CG1299	FBgn0035501	Shawl	FBgn0085395
igl	FBgn0013467	VhaM9.7-a	FBgn0035521	TrissinR	FBgn0085410
ND2	FBgn0013680	DopEcR	FBgn0035538	CG34384	FBgn0085413
ND6	FBgn0013685	CG13722	FBgn0035553	dpr12	FBgn0085414
phyl	FBgn0013725	Lkr	FBgn0035610	CG34396	FBgn0085425
Gycalpha99B	FBgn0013972	CG10483	FBgn0035649	Rgk3	FBgn0085426
Gycbeta100B	FBgn0013973	axed	FBgn0035708	CG34402	FBgn0085431
Calx	FBgn0013995	CG8519	FBgn0035711	stmA	FBgn0086784
tim	FBgn0014396	unc-13-4A	FBgn0035756	sls	FBgn0086906
Hr38	FBgn0014859	frac	FBgn0035798	Rab26	FBgn0086913
Ag5r	FBgn0015010	CG6282	FBgn0035914	5-HT2A	FBgn0087012
alpha-Est8	FBgn0015576	S-Lap1	FBgn0035915	CG42232	FBgn0250754
alpha-Est9	FBgn0015577	Zasp66	FBgn0035917	CG33521	FBgn0250819
lbm	FBgn0016032	Cpr67B	FBgn0035985	CG2016	FBgn0250839

nompA	FBgn0016047	CG14142	FBgn0036143	beat-VII	FBgn0250908
vri	FBgn0016076	Muc68Ca	FBgn0036181	Octbeta3R	FBgn0250910
nompC	FBgn0016920	CrzR	FBgn0036278	futsch	FBgn0259108
qm	FBgn0019662	Ent3	FBgn0036319	Ndae1	FBgn0259111
mspo	FBgn0020269	CG10154	FBgn0036361	CG42260	FBgn0259145
TM4SF	FBgn0020372	CG14109	FBgn0036364	fid	FBgn0259146
Tsf1	FBgn0022355	CG10738	FBgn0036368	CG42313	FBgn0259213
Sodh-2	FBgn0022359	CG10089	FBgn0036369	RhoGAP102A	FBgn0259216
Pka-R2	FBgn0022382	CG10710	FBgn0036377	CG42319	FBgn0259219
amon	FBgn0023179	CG8745	FBgn0036381	CG42322	FBgn0259222
CG17778	FBgn0023534	CG17364	FBgn0036391	CCKLR-17D1	FBgn0259231
Ac78C	FBgn0024150	upSET	FBgn0036398	CG42339	FBgn0259241
gprs	FBgn0024232	CG5830	FBgn0036556	sqa	FBgn0259678
RSG7	FBgn0024941	CG13055	FBgn0036583	Pkcdelta	FBgn0259680
Oamb	FBgn0024944	Cyp312a1	FBgn0036778	CG42402	FBgn0259821
CG2680	FBgn0024995	CG14075	FBgn0036835	Ca-beta	FBgn0259822
Rab27	FBgn0025382	CG14086	FBgn0036860	CG42450	FBgn0259927
PH4alphaMP	FBgn0026190	Gbs-76A	FBgn0036862	CG42534	FBgn0260487
Ndg	FBgn0026403	CG9452	FBgn0036877	Mp	FBgn0260660
GABA-B-R2	FBgn0027575	CG9368	FBgn0036890	CG42588	FBgn0260965
CG5867	FBgn0027586	CG14186	FBgn0036935	Syt14	FBgn0261086
CG1688	FBgn0027589	CG13248	FBgn0036984	Sytalpha	FBgn0261089
CG2082	FBgn0027608	Cpr78E	FBgn0037114	Sytbeta	FBgn0261090
jdp	FBgn0027654	CG14572	FBgn0037128	NA	FBgn0261548
kek3	FBgn0028370	SLC22A	FBgn0037140	CG42675	FBgn0261561
Tob	FBgn0028397	CG11370	FBgn0037181	CG42700	FBgn0261611
GluRIID	FBgn0028422	CG1090	FBgn0037238	SLO2	FBgn0261698
CG30116	FBgn0028496	CG1113	FBgn0037304	kcc	FBgn0261794
CG3530	FBgn0028497	CG14669	FBgn0037326	CG42750	FBgn0261804
Nckx30C	FBgn0028704	Neurochondrin	FBgn0037447	CG42788	FBgn0261859
nAChRalpha5	FBgn0028875	CG15186	FBgn0037448	CG42795	FBgn0261928
CG33090	FBgn0028916	thw	FBgn0037487	CG42817	FBgn0261999
Patsas	FBgn0029137	CG3014	FBgn0037519	CG42822	FBgn0262004
SPR	FBgn0029768	CG2993	FBgn0037521	bru2	FBgn0262475
CG4660	FBgn0029839	mAChR-B	FBgn0037546	Rbp	FBgn0262483
Nep1	FBgn0029843	CG9626	FBgn0037565	CG43102	FBgn0262562
CG14445	FBgn0029851	Cyp313b1	FBgn0037601	Shab	FBgn0262593
CG15894	FBgn0029864	CG9801	FBgn0037623	Sap130	FBgn0262714
CG12541	FBgn0029930	Task7	FBgn0037690	Pal2	FBgn0262728
CG4607	FBgn0029932	CG16779	FBgn0037698	Gfrl	FBgn0262869
dpr14	FBgn0029974	CG8301	FBgn0037717	cac	FBgn0263111

fend	FBgn0030090	CG12950	FBgn0037736	tx	FBgn0263118
SmydA-9	FBgn0030102	CG8500	FBgn0037754	Cngl	FBgn0263257
CG15247	FBgn0030156	CG14688	FBgn0037819	CG11000	FBgn0263353
SmydA-4	FBgn0030257	CG14695	FBgn0037850	CG42784	FBgn0263354
hec	FBgn0030437	dpr5	FBgn0037908	NA	FBgn0263376
CG13403	FBgn0030544	GstD11	FBgn0038029	Ih	FBgn0263397
CG9413	FBgn0030574	Octbeta2R	FBgn0038063	CG43707	FBgn0263846
Rab3-GEF	FBgn0030613	CG6753	FBgn0038070	CG43729	FBgn0263980
Lrp4	FBgn0030706	CG11668	FBgn0038113	GluRIB	FBgn0264000
CG4678	FBgn0030778	CG9813	FBgn0038143	dysc	FBgn0264006
CG5162	FBgn0030828	CG9297	FBgn0038181	Slob	FBgn0264087
CG12990	FBgn0030859	CCHa1	FBgn0038199	NA	FBgn0264255
CCKLR-17D3	FBgn0030954	CG14356	FBgn0038207	CG43897	FBgn0264489
CG7058	FBgn0030961	CG14853	FBgn0038246	Fife	FBgn0264606
CG7378	FBgn0030976	CG14855	FBgn0038260	Mhc	FBgn0264695
CG12531	FBgn0031064	dpr9	FBgn0038282	Rgk1	FBgn0264753
CG9572	FBgn0031089	AOX4	FBgn0038350	Pde1c	FBgn0264815
CG4213	FBgn0031251	CG8925	FBgn0038404	NA	FBgn0264857
CG11835	FBgn0031264	CG14880	FBgn0038422	CG44085	FBgn0264894
IA-2	FBgn0031294	CG7587	FBgn0038523	pHCl-1	FBgn0264908
CG4577	FBgn0031306	TyrRII	FBgn0038541	CG44153	FBgn0265002
MFS3	FBgn0031307	TyrR	FBgn0038542	St3	FBgn0265052
CG5080	FBgn0031313	CG7708	FBgn0038641	CG44245	FBgn0265180
CG15385	FBgn0031397	CG18208	FBgn0038653	CG44247	FBgn0265182
CG31689	FBgn0031449	unc79	FBgn0038693	Vha68-1	FBgn0265262
CG10019	FBgn0031568	CG17190	FBgn0038761	tn	FBgn0265356
CG15431	FBgn0031602	CG5023	FBgn0038774	CG44422	FBgn0265595
CG12194	FBgn0031636	Ktl	FBgn0038839	rad	FBgn0265597
hoe2	FBgn0031649	Nrx-1	FBgn0038975	Ric	FBgn0265605
CG14024	FBgn0031697	Octbeta1R	FBgn0038980	rdgC	FBgn0265959
CG9021	FBgn0031747	CG10175	FBgn0039084	Dop1R2	FBgn0266137
CG13999	FBgn0031753	beat-IV	FBgn0039089	NA	FBgn0266180
CG13995	FBgn0031770	CG13650	FBgn0039277	NA	FBgn0266227
Daxx	FBgn0031820	CG11852	FBgn0039297	CngB	FBgn0266346
CG11319	FBgn0031835	CG5890	FBgn0039380	CG45067	FBgn0266437
CG11221	FBgn0031855	CG6142	FBgn0039415	CG45076	FBgn0266446
LUBEL	FBgn0031857	CG6403	FBgn0039453	CG45263	FBgn0266801
CG18304	FBgn0031869	CG5646	FBgn0039525	NA	FBgn0266901
CG5171	FBgn0031907	Tusp	FBgn0039530	unc-104	FBgn0267002
CG5177	FBgn0031908	unc80	FBgn0039536	CG32700	FBgn0267253
CG6055	FBgn0031918	CG11898	FBgn0039645	Glut4EF	FBgn0267336

Scgalpha	FBgn0032013	jus	FBgn0039647		

MB-enriched genes Adult					
Gene Symbol	**Flybase ID**	**Gene Symbol**	**Flybase ID**	**Gene Symbol**	**Flybase ID**
a	FBgn0000008	CG10362	FBgn0030358	Nlg1	FBgn0051146
Act87E	FBgn0000046	hec	FBgn0030437	CG31191	FBgn0051191
Pka-C1	FBgn0000273	cactin	FBgn0031114	CG31523	FBgn0051523
cos	FBgn0000352	CG3625	FBgn0031245	CG31760	FBgn0051760
fz	FBgn0001085	CG4133	FBgn0031257	CG32204	FBgn0052204
Hsc70-3	FBgn0001218	CG11835	FBgn0031264	PVRAP	FBgn0052406
ImpL3	FBgn0001258	MFS3	FBgn0031307	Dop2R	FBgn0053517
Mp20	FBgn0002789	CG11319	FBgn0031835	Unc-89	FBgn0053519
Prm	FBgn0003149	CG11221	FBgn0031855	Shawl	FBgn0085395
rut	FBgn0003301	CG3838	FBgn0032130	Rgk3	FBgn0085426
NA	FBgn0003887	CG10132	FBgn0032798	CG34402	FBgn0085431
NA	FBgn0004028	sNPF	FBgn0032840	sls	FBgn0086906
Tm2	FBgn0004117	Hr51	FBgn0034012	Mlp60A	FBgn0259209
ey	FBgn0005558	Asph	FBgn0034075	CG42319	FBgn0259219
bt	FBgn0005666	CG5065	FBgn0034145	CG42339	FBgn0259241
dac	FBgn0005677	MFS16	FBgn0034611	Pka-R1	FBgn0259243
Dop1R1	FBgn0011582	CG6044	FBgn0034725	Pkcdelta	FBgn0259680
Elk	FBgn0011589	GlyT	FBgn0034911	CG42402	FBgn0259821
Hsp70Ba	FBgn0013278	yki	FBgn0034970	Hip14	FBgn0259824
phyl	FBgn0013725	Kah	FBgn0035144	dl	FBgn0260632
Hr38	FBgn0014859	GC	FBgn0035245	bond	FBgn0260942
CCT3	FBgn0015019	CG13921	FBgn0035267	Baldspot	FBgn0260960
BEAF-32	FBgn0015602	SP1173	FBgn0035710	Sytalpha	FBgn0261089
Rbf	FBgn0015799	tow	FBgn0035719	Ppcs	FBgn0261285
toy	FBgn0019650	CG6765	FBgn0035903	NA	FBgn0261548
qm	FBgn0019662	Zasp66	FBgn0035917	Sap130	FBgn0262714
mspo	FBgn0020269	CG5830	FBgn0036556	mub	FBgn0262737
Pka-R2	FBgn0022382	CG13055	FBgn0036583	SERCA	FBgn0263006
amon	FBgn0023179	CG9368	FBgn0036890	5-HT1B	FBgn0263116
CG3630	FBgn0023540	CG8500	FBgn0037754	CG43897	FBgn0264489
Ac78C	FBgn0024150	CG7708	FBgn0038641	Rgk1	FBgn0264753
gprs	FBgn0024232	SIFaR	FBgn0038880	tn	FBgn0265356
Oamb	FBgn0024944	Lgr3	FBgn0039354	rad	FBgn0265597
CG5867	FBgn0027586	dysf	FBgn0039411	coro	FBgn0265935
jdp	FBgn0027654	wat	FBgn0039620	CG44774	FBgn0266000

Dgp-1	FBgn0027836	jus	FBgn0039647	Dop1R2	FBgn0266137
CG2938	FBgn0029685	tamo	FBgn0041582	btsz	FBgn0266756
Nep1	FBgn0029843	prt	FBgn0043005	CG32700	FBgn0267253
CG15894	FBgn0029864	metro	FBgn0050021		
fend	FBgn0030090	CG30158	FBgn0050158		

Appendix D Differentially expressed genes in SWI/SNF-KD MB and EcR-B1^{DN} MB Larvae

Upregulated genes E(y)3-KD MB					
Gene Symbol	**Flybase ID**	**Gene Symbol**	**Flybase ID**	**Gene Symbol**	**Flybase ID**
nAChRalpha1	FBgn0000036	CG4502	FBgn0031896	CG31635	FBgn0051635
nAChRbeta1	FBgn0000038	CG7781	FBgn0032021	wry	FBgn0051665
cm	FBgn0000330	nAChRalpha6	FBgn0032151	CG31712	FBgn0051712
Hr3	FBgn0000448	Schip1	FBgn0032221	fred	FBgn0051774
E(Pc)	FBgn0000581	kek4	FBgn0032484	Cda5	FBgn0051973
ftz	FBgn0001077	CG10283	FBgn0032681	anne	FBgn0052000
g	FBgn0001087	sNPF	FBgn0032840	CG32017	FBgn0052017
gt	FBgn0001150	mRpS18B	FBgn0032849	CG32066	FBgn0052066
Ca-alpha1D	FBgn0001991	nrv3	FBgn0032946	Ndfip	FBgn0052177
rib	FBgn0003254	CG2225	FBgn0032957	CG32204	FBgn0052204
sei	FBgn0003353	Gadd45	FBgn0033153	CG32243	FBgn0052243
v	FBgn0003965	CG1358	FBgn0033196	Hers	FBgn0052529
Syt1	FBgn0004242	CG14762	FBgn0033250	Muc14A	FBgn0052580
svr	FBgn0004648	CG12913	FBgn0033500	CG32647	FBgn0052647
scrt	FBgn0004880	CG6329	FBgn0033872	CG32772	FBgn0052772
orb	FBgn0004882	VGAT	FBgn0033911	CG32944	FBgn0052944
gol	FBgn0004919	Usp20-33	FBgn0033916	CG33203	FBgn0053203
upd1	FBgn0004956	Arc2	FBgn0033928	dpr7	FBgn0053481
robo1	FBgn0005631	jef	FBgn0033958	CG33494	FBgn0053494
Ets21C	FBgn0005660	Hr51	FBgn0034012	upd3	FBgn0053542
comm	FBgn0010105	tun	FBgn0034046	CG33543	FBgn0053543
alpha-Cat	FBgn0010215	Mlf	FBgn0034051	NA	FBgn0053653
tutl	FBgn0010473	CG5065	FBgn0034145	CG40178	FBgn0058178
TrpRS	FBgn0010803	HPS4	FBgn0034261	NA	FBgn0058196
Sema1a	FBgn0011259	CG10911	FBgn0034295	CG13197	FBgn0062449
Elk	FBgn0011589	PIP5K59B	FBgn0034789	dyl	FBgn0066365
Nos	FBgn0011676	Orcokinin	FBgn0034935	CG34357	FBgn0085386
mtd	FBgn0013576	Pask	FBgn0034950	shakB	FBgn0085387

phyl	FBgn0013725	CG14982	FBgn0035477	pan	FBgn0085432
sced	FBgn0013732	CG12605	FBgn0035481	CG34409	FBgn0085438
Gycbeta100B	FBgn0013973	CG10289	FBgn0035688	sif	FBgn0085447
sty	FBgn0014388	CG10077	FBgn0035720	sra	FBgn0086370
Hr38	FBgn0014859	CG4328	FBgn0036274	lap	FBgn0086372
chn	FBgn0015371	Ent3	FBgn0036319	nAChRalpha7	FBgn0086778
toc	FBgn0015600	CG13055	FBgn0036583	mmd	FBgn0259110
CaMKI	FBgn0016126	CG18265	FBgn0036725	CG42313	FBgn0259213
Pdp1	FBgn0016694	CG8786	FBgn0036897	CG42324	FBgn0259224
klg	FBgn0017590	ICA69	FBgn0037050	CG42337	FBgn0259239
toy	FBgn0019650	CG10508	FBgn0037060	CG42339	FBgn0259241
NA	FBgn0019948	CG7166	FBgn0037107	CG42492	FBgn0259994
CG4050	FBgn0020312	CG12768	FBgn0037206	GABA-B-R1	FBgn0260446
Spred	FBgn0020767	CG14669	FBgn0037326	qvr	FBgn0260499
l(2)k01209	FBgn0022029	PEK	FBgn0037327	dpr21	FBgn0260995
amon	FBgn0023179	kat-60L1	FBgn0037375	stj	FBgn0261041
Ac3	FBgn0023416	CG17816	FBgn0037525	Syt14	FBgn0261086
CG32809	FBgn0023531	Ada2b	FBgn0037555	Sytalpha	FBgn0261089
Ac78C	FBgn0024150	GstZ2	FBgn0037697	Ppcs	FBgn0261285
gprs	FBgn0024232	CG16779	FBgn0037698	CG42700	FBgn0261611
Slip1	FBgn0024728	CG8301	FBgn0037717	fwe	FBgn0261722
Actbeta	FBgn0024913	CG14372	FBgn0038156	aPKC	FBgn0261854
CG3719	FBgn0024986	CG12402	FBgn0038202	CG42788	FBgn0261859
Mur2B	FBgn0025390	Pde6	FBgn0038237	FoxP	FBgn0262477
Sik2	FBgn0025625	dpr9	FBgn0038282	Rbp	FBgn0262483
unc-13	FBgn0025726	CG7708	FBgn0038641	dtn	FBgn0262730
Eph	FBgn0025936	CG6026	FBgn0038676	NA	FBgn0262742
IntS4	FBgn0026679	unc79	FBgn0038693	cac	FBgn0263111
miple1	FBgn0027111	CG4662	FBgn0038735	Cngl	FBgn0263257
Dnz1	FBgn0027453	CG16791	FBgn0038881	NA	FBgn0263376
Cdk5alpha	FBgn0027491	CG7059	FBgn0038957	nwk	FBgn0263456
CG6495	FBgn0027550	Nrx-1	FBgn0038975	Vsx2	FBgn0263512
GABA-B-R2	FBgn0027575	Bili	FBgn0039282	NA	FBgn0263660
Dgp-1	FBgn0027836	CG10420	FBgn0039296	CG17684	FBgn0263780
rdgBbeta	FBgn0027872	Tusp	FBgn0039530	bru3	FBgn0264001
Tob	FBgn0028397	unc80	FBgn0039536	NA	FBgn0264255
CG15270	FBgn0028879	DIP-gamma	FBgn0039617	orb2	FBgn0264307
CG4168	FBgn0028888	CG11317	FBgn0039816	ab	FBgn0264442
CG4935	FBgn0028897	CG12054	FBgn0039831	CG43861	FBgn0264443
CG33090	FBgn0028916	Syt7	FBgn0039900	CaMKII	FBgn0264607
trbl	FBgn0028978	Asator	FBgn0039908	RhoGEF3	FBgn0264707

onecut	FBgn0028996	PIP4K	FBgn0039924	Rgk1	FBgn0264753
Men-b	FBgn0029155	CG11155	FBgn0039927	NA	FBgn0264793
CG12239	FBgn0029810	CG12061	FBgn0040031	NA	FBgn0264822
spidey	FBgn0029975	CG17698	FBgn0040056	pHCl-1	FBgn0264908
CG2247	FBgn0030320	Aplip1	FBgn0040281	Dscam2	FBgn0265296
Rbp1-like	FBgn0030479	Ephrin	FBgn0040324	NA	FBgn0265379
CG9164	FBgn0030634	Unc-76	FBgn0040395	rad	FBgn0265597
Lrp4	FBgn0030706	Alk	FBgn0040505	zyd	FBgn0265767
stas	FBgn0030850	CG17193	FBgn0040571	ttv	FBgn0265974
upd2	FBgn0030904	dpr1	FBgn0040726	CG44837	FBgn0266100
Usp2	FBgn0031187	CG8620	FBgn0040837	NA	FBgn0266227
ND-15	FBgn0031228	hoe1	FBgn0041150	nAChRalpha4	FBgn0266347
CG3625	FBgn0031245	cpx	FBgn0041605	CG45002	FBgn0266354
CG4552	FBgn0031304	rho-5	FBgn0041723	tau	FBgn0266579
CG3104	FBgn0031473	CG32165	FBgn0042178	CG45263	FBgn0266801
CG10019	FBgn0031568	CG18870	FBgn0042180	CG32486	FBgn0266918
CG15431	FBgn0031602	Nfl	FBgn0042696	CG32700	FBgn0267253
CG15630	FBgn0031627	metro	FBgn0050021	Myo81F	FBgn0267431
CG3294	FBgn0031628	mtt	FBgn0050361	NA	FBgn0267571
CG15628	FBgn0031632	CG31064	FBgn0051064	NA	FBgn0267579
CG4230	FBgn0031683	mRRF2	FBgn0051159	NA	FBgn0267666
CG14024	FBgn0031697	CG31221	FBgn0051221		
CG17378	FBgn0031858	CG31223	FBgn0051223		

Downregulated genes E(y)3-KD MB					
Gene Symbol	**Flybase ID**	**Gene Symbol**	**Flybase ID**	**Gene Symbol**	**Flybase ID**
b	FBgn0000153	CG15282	FBgn0028855	CG6163	FBgn0036155
bw	FBgn0000241	NimC2	FBgn0028939	CG10657	FBgn0036289
cni	FBgn0000339	NA	FBgn0029003	CG8100	FBgn0036410
NA	FBgn0000556	aru	FBgn0029095	CG7402	FBgn0036768
eEF2	FBgn0000559	eEF1gamma	FBgn0029176	CG9449	FBgn0036875
Eip71CD	FBgn0000565	spirit	FBgn0030051	CG9451	FBgn0036876
Fbp1	FBgn0000639	Rbm13	FBgn0030067	CG9231	FBgn0036887
Fbp2	FBgn0000640	CG12118	FBgn0030101	CG15881	FBgn0036909
Gld	FBgn0001112	p24-1	FBgn0030341	Cpr78E	FBgn0037114
Hsp27	FBgn0001226	CG8206	FBgn0030679	CG11370	FBgn0037181
janA	FBgn0001280	CG9782	FBgn0030763	CG1113	FBgn0037304
NA	FBgn0001301	CG6891	FBgn0030955	CG1208	FBgn0037386
l(2)gl	FBgn0002121	CG7889	FBgn0031003	CG14598	FBgn0037503

NA	FBgn0002526	CG14207	FBgn0031037	CG2781	FBgn0037534
Lcp2	FBgn0002533	cold	FBgn0031268	CG2767	FBgn0037537
E(spl)m5-HLH	FBgn0002631	CG5397	FBgn0031327	DppIII	FBgn0037580
Rpn8	FBgn0002787	Cyp28d1	FBgn0031689	skap	FBgn0037643
CG2841	FBgn0003159	Oscillin	FBgn0031717	CG12224	FBgn0037974
Pu	FBgn0003162	CG9021	FBgn0031747	CG5167	FBgn0038038
RpLP2	FBgn0003274	CG6055	FBgn0031918	NijC	FBgn0038079
ry	FBgn0003308	CG13796	FBgn0031939	Npc2b	FBgn0038198
Sgs1	FBgn0003372	CG7778	FBgn0032025	CG5866	FBgn0038508
Sgs3	FBgn0003373	Uba4	FBgn0032054	pasi1	FBgn0038545
Sgs5	FBgn0003375	eEF1delta	FBgn0032198	CG7342	FBgn0038716
Sgs7	FBgn0003377	Usp14	FBgn0032216	CG4538	FBgn0038745
Sgs8	FBgn0003378	CG17107	FBgn0032281	CG10175	FBgn0039084
alphaTub85E	FBgn0003886	Samuel	FBgn0032330	CG13627	FBgn0039217
Prosalpha4	FBgn0004066	AstC	FBgn0032336	CG11089	FBgn0039241
Hrb87F	FBgn0004237	CG6287	FBgn0032350	CG10514	FBgn0039312
Eig71Ee	FBgn0004592	CG10343	FBgn0032703	CG9747	FBgn0039754
Mlc-c	FBgn0004687	CG17323	FBgn0032713	Rpt6R	FBgn0039788
tok	FBgn0004885	CG10237	FBgn0032783	eIF3d1	FBgn0040227
Scsalpha	FBgn0004888	CG10026	FBgn0032785	GNBP3	FBgn0040321
Prat	FBgn0004901	CG9248	FBgn0032923	CG13551	FBgn0040660
RpL23	FBgn0010078	Tsp42Ep	FBgn0033137	CG11368	FBgn0040923
Gel	FBgn0010225	CG2121	FBgn0033289	Tep2	FBgn0041182
GstS1	FBgn0010226	Cpr47Ee	FBgn0033602	AttB	FBgn0041581
Uch	FBgn0010288	Sod3	FBgn0033631	Capr	FBgn0042134
Dro	FBgn0010388	ERp60	FBgn0033663	NA	FBgn0050029
TpnC73F	FBgn0010424	CG8501	FBgn0033724	Obp49a	FBgn0050052
wal	FBgn0010516	Cpr49Ac	FBgn0033725	CG31075	FBgn0051075
Aldh-III	FBgn0010548	Cpr49Ag	FBgn0033730	CG31100	FBgn0051100
Prosbeta1	FBgn0010590	Cpr49Ah	FBgn0033731	CG31321	FBgn0051321
Srp54k	FBgn0010747	ItgaPS4	FBgn0034005	CG31344	FBgn0051344
ox	FBgn0011227	Cyp4aa1	FBgn0034053	Cpr65Aw	FBgn0052404
Uch-L5	FBgn0011327	krimp	FBgn0034098	NA	FBgn0052865
NA	FBgn0012042	CG6426	FBgn0034162	AlkB	FBgn0065035
AhcyL2	FBgn0015011	CG4847	FBgn0034229	Neb-cGP	FBgn0083167
CCT3	FBgn0015019	CG10936	FBgn0034253	CG34227	FBgn0085256
Rpt2	FBgn0015282	eIF3c	FBgn0034258	Shroom	FBgn0085408
Rpn10	FBgn0015283	CG5756	FBgn0034301	Prosalpha2	FBgn0086134
Shark	FBgn0015295	nopo	FBgn0034314	vvl	FBgn0086680
Hmu	FBgn0015737	Obp56h	FBgn0034475	5-HT2A	FBgn0087012
ATPsynB	FBgn0019644	CG3264	FBgn0034712	AGO3	FBgn0250816

Orct	FBgn0019952	CG9877	FBgn0034819	Prosalpha6	FBgn0250843
geko	FBgn0020300	CG3500	FBgn0034849	pot	FBgn0250871
pug	FBgn0020385	CG9812	FBgn0034860	Cht10	FBgn0250907
Idgf3	FBgn0020414	CG5554	FBgn0034914	CG42319	FBgn0259219
Oat	FBgn0022774	RpL12	FBgn0034968	NimC1	FBgn0259896
Prosbeta2	FBgn0023174	CG2811	FBgn0035082	Nop60B	FBgn0259937
Plap	FBgn0024314	Phk-3	FBgn0035089	CG17337	FBgn0259979
Pcd	FBgn0024841	Vdup1	FBgn0035103	CG42500	FBgn0260226
NA	FBgn0025117	CG5687	FBgn0035293	TER94	FBgn0261014
PH4alphaMP	FBgn0026190	CG1139	FBgn0035300	rtv	FBgn0261277
Ndg	FBgn0026403	CG15822	FBgn0035308	Prosalpha3	FBgn0261394
fat-spondin	FBgn0026721	CG14964	FBgn0035410	Rpn3	FBgn0261396
Dp1	FBgn0027835	ckd	FBgn0035427	Lmpt	FBgn0261565
CAH2	FBgn0027843	CG1136	FBgn0035490	RpL37A	FBgn0261608
jbug	FBgn0028371	RhoGEF64C	FBgn0035574	l(2)41Ab	FBgn0262123
TotA	FBgn0028396	CG10576	FBgn0035630	magu	FBgn0262169
ics	FBgn0028546	Txl	FBgn0035631	DNA-ligI	FBgn0262619
NA	FBgn0028665	CG13676	FBgn0035844	CG43163	FBgn0262719
Vha100-2	FBgn0028670	GstO3	FBgn0035904	Vha68-2	FBgn0263598
Rpt5	FBgn0028684	TrpA1	FBgn0035934	yin	FBgn0265575
Rpt4	FBgn0028685	Dhpr	FBgn0035964	Fhos	FBgn0266084
Rpt3	FBgn0028686	Slc45-1	FBgn0035968	Sem1	FBgn0266666
Rpn11	FBgn0028694	PGRP-LC	FBgn0035976	stac	FBgn0266719
Rpn1	FBgn0028695	PGRP-LF	FBgn0035977	Yeti	FBgn0267398
eEF1beta	FBgn0028737	CG6175	FBgn0036152		

Upregulated genes Snr1-KD MB					
Gene Symbol	**Flybase ID**	**Gene Symbol**	**Flybase ID**	**Gene Symbol**	**Flybase ID**
Ald	FBgn0000064	GlcAT-S	FBgn0032135	Obp99a	FBgn0039678
ftz-f1	FBgn0001078	Pect	FBgn0032482	CG12071	FBgn0039808
Hex-A	FBgn0001186	Ttc19	FBgn0032744	CG15864	FBgn0040528
lin	FBgn0002552	CG17544	FBgn0032775	CG17193	FBgn0040571
MtnA	FBgn0002868	Hasp	FBgn0032797	Ir41a	FBgn0040849
Atpalpha	FBgn0002921	nrv3	FBgn0032946	hoe1	FBgn0041150
Pgi	FBgn0003074	Gadd45	FBgn0033153	Slbp	FBgn0041186
r-l	FBgn0003257	CG1358	FBgn0033196	cpx	FBgn0041605
Jon99Ciii	FBgn0003356	CG2064	FBgn0033205	Hexo2	FBgn0041629
Jon99Ciii	FBgn0003357	ACC	FBgn0033246	CG18764	FBgn0042205
tipE	FBgn0003710	CG12769	FBgn0033252	Proc	FBgn0045038

NA	FBgn0003732	PPO2	FBgn0033367	NA	FBgn0050118
porin	FBgn0004363	CG13743	FBgn0033368	CG30158	FBgn0050158
Mdr65	FBgn0004513	CG12909	FBgn0033507	CG30172	FBgn0050172
Gad1	FBgn0004516	CG11883	FBgn0033538	CG30203	FBgn0050203
B52	FBgn0004587	Sln	FBgn0033657	CG30389	FBgn0050389
Sam-S	FBgn0005278	CG6329	FBgn0033872	CG31030	FBgn0051030
Nup214	FBgn0010660	CG12868	FBgn0033945	CG31191	FBgn0051191
Nos	FBgn0011676	tun	FBgn0034046	CG31301	FBgn0051301
Dh44	FBgn0012344	Mlf	FBgn0034051	CG31706	FBgn0051706
sced	FBgn0013732	CG8060	FBgn0034113	fred	FBgn0051774
Gycalpha99B	FBgn0013972	HPS4	FBgn0034261	CG32066	FBgn0052066
Gycbeta100B	FBgn0013973	Mctp	FBgn0034389	CG32204	FBgn0052204
Sr-CI	FBgn0014033	Oatp58Dc	FBgn0034716	PMP34	FBgn0052250
Hr38	FBgn0014859	CG4250	FBgn0034761	CG32392	FBgn0052392
Mcm2	FBgn0014861	thoc5	FBgn0034939	PVRAP	FBgn0052406
Rbf	FBgn0015799	CG3860	FBgn0034951	Cubn	FBgn0052702
vkg	FBgn0016075	Nplp1	FBgn0035092	dpr4	FBgn0053512
Pdp1	FBgn0016694	Sf3b3	FBgn0035162	SIFa	FBgn0053527
Gs1l	FBgn0019982	Trh	FBgn0035187	CG33543	FBgn0053543
Gcn5	FBgn0020388	CNMa	FBgn0035282	CG40470	FBgn0058470
Gpo-1	FBgn0022160	CG10866	FBgn0035475	Dgk	FBgn0085390
Cbp80	FBgn0022942	CG1265	FBgn0035517	CG34370	FBgn0085399
CG17778	FBgn0023534	CG10467	FBgn0035679	CG34409	FBgn0085438
gprs	FBgn0024232	CG4476	FBgn0035969	spok	FBgn0086917
foi	FBgn0024236	CG3689	FBgn0035987	CG42235	FBgn0250757
NTPase	FBgn0024947	CG8177	FBgn0036043	CG42255	FBgn0259140
Inos	FBgn0025885	GlcAT-P	FBgn0036144	CG42337	FBgn0259239
mbo	FBgn0026207	CG8745	FBgn0036381	Pka-R1	FBgn0259243
Eaat1	FBgn0026439	CG17364	FBgn0036391	nvd	FBgn0259697
NA	FBgn0027571	CG7841	FBgn0036502	zld	FBgn0259789
jdp	FBgn0027654	CG13055	FBgn0036583	CG42495	FBgn0260027
Dgp-1	FBgn0027836	CG13025	FBgn0036660	CG42542	FBgn0260659
rdgBbeta	FBgn0027872	Mip	FBgn0036713	Pdfr	FBgn0260753
Tob	FBgn0028397	CG18265	FBgn0036725	Sytalpha	FBgn0261089
NimB4	FBgn0028542	Gabat	FBgn0036927	Ppcs	FBgn0261285
beat-Ic	FBgn0028644	obst-F	FBgn0036947	scra	FBgn0261385
Nckx30C	FBgn0028704	atk	FBgn0036995	GLS	FBgn0261625
CG18273	FBgn0029525	CG11399	FBgn0037021	fwe	FBgn0261722
CG3009	FBgn0029720	DNApol-eta	FBgn0037141	mi	FBgn0261786
CG15765	FBgn0029814	Skp2	FBgn0037236	kcc	FBgn0261794
Tsp5D	FBgn0029837	CG17816	FBgn0037525	CG42817	FBgn0261999

dpr14	FBgn0029974	CG8861	FBgn0037676	CG43066	FBgn0262476
spidey	FBgn0029975	CG8301	FBgn0037717	CG43085	FBgn0262531
CG2260	FBgn0030000	CG5276	FBgn0037900	NA	FBgn0262789
CG16892	FBgn0030122	dpr5	FBgn0037908	Hk	FBgn0263220
Cyp4g15	FBgn0030304	Elp1	FBgn0037926	NA	FBgn0263376
mRpS25	FBgn0030572	GstD11	FBgn0038029	Slob	FBgn0264087
CG9609	FBgn0030787	CG5641	FBgn0038046	ab	FBgn0264442
et	FBgn0031055	Gnmt	FBgn0038074	cv-d	FBgn0265048
mRpL10	FBgn0031231	UQCR-C1	FBgn0038271	Neto	FBgn0265416
CG4291	FBgn0031287	Sdr	FBgn0038279	zyd	FBgn0265767
CG4629	FBgn0031299	dpr9	FBgn0038282	NA	FBgn0266214
eys	FBgn0031414	mRpS10	FBgn0038307	NA	FBgn0266227
Cep97	FBgn0031575	CG6118	FBgn0038339	NA	FBgn0266414
CG15630	FBgn0031627	CG15803	FBgn0038606	ringer	FBgn0266417
Jon25Biii	FBgn0031653	unc79	FBgn0038693	NA	FBgn0266886
CG9107	FBgn0031764	Ktl	FBgn0038839	NA	FBgn0267665
CG7781	FBgn0032021	Octbeta1R	FBgn0038980		
CG7627	FBgn0032026	CG11897	FBgn0039644		

Downregulated genes Snr1-KD MB					
Gene Symbol	**Flybase ID**	**Gene Symbol**	**Flybase ID**	**Gene Symbol**	**Flybase ID**
chic	FBgn0000308	CG5001	FBgn0031322	CG7720	FBgn0038652
crc	FBgn0000370	Wdr62	FBgn0031374	CG18208	FBgn0038653
Sap-r	FBgn0000416	CG31689	FBgn0031449	CG4733	FBgn0038744
Ddc	FBgn0000422	CG9664	FBgn0031515	CG4538	FBgn0038745
Pka-C3	FBgn0000489	CG9663	FBgn0031516	CG17111	FBgn0039048
EcR	FBgn0000546	CG3277	FBgn0031518	spas	FBgn0039141
Gs2	FBgn0001145	CG3036	FBgn0031645	CG7016	FBgn0039238
Hsp27	FBgn0001226	CG14024	FBgn0031697	CG5639	FBgn0039527
NA	FBgn0001234	obst-E	FBgn0031737	AstA-R2	FBgn0039595
hth	FBgn0001235	CG11034	FBgn0031741	wat	FBgn0039620
knrl	FBgn0001323	CG13995	FBgn0031770	Ctl2	FBgn0039637
Prosbeta6	FBgn0002284	Tsp	FBgn0031850	Kul	FBgn0039688
Rpn8	FBgn0002787	CG18304	FBgn0031869	Rpt6R	FBgn0039788
CG2841	FBgn0003159	CG5171	FBgn0031907	CG15547	FBgn0039809
Sgs1	FBgn0003372	CG5177	FBgn0031908	CG1674	FBgn0039897
Sgs3	FBgn0003373	SLC5A11	FBgn0031998	mav	FBgn0039914
Sgs7	FBgn0003377	Usp14	FBgn0032216	CG11380	FBgn0040359
Sgs8	FBgn0003378	Samuel	FBgn0032330	CG5254	FBgn0040383

shd	FBgn0003388	CG6770	FBgn0032400	CG13551	FBgn0040660
sog	FBgn0003463	CG9934	FBgn0032467	Muc26B	FBgn0040950
sqh	FBgn0003514	DnaJ-H	FBgn0032474	CG30427	FBgn0043792
wbl	FBgn0004003	CG5953	FBgn0032587	Atg2	FBgn0044452
Eig71Ee	FBgn0004592	Trpgamma	FBgn0032593	CG3502	FBgn0046253
GluRIIA	FBgn0004620	kon	FBgn0032683	CG30345	FBgn0050345
retn	FBgn0004795	CG17323	FBgn0032713	CG30440	FBgn0050440
tok	FBgn0004885	CG10623	FBgn0032727	NA	FBgn0051044
Hnf4	FBgn0004914	CG10431	FBgn0032730	CG31102	FBgn0051102
NA	FBgn0005592	CG10237	FBgn0032783	Nlg1	FBgn0051146
CanA1	FBgn0010015	Pomp	FBgn0032884	Gba1a	FBgn0051148
Gel	FBgn0010225	CG3651	FBgn0032974	GluRIIE	FBgn0051201
TpnC73F	FBgn0010424	Strica	FBgn0033051	NKCC	FBgn0051547
NAT1	FBgn0010488	CG2121	FBgn0033289	NA	FBgn0051728
dmGlut	FBgn0010497	CG1418	FBgn0033468	Adi1	FBgn0052068
Aldh-III	FBgn0010548	CG12910	FBgn0033502	CG32137	FBgn0052137
poe	FBgn0011230	CAP	FBgn0033504	AMPdeam	FBgn0052626
Trp1	FBgn0011584	CG9003	FBgn0033639	Mical	FBgn0053208
Pex1	FBgn0013563	Sobp	FBgn0033654	form3	FBgn0053556
Awh	FBgn0013751	CG8888	FBgn0033679	CG33970	FBgn0053970
Rho1	FBgn0014020	Cpr49Ac	FBgn0033725	CG33978	FBgn0053978
AhcyL2	FBgn0015011	CG6357	FBgn0033875	Ube3a	FBgn0061469
Fer1HCH	FBgn0015222	Dh44-R1	FBgn0033932	EMRE	FBgn0062440
Rpt2	FBgn0015282	Achl	FBgn0033936	tmod	FBgn0082582
Rpn10	FBgn0015283	Asph	FBgn0034075	Nlg4	FBgn0083975
nrv1	FBgn0015776	Ptp52F	FBgn0034085	Pvf3	FBgn0085407
Rab7	FBgn0015795	CG4945	FBgn0034137	TrissinR	FBgn0085410
Drip	FBgn0015872	CG10953	FBgn0034204	Nox	FBgn0085428
stumps	FBgn0020299	CG10936	FBgn0034253	CG34417	FBgn0085446
pio	FBgn0020521	CG5756	FBgn0034301	CG41378	FBgn0085638
Xbp1	FBgn0021872	cer	FBgn0034443	NA	FBgn0085732
Ac13E	FBgn0022710	Fem-1	FBgn0034542	Prosalpha2	FBgn0086134
RpL39	FBgn0023170	CG11073	FBgn0034693	Ubi-p5E	FBgn0086558
Prosbeta2	FBgn0023174	sona	FBgn0034903	sls	FBgn0086906
Prosalpha7	FBgn0023175	CG16786	FBgn0034974	CG41520	FBgn0087011
CG2865	FBgn0023526	Phk-3	FBgn0035089	5-HT2A	FBgn0087012
CG3630	FBgn0023540	Kah	FBgn0035144	AGO3	FBgn0250816
Naa30A	FBgn0024362	CG1139	FBgn0035300	CG2016	FBgn0250839
Mhcl	FBgn0026059	CG1136	FBgn0035490	Prosalpha6	FBgn0250843
cib	FBgn0026084	slow	FBgn0035539	Cht10	FBgn0250907
PH4alphaMP	FBgn0026190	CG13722	FBgn0035553	RhoGAP102A	FBgn0259216

Dronc	FBgn0026404	CG13705	FBgn0035582	CG42319	FBgn0259219
Rad23	FBgn0026777	blanks	FBgn0035608	laccase2	FBgn0259247
Stam	FBgn0027363	frm	FBgn0035612	sqa	FBgn0259678
CG4757	FBgn0027584	Sf3b6	FBgn0035692	Pkcdelta	FBgn0259680
CG8740	FBgn0027585	Sh3beta	FBgn0035772	Nost	FBgn0259734
CG2082	FBgn0027608	CG4911	FBgn0035959	CG42390	FBgn0259736
Dp1	FBgn0027835	Dhpr	FBgn0035964	CG42524	FBgn0260429
fal	FBgn0028380	Ufd1-like	FBgn0036136	CG12163	FBgn0260462
chm	FBgn0028387	CG6175	FBgn0036152	serp	FBgn0260653
ics	FBgn0028546	CG11652	FBgn0036194	TER94	FBgn0261014
lqf	FBgn0028582	CG11658	FBgn0036196	verm	FBgn0261341
qsm	FBgn0028622	CG11529	FBgn0036264	capt	FBgn0261458
Sur	FBgn0028675	CG14117	FBgn0036331	haf	FBgn0261509
Rpt5	FBgn0028684	CG14109	FBgn0036364	CG42671	FBgn0261553
Rpn7	FBgn0028688	CG13033	FBgn0036638	Thor	FBgn0261560
Rpn6	FBgn0028689	CG9701	FBgn0036659	RpL37A	FBgn0261608
Rpn5	FBgn0028690	CG6664	FBgn0036685	CG42749	FBgn0261803
Rpn9	FBgn0028691	CG13731	FBgn0036717	CG42822	FBgn0262004
Rpn2	FBgn0028692	Cyp12c1	FBgn0036806	Spn77Ba	FBgn0262057
Rpn12	FBgn0028693	CG14073	FBgn0036814	l(2)41Ab	FBgn0262123
Rpn1	FBgn0028695	MESR6	FBgn0036846	Skeletor	FBgn0262717
CG31817	FBgn0028899	CG9449	FBgn0036875	milt	FBgn0262872
Prosbeta5	FBgn0029134	CG7668	FBgn0036929	cnc	FBgn0262975
HIP-R	FBgn0029676	eRF1	FBgn0036974	NA	FBgn0263039
CG5921	FBgn0029835	CG5618	FBgn0036975	Cht6	FBgn0263132
CG11700	FBgn0029856	CG5969	FBgn0036998	NA	FBgn0263380
CG14439	FBgn0029898	CG5059	FBgn0037007	hppy	FBgn0263395
UbcE2H	FBgn0029996	Rcd2	FBgn0037012	NA	FBgn0263617
spirit	FBgn0030051	CG14642	FBgn0037222	NA	FBgn0263659
SmydA-9	FBgn0030102	CG1113	FBgn0037304	NA	FBgn0264439
CG17754	FBgn0030114	CG1239	FBgn0037368	how	FBgn0264491
CG15211	FBgn0030234	Neurochondrin	FBgn0037447	CG1172	FBgn0264712
Sclp	FBgn0030357	CG15186	FBgn0037448	NA	FBgn0264834
GstT4	FBgn0030484	CG2781	FBgn0037534	CG44085	FBgn0264894
CG15756	FBgn0030493	CG3223	FBgn0037538	tn	FBgn0265356
CG12481	FBgn0030542	CG9626	FBgn0037565	yin	FBgn0265575
CG11590	FBgn0030545	GCC185	FBgn0037979	Zasp52	FBgn0265991
CG13012	FBgn0030769	CG6753	FBgn0038070	rudhira	FBgn0266019
CG4829	FBgn0030796	NijC	FBgn0038079	CG45050	FBgn0266410
CG13003	FBgn0030798	Paip2	FBgn0038100	Sem1	FBgn0266666
RhoGAP15B	FBgn0030808	PK2-R2	FBgn0038139	Svil	FBgn0266696

Ubr1	FBgn0030809	CG9312	FBgn0038179	stac	FBgn0266719
CG5445	FBgn0030838	Cht5	FBgn0038180	Snap24	FBgn0266720
wgn	FBgn0030941	Mur89F	FBgn0038492	NA	FBgn0267073
CG6891	FBgn0030955	CG7587	FBgn0038523	Yeti	FBgn0267398
CG4213	FBgn0031251	Muc91C	FBgn0038642	NA	FBgn0267793

Upregulated genes Bap60-KD MB		**Downregulated genes Bap60-KD MB**	
Gene Symbol	**Flybase ID**	**Gene Symbol**	**Flybase ID**
TBCB	FBgn0034451	Sgs3	FBgn0003373
CG30096	FBgn0050096	Sgs7	FBgn0003377
dyl	FBgn0066365	Sgs8	FBgn0003378
upd2	FBgn0030904	Eig71Ee	FBgn0004592
		NA	FBgn0262722
		tim	FBgn0014396

Upregulated genes EcR-B1^{DN}-KD MB					
Gene Symbol	**Flybase ID**	**Gene Symbol**	**Flybase ID**	**Gene Symbol**	**Flybase ID**
CecC	FBgn0000279	Strica	FBgn0033051	Gclc	FBgn0040319
Col4a1	FBgn0000299	SCAP	FBgn0033052	CG17193	FBgn0040571
cv-2	FBgn0000395	CG14591	FBgn0033054	Nplp2	FBgn0040813
NA	FBgn0000409	CCHa2-R	FBgn0033058	CG8620	FBgn0040837
eag	FBgn0000535	Gadd45	FBgn0033153	hoe1	FBgn0041150
ftz-f1	FBgn0001078	CG2064	FBgn0033205	Socs36E	FBgn0041184
GstD1	FBgn0001149	Nop17l	FBgn0033224	Pcyt1	FBgn0041342
Hex-A	FBgn0001186	CG1882	FBgn0033226	cpx	FBgn0041605
NA	FBgn0001332	ACC	FBgn0033246	Hexo2	FBgn0041629
MtnA	FBgn0002868	CG12769	FBgn0033252	Proc	FBgn0045038
mus205	FBgn0002891	CG8708	FBgn0033271	NT5E-2	FBgn0050104
Atpalpha	FBgn0002921	spab	FBgn0033358	NA	FBgn0050118
NA	FBgn0004168	CG13743	FBgn0033368	CG30172	FBgn0050172
porin	FBgn0004363	ths	FBgn0033652	CG30203	FBgn0050203
Mdr65	FBgn0004513	Drl-2	FBgn0033791	CG30389	FBgn0050389
Gad1	FBgn0004516	CG17047	FBgn0033827	PH4alphaSG1	FBgn0051014
Cbp53E	FBgn0004580	bbc	FBgn0033844	CG31030	FBgn0051030
GluRIA	FBgn0004619	CG6329	FBgn0033872	CG31221	FBgn0051221
TkR86C	FBgn0004841	Arc2	FBgn0033928	CG31496	FBgn0051496
upd1	FBgn0004956	tun	FBgn0034046	nolo	FBgn0051619
Ets21C	FBgn0005660	CG5065	FBgn0034145	smog	FBgn0051660

Con	FBgn0005775	HPS4	FBgn0034261	fred	FBgn0051774
GstD2	FBgn0010038	CG5002	FBgn0034275	Cda5	FBgn0051973
GstD3	FBgn0010039	dpr13	FBgn0034286	CG32066	FBgn0052066
hig	FBgn0010114	Muc55B	FBgn0034294	CG32198	FBgn0052198
RpA-70	FBgn0010173	CG10911	FBgn0034295	CG32204	FBgn0052204
Tbh	FBgn0010329	GstE1	FBgn0034335	PVRAP	FBgn0052406
Nc73EF	FBgn0010352	Rcd6	FBgn0034530	stx	FBgn0052676
Cyp18a1	FBgn0010383	rad50	FBgn0034728	CG32758	FBgn0052758
Phb2	FBgn0010551	CG10384	FBgn0034731	AGBE	FBgn0053138
MFS14	FBgn0010651	CG13560	FBgn0034899	Hs3st-A	FBgn0053147
La	FBgn0011638	CG11300	FBgn0034901	dpr11	FBgn0053202
Nos	FBgn0011676	GlyT	FBgn0034911	CG33203	FBgn0053203
AcCoAS	FBgn0012034	CG16787	FBgn0034940	CG33267	FBgn0053267
Hr38	FBgn0014859	CG3860	FBgn0034951	dpr3	FBgn0053516
Hsp60A	FBgn0015245	CG13579	FBgn0035010	obst-H	FBgn0053983
CG14906	FBgn0015351	Nplp1	FBgn0035092	dyl	FBgn0066365
nAChRalpha3	FBgn0015519	Gale	FBgn0035147	Frq2	FBgn0083228
NA	FBgn0015541	Pcyt2	FBgn0035231	Dgk	FBgn0085390
toc	FBgn0015600	DopEcR	FBgn0035538	CG34370	FBgn0085399
vkg	FBgn0016075	CG4611	FBgn0035591	Epac	FBgn0085421
Pdp1	FBgn0016694	CG8641	FBgn0035733	CG34393	FBgn0085422
dos	FBgn0016794	unc-13-4A	FBgn0035756	NaCP60E	FBgn0085434
Gs1l	FBgn0019982	CG7506	FBgn0035805	CG34409	FBgn0085438
mGluR	FBgn0019985	path	FBgn0036007	CG12484	FBgn0086604
Gcn5	FBgn0020388	CG14142	FBgn0036143	spin	FBgn0086676
Idgf3	FBgn0020414	GlcAT-P	FBgn0036144	jeb	FBgn0086677
Gpo-1	FBgn0022160	Muc68Ca	FBgn0036181	chinmo	FBgn0086758
CG17778	FBgn0023534	RpL10Ab	FBgn0036213	nAChRalpha7	FBgn0086778
CG17896	FBgn0023537	CG10960	FBgn0036316	futsch	FBgn0259108
gprs	FBgn0024232	Toll-6	FBgn0036494	CG42268	FBgn0259163
foi	FBgn0024236	CG13024	FBgn0036665	ome	FBgn0259175
NTPase	FBgn0024947	CG5535	FBgn0036764	CG42342	FBgn0259244
CG3719	FBgn0024986	AstC-R2	FBgn0036789	zld	FBgn0259789
Rab27	FBgn0025382	MYPT-75D	FBgn0036801	GABA-B-R1	FBgn0260446
Mgstl	FBgn0025814	Mkp3	FBgn0036844	CG42540	FBgn0260657
Traf4	FBgn0026319	CG14086	FBgn0036860	Chchd2	FBgn0260747
Mpcp2	FBgn0026409	Gabat	FBgn0036927	Baldspot	FBgn0260960
Eaat2	FBgn0026438	CG14186	FBgn0036935	CG42594	FBgn0260971
Eaat1	FBgn0026439	CG5664	FBgn0037082	Sytalpha	FBgn0261089
CG5991	FBgn0026576	Syn1	FBgn0037130	SREBP	FBgn0261283
Ady43A	FBgn0026602	CG1090	FBgn0037238	Ppcs	FBgn0261285

IntS4	FBgn0026679	POLDIP2	FBgn0037329	RpL8	FBgn0261602
ThrRS	FBgn0027081	kat-60L1	FBgn0037375	GLS	FBgn0261625
NA	FBgn0027493	CG17816	FBgn0037525	fwe	FBgn0261722
NA	FBgn0027571	CG8861	FBgn0037676	kcc	FBgn0261794
Dgp-1	FBgn0027836	Teh1	FBgn0037766	sdt	FBgn0261873
CG6424	FBgn0028494	dpr15	FBgn0037993	CG42807	FBgn0261989
beat-Ic	FBgn0028644	GstD9	FBgn0038020	CadN2	FBgn0262018
CG15270	FBgn0028879	CG5167	FBgn0038038	CG43066	FBgn0262476
trbl	FBgn0028978	CG6225	FBgn0038072	CG43117	FBgn0262577
Spn55B	FBgn0028983	beat-Vc	FBgn0038084	Acsl	FBgn0263120
CG3009	FBgn0029720	beat-Va	FBgn0038087	Hk	FBgn0263220
SPR	FBgn0029768	CG7381	FBgn0038098	Mocs1	FBgn0263241
CG4096	FBgn0029791	CG14850	FBgn0038239	scrib	FBgn0263289
dpr14	FBgn0029974	CG14852	FBgn0038242	CG11000	FBgn0263353
spidey	FBgn0029975	UQCR-C1	FBgn0038271	nwk	FBgn0263456
CG12112	FBgn0030048	Gyc88E	FBgn0038295	NA	FBgn0263660
CG11695	FBgn0030316	obe	FBgn0038344	CG43689	FBgn0263772
CG1578	FBgn0030336	CG14879	FBgn0038419	CG43693	FBgn0263776
CG4407	FBgn0030431	CG14907	FBgn0038455	CG43729	FBgn0263980
CG1998	FBgn0030485	CG18213	FBgn0038470	cpo	FBgn0263995
CG9411	FBgn0030569	CG15803	FBgn0038606	CG43783	FBgn0264305
Lrp4	FBgn0030706	unc79	FBgn0038693	CG43778	FBgn0264308
upd2	FBgn0030904	MFS9	FBgn0038799	CG43795	FBgn0264339
CG7990	FBgn0030997	Ktl	FBgn0038839	Ca-alpha1T	FBgn0264386
Cp110	FBgn0031191	CG6678	FBgn0038917	RhoGEF3	FBgn0264707
CG4133	FBgn0031257	Pebp1	FBgn0038973	CG44040	FBgn0264832
CG13947	FBgn0031277	Octbeta1R	FBgn0038980	koi	FBgn0265003
CG5080	FBgn0031313	Cow	FBgn0039054	cv-d	FBgn0265048
mio	FBgn0031399	CG4467	FBgn0039064	Vha68-1	FBgn0265262
VGlut	FBgn0031424	CG10184	FBgn0039094	Neto	FBgn0265416
CG3714	FBgn0031589	CG10420	FBgn0039296	CG44837	FBgn0266100
CG9109	FBgn0031765	Ssadh	FBgn0039349	NA	FBgn0266214
CG14535	FBgn0031955	CG14237	FBgn0039428	NA	FBgn0266227
CG7781	FBgn0032021	unc80	FBgn0039536	FeCH	FBgn0266268
CG7627	FBgn0032026	beat-VI	FBgn0039584	CG45002	FBgn0266354
Dh31	FBgn0032048	DIP-gamma	FBgn0039617	ringer	FBgn0266417
CG3838	FBgn0032130	CG11897	FBgn0039644	NA	FBgn0266846
GlcAT-S	FBgn0032135	CG11898	FBgn0039645	NA	FBgn0266886
MRP	FBgn0032456	jus	FBgn0039647	AOX1	FBgn0267408
Ttc19	FBgn0032744	CG7920	FBgn0039737	NA	FBgn0267635
CG17544	FBgn0032775	CG9743	FBgn0039756	NA	FBgn0267665

nrv3	FBgn0032946	PH4alphaSG2	FBgn0039779		

Downregulated genes EcR-B1^{DN}-KD MB					
Gene Symbol	**Flybase ID**	**Gene Symbol**	**Flybase ID**	**Gene Symbol**	**Flybase ID**
Act87E	FBgn0000046	Tsp	FBgn0031850	CG18528	FBgn0039189
chic	FBgn0000308	CG11221	FBgn0031855	dsd	FBgn0039528
DNaseII	FBgn0000477	CG18304	FBgn0031869	CG11873	FBgn0039633
Pka-C3	FBgn0000489	CG5171	FBgn0031907	CG9682	FBgn0039760
EcR	FBgn0000546	CG5177	FBgn0031908	CG1674	FBgn0039897
Eip74EF	FBgn0000567	CG7102	FBgn0031961	mav	FBgn0039914
Eip75B	FBgn0000568	CG14277	FBgn0032008	CG12061	FBgn0040031
ems	FBgn0000576	Usp14	FBgn0032216	GNBP3	FBgn0040321
FER	FBgn0000723	CG17107	FBgn0032281	Atx2	FBgn0041188
hth	FBgn0001235	CG7294	FBgn0032284	Hexo1	FBgn0041630
NA	FBgn0001301	Samuel	FBgn0032330	Atg2	FBgn0044452
kni	FBgn0001320	CG16854	FBgn0032338	GluRIIC	FBgn0046113
knrl	FBgn0001323	Trpgamma	FBgn0032593	CG30015	FBgn0050015
l(3)mbn	FBgn0002440	CG10211	FBgn0032685	CG30026	FBgn0050026
Lcp1	FBgn0002531	CG10623	FBgn0032727	CG30089	FBgn0050089
Map205	FBgn0002645	CG17350	FBgn0032772	CG30392	FBgn0050392
Rpn8	FBgn0002787	CG10237	FBgn0032783	CG30438	FBgn0050438
sog	FBgn0003463	CG14764	FBgn0033236	CG30440	FBgn0050440
tud	FBgn0003891	sand	FBgn0033257	NA	FBgn0051044
wbl	FBgn0004003	BBS4	FBgn0033578	CG31103	FBgn0051103
NA	FBgn0004028	Sod3	FBgn0033631	CG31104	FBgn0051104
up	FBgn0004169	CG9005	FBgn0033638	Nlg1	FBgn0051146
Hrb87F	FBgn0004237	CG9003	FBgn0033639	CG31176	FBgn0051176
Cyp1	FBgn0004432	Sobp	FBgn0033654	CG31321	FBgn0051321
Plc21C	FBgn0004611	exp	FBgn0033668	sals	FBgn0051374
retn	FBgn0004795	CG8888	FBgn0033679	CG31475	FBgn0051475
bowl	FBgn0004893	CG10205	FBgn0033970	NA	FBgn0051728
NA	FBgn0005592	Cyp4aa1	FBgn0034053	NA	FBgn0051781
Sox14	FBgn0005612	casp	FBgn0034068	CG31997	FBgn0051997
CanA1	FBgn0010015	Asph	FBgn0034075	Cpr66D	FBgn0052029
Gel	FBgn0010225	CG4945	FBgn0034137	Cpr65Aw	FBgn0052404
corto	FBgn0010313	CG4847	FBgn0034229	Cpr65Av	FBgn0052405
TpnC73F	FBgn0010424	CG10936	FBgn0034253	X11Lbeta	FBgn0052677
emp	FBgn0010435	CG5756	FBgn0034301	CG32816	FBgn0052816
l(2)01289	FBgn0010482	CG15080	FBgn0034391	Mical	FBgn0053208

NAT1	FBgn0010488	cer	FBgn0034443	form3	FBgn0053556
msn	FBgn0010909	CG11073	FBgn0034693	CG33978	FBgn0053978
poe	FBgn0011230	CG3649	FBgn0034785	CG40006	FBgn0058006
Klp3A	FBgn0011606	PIP5K59B	FBgn0034789	NA	FBgn0058469
tsr	FBgn0011726	NA	FBgn0034967	Lasp	FBgn0063485
COX2	FBgn0013675	CG16786	FBgn0034974	tmod	FBgn0082582
Rho1	FBgn0014020	Vdup1	FBgn0035103	CG34120	FBgn0083956
bnl	FBgn0014135	Kah	FBgn0035144	CG34355	FBgn0085384
tim	FBgn0014396	Ctr9	FBgn0035205	CG34398	FBgn0085427
Rpt2	FBgn0015282	CG1139	FBgn0035300	CG34417	FBgn0085446
alpha-Est8	FBgn0015576	spz5	FBgn0035379	sls	FBgn0086906
nompA	FBgn0016047	CG11486	FBgn0035397	CG41520	FBgn0087011
vri	FBgn0016076	CG14964	FBgn0035410	5-HT2A	FBgn0087012
sba	FBgn0016754	CG1136	FBgn0035490	CG33521	FBgn0250819
CG2865	FBgn0023526	CG11350	FBgn0035552	Cht10	FBgn0250907
CG2924	FBgn0023528	CG13705	FBgn0035582	grh	FBgn0259211
CG3630	FBgn0023540	blanks	FBgn0035608	CG42319	FBgn0259219
Ac78C	FBgn0024150	Jon65Aiii	FBgn0035665	laccase2	FBgn0259247
drm	FBgn0024244	Jon65Ai	FBgn0035667	Pkcdelta	FBgn0259680
Naa30A	FBgn0024362	Sf3b6	FBgn0035692	Nost	FBgn0259734
Lip2	FBgn0024740	CG8519	FBgn0035711	Su(var)3-3	FBgn0260397
Tnpo	FBgn0024921	Sh3beta	FBgn0035772	HIP-R	FBgn0260484
par-6	FBgn0026192	CG8209	FBgn0035830	serp	FBgn0260653
Rad23	FBgn0026777	CG13676	FBgn0035844	Mp	FBgn0260660
CG1688	FBgn0027589	Zasp66	FBgn0035917	TER94	FBgn0261014
GV1	FBgn0027790	CG4911	FBgn0035959	verm	FBgn0261341
chm	FBgn0028387	CG14109	FBgn0036364	Prosalpha3	FBgn0261394
qsm	FBgn0028622	mop	FBgn0036448	Rpn3	FBgn0261396
Rpt4	FBgn0028685	CG17032	FBgn0036547	haf	FBgn0261509
Rpn7	FBgn0028688	CG5830	FBgn0036556	CG42674	FBgn0261556
Rpn6	FBgn0028689	CG13731	FBgn0036717	RpL37A	FBgn0261608
Rpn2	FBgn0028692	CG14073	FBgn0036814	CG42700	FBgn0261611
Rpn1	FBgn0028695	MESR6	FBgn0036846	CG42749	FBgn0261803
nerfin-1	FBgn0028999	CG9449	FBgn0036875	NA	FBgn0262108
Tollo	FBgn0029114	CG7668	FBgn0036929	RanBPM	FBgn0262114
CG11700	FBgn0029856	CG5059	FBgn0037007	Tl	FBgn0262473
UbcE2H	FBgn0029996	CG14642	FBgn0037222	Skeletor	FBgn0262717
CG12115	FBgn0030097	spartin	FBgn0037265	cnc	FBgn0262975
SmydA-9	FBgn0030102	plh	FBgn0037292	Cht6	FBgn0263132
CG2145	FBgn0030251	CG1113	FBgn0037304	Coop	FBgn0263240
CG15201	FBgn0030272	CG14669	FBgn0037326	Vsx2	FBgn0263512

Lint-1	FBgn0030274	Neurochondrin	FBgn0037447	NA	FBgn0264084
PGRP-SA	FBgn0030310	CG15186	FBgn0037448	CG43861	FBgn0264443
Sclp	FBgn0030357	CG3014	FBgn0037519	how	FBgn0264491
CG15027	FBgn0030611	CG2767	FBgn0037537	NA	FBgn0264745
CG9095	FBgn0030617	CG9626	FBgn0037565	NA	FBgn0264834
CG9782	FBgn0030763	CG9801	FBgn0037623	smt3	FBgn0264922
CG13003	FBgn0030798	GstZ2	FBgn0037697	CG44242	FBgn0265177
CG12990	FBgn0030859	CG14715	FBgn0037930	tn	FBgn0265356
CG15046	FBgn0030927	NijC	FBgn0038079	CG44422	FBgn0265595
obst-A	FBgn0031097	Paip2	FBgn0038100	Bx	FBgn0265598
CG3625	FBgn0031245	CG8031	FBgn0038110	Dop1R2	FBgn0266137
CG11835	FBgn0031264	CG9312	FBgn0038179	NA	FBgn0266315
CG5001	FBgn0031322	Cht5	FBgn0038180	CG45076	FBgn0266446
CG9663	FBgn0031516	TyrR	FBgn0038542	Sem1	FBgn0266666
CG3277	FBgn0031518	CG18208	FBgn0038653	NA	FBgn0266901
Jon25Bii	FBgn0031654	CG4538	FBgn0038745	Glut4EF	FBgn0267336
CG14024	FBgn0031697	CG5326	FBgn0038983	NA	FBgn0267704

Appendix E Differentially accessible genes in larval SWI/SNF-KD MBs

More accessible genes E(y)3-KD MB					
Gene Symbol	**Flybase ID**	**Gene Symbol**	**Flybase ID**	**Gene Symbol**	**Flybase ID**
NA	FBgn0058469	NA	FBgn0263410	Nep1	FBgn0029843
NA	FBgn0058469	NA	FBgn0264940	CG43347	FBgn0263072
NA	FBgn0058469	CG13442	FBgn0034546	CG42650	FBgn0261502
NA	FBgn0053653	kek1	FBgn0015399	NA	FBgn0283558
NA	FBgn0058469	CG34274	FBgn0085303	tnc	FBgn0039257
CG9380	FBgn0035094	CG1677	FBgn0029941	Tengl4	FBgn0037857
NA	FBgn0053653	CG3655	FBgn0040397	NA	FBgn0265421
NA	FBgn0053653	Ptpa	FBgn0016698	Hr3	FBgn0000448
NA	FBgn0058469	NA	FBgn0267603	NA	FBgn0266238
CG9380	FBgn0035094	CG34274	FBgn0085303	PsGEF	FBgn0264598
NA	FBgn0053653	bru3	FBgn0264001	beat-VII	FBgn0250908
tun	FBgn0034046	NA	FBgn0267653	CG3491	FBgn0028887
NA	FBgn0053653	CG2209	FBgn0030441	beat-IIIb	FBgn0053179
CG12594	FBgn0037941	Rdl	FBgn0004244	jeb	FBgn0086677
CG9380	FBgn0035094	NA	FBgn0267471	Dscam3	FBgn0261046
CG43902	FBgn0264503	CG11029	FBgn0031735	CG34106	FBgn0083942
mAChR-B	FBgn0037546	Dhit	FBgn0028743	NA	FBgn0266892

NA	FBgn0265047	bru3	FBgn0264001	NA	FBgn0266036
CG45002	FBgn0266354	Mef2	FBgn0011656	NA	FBgn0267681
CG6282	FBgn0035914	NA	FBgn0267266	hth	FBgn0001235
CG44815	FBgn0266050	NA	FBgn0065096	CG6154	FBgn0039420
Ten-a	FBgn0267001	Rbp6	FBgn0260943	Dscam2	FBgn0265296
CG7372	FBgn0036522	CG9380	FBgn0035094	tx	FBgn0263118
dpr8	FBgn0052600	CG3556	FBgn0029708	CG31769	FBgn0051769
hppy	FBgn0263395	Cyp12e1	FBgn0037817	NA	FBgn0266213
NA	FBgn0266897	Octbeta1R	FBgn0038980	CG43729	FBgn0263980
NA	FBgn0265420	SkpE	FBgn0031074	NA	FBgn0003374
CG9815	FBgn0034861	NA	FBgn0267600	ChAT	FBgn0000303
NA	FBgn0262369	Kr	FBgn0001325	CG34286	FBgn0085315
Sema2b	FBgn0264273	CG1504	FBgn0031100	nAChRalpha5	FBgn0028875
CG12693	FBgn0029705	DNaseII	FBgn0000477	tow	FBgn0035719
Pkn	FBgn0020621	NA	FBgn0265365	bru3	FBgn0264001
NA	FBgn0267107	CG11873	FBgn0039633	NA	FBgn0263332
Or24a	FBgn0026394	NA	FBgn0266306	CG3483	FBgn0035005
CG43231	FBgn0262876	NA	FBgn0262415	Mctp	FBgn0034389
NA	FBgn0264367	CG32333	FBgn0052333	Amy-p	FBgn0000079
CG5171	FBgn0031907	NA	FBgn0267600	Imp	FBgn0285926
NA	FBgn0265196	Or63a	FBgn0035382	NA	FBgn0284238
NA	FBgn0267269	NijA	FBgn0036101	NA	FBgn0266832
CG45002	FBgn0266354	pdm3	FBgn0261588	NA	FBgn0265679
shep	FBgn0052423	NijA	FBgn0036101	CG17193	FBgn0040571
C901	FBgn0021742	Cyp49a1	FBgn0033524	NA	FBgn0284415
Dop2R	FBgn0053517	CG15712	FBgn0034131	CG15446	FBgn0031155
Pkg21D	FBgn0000442	ey	FBgn0005558	NA	FBgn0264703
NA	FBgn0263778	CG17364	FBgn0036391	NA	FBgn0267910
apt	FBgn0015903	unc-13-4A	FBgn0035756	Ih	FBgn0263397
pros	FBgn0004595	NA	FBgn0267032	CG30158	FBgn0050158
Cnx99A	FBgn0015622	CG13192	FBgn0033653	wcy	FBgn0030812
nAChRalpha1	FBgn0000036	NA	FBgn0264957	CG46301	FBgn0283651
NA	FBgn0053504	bi	FBgn0000179	Tet	FBgn0263392
CG3517	FBgn0038706	NA	FBgn0267799	haf	FBgn0261509
shakB	FBgn0085387	MtnC	FBgn0038790	CG34113	FBgn0083949
CG15198	FBgn0030283	be	FBgn0052594	CG8929	FBgn0034504
CG32115	FBgn0052115	tmod	FBgn0082582	CG32396	FBgn0052396
CG43192	FBgn0262821	CG14491	FBgn0034284	rn	FBgn0267337
CG12200	FBgn0031018	NA	FBgn0262025	KrT95D	FBgn0020647
Menl-2	FBgn0029153	NA	FBgn0262315	CG18480	FBgn0028518
NA	FBgn0267088	CG32846	FBgn0052846	NA	FBgn0264485

s-cup	FBgn0050044	Dys	FBgn0260003	CG45002	FBgn0266354
CG33667	FBgn0053667	CG5773	FBgn0034290	CG8177	FBgn0036043
NA	FBgn0264882	fz	FBgn0001085	CG42878	FBgn0262170
wake	FBgn0266418	trv	FBgn0085391	AstA-R2	FBgn0039595
NA	FBgn0266179	rst	FBgn0003285	ST6Gal	FBgn0035050
CG5906	FBgn0036217	cpx	FBgn0041605	Slob	FBgn0264087
CG9380	FBgn0035094	NA	FBgn0263406	SoxN	FBgn0029123
NA	FBgn0265793	Nep3	FBgn0031081	fne	FBgn0086675
Dif	FBgn0011274	CG43373	FBgn0263131	ACXC	FBgn0040508
NA	FBgn0259996	CG6726	FBgn0039049	sm	FBgn0003435
NA	FBgn0263501	Eip75B	FBgn0000568	NA	FBgn0051331
CG15472	FBgn0029724	NA	FBgn0267671	CG42323	FBgn0259223
CG10993	FBgn0030524	CG11828	FBgn0039616	Abd-B	FBgn0000015
CG1137	FBgn0037454	dpr15	FBgn0037993	5-HT1B	FBgn0263116
px	FBgn0003175	obst-B	FBgn0027600	Dys	FBgn0260003
CG12885	FBgn0039523	glob1	FBgn0027657	brp	FBgn0259246
CG12484	FBgn0086604	NA	FBgn0267962	CG7990	FBgn0030997
Toll-6	FBgn0036494	CG7311	FBgn0028848	CG15719	FBgn0030440
NA	FBgn0265814	inaD	FBgn0001263	CG42337	FBgn0259239
NA	FBgn0267741	CG16894	FBgn0034483	nvy	FBgn0005636
CG42389	FBgn0259735	zf30C	FBgn0270924	CG30270	FBgn0061435
CG6614	FBgn0032369	sty	FBgn0014388	CG42750	FBgn0261804
CG45545	FBgn0267105	VAChT	FBgn0270928	Hr4	FBgn0264562
CG12498	FBgn0040356	CG43335	FBgn0263040	kek6	FBgn0039862
CG14077	FBgn0036830	CG9101	FBgn0030622	unc-104	FBgn0267002
robo3	FBgn0041097	NA	FBgn0265147	CG43066	FBgn0262476
NA	FBgn0266416	NA	FBgn0266097	can	FBgn0011569
NA	FBgn0266957	NA	FBgn0086034	CG42321	FBgn0259221
CG12729	FBgn0029816	NA	FBgn0264337	disco-r	FBgn0285879
Osi20	FBgn0037430	Octbeta2R	FBgn0038063	CG44290	FBgn0265317
mAChR-B	FBgn0037546	CG43188	FBgn0262817	nAChRbeta1	FBgn0000038
beat-IIIa	FBgn0265607	NA	FBgn0267800	NA	FBgn0267306
Cpn	FBgn0261714	CG43783	FBgn0264305	NA	FBgn0261700
CG17003	FBgn0031082	NA	FBgn0262963	CG9698	FBgn0039784
CanA-14F	FBgn0267912	CG31921	FBgn0051921	CG6220	FBgn0033865
CG32698	FBgn0052698	Slc45-1	FBgn0035968	Pkc53E	FBgn0003091
CG4073	FBgn0037827	CG8654	FBgn0034479	NA	FBgn0266830
Cpr76Ba	FBgn0036878	CG6966	FBgn0038286	CG34114	FBgn0083950
trv	FBgn0085391	CG14985	FBgn0035482	CG12538	FBgn0038157
CG17349	FBgn0032771	mam	FBgn0002643	Octbeta3R	FBgn0250910
NA	FBgn0085337	NA	FBgn0265640	NA	FBgn0267579

NA	FBgn0262243	Rbfox1	FBgn0052062	sdt	FBgn0261873
bru1	FBgn0000114	CG9570	FBgn0031085	Tollo	FBgn0029114
r-cup	FBgn0031142	bru3	FBgn0264001	MsR1	FBgn0035331
NA	FBgn0267710	NA	FBgn0265444	NA	FBgn0086037
CG45002	FBgn0266354	NA	FBgn0053653	Rh3	FBgn0003249
CG12716	FBgn0030439	CadN2	FBgn0262018	CG30413	FBgn0050413
CG10384	FBgn0034731	CG6244	FBgn0036531	GluClalpha	FBgn0024963
CG6023	FBgn0030912	CG33463	FBgn0053463	CG45116	FBgn0266591
CG6660	FBgn0039030	alphaKap4	FBgn0035657	CG43231	FBgn0262876
Frq2	FBgn0083228	CG7329	FBgn0032271	Con	FBgn0005775
NA	FBgn0267149	CG13766	FBgn0031834	NA	FBgn0267470
CG31337	FBgn0051337	NA	FBgn0052748	NA	FBgn0264880
CG10139	FBgn0033951	Dop1R1	FBgn0011582	Hs3st-A	FBgn0053147
chrb	FBgn0036165	NA	FBgn0266781	CG5048	FBgn0036437
twz	FBgn0034636	CG17321	FBgn0032719	NA	FBgn0020556
NA	FBgn0267293	drl	FBgn0015380	CG7251	FBgn0031723
CG15333	FBgn0029989	Sfp70A4	FBgn0259970	NA	FBgn0267752
CG1722	FBgn0031168	sdt	FBgn0261873	amon	FBgn0023179
NA	FBgn0267746	Ald	FBgn0000064	NA	FBgn0051331
Sgt	FBgn0032640	NA	FBgn0265755	ham	FBgn0045852
CG43778	FBgn0264308	Gr47a	FBgn0041242	MFS9	FBgn0038799
CG15631	FBgn0031626	fred	FBgn0051774	Fur1	FBgn0004509
GluRIB	FBgn0264000	bol	FBgn0011206	dpr12	FBgn0085414
NA	FBgn0267559	CG43844	FBgn0264426	Tpl94D	FBgn0051281
Oaz	FBgn0284250	orb	FBgn0004882	px	FBgn0003175
CG43843	FBgn0264395	NA	FBgn0264879	NA	FBgn0262400
dpr6	FBgn0040823	NA	FBgn0265537	CG12147	FBgn0037325
NA	FBgn0266401	dnc	FBgn0000479	CG15117	FBgn0034417
CG34357	FBgn0085386	CG13912	FBgn0035186	NA	FBgn0267763
bru1	FBgn0000114	CG4960	FBgn0039371	inc	FBgn0025394
NA	FBgn0267960	NA	FBgn0262972	Kdm4B	FBgn0053182
CG15570	FBgn0029697	NA	FBgn0266023	hwt	FBgn0264542
GluRIB	FBgn0264000	sif	FBgn0085447	Ptp99A	FBgn0004369
CG46308	FBgn0284224	CG34026	FBgn0054026	NA	FBgn0267399
NA	FBgn0263618	CG45263	FBgn0266801	CG9413	FBgn0030574
NA	FBgn0263499	NA	FBgn0262027	cpo	FBgn0263995
Drl-2	FBgn0033791	CG11192	FBgn0034507	CG43231	FBgn0262876
CG17122	FBgn0036962	CG42613	FBgn0261262	CG12484	FBgn0086604
NA	FBgn0267032	CG14891	FBgn0038445	Pde6	FBgn0038237
Naam	FBgn0051216	scramb1	FBgn0052056	TfAP-2	FBgn0261953
CG31128	FBgn0051128	Eip75B	FBgn0000568	NA	FBgn0267658

NA	FBgn0263537	CG10038	FBgn0038013	Sap47	FBgn0013334
gskt	FBgn0046332	NA	FBgn0267315	CG15236	FBgn0033108
Ser7	FBgn0019929	CG15576	FBgn0029700	CG32264	FBgn0052264
CG5171	FBgn0031907	CG3795	FBgn0025378	CG32246	FBgn0052246
NA	FBgn0267259	CG12347	FBgn0038558	igl	FBgn0013467
Rbp6	FBgn0260943	04-Sep	FBgn0259923	dnc	FBgn0000479
CG17944	FBgn0037500	CG10947	FBgn0032857	MED15	FBgn0027592
fest	FBgn0034435	NA	FBgn0263533	PNPase	FBgn0039846
CG43230	FBgn0262875	NA	FBgn0086030	ACXC	FBgn0040508
NA	FBgn0266775	CG11317	FBgn0039816	Ets65A	FBgn0005658
CG8160	FBgn0034011	dpr8	FBgn0052600	NA	FBgn0262898
NA	FBgn0262025	CG46301	FBgn0283651	GstZ2	FBgn0037697
NA	FBgn0264940	NA	FBgn0261924	Rbp6	FBgn0260943
Or45a	FBgn0033404	alpha-Est10	FBgn0015569	Rab26	FBgn0086913
NA	FBgn0264428	Ktl	FBgn0038839	NA	FBgn0264506
CrzR	FBgn0036278	CG15878	FBgn0035316	Snoo	FBgn0085450
Mob2	FBgn0259481	CG13045	FBgn0036596	CG13323	FBgn0033788
CG11898	FBgn0039645	CG43066	FBgn0262476	CG18265	FBgn0036725
NA	FBgn0265585	A16	FBgn0028965	CG5213	FBgn0038345
cpo	FBgn0263995	CG17744	FBgn0035730	NA	FBgn0262989
Sdc	FBgn0010415	Ugt37b1	FBgn0026755	CG12531	FBgn0031064
l(3)72Dr	FBgn0263608	NA	FBgn0262389	slo	FBgn0003429
NA	FBgn0264843	Nlg3	FBgn0083963	Cow	FBgn0039054
NA	FBgn0266245	NA	FBgn0267932	mAChR-A	FBgn0000037
NA	FBgn0265869	CecC	FBgn0000279	mub	FBgn0262737
GluRIB	FBgn0264000	CG14810	FBgn0029589	ush	FBgn0003963
CG13481	FBgn0036421	NA	FBgn0039582	NA	FBgn0265073
Abd-B	FBgn0000015	CG33143	FBgn0053143	heph	FBgn0011224
NA	FBgn0267671	CG9967	FBgn0031413	CG32333	FBgn0052333
Cpr12A	FBgn0030494	NA	FBgn0264678	CG30419	FBgn0050419
CG34286	FBgn0085315	CG11768	FBgn0037625	Ktl	FBgn0038839
betaNACtes3	FBgn0052601	CG31760	FBgn0051760	sll	FBgn0038524
CG13407	FBgn0038931	NA	FBgn0266781	shn	FBgn0003396
CG6629	FBgn0037860	NA	FBgn0264787	mago	FBgn0002736
CG43074	FBgn0262484	DNaseII	FBgn0000477	tna	FBgn0026160
pyd	FBgn0262614	CG31813	FBgn0051813	Fili	FBgn0085397
NA	FBgn0266985	CG7560	FBgn0036157	SP2353	FBgn0034070
Snoo	FBgn0085450	Loxl1	FBgn0039848	RhoGAP100F	FBgn0039883
NA	FBgn0067407	Or67d	FBgn0036080	CG43102	FBgn0262562
Gycbeta100B	FBgn0013973	danr	FBgn0039283	CG42795	FBgn0261928
CG45263	FBgn0266801	CG43066	FBgn0262476	Tb	FBgn0243586

dnc	FBgn0000479	mAChR-B	FBgn0037546	CASK	FBgn0013759
NA	FBgn0267715	unc80	FBgn0039536	RhoGEF3	FBgn0264707
CG42663	FBgn0261545	Corin	FBgn0033192	NA	FBgn0266831
kn	FBgn0001319	NA	FBgn0052449	CG3199	FBgn0038210
NA	FBgn0267746	CG11997	FBgn0037662	Ca-beta	FBgn0259822
NA	FBgn0086060	NA	FBgn0267579	Nlg2	FBgn0031866
inaC	FBgn0004784	CG12784	FBgn0038356	Blimp-1	FBgn0035625
NA	FBgn0267935	Pde1c	FBgn0264815	tun	FBgn0034046
CG42523	FBgn0260428	CG43335	FBgn0263040	CG9328	FBgn0032886
CG15578	FBgn0040905	lov	FBgn0266129	Oseg2	FBgn0035317
CG12374	FBgn0033774	sgg	FBgn0003371	cpx	FBgn0041605
NA	FBgn0267399	ACXC	FBgn0040508	Ca-beta	FBgn0259822
Rbp6	FBgn0260943	CG15803	FBgn0038606	NA	FBgn0265763
NA	FBgn0051588	NA	FBgn0263453	CG4502	FBgn0031896
fru	FBgn0004652	fog	FBgn0000719	IA-2	FBgn0031294
DIP-alpha	FBgn0052791	trv	FBgn0085391	NA	FBgn0262367
NA	FBgn0266908	Mmp2	FBgn0033438	Gug	FBgn0010825
CG10936	FBgn0034253	app	FBgn0260941	sif	FBgn0085447
NA	FBgn0284409	CG32052	FBgn0044328	simj	FBgn0010762
CG9107	FBgn0031764	CanA-14F	FBgn0267912	dve	FBgn0020307
NA	FBgn0264857	CG34113	FBgn0083949	Spn28Db	FBgn0053121
CG34384	FBgn0085413	dan	FBgn0039286	CG45071	FBgn0266441
CG43236	FBgn0262881	sno	FBgn0265630	Sidpn	FBgn0032741
NA	FBgn0262546	CG31741	FBgn0051741	CG13954	FBgn0033405
NA	FBgn0264787	CG45603	FBgn0267163	CG46301	FBgn0283651
NA	FBgn0263503	NA	FBgn0263557	NA	FBgn0262319
CG1958	FBgn0029940	CG34188	FBgn0085217	Elk	FBgn0011589
NA	FBgn0259996	bru2	FBgn0262475		

Less accessible genes E(y)3-KD MB					
Gene Symbol	**Flybase ID**	**Gene Symbol**	**Flybase ID**	**Gene Symbol**	**Flybase ID**
l(3)neo38	FBgn0265276	mino	FBgn0027579	CG43207	FBgn0262843
Maf1	FBgn0267861	Spt20	FBgn0036374	CG18508	FBgn0028746
vri	FBgn0016076	E(spl)m3-HLH	FBgn0002609	cv-c	FBgn0285955
y	FBgn0004034	AdoR	FBgn0039747	Klp59D	FBgn0034827
Gadd45	FBgn0033153	loco	FBgn0020278	CG6231	FBgn0038720
Trf	FBgn0010287	ko	FBgn0020294	Imp	FBgn0285926
brk	FBgn0024250	CG6123	FBgn0030913	KP78b	FBgn0026063
stwl	FBgn0003459	AdamTS-A	FBgn0038341	dpy	FBgn0053196

CG7653	FBgn0028935	UBL3	FBgn0026076	CG31689	FBgn0031449
jing	FBgn0086655	CG43248	FBgn0262893	CG9650	FBgn0029939
lbm	FBgn0016032	dpp	FBgn0000490	CG9743	FBgn0039756
tefu	FBgn0045035	ps	FBgn0261552	ckd	FBgn0035427
Hsp23	FBgn0001224	NA	FBgn0266398	CG2247	FBgn0030320
CG4572	FBgn0038738	Moe	FBgn0011661	CG32103	FBgn0052103
Dak1	FBgn0028833	Unc-76	FBgn0040395	NA	FBgn0263555
CG7653	FBgn0028935	grh	FBgn0259211	NA	FBgn0263617
CG3987	FBgn0038292	br	FBgn0283451	GEFmeso	FBgn0050115
NA	FBgn0011891	NA	FBgn0086081	Dad	FBgn0020493
trv	FBgn0085391	for	FBgn0000721	CG6006	FBgn0063649
Synd	FBgn0053094	E(spl)m7-HLH	FBgn0002633	raw	FBgn0003209
ifc	FBgn0001941	CG34317	FBgn0085346	l(2)37Cg	FBgn0086447
CG6550	FBgn0034214	CG13921	FBgn0035267	Mur2B	FBgn0025390
spin	FBgn0086676	shot	FBgn0013733	CCHa1	FBgn0038199
mfrn	FBgn0039561	aru	FBgn0029095	fus	FBgn0023441
mthl5	FBgn0037960	Asciz	FBgn0035407	NA	FBgn0267087
01-Sep	FBgn0011710	NA	FBgn0263555	CG10924	FBgn0034356
MEP-1	FBgn0035357	Xrp1	FBgn0261113	FER	FBgn0000723
NA	FBgn0267779	CG17896	FBgn0023537	wdp	FBgn0034718
bbx	FBgn0024251	NA	FBgn0266398	nub	FBgn0085424
br	FBgn0283451	sd	FBgn0003345	NA	FBgn0262444
CG11447	FBgn0038737	aop	FBgn0000097	CG18284	FBgn0043825
stv	FBgn0086708	NA	FBgn0266706	NA	FBgn0263019
Pka-R1	FBgn0259243	EcR	FBgn0000546	Ets21C	FBgn0005660
Syp	FBgn0038826	CG11438	FBgn0037164	CG42389	FBgn0259735
Thor	FBgn0261560	vri	FBgn0016076	CG32137	FBgn0052137
CG6044	FBgn0034725	par-1	FBgn0260934	ec	FBgn0000542
HDAC6	FBgn0026428	Lpin	FBgn0263593	AspRS	FBgn0002069
CG31668	FBgn0051668	CG14478	FBgn0028953	bnl	FBgn0014135
NA	FBgn0265830	CG4199	FBgn0025628	CG9436	FBgn0033101
NA	FBgn0265957	CG10924	FBgn0034356	blow	FBgn0004133
NA	FBgn0267633	NA	FBgn0265682	CG31729	FBgn0051729
NA	FBgn0264549	Ser	FBgn0004197	CG6145	FBgn0033853
shn	FBgn0003396	mnd	FBgn0002778	dpp	FBgn0000490
bowl	FBgn0004893	CG12880	FBgn0046258	Ppn	FBgn0003137
CG5984	FBgn0039500	CG30403	FBgn0050403	IP3K1	FBgn0032147
tkv	FBgn0003716	NA	FBgn0051044	d	FBgn0262029
ck	FBgn0000317	CG9747	FBgn0039754	Shroom	FBgn0085408
CG32137	FBgn0052137	CG2915	FBgn0033241	CG8306	FBgn0034142
NA	FBgn0266620	CG16989	FBgn0025621	NA	FBgn0011916

Coop	FBgn0263240	CG6175	FBgn0036152	Inx3	FBgn0265274
Vha44	FBgn0262511	Syp	FBgn0038826	ben	FBgn0000173
trx	FBgn0003862	NA	FBgn0267634	Tollo	FBgn0029114
CG5830	FBgn0036556	CG6163	FBgn0036155	Tsp42Ea	FBgn0029508
Mur2B	FBgn0025390	CG6175	FBgn0036152	aop	FBgn0000097
EcR	FBgn0000546	cv-2	FBgn0000395	MFS14	FBgn0010651
l(1)G0193	FBgn0027280	LpR2	FBgn0051092	CG12560	FBgn0031974
NA	FBgn0284410	CREG	FBgn0025456	CG3788	FBgn0034800
babo	FBgn0011300	EcR	FBgn0000546	NA	FBgn0267679
gem	FBgn0050011	Ser	FBgn0004197	shg	FBgn0003391
bdg	FBgn0034049	ttk	FBgn0003870	NA	FBgn0265888
CG30069	FBgn0050069	gish	FBgn0250823	NA	FBgn0065095
gukh	FBgn0026239	CG12078	FBgn0035426	NA	FBgn0265924
neo	FBgn0039704	fng	FBgn0011591	CG15522	FBgn0039723
Rip11	FBgn0027335	NA	FBgn0266808	Dl	FBgn0000463
NA	FBgn0051885	CG42637	FBgn0261360	CrebB	FBgn0265784
Fas3	FBgn0000636	Lmpt	FBgn0261565	ft	FBgn0001075
Su(P)	FBgn0004465	CG11791	FBgn0039266	Tgi	FBgn0036373
Tollo	FBgn0029114	Ugt86Da	FBgn0040259	foxo	FBgn0038197
Spn42Da	FBgn0265137	dl	FBgn0260632	crc	FBgn0000370
stg	FBgn0003525	mfrn	FBgn0039561	CG7149	FBgn0031948
CG5346	FBgn0038981	E(spl)malpha-BFM	FBgn0002732	CG43337	FBgn0263042
CG32698	FBgn0052698	NA	FBgn0265525	NA	FBgn0267576
CG13252	FBgn0037016	NA	FBgn0052481	br	FBgn0283451
CG13437	FBgn0034541	pdgy	FBgn0027601	NA	FBgn0266986
CG11899	FBgn0014427	CG31028	FBgn0051028	hid	FBgn0003997
NA	FBgn0264869	CLIP-190	FBgn0020503	Mrp4	FBgn0263316
Trxr-1	FBgn0020653	Picot	FBgn0024315	CG5953	FBgn0032587
klar	FBgn0001316	CG14502	FBgn0034321	bark	FBgn0031571
vri	FBgn0016076	NA	FBgn0267169	GstD1	FBgn0001149
bowl	FBgn0004893	CG11275	FBgn0034706	ATP8B	FBgn0037989
NA	FBgn0266161	CG32026	FBgn0052026	NA	FBgn0266973
Fhos	FBgn0266084	CG17834	FBgn0028394	CG31743	FBgn0032618
RhoGEF2	FBgn0023172	EcR	FBgn0000546	N	FBgn0004647
rau	FBgn0031745	magu	FBgn0262169	Lsd-2	FBgn0030608
NA	FBgn0267769	foxo	FBgn0038197	sob	FBgn0004892
E(spl)mbeta-HLH	FBgn0002733	NA	FBgn0265705	Pdp1	FBgn0016694
Cad99C	FBgn0039709	Pino	FBgn0016926	Cyp28d2	FBgn0031688
DIP1	FBgn0024807	CG4374	FBgn0039078	Cln7	FBgn0035767
CG32813	FBgn0052813	CG43245	FBgn0262890	Shroom	FBgn0085408

bib	FBgn0000180	NA	FBgn0054052	pk	FBgn0003090
mamo	FBgn0267033	E(spl)malpha-BFM	FBgn0002732	melt	FBgn0023001
NA	FBgn0266148	CG13895	FBgn0035158	Shroom	FBgn0085408
nkd	FBgn0002945	btsz	FBgn0266756	Shroom	FBgn0085408
E(spl)m2-BFM	FBgn0002592	Gli	FBgn0001987		

More accessible genes Snr1-KD MB					
Gene Symbol	**Flybase ID**	**Gene Symbol**	**Flybase ID**	**Gene Symbol**	**Flybase ID**
NA	FBgn0058469	NA	FBgn0085784	CG14546	FBgn0039395
NA	FBgn0058469	NA	FBgn0053653	NA	FBgn0266762
NA	FBgn0058469	vn	FBgn0003984	Or94a	FBgn0039033
NA	FBgn0058469	Gr98a	FBgn0039520	CG40228	FBgn0063670
CG40439	FBgn0284080	CG3215	FBgn0034825	CG14756	FBgn0033275
DIP-delta	FBgn0085420	CG13801	FBgn0035332	CG41378	FBgn0085638
CG40439	FBgn0284080	scro	FBgn0028993	NA	FBgn0265841
CG33299	FBgn0053299	Ugt36Ba	FBgn0040262	Cyp6a14	FBgn0033302
E5	FBgn0008646	CG41099	FBgn0039955	Sfp93F	FBgn0261060
NA	FBgn0265163	NA	FBgn0085786	CG43795	FBgn0264339
NA	FBgn0267608	NA	FBgn0061188	haf	FBgn0261509
beta4GalT7	FBgn0039258	NA	FBgn0259853	NA	FBgn0266412
NA	FBgn0263519	NA	FBgn0267603	frm	FBgn0035612
NA	FBgn0265766	CG30265	FBgn0050265	NA	FBgn0266762
dtr	FBgn0023090	CG1315	FBgn0026565	Pkn	FBgn0020621
GluRIIC	FBgn0046113	CG34300	FBgn0085329	CG34307	FBgn0085336
Gr22e	FBgn0045497	Acp62F	FBgn0020509	NA	FBgn0263764
ndl	FBgn0002926	MFS17	FBgn0058263	NA	FBgn0267775
CG14838	FBgn0035799	NA	FBgn0266257	NA	FBgn0267537
NA	FBgn0267452	CG3517	FBgn0038706	hppy	FBgn0263395
sick	FBgn0263873	Pkg21D	FBgn0000442	CG40228	FBgn0063670
CG15262	FBgn0028852	NA	FBgn0267308	NA	FBgn0267132
CG42694	FBgn0261584	Dscam3	FBgn0261046	CG2150	FBgn0003065
NA	FBgn0267608	Fur1	FBgn0004509	NA	FBgn0267524
CG3942	FBgn0038008	pyr	FBgn0033649	NA	FBgn0265765
dsx-c73A	FBgn0261799	NA	FBgn0266009	CG42741	FBgn0261705
CG4066	FBgn0038011	hth	FBgn0001235	S-Lap3	FBgn0045770
CG15820	FBgn0035312	CG9997	FBgn0039597	NA	FBgn0085786
CG17018	FBgn0039972	NA	FBgn0267524	NA	FBgn0266232
CG45781	FBgn0267428	Nep4	FBgn0038818	NA	FBgn0264548

NA	FBgn0058182	CG31445	FBgn0051445	CG9312	FBgn0038179
CG31213	FBgn0051213	NA	FBgn0267117	ine	FBgn0011603
NA	FBgn0058182	CG43694	FBgn0263777	NA	FBgn0267460
CG44098	FBgn0264907	pnt	FBgn0003118	CG13581	FBgn0035014
CG45781	FBgn0267428	Obp57b	FBgn0043534	18w	FBgn0004364
CG15580	FBgn0037398	Traf4	FBgn0026319	NA	FBgn0267704
beat-Vc	FBgn0038084	CG8141	FBgn0038125	NA	FBgn0265820
CG14257	FBgn0039479	Acam	FBgn0011273	Cyt-b5-r	FBgn0000406
CG12158	FBgn0040775	Obp56d	FBgn0034470	CG34171	FBgn0085200
CG18577	FBgn0037870	CG4706	FBgn0037862	NA	FBgn0067407
CG5767	FBgn0034292	NA	FBgn0264880	NA	FBgn0267799
NA	FBgn0058182	CG4704	FBgn0039029	NA	FBgn0267786
TwdlT	FBgn0029170	Ir52b	FBgn0050469	Gr22e	FBgn0045497
NA	FBgn0265681	NA	FBgn0085784	NA	FBgn0011855
Gr59d	FBgn0041236	NA	FBgn0086032	NA	FBgn0263664
pHCl-2	FBgn0039840	CG34278	FBgn0085307	CG9168	FBgn0035216
CG17018	FBgn0039972	CG41099	FBgn0039955	bbg	FBgn0087007
NA	FBgn0267769	dpr21	FBgn0260995	Best4	FBgn0036491
Adgf-A2	FBgn0043025	SA-2	FBgn0043865	MFS17	FBgn0058263
NA	FBgn0267133	NA	FBgn0266764	NA	FBgn0085784
CG13713	FBgn0042199	NA	FBgn0264726	Tsp29Fa	FBgn0032074
Ccp84Aa	FBgn0004783	CG13315	FBgn0040827	yip3	FBgn0040063
RYa	FBgn0085512	CG9380	FBgn0035094	CG31245	FBgn0051245
NA	FBgn0262542	CG43732	FBgn0263983	NA	FBgn0267519
NA	FBgn0266762	CG45781	FBgn0267428	mthl12	FBgn0045442
RYa	FBgn0085512	CG31176	FBgn0051176	tnc	FBgn0039257
NA	FBgn0085664	Fis1	FBgn0039969	CG10559	FBgn0039323
CG31087	FBgn0051087	NA	FBgn0039656	CG32834	FBgn0052834
CG40439	FBgn0284080	ND-49L	FBgn0039331	NA	FBgn0085784
rau	FBgn0031745	NA	FBgn0259838	CCAP-R	FBgn0039396
NA	FBgn0085784	CG5623	FBgn0038357	NA	FBgn0265840
BigH1	FBgn0038252	CG9107	FBgn0031764	Jon99Ciii	FBgn0003356
NA	FBgn0264880	NA	FBgn0266007	Ir92a	FBgn0038789
NA	FBgn0264905	NA	FBgn0263500	CG33970	FBgn0053970
DNApol-alpha180	FBgn0259113	CG42355	FBgn0259701	NA	FBgn0266909
CG15800	FBgn0034904	CG14395	FBgn0038073	rau	FBgn0031745
CG31928	FBgn0051928	Or43b	FBgn0026393	d4	FBgn0033015
TwdlT	FBgn0029170	CG43742	FBgn0263999	tnc	FBgn0039257
bab2	FBgn0025525	CG14546	FBgn0039395	NA	FBgn0053653
NA	FBgn0264429	CG6901	FBgn0038414	CG18132	FBgn0031345
CCAP-R	FBgn0039396	Pka-C2	FBgn0000274	CG31296	FBgn0051296

eIF4E4	FBgn0035709	Ets98B	FBgn0005659	Cad86C	FBgn0261053
Gld2	FBgn0038934	NA	FBgn0058182	Yeti	FBgn0267398
ems	FBgn0000576	CG40178	FBgn0058178	CG4793	FBgn0028514
klar	FBgn0001316	MFS17	FBgn0058263	CG18493	FBgn0038701
CG12009	FBgn0035430	CG14740	FBgn0037988	Der-2	FBgn0038438
CG30049	FBgn0050049	CG13559	FBgn0034870	CG11550	FBgn0039864
NA	FBgn0265843	Dyrk2	FBgn0016930	CG16894	FBgn0034483
CG5849	FBgn0038897	NA	FBgn0086022	NA	FBgn0265844
NA	FBgn0266876	NA	FBgn0267133	NA	FBgn0265843
NA	FBgn0267645	CG13539	FBgn0034833	CG11106	FBgn0030280
NA	FBgn0265896	NA	FBgn0267524	NA	FBgn0267688
CG9109	FBgn0031765	Act79B	FBgn0000045	Fst	FBgn0037724
NA	FBgn0259853	CG3330	FBgn0039511	CG14506	FBgn0039659
CG45781	FBgn0267428	NA	FBgn0266415	CG17018	FBgn0039972
CG14280	FBgn0038695	CG13705	FBgn0035582	NA	FBgn0267801
CG7675	FBgn0038610	CG17111	FBgn0039048	NA	FBgn0264375
CG40439	FBgn0284080	CG13658	FBgn0039315	NA	FBgn0266159
NA	FBgn0085810	NA	FBgn0266323	NA	FBgn0267524
NA	FBgn0266840	CG31750	FBgn0046888	NA	FBgn0260435
CG31928	FBgn0051928	CG8483	FBgn0038126	ND-B14.5AL	FBgn0037172
ine	FBgn0011603	CG31077	FBgn0051077	CG1137	FBgn0037454
CG15800	FBgn0034904	CG34289	FBgn0085318	msopa	FBgn0004414
NA	FBgn0002526	CG41378	FBgn0085638	CG31437	FBgn0051437
zormin	FBgn0052311	NA	FBgn0267023	CG3492	FBgn0035007
NA	FBgn0267922	CG2955	FBgn0031585	hdc	FBgn0010113
CCY	FBgn0267592	pyr	FBgn0033649	nahoda	FBgn0034797
NA	FBgn0085786	CG32249	FBgn0052249	NA	FBgn0266234
CheA84a	FBgn0261290	CG7362	FBgn0038258	NA	FBgn0262106
Wdr62	FBgn0031374	Cnx99A	FBgn0015622	ine	FBgn0011603
CG17278	FBgn0046763	NA	FBgn0283501	Obp56i	FBgn0043532
NA	FBgn0267430	CG13712	FBgn0035570	CG9380	FBgn0035094
Cyp12a4	FBgn0038681	CG8501	FBgn0033724	ine	FBgn0011603
NA	FBgn0011869	CG43307	FBgn0262999	NA	FBgn0085664
CG4714	FBgn0033819	Myo81F	FBgn0267431	NA	FBgn0265841
CG9109	FBgn0031765	SoxN	FBgn0029123	Ugt36Ba	FBgn0040262
rdo	FBgn0243486	CG40439	FBgn0284080	sunz	FBgn0037462
NA	FBgn0263551	CG13590	FBgn0035012	CG30463	FBgn0050463
CG31262	FBgn0051262	Adhr	FBgn0000056	Muc96D	FBgn0051439
Spn100A	FBgn0039795	CG17110	FBgn0039050	NA	FBgn0267683
dpr11	FBgn0053202	NA	FBgn0053653	Act57B	FBgn0000044
NA	FBgn0265382	NA	FBgn0267143	MFS17	FBgn0058263

NA	FBgn0267133	NA	FBgn0266203	CG34433	FBgn0085462
CG10126	FBgn0038088	tll	FBgn0003720	CG31013	FBgn0051013
CG17109	FBgn0039051	Dnah3	FBgn0035581	CG34433	FBgn0085462
CG43742	FBgn0263999	CG31051	FBgn0051051	CG11029	FBgn0031735
CG14506	FBgn0039659	CG9380	FBgn0035094	Spt3	FBgn0037981
CG1315	FBgn0026565	NA	FBgn0266747	Gr92a	FBgn0045471
PpN58A	FBgn0025573	Art6	FBgn0038189	LysP	FBgn0004429
NA	FBgn0267769	Syx17	FBgn0035540	nompB	FBgn0016919
NA	FBgn0265843	lov	FBgn0266129	NA	FBgn0267939
NA	FBgn0266909	NA	FBgn0262425	Klp59D	FBgn0034827
CG41562	FBgn0085693	NA	FBgn0266873	Or59b	FBgn0034865
CG4021	FBgn0034659	NA	FBgn0265653	ND-AGGG	FBgn0085736
mey	FBgn0039851	CG17109	FBgn0039051	CG10814	FBgn0033830
fred	FBgn0051774	CG14506	FBgn0039659	NA	FBgn0264428
CG3347	FBgn0031513	NA	FBgn0266816	NA	FBgn0262172
CG42741	FBgn0261705	CG14354	FBgn0039376	NA	FBgn0266762
CG10479	FBgn0035656	CG10177	FBgn0039083	tmod	FBgn0082582
CG13589	FBgn0035011	NA	FBgn0266842	NA	FBgn0265945
ms(3)76Ba	FBgn0036868	TkR99D	FBgn0004622	CG1139	FBgn0035300
CG1544	FBgn0039827	Or94a	FBgn0039033	Obp83g	FBgn0046875
NA	FBgn0265765	fz2	FBgn0016797	NA	FBgn0267710
NA	FBgn0265844	rdo	FBgn0243486	ine	FBgn0011603
Cyp6a18	FBgn0039519	CG14317	FBgn0038566	CG6293	FBgn0037807
NA	FBgn0267133	sala	FBgn0003313	NA	FBgn0265305
CG4374	FBgn0039078	NA	FBgn0267787	NA	FBgn0267133
CG41099	FBgn0039955	CG31296	FBgn0051296	NA	FBgn0267524
NA	FBgn0267133	CG17278	FBgn0046763	betaTub60D	FBgn0003888
NA	FBgn0051432	NA	FBgn0262887	NA	FBgn0262025
NA	FBgn0267620	CG40439	FBgn0058439	CG14062	FBgn0039592
NA	FBgn0265728	NA	FBgn0266401	CG42357	FBgn0259703
CG40439	FBgn0284080	CG4390	FBgn0038771	NA	FBgn0265062
Klp59C	FBgn0034824	osp	FBgn0003016	NA	FBgn0267526
NA	FBgn0265420	Art9	FBgn0038188	CG34371	FBgn0085400
NA	FBgn0267519	NA	FBgn0011897	CG4073	FBgn0037827
CrzR	FBgn0036278	cher	FBgn0014141	NA	FBgn0028889
SA-2	FBgn0043865	CG7794	FBgn0038565	18w	FBgn0004364
Ir94f	FBgn0051225	CG40439	FBgn0284080	CG10589	FBgn0037035
LpR2	FBgn0051092	NA	FBgn0266747	CG9380	FBgn0035094
NA	FBgn0259861	Osi6	FBgn0027527	nyo	FBgn0039852
NA	FBgn0264880	NA	FBgn0085786	CG1137	FBgn0037454
NimB4	FBgn0028542	Cpr49Aa	FBgn0050045	klar	FBgn0001316

CG33012	FBgn0053012	HP6	FBgn0031613	NA	FBgn0267724
Or23a	FBgn0026395	CrzR	FBgn0036278	NA	FBgn0265766
CG42370	FBgn0259716	CG17928	FBgn0032603	NA	FBgn0263657
Gbp3	FBgn0039031	NA	FBgn0267775	CG44290	FBgn0265317
CG3916	FBgn0038003	NA	FBgn0085786	MsR1	FBgn0035331
beat-IIa	FBgn0038498	NA	FBgn0058182	CG41562	FBgn0085693
NA	FBgn0265592	NA	FBgn0003926	Ptp99A	FBgn0004369
lmd	FBgn0039039	NA	FBgn0263618	how	FBgn0264491
NA	FBgn0265766	NA	FBgn0263664	sxc	FBgn0261403
Ir94g	FBgn0039079	CG15408	FBgn0031523	NA	FBgn0265842
ND-AGGG	FBgn0085736	NA	FBgn0267602	NA	FBgn0053653
CG16837	FBgn0035009	CG4554	FBgn0034734	mey	FBgn0039851
Ir94h	FBgn0039080	Dhc93AB	FBgn0013812	neo	FBgn0039704
CG9109	FBgn0031765	NA	FBgn0264857	Acp36DE	FBgn0011559
CG4073	FBgn0037827	CG43694	FBgn0263777	dan	FBgn0039286
CG14257	FBgn0039479	NA	FBgn0263618	Pgam5-2	FBgn0035004
CG3330	FBgn0039511	NA	FBgn0263874	Prosbeta5R2	FBgn0051742
NA	FBgn0085664	CG41520	FBgn0087011	Tmc	FBgn0267796
NA	FBgn0267524	Or24a	FBgn0026394	CG1894	FBgn0039585
NA	FBgn0267744	nyo	FBgn0039852	CG6040	FBgn0038679
AOX4	FBgn0038350	NA	FBgn0264889	CG31128	FBgn0051128
CG4372	FBgn0034665	Ser	FBgn0004197	CG3517	FBgn0038706
NA	FBgn0266010	ine	FBgn0011603	Thd1	FBgn0026869
2mit	FBgn0260793	NA	FBgn0267719	Su(var)3-3	FBgn0260397
CG42710	FBgn0261627	CG40228	FBgn0063670	orb	FBgn0004882
CG7720	FBgn0038652	CG10170	FBgn0039085	CG10321	FBgn0034643
NA	FBgn0085664	NA	FBgn0052480	NA	FBgn0267143
NA	FBgn0267133	CG7465	FBgn0035551	NA	FBgn0265945
CG42685	FBgn0261571	CG5024	FBgn0039373	NA	FBgn0267123
Dhc98D	FBgn0013813	Act79B	FBgn0000045	Vha100-3	FBgn0028669
CG3483	FBgn0035005	mey	FBgn0039851	ppk15	FBgn0039424
NA	FBgn0266087	Svil	FBgn0266696	dpr17	FBgn0051361
NA	FBgn0266380	NA	FBgn0266909	NA	FBgn0267269
CG42714	FBgn0261631	CG30268	FBgn0050268	MsR1	FBgn0035331
NA	FBgn0267133	HP1e	FBgn0037675	NA	FBgn0267122
NA	FBgn0264338	NA	FBgn0267646	NA	FBgn0267787
CG42493	FBgn0260007	NA	FBgn0265892	CG15343	FBgn0030029
Or43b	FBgn0026393	CG43203	FBgn0262839	NA	FBgn0284415
CG4907	FBgn0039010	beat-Vc	FBgn0038084	mtt	FBgn0050361
CG17211	FBgn0032414	Jon99Ciii	FBgn0003357	CG10184	FBgn0039094
Gr98a	FBgn0039520	CG14257	FBgn0039479	NA	FBgn0267149

Prtl99C	FBgn0039707	CG40178	FBgn0058178	NA	FBgn0262382
SA-2	FBgn0043865	CG44290	FBgn0265317	scb	FBgn0003328
CG45781	FBgn0267428	NA	FBgn0051432	CG42534	FBgn0260487
CG3734	FBgn0038700	NA	FBgn0267958	pHCl-2	FBgn0039840
CG30048	FBgn0050048	CG40228	FBgn0063670	bbg	FBgn0087007
CG32488	FBgn0052488	dsx	FBgn0000504	MFS17	FBgn0058263
BG642163	FBgn0083938	NA	FBgn0266887	NA	FBgn0267715
CG44569	FBgn0265762	CG43896	FBgn0264488	Tb	FBgn0243586
AOX3	FBgn0038349	CG42238	FBgn0250867	Sfp65A	FBgn0259969
glob2	FBgn0250846	CG43188	FBgn0262817	NA	FBgn0053653
CG10750	FBgn0032769	NA	FBgn0266226	CG4572	FBgn0038738
HP6	FBgn0031613	TrissinR	FBgn0085410		
CG41378	FBgn0085638	NA	FBgn0264548		

Less accessible genes Snr1-KD MB					
Gene Symbol	**Flybase ID**	**Gene Symbol**	**Flybase ID**	**Gene Symbol**	**Flybase ID**
MTA1-like	FBgn0027951	Nup205	FBgn0031078	EcR	FBgn0000546
Atet	FBgn0020762	CG4287	FBgn0038388	Top3beta	FBgn0026015
mAChR-A	FBgn0000037	CG13907	FBgn0035173	Ptpmeg2	FBgn0028341
Ufl1	FBgn0037467	CG12702	FBgn0031070	sno	FBgn0265630
Fer2LCH	FBgn0015221	Bacc	FBgn0031453	Hex-A	FBgn0001186
bin3	FBgn0263144	CG33798	FBgn0053798	para	FBgn0285944
Bsg	FBgn0261822	Socs36E	FBgn0041184	Rab10	FBgn0015789
14-3-3epsilon	FBgn0020238	Crtc	FBgn0036746	CG9281	FBgn0030672
alphaTub84B	FBgn0003884	eas	FBgn0000536	Gbeta13F	FBgn0001105
GC	FBgn0035245	CG9821	FBgn0037636	wcy	FBgn0030812
mtSSB	FBgn0010438	NA	FBgn0264940	Fur2	FBgn0004598
Blimp-1	FBgn0035625	Ppa	FBgn0020257	TRAM	FBgn0040340
CG9331	FBgn0032889	Gfat2	FBgn0039580	CG15296	FBgn0030215
CG31522	FBgn0051522	hiw	FBgn0030600	NA	FBgn0029003
CG16896	FBgn0035073	inc	FBgn0025394	Smr	FBgn0265523
NA	FBgn0262319	toy	FBgn0019650	zf30C	FBgn0270924
NA	FBgn0262400	yps	FBgn0022959	CG9921	FBgn0030743
stj	FBgn0261041	vri	FBgn0016076	oc	FBgn0004102
CG45075	FBgn0266445	msn	FBgn0010909	tay	FBgn0260938
Tet	FBgn0263392	RpLP2	FBgn0003274	CG14810	FBgn0029589
ssp3	FBgn0032723	CG34172	FBgn0085201	lin-52	FBgn0029800
NA	FBgn0266831	chif	FBgn0000307	bif	FBgn0014133
RpS9	FBgn0010408	br	FBgn0283451	NA	FBgn0267099

tna	FBgn0026160	NA	FBgn0267201	NA	FBgn0264390
par-1	FBgn0260934	svr	FBgn0004648	zfh2	FBgn0004607
CG15233	FBgn0033076	not	FBgn0013717	Pfrx	FBgn0027621
eff	FBgn0011217	CG6785	FBgn0032399	CG32698	FBgn0052698
chic	FBgn0000308	Pka-C1	FBgn0000273	dpr14	FBgn0029974
NA	FBgn0266830	CG15465	FBgn0029746	br	FBgn0283451
CG11486	FBgn0035397	dnc	FBgn0000479	Nup93-1	FBgn0027537
cpx	FBgn0041605	en	FBgn0000577	shn	FBgn0003396
plum	FBgn0039431	SrpRbeta	FBgn0011509	Vsp37A	FBgn0016038
l(1)G0156	FBgn0027291	NA	FBgn0267559	CG12581	FBgn0037213
Spn28Db	FBgn0053121	Rh5	FBgn0014019	Lcch3	FBgn0010240
ckn	FBgn0033987	RpS17	FBgn0005533	CG14234	FBgn0031065
GstZ2	FBgn0037697	ras	FBgn0003204	cib	FBgn0026084
l(3)04053	FBgn0010830	Ars2	FBgn0033062	su(sable)	FBgn0003575
NA	FBgn0011938	Daxx	FBgn0031820	alpha-Man-Ia	FBgn0259170
ush	FBgn0003963	NA	FBgn0011891	BtbVII	FBgn0263108
CG3434	FBgn0036000	THADA	FBgn0031077	sol	FBgn0003464
NA	FBgn0012024	CG12395	FBgn0030722	spri	FBgn0085443
subdued	FBgn0038721	crol	FBgn0020309	CG9413	FBgn0030574
CG10098	FBgn0037472	Sema1b	FBgn0016059	CG13323	FBgn0033788
shn	FBgn0003396	hang	FBgn0026575	Tlk	FBgn0283657
cpx	FBgn0041605	NA	FBgn0275433	chm	FBgn0028387
mts	FBgn0004177	ifc	FBgn0001941	CG5273	FBgn0040382
NA	FBgn0265153	dnc	FBgn0000479	CG1677	FBgn0029941
NA	FBgn0267702	Zip99C	FBgn0039714	CHES-1-like	FBgn0029504
NA	FBgn0052449	CanA-14F	FBgn0267912	fliI	FBgn0000709
Tet	FBgn0263392	dlg1	FBgn0001624	Socs16D	FBgn0030869
jp	FBgn0032129	slgA	FBgn0003423	CG9413	FBgn0030574
Mpc1	FBgn0038662	CG17124	FBgn0032297	CG43347	FBgn0263072
l(3)neo38	FBgn0265276	Cerk	FBgn0037315	CG9650	FBgn0029939
Vha16-1	FBgn0262736	br	FBgn0283451	RpS3A	FBgn0017545
NA	FBgn0263486	Srpk79D	FBgn0025702	NA	FBgn0267100
CycG	FBgn0039858	Pfk	FBgn0003071	CG4078	FBgn0029798
CG10082	FBgn0034644	CG7326	FBgn0030970	CG3842	FBgn0029866
Ext2	FBgn0029175	NA	FBgn0065095	Ubr3	FBgn0260970
fax	FBgn0014163	Sh	FBgn0003380	HDAC4	FBgn0041210
Ald	FBgn0000064	NA	FBgn0065095	CG4766	FBgn0027546
CG10019	FBgn0031568	Raf	FBgn0003079	CG3775	FBgn0030425
Eip74EF	FBgn0000567	Mnt	FBgn0023215	CG32521	FBgn0052521
NAT1	FBgn0010488	CG43245	FBgn0262890	CG44774	FBgn0266000
vimar	FBgn0022960	Vsx2	FBgn0263512	IntS4	FBgn0026679

CG13323	FBgn0033788	CG43245	FBgn0262890	stnB	FBgn0016975
CG6005	FBgn0038672	CG3638	FBgn0261444	Arp2	FBgn0011742
CG6767	FBgn0036030	NA	FBgn0263345	CG42580	FBgn0260870
P5CDh1	FBgn0037138	corto	FBgn0010313	CG12991	FBgn0030847
CCT5	FBgn0010621	NA	FBgn0264826	CG4661	FBgn0030429
trh	FBgn0262139	CG42700	FBgn0261611	alpha-Man-Ia	FBgn0259170
NA	FBgn0051331	cdc14	FBgn0031952	NA	FBgn0047092
NA	FBgn0266819	Hr51	FBgn0034012	dnc	FBgn0000479
CG9663	FBgn0031516	CG1504	FBgn0031100	CG6767	FBgn0036030
cbt	FBgn0043364	Corin	FBgn0033192	snz	FBgn0029976
pdm3	FBgn0261588	NA	FBgn0267962	CG18508	FBgn0028746
CG5380	FBgn0038951	NA	FBgn0264787	CG9784	FBgn0030761
chinmo	FBgn0086758	Pkn	FBgn0020621	CG12643	FBgn0040942
Ppat-Dpck	FBgn0035632	CG12091	FBgn0035228	ari-1	FBgn0017418
Hr3	FBgn0000448	unc-119	FBgn0025549	Mnt	FBgn0023215
CG18371	FBgn0033893	CG3078	FBgn0023524	CG9650	FBgn0029939
Msp300	FBgn0261836	RpL28	FBgn0035422	CG30020	FBgn0050020
put	FBgn0003169	disco-r	FBgn0285879	CG7556	FBgn0030990
CG6163	FBgn0036155	Mef2	FBgn0011656	inaE	FBgn0261244
cnk	FBgn0021818	sgg	FBgn0003371	CG34449	FBgn0085478
PRAS40	FBgn0267824	Pp2C1	FBgn0022768	Appl	FBgn0000108
HnRNP-K	FBgn0267791	velo	FBgn0035713	CG11138	FBgn0030400
tara	FBgn0040071	CG6201	FBgn0032343	CG30389	FBgn0050389
Reph	FBgn0021800	sbb	FBgn0285917	Tango13	FBgn0086674
NA	FBgn0266209	e(y)3	FBgn0087008	ey	FBgn0005558
Stat92E	FBgn0016917	lig	FBgn0020279	Kap3	FBgn0028421
Syp	FBgn0038826	CG6220	FBgn0033865	Cyp1	FBgn0004432
Inos	FBgn0025885	mib2	FBgn0086442	NA	FBgn0265454
CG12054	FBgn0039831	Nf1	FBgn0015269	Scgdelta	FBgn0025391
CG7879	FBgn0035235	KrT95D	FBgn0020647	CG15894	FBgn0029864
simj	FBgn0010762	CG18265	FBgn0036725	RunxA	FBgn0083981
NTPase	FBgn0024947	CG11658	FBgn0036196	muc	FBgn0283658
NA	FBgn0267579	CG13894	FBgn0035157	Usp2	FBgn0031187
CadN	FBgn0015609	CG7990	FBgn0030997	brk	FBgn0024250
Ssdp	FBgn0011481	Tango5	FBgn0052675	bbx	FBgn0024251
NA	FBgn0052272	CG16779	FBgn0037698	Pat1	FBgn0029878
Dys	FBgn0260003	BTBD9	FBgn0030228	CG42450	FBgn0259927
CG11000	FBgn0263353	Taf4	FBgn0010280	brk	FBgn0024250
Ca-beta	FBgn0259822	NA	FBgn0052748	CG11566	FBgn0031159
Pka-R2	FBgn0022382	Spt6	FBgn0028982	CG2889	FBgn0030206
NK7.1	FBgn0024321	NA	FBgn0001079	SkpA	FBgn0025637

CtBP	FBgn0020496	Amun	FBgn0030328	NA	FBgn0267741
dos	FBgn0016794	Raf	FBgn0003079	nej	FBgn0261617
CG33203	FBgn0053203	bi	FBgn0000179	CG43783	FBgn0264305
B4	FBgn0023407	NetB	FBgn0015774	lva	FBgn0029688
alt	FBgn0038535	Tlk	FBgn0283657	CrebB	FBgn0265784
Syx1A	FBgn0013343	NA	FBgn0027493	rst	FBgn0003285
CG31769	FBgn0051769	zfh2	FBgn0004607	Rbp	FBgn0262483
CG45116	FBgn0266591	Stt3A	FBgn0031149	NA	FBgn0264678
Sidpn	FBgn0032741	gw	FBgn0051992	CG32813	FBgn0052813
Rgl	FBgn0026376	CG45071	FBgn0266441	CG11138	FBgn0030400
CG14505	FBgn0034327	NA	FBgn0264439	CG12112	FBgn0030048
mor	FBgn0002783	SPoCk	FBgn0052451	CG6867	FBgn0030887
Eip74EF	FBgn0000567	CG3703	FBgn0040348	Mekk1	FBgn0024329
jumu	FBgn0015396	CG9413	FBgn0030574	CkIIbeta	FBgn0000259
CG13321	FBgn0033787	CanA-14F	FBgn0267912	tth	FBgn0030502
CG13204	FBgn0033627	CG6424	FBgn0028494	CG3842	FBgn0029866
Akap200	FBgn0027932	tou	FBgn0033636	CG4496	FBgn0031894
NA	FBgn0086080	fs(1)h	FBgn0004656	unc-119	FBgn0025549
NA	FBgn0265153	alpha-Man-IIb	FBgn0026616	Tis11	FBgn0011837
bor	FBgn0040237	lola	FBgn0283521	CG1718	FBgn0031170
btsz	FBgn0266756	ey	FBgn0005558	CG14442	FBgn0029893
Cka	FBgn0044323	Oaz	FBgn0284250	mahe	FBgn0029979
NA	FBgn0267634	X11Lbeta	FBgn0052677	Gga	FBgn0030141
HmgZ	FBgn0010228	Act5C	FBgn0000042	l(1)G0196	FBgn0027279
sm	FBgn0003435	rictor	FBgn0031006	CHES-1-like	FBgn0029504
CG11883	FBgn0033538	srl	FBgn0037248	mamo	FBgn0267033
smg	FBgn0016070	Nmdar2	FBgn0053513	MED22	FBgn0040339
Trl	FBgn0013263	VhaSFD	FBgn0027779	Trf2	FBgn0261793
futsch	FBgn0259108	ERp60	FBgn0033663	NA	FBgn0264678
grp	FBgn0261278	Pp2C1	FBgn0022768	br	FBgn0283451
CG11873	FBgn0039633	Appl	FBgn0000108	CG14621	FBgn0031183
tara	FBgn0040071	disco	FBgn0000459	NA	FBgn0265830
CG34347	FBgn0085376	Dlic	FBgn0030276	CG12531	FBgn0031064
pk	FBgn0003090	para	FBgn0285944	CG15373	FBgn0030889
Dpit47	FBgn0266518	D19B	FBgn0022699	Hers	FBgn0052529
Atx2	FBgn0041188	dac	FBgn0005677	sdt	FBgn0261873
CG42784	FBgn0263354	CG15719	FBgn0030440	CHES-1-like	FBgn0029504
bin3	FBgn0263144	ome	FBgn0259175	NA	FBgn0264678
mei-P26	FBgn0026206	fzr	FBgn0262699	fend	FBgn0030090
eRF3	FBgn0020443	bma	FBgn0085385	Trxr-1	FBgn0020653
CG2246	FBgn0039790	Cyp308a1	FBgn0030949	rut	FBgn0003301

NA	FBgn0265419	mim	FBgn0053558	CG11151	FBgn0030519
FASN1	FBgn0283427	vri	FBgn0016076	CG14212	FBgn0031045
CalpA	FBgn0012051	CG32590	FBgn0052590	His3.3B	FBgn0004828
MESR6	FBgn0036846	CG42337	FBgn0259239	CG15312	FBgn0030174
Sox14	FBgn0005612	Tpr2	FBgn0032586	ph-d	FBgn0004860
Sirt1	FBgn0024291	shn	FBgn0003396	CG11566	FBgn0031159
CG16972	FBgn0032481	dsd	FBgn0039528	prage	FBgn0283741
Sh	FBgn0003380	rdgB	FBgn0003218	Raf	FBgn0003079
Tet	FBgn0263392	CG18766	FBgn0042111	UBL3	FBgn0026076
Iris	FBgn0031305	CG9328	FBgn0032886	DIP-alpha	FBgn0052791
CG9084	FBgn0033582	hwt	FBgn0264542	btd	FBgn0000233
mtd	FBgn0013576	CG3690	FBgn0040350	exd	FBgn0000611
hwt	FBgn0264542	Eip74EF	FBgn0000567	CrebB	FBgn0265784
NA	FBgn0267219	Adar	FBgn0026086	CG6961	FBgn0030959
NA	FBgn0262367	Rbf	FBgn0015799	NA	FBgn0263334
dunk	FBgn0083973	CBP	FBgn0026144	NA	FBgn0266350
TER94	FBgn0261014	sqz	FBgn0010768	vap	FBgn0003969
Hrb27C	FBgn0004838	Naa15-16	FBgn0031020	MFS10	FBgn0030452
CG14762	FBgn0033250	Tango14	FBgn0031312	pico	FBgn0261811
NA	FBgn0267203	CanA-14F	FBgn0267912	arm	FBgn0000117
CG12173	FBgn0037305	glob1	FBgn0027657	tup	FBgn0003896
CG32547	FBgn0052547	NA	FBgn0053294	Hers	FBgn0052529
NA	FBgn0052826	elav	FBgn0260400	SkpD	FBgn0026174
cnn	FBgn0013765	CG10565	FBgn0037051	psq	FBgn0263102
NA	FBgn0265955	babo	FBgn0011300	A16	FBgn0028965
pros	FBgn0004595	CG18467	FBgn0034218	RSG7	FBgn0024941
Sin3A	FBgn0022764	mlt	FBgn0265512	dpr8	FBgn0052600
eIF3b	FBgn0034237	NA	FBgn0267752	NA	FBgn0265830
east	FBgn0261954	cac	FBgn0263111	c11.1	FBgn0040236
metro	FBgn0050021	NA	FBgn0086080	sd	FBgn0003345
Ih	FBgn0263397	CG8173	FBgn0030864	Ahcy	FBgn0014455
jumu	FBgn0015396	BCL7-like	FBgn0026149	Shroom	FBgn0085408
CG2865	FBgn0023526	CG11448	FBgn0024985	Drak	FBgn0052666
gem	FBgn0050011	ras	FBgn0003204	CG6481	FBgn0030936
NA	FBgn0265924	disco-r	FBgn0285879	CG43347	FBgn0263072
msn	FBgn0010909	NA	FBgn0065095	shakB	FBgn0085387
NA	FBgn0051331	Ubqn	FBgn0031057	sesB	FBgn0003360
CG42788	FBgn0261859	Mur2B	FBgn0025390	CG1998	FBgn0030485
l(3)neo38	FBgn0265276	Cngl	FBgn0263257	CG12576	FBgn0031190
hth	FBgn0001235	CG45603	FBgn0267163	mam	FBgn0002643
CG9328	FBgn0032886	EcR	FBgn0000546	l(1)G0193	FBgn0027280

mrt	FBgn0039507	nmo	FBgn0011817	CG1640	FBgn0030478
sax	FBgn0003317	Pka-R1	FBgn0259243	rdgA	FBgn0261549
CG5937	FBgn0029834	sta	FBgn0003517	RabX2	FBgn0030200
Syx1A	FBgn0013343	CG43736	FBgn0263993	CG14810	FBgn0029589
sll	FBgn0038524	br	FBgn0283451	CG33795	FBgn0053795
RpS11	FBgn0033699	Sh	FBgn0003380	unc	FBgn0003950
CG3719	FBgn0024986	Tlk	FBgn0283657	Tlk	FBgn0283657
NA	FBgn0267668	tou	FBgn0033636	CG17598	FBgn0031194
mura	FBgn0037705	RpII215	FBgn0003277	Rip11	FBgn0027335
wapl	FBgn0004655	Shmt	FBgn0029823	CG7332	FBgn0030973
tara	FBgn0040071	NA	FBgn0086037	CG14408	FBgn0030581
14-3-3zeta	FBgn0004907	Dif	FBgn0011274	nej	FBgn0261617
NA	FBgn0263483	Rh5	FBgn0014019	CHES-1-like	FBgn0029504
px	FBgn0003175	CG2691	FBgn0030504	CG2918	FBgn0023529
hrg	FBgn0015949	Raf	FBgn0003079	CG7058	FBgn0030961
Nep1	FBgn0029843	CG15233	FBgn0033076	Syb	FBgn0003660
ATPsynC	FBgn0039830	Ube3a	FBgn0061469	NA	FBgn0264676
CG6044	FBgn0034725	Raf	FBgn0003079	Cdc7	FBgn0028360
CG2924	FBgn0023528	mamo	FBgn0267033	Rala	FBgn0015286
NA	FBgn0283558	Ten-a	FBgn0267001	CG43902	FBgn0264503
hid	FBgn0003997	amon	FBgn0023179	CG16721	FBgn0029820
NA	FBgn0283426	NA	FBgn0266892	HDAC6	FBgn0026428
pan	FBgn0085432	Tob	FBgn0028397	Fnta	FBgn0031633
Su(z)2	FBgn0265623	Rab3-GEF	FBgn0030613	CG8128	FBgn0030668
CG32085	FBgn0052085	RhoGAP19D	FBgn0031118	NA	FBgn0267162
Rph	FBgn0030230	Act5C	FBgn0000042	l(1)G0320	FBgn0028327
CG1427	FBgn0037347	NA	FBgn0263039	mamo	FBgn0267033
prtp	FBgn0030329	dnc	FBgn0000479	CG15309	FBgn0030183
CG17544	FBgn0032775	Wee1	FBgn0011737	Tak1	FBgn0026323
Reph	FBgn0021800	ph-p	FBgn0004861	l(1)1Bi	FBgn0001341
NA	FBgn0265427	Ten-a	FBgn0267001	NA	FBgn0267067
tipE	FBgn0003710	scramb1	FBgn0052056	CG1582	FBgn0030246
CG9171	FBgn0031738	dpr8	FBgn0052600	Syx16	FBgn0031106
Gug	FBgn0010825	NA	FBgn0086667	CG15891	FBgn0029860
Sxl	FBgn0264270	CG7231	FBgn0031968	CG14810	FBgn0029589
Uba1	FBgn0023143	NA	FBgn0052493	bbx	FBgn0024251
sba	FBgn0016754	CG5953	FBgn0032587	hwt	FBgn0264542
cg	FBgn0000289	CG6379	FBgn0029693	Grip	FBgn0029830
Galphao	FBgn0001122	Gug	FBgn0010825	CG12498	FBgn0040356
CG44838	FBgn0266101	CG4660	FBgn0029839	dnc	FBgn0000479
CG6231	FBgn0038720	CG1722	FBgn0031168	ph-p	FBgn0004861

VAChT	FBgn0270928	NA	FBgn0264703	psq	FBgn0263102
NA	FBgn0266830	Hk	FBgn0263220	CG44422	FBgn0265595
trv	FBgn0085391	Awh	FBgn0013751	CG9411	FBgn0030569
ps	FBgn0261552	CG6481	FBgn0030936	Pmp70	FBgn0031069
jim	FBgn0027339	NA	FBgn0267169	NA	FBgn0011951
CG14434	FBgn0029915	Raf	FBgn0003079	CG18508	FBgn0028746
NA	FBgn0267910	01-Sep	FBgn0011710	Ubr1	FBgn0030809
fne	FBgn0086675	Mur2B	FBgn0025390	UbcE2H	FBgn0029996
Kdm4B	FBgn0053182	Calr	FBgn0005585	Rcd-1	FBgn0031047
SH3PX1	FBgn0040475	pod1	FBgn0029903	CG6106	FBgn0030914
crol	FBgn0020309	Smox	FBgn0025800	SK	FBgn0029761
CG4230	FBgn0031683	Tomosyn	FBgn0030412	CG32806	FBgn0052806
CG7971	FBgn0035253	CG1578	FBgn0030336	B-H2	FBgn0004854
kdn	FBgn0261955	Atf3	FBgn0028550	shakB	FBgn0085387
Mob2	FBgn0259481	MAPk-Ak2	FBgn0013987	CG7378	FBgn0030976
CG42492	FBgn0259994	NA	FBgn0263039	Yippee	FBgn0026749
CG11399	FBgn0037021	fz4	FBgn0027342	pdgy	FBgn0027601
Rab27	FBgn0025382	Hsc70-3	FBgn0001218	Roc1a	FBgn0025638
CG3634	FBgn0037026	CG42240	FBgn0250869	CG5004	FBgn0260748
jim	FBgn0027339	CG1958	FBgn0029940	CG14441	FBgn0029895
Kdm2	FBgn0037659	CG8300	FBgn0029937	CG15200	FBgn0030278
ND-SGDH	FBgn0011455	Top1	FBgn0004924	NA	FBgn0267068
MtnC	FBgn0038790	Ptp10D	FBgn0004370	betaNACtes3	FBgn0052601
pum	FBgn0003165	bip1	FBgn0026263	Pfrx	FBgn0027621
ey	FBgn0005558	deltaCOP	FBgn0028969	CG12155	FBgn0029957
unc-5	FBgn0034013	HDAC4	FBgn0041210	Ptpmeg2	FBgn0028341
sn	FBgn0003447	Svil	FBgn0266696	N	FBgn0004647
Cyp28d2	FBgn0031688	NA	FBgn0265866	l(1)G0334	FBgn0028325
pnr	FBgn0003117	CG34172	FBgn0085201	RpL31	FBgn0285949
upSET	FBgn0036398	Cdc7	FBgn0028360	ben	FBgn0000173
Lk6	FBgn0017581	Tlk	FBgn0283657	Tlk	FBgn0283657
CG32532	FBgn0052532	CG14810	FBgn0029589	NA	FBgn0265705
dikar	FBgn0261934	sgg	FBgn0003371	CG9380	FBgn0035094
CG9328	FBgn0032886	AMPdeam	FBgn0052626	CG43759	FBgn0264090
CG45050	FBgn0266410	dtn	FBgn0262730	mamo	FBgn0267033
CG16721	FBgn0029820	HP5	FBgn0030301	Sap30	FBgn0030788
Sox102F	FBgn0039938	CG32506	FBgn0052506	NA	FBgn0263503
Mondo	FBgn0032940	CG32809	FBgn0023531	RhoGAP19D	FBgn0031118
brat	FBgn0010300	PhKgamma	FBgn0011754	Tlk	FBgn0283657
CG4935	FBgn0028897	east	FBgn0261954		

More accessible genes Bap60-KD MB					
Gene Symbol	Flybase ID	Gene Symbol	Flybase ID	Gene Symbol	Flybase ID
NA	FBgn0053653	CG13658	FBgn0039315	NA	FBgn0267519
CG44290	FBgn0265317	NA	FBgn0266323	mthl12	FBgn0045442
Oatp58Db	FBgn0034715	CG31750	FBgn0046888	tnc	FBgn0039257
CG44290	FBgn0265317	CG8483	FBgn0038126	CG10559	FBgn0039323
CG4021	FBgn0034659	CG31077	FBgn0051077	CG32834	FBgn0052834
mey	FBgn0039851	CG34289	FBgn0085318	NA	FBgn0085784
fred	FBgn0051774	CG41378	FBgn0085638	CCAP-R	FBgn0039396
CG3347	FBgn0031513	NA	FBgn0267023	NA	FBgn0265840
CG42741	FBgn0261705	CG2955	FBgn0031585	Jon99Ciii	FBgn0003356
CG10479	FBgn0035656	pyr	FBgn0033649	Ir92a	FBgn0038789
CG13589	FBgn0035011	CG32249	FBgn0052249	CG33970	FBgn0053970
ms(3)76Ba	FBgn0036868	CG7362	FBgn0038258	px	FBgn0003175
CG1544	FBgn0039827	Cnx99A	FBgn0015622	NA	FBgn0266909
NA	FBgn0265765	NA	FBgn0283501	rau	FBgn0031745
NA	FBgn0265844	CG13712	FBgn0035570	d4	FBgn0033015
Cyp6a18	FBgn0039519	CG8501	FBgn0033724	tnc	FBgn0039257
NA	FBgn0267133	CG43307	FBgn0262999	NA	FBgn0053653
CG4374	FBgn0039078	Myo81F	FBgn0267431	CG18132	FBgn0031345
CG41099	FBgn0039955	SoxN	FBgn0029123	CG45781	FBgn0267428
NA	FBgn0267133	CG40439	FBgn0284080	CG31296	FBgn0051296
NA	FBgn0051432	CG13590	FBgn0035012	Cad86C	FBgn0261053
NA	FBgn0267620	Adhr	FBgn0000056	Yeti	FBgn0267398
NA	FBgn0265728	CG17110	FBgn0039050	CG4793	FBgn0028514
CG40439	FBgn0284080	NA	FBgn0053653	CG18493	FBgn0038701
Klp59C	FBgn0034824	NA	FBgn0267143	Der-2	FBgn0038438
NA	FBgn0265420	NA	FBgn0266203	CG11550	FBgn0039864
NA	FBgn0267519	tll	FBgn0003720	CG16894	FBgn0034483
CrzR	FBgn0036278	Dnah3	FBgn0035581	NA	FBgn0265844
SA-2	FBgn0043865	CG31051	FBgn0051051	NA	FBgn0265843
Ir94f	FBgn0051225	CG9380	FBgn0035094	CG11106	FBgn0030280
LpR2	FBgn0051092	NA	FBgn0266747	NA	FBgn0267688
NA	FBgn0259861	Art6	FBgn0038189	Fst	FBgn0037724
NA	FBgn0264880	Syx17	FBgn0035540	CG14506	FBgn0039659
NimB4	FBgn0028542	lov	FBgn0266129	NA	FBgn0085786
CG33012	FBgn0053012	NA	FBgn0262425	klar	FBgn0001316
Or23a	FBgn0026395	NA	FBgn0266873	CG17018	FBgn0039972
CG42370	FBgn0259716	NA	FBgn0265653	NA	FBgn0267801
Gbp3	FBgn0039031	CG17109	FBgn0039051	NA	FBgn0264375
CG3916	FBgn0038003	CG14506	FBgn0039659	NA	FBgn0266159

beat-IIa	FBgn0038498	NA	FBgn0266816	NA	FBgn0267524
NA	FBgn0265592	CG14354	FBgn0039376	NA	FBgn0260435
lmd	FBgn0039039	CG10177	FBgn0039083	ND-B14.5AL	FBgn0037172
NA	FBgn0265766	NA	FBgn0266842	CG1137	FBgn0037454
Ir94g	FBgn0039079	TkR99D	FBgn0004622	msopa	FBgn0004414
ND-AGGG	FBgn0085736	Or94a	FBgn0039033	CG31437	FBgn0051437
CG16837	FBgn0035009	fz2	FBgn0016797	CG3492	FBgn0035007
Ir94h	FBgn0039080	rdo	FBgn0243486	hdc	FBgn0010113
CG9109	FBgn0031765	CG14317	FBgn0038566	nahoda	FBgn0034797
CG4073	FBgn0037827	sala	FBgn0003313	NA	FBgn0266234
CG14257	FBgn0039479	NA	FBgn0267787	NA	FBgn0262106
CG3330	FBgn0039511	CG31296	FBgn0051296	ine	FBgn0011603
NA	FBgn0085664	CG17278	FBgn0046763	Obp56i	FBgn0043532
NA	FBgn0267524	NA	FBgn0262887	CG9380	FBgn0035094
NA	FBgn0267744	CG40439	FBgn0058439	ine	FBgn0011603
AOX4	FBgn0038350	NA	FBgn0266401	NA	FBgn0085664
CG4372	FBgn0034665	CG4390	FBgn0038771	NA	FBgn0265841
NA	FBgn0266010	osp	FBgn0003016	Ugt36Ba	FBgn0040262
2mit	FBgn0260793	Art9	FBgn0038188	sunz	FBgn0037462
CG42710	FBgn0261627	NA	FBgn0011897	CG30463	FBgn0050463
CG7720	FBgn0038652	cher	FBgn0014141	Muc96D	FBgn0051439
NA	FBgn0085664	CG7794	FBgn0038565	NA	FBgn0267683
NA	FBgn0267133	CG40439	FBgn0284080	Act57B	FBgn0000044
CG42685	FBgn0261571	NA	FBgn0085786	MFS17	FBgn0058263
Dhc98D	FBgn0013813	NA	FBgn0266747	CG34433	FBgn0085462
CG3483	FBgn0035005	Osi6	FBgn0027527	CG31013	FBgn0051013
NA	FBgn0266087	NA	FBgn0085786	CG34433	FBgn0085462
NA	FBgn0266380	Cpr49Aa	FBgn0050045	CG34289	FBgn0085318
CG42714	FBgn0261631	HP6	FBgn0031613	CG11029	FBgn0031735
NA	FBgn0267133	CrzR	FBgn0036278	Spt3	FBgn0037981
NA	FBgn0264338	CG17928	FBgn0032603	Gr92a	FBgn0045471
CG42493	FBgn0260007	NA	FBgn0267775	LysP	FBgn0004429
Or43b	FBgn0026393	NA	FBgn0085786	nompB	FBgn0016919
CG4907	FBgn0039010	NA	FBgn0058182	NA	FBgn0267939
CG17211	FBgn0032414	NA	FBgn0003926	Klp59D	FBgn0034827
Gr98a	FBgn0039520	NA	FBgn0263618	Or59b	FBgn0034865
Prtl99C	FBgn0039707	NA	FBgn0263664	ND-AGGG	FBgn0085736
SA-2	FBgn0043865	CG15408	FBgn0031523	CG10814	FBgn0033830
CG45781	FBgn0267428	NA	FBgn0267602	NA	FBgn0264428
CG3734	FBgn0038700	CG4554	FBgn0034734	NA	FBgn0262172
CG30048	FBgn0050048	Dhc93AB	FBgn0013812	NA	FBgn0266762

CG32488	FBgn0052488	NA	FBgn0264857	tmod	FBgn0082582
BG642163	FBgn0083938	CG43694	FBgn0263777	NA	FBgn0265945
CG44569	FBgn0265762	NA	FBgn0263618	CG1139	FBgn0035300
AOX3	FBgn0038349	NA	FBgn0263874	Obp83g	FBgn0046875
glob2	FBgn0250846	CG41520	FBgn0087011	NA	FBgn0267710
CG10750	FBgn0032769	Or24a	FBgn0026394	ine	FBgn0011603
HP6	FBgn0031613	nyo	FBgn0039852	CG6293	FBgn0037807
CG41378	FBgn0085638	NA	FBgn0264889	NA	FBgn0265305
NA	FBgn0085784	Ser	FBgn0004197	NA	FBgn0267133
NA	FBgn0053653	ine	FBgn0011603	NA	FBgn0267524
vn	FBgn0003984	NA	FBgn0267719	betaTub60D	FBgn0003888
Gr98a	FBgn0039520	CG40228	FBgn0063670	Jon99Ciii	FBgn0003356
CG3215	FBgn0034825	CG10170	FBgn0039085	NA	FBgn0262025
CG13801	FBgn0035332	NA	FBgn0052480	CG14062	FBgn0039592
scro	FBgn0028993	CG7465	FBgn0035551	CG42357	FBgn0259703
Ugt36Ba	FBgn0040262	CG5024	FBgn0039373	tmod	FBgn0082582
CG41099	FBgn0039955	Act79B	FBgn0000045	NA	FBgn0265062
NA	FBgn0085786	mey	FBgn0039851	NA	FBgn0267526
NA	FBgn0061188	Svil	FBgn0266696	CG34371	FBgn0085400
NA	FBgn0259853	NA	FBgn0266909	CG4073	FBgn0037827
NA	FBgn0267603	CG30268	FBgn0050268	NA	FBgn0028889
CG30265	FBgn0050265	HP1e	FBgn0037675	18w	FBgn0004364
CG1315	FBgn0026565	NA	FBgn0267646	CG10589	FBgn0037035
CG34300	FBgn0085329	NA	FBgn0265892	CG9380	FBgn0035094
Acp62F	FBgn0020509	CG31176	FBgn0051176	CG41562	FBgn0085693
MFS17	FBgn0058263	CG43203	FBgn0262839	nyo	FBgn0039852
NA	FBgn0266257	beat-Vc	FBgn0038084	NA	FBgn0265843
CG3517	FBgn0038706	Jon99Ciii	FBgn0003357	CG1137	FBgn0037454
Pkg21D	FBgn0000442	CG14257	FBgn0039479	CG34433	FBgn0085462
NA	FBgn0053653	CG40178	FBgn0058178	klar	FBgn0001316
NA	FBgn0267308	CG44290	FBgn0265317	NA	FBgn0267724
Dscam3	FBgn0261046	NA	FBgn0051432	NA	FBgn0265766
Fur1	FBgn0004509	NA	FBgn0267958	NA	FBgn0263657
pyr	FBgn0033649	CG40228	FBgn0063670	CG44290	FBgn0265317
NA	FBgn0266009	dsx	FBgn0000504	MsR1	FBgn0035331
hth	FBgn0001235	NA	FBgn0266887	CG41562	FBgn0085693
CG9997	FBgn0039597	CG43896	FBgn0264488	Ptp99A	FBgn0004369
NA	FBgn0267524	CG42238	FBgn0250867	how	FBgn0264491
Nep4	FBgn0038818	CG43188	FBgn0262817	sxc	FBgn0261403
CG31445	FBgn0051445	NA	FBgn0266226	NA	FBgn0265842
NA	FBgn0267117	TrissinR	FBgn0085410	NA	FBgn0053653

CG43694	FBgn0263777	NA	FBgn0264548	mey	FBgn0039851
pnt	FBgn0003118	CG14546	FBgn0039395	neo	FBgn0039704
Obp57b	FBgn0043534	NA	FBgn0266762	Acp36DE	FBgn0011559
Traf4	FBgn0026319	Or94a	FBgn0039033	dan	FBgn0039286
CG8141	FBgn0038125	CG40228	FBgn0063670	Pgam5-2	FBgn0035004
Acam	FBgn0011273	CG14756	FBgn0033275	Prosbeta5R2	FBgn0051742
Obp56d	FBgn0034470	CG41378	FBgn0085638	Tmc	FBgn0267796
CG4706	FBgn0037862	NA	FBgn0265841	CG42523	FBgn0260428
NA	FBgn0264880	Cyp6a14	FBgn0033302	CG1894	FBgn0039585
CG4704	FBgn0039029	Sfp93F	FBgn0261060	CG6040	FBgn0038679
Ir52b	FBgn0050469	CG43795	FBgn0264339	CG31128	FBgn0051128
NA	FBgn0085784	haf	FBgn0261509	CG3517	FBgn0038706
NA	FBgn0086032	NA	FBgn0266412	Thd1	FBgn0026869
CG34278	FBgn0085307	frm	FBgn0035612	Su(var)3-3	FBgn0260397
CG41099	FBgn0039955	NA	FBgn0266762	orb	FBgn0004882
dpr21	FBgn0260995	Pkn	FBgn0020621	CG10321	FBgn0034643
SA-2	FBgn0043865	CG34307	FBgn0085336	NA	FBgn0267143
NA	FBgn0266764	NA	FBgn0263764	haf	FBgn0261509
NA	FBgn0264726	NA	FBgn0267775	NA	FBgn0265945
CG13315	FBgn0040827	NA	FBgn0267537	NA	FBgn0267123
CG9380	FBgn0035094	hppy	FBgn0263395	Vha100-3	FBgn0028669
CG43732	FBgn0263983	CG40228	FBgn0063670	NA	FBgn0067407
CG45781	FBgn0267428	NA	FBgn0267132	NA	FBgn0267787
CG31176	FBgn0051176	CG2150	FBgn0003065	ppk15	FBgn0039424
Fis1	FBgn0039969	NA	FBgn0267524	dpr17	FBgn0051361
NA	FBgn0039656	NA	FBgn0265765	NA	FBgn0267269
ND-49L	FBgn0039331	CG42741	FBgn0261705	MsR1	FBgn0035331
NA	FBgn0259838	S-Lap3	FBgn0045770	NA	FBgn0262382
CG5623	FBgn0038357	NA	FBgn0085786	Sfp65A	FBgn0259969
CG9107	FBgn0031764	NA	FBgn0266232	mtt	FBgn0050361
NA	FBgn0266007	NA	FBgn0264548	NA	FBgn0267122
NA	FBgn0263500	CG9312	FBgn0038179	NA	FBgn0267787
CG42355	FBgn0259701	ine	FBgn0011603	CG15343	FBgn0030029
CG14395	FBgn0038073	NA	FBgn0267460	NA	FBgn0284415
Or43b	FBgn0026393	CG13581	FBgn0035014	mtt	FBgn0050361
CG43742	FBgn0263999	18w	FBgn0004364	CG10184	FBgn0039094
CG14546	FBgn0039395	NA	FBgn0267704	NA	FBgn0267149
CG6901	FBgn0038414	NA	FBgn0265820	NA	FBgn0262382
Pka-C2	FBgn0000274	Cyt-b5-r	FBgn0000406	scb	FBgn0003328
Ets98B	FBgn0005659	CG34171	FBgn0085200	CG15117	FBgn0034417
NA	FBgn0058182	NA	FBgn0067407	CG42534	FBgn0260487

CG40178	FBgn0058178	NA	FBgn0267799	NA	FBgn0263618
MFS17	FBgn0058263	NA	FBgn0267786	pHCl-2	FBgn0039840
CG14740	FBgn0037988	Gr22e	FBgn0045497	bbg	FBgn0087007
CG13559	FBgn0034870	CG15820	FBgn0035312	MFS17	FBgn0058263
Dyrk2	FBgn0016930	NA	FBgn0011855	NA	FBgn0267715
NA	FBgn0086022	NA	FBgn0263664	MsR1	FBgn0035331
NA	FBgn0267133	CG9168	FBgn0035216	Prosbeta5R2	FBgn0051742
CG13539	FBgn0034833	bbg	FBgn0087007	Tb	FBgn0243586
NA	FBgn0267524	Best4	FBgn0036491	Sfp65A	FBgn0259969
Act79B	FBgn0000045	MFS17	FBgn0058263	Tb	FBgn0243586
CG3330	FBgn0039511	NA	FBgn0085784	NA	FBgn0053653
NA	FBgn0266415	Tsp29Fa	FBgn0032074	CG15343	FBgn0030029
CG13705	FBgn0035582	yip3	FBgn0040063	CG4572	FBgn0038738
CG17111	FBgn0039048	CG31245	FBgn0051245		

Less accessible genes Bap60-KD MB					
Gene Symbol	**Flybase ID**	**Gene Symbol**	**Flybase ID**	**Gene Symbol**	**Flybase ID**
MTA1-like	FBgn0027951	Kdm4B	FBgn0053182	MAPk-Ak2	FBgn0013987
Atet	FBgn0020762	SH3PX1	FBgn0040475	NA	FBgn0263039
mAChR-A	FBgn0000037	crol	FBgn0020309	fz4	FBgn0027342
Ufl1	FBgn0037467	CG4230	FBgn0031683	Hsc70-3	FBgn0001218
14-3-3zeta	FBgn0004907	CG7971	FBgn0035253	CG42240	FBgn0250869
tara	FBgn0040071	kdn	FBgn0261955	CG1958	FBgn0029940
Fer2LCH	FBgn0015221	Mob2	FBgn0259481	CG8300	FBgn0029937
bin3	FBgn0263144	CG42492	FBgn0259994	Top1	FBgn0004924
Bsg	FBgn0261822	CG11399	FBgn0037021	Ptp10D	FBgn0004370
14-3-3epsilon	FBgn0020238	Rab27	FBgn0025382	bip1	FBgn0026263
alphaTub84B	FBgn0003884	CG3634	FBgn0037026	deltaCOP	FBgn0028969
GC	FBgn0035245	jim	FBgn0027339	HDAC4	FBgn0041210
mtSSB	FBgn0010438	Kdm2	FBgn0037659	Svil	FBgn0266696
Blimp-1	FBgn0035625	ND-SGDH	FBgn0011455	NA	FBgn0265866
CG9331	FBgn0032889	MtnC	FBgn0038790	CG34172	FBgn0085201
Trl	FBgn0013263	pum	FBgn0003165	Cdc7	FBgn0028360
CG31522	FBgn0051522	ey	FBgn0005558	Tlk	FBgn0283657
CG16896	FBgn0035073	unc-5	FBgn0034013	CG14810	FBgn0029589
NA	FBgn0262319	sn	FBgn0003447	sgg	FBgn0003371
NA	FBgn0262400	NA	FBgn0262378	Mondo	FBgn0032940
pros	FBgn0004595	Cyp28d2	FBgn0031688	AMPdeam	FBgn0052626
alphaTub84B	FBgn0003884	pnr	FBgn0003117	dtn	FBgn0262730

stj	FBgn0261041	S	FBgn0003310	HP5	FBgn0030301
CG45075	FBgn0266445	upSET	FBgn0036398	CG32506	FBgn0052506
Tet	FBgn0263392	Lk6	FBgn0017581	CG32809	FBgn0023531
NA	FBgn0011938	CG32532	FBgn0052532	PhKgamma	FBgn0011754
CG46301	FBgn0283651	dikar	FBgn0261934	east	FBgn0261954
ssp3	FBgn0032723	CG9328	FBgn0032886	EcR	FBgn0000546
NA	FBgn0266831	CG45050	FBgn0266410	Top3beta	FBgn0026015
cbt	FBgn0043364	CG16721	FBgn0029820	Ptpmeg2	FBgn0028341
RpS9	FBgn0010408	Sox102F	FBgn0039938	sno	FBgn0265630
tna	FBgn0026160	Mondo	FBgn0032940	Hex-A	FBgn0001186
par-1	FBgn0260934	brat	FBgn0010300	para	FBgn0285944
Sidpn	FBgn0032741	CG4935	FBgn0028897	Rab10	FBgn0015789
CG15233	FBgn0033076	Calr	FBgn0005585	CG9281	FBgn0030672
eff	FBgn0011217	Nup205	FBgn0031078	Gbeta13F	FBgn0001105
chic	FBgn0000308	CG4287	FBgn0038388	wcy	FBgn0030812
NA	FBgn0266830	CG13907	FBgn0035173	Fur2	FBgn0004598
CG11486	FBgn0035397	CG12702	FBgn0031070	TRAM	FBgn0040340
cpx	FBgn0041605	Bacc	FBgn0031453	CG15296	FBgn0030215
plum	FBgn0039431	CG33798	FBgn0053798	NA	FBgn0029003
l(1)G0156	FBgn0027291	brat	FBgn0010300	Smr	FBgn0265523
Spn28Db	FBgn0053121	Socs36E	FBgn0041184	zf30C	FBgn0270924
Sox14	FBgn0005612	Crtc	FBgn0036746	CG9921	FBgn0030743
ckn	FBgn0033987	eas	FBgn0000536	oc	FBgn0004102
GstZ2	FBgn0037697	CG9821	FBgn0037636	tay	FBgn0260938
l(3)04053	FBgn0010830	NA	FBgn0264940	CG14810	FBgn0029589
NA	FBgn0011938	Ppa	FBgn0020257	lin-52	FBgn0029800
ush	FBgn0003963	Gfat2	FBgn0039580	bif	FBgn0014133
CG3434	FBgn0036000	hiw	FBgn0030600	NA	FBgn0267099
NA	FBgn0012024	inc	FBgn0025394	NA	FBgn0264390
subdued	FBgn0038721	toy	FBgn0019650	zfh2	FBgn0004607
Rh5	FBgn0014019	spin	FBgn0086676	Pfrx	FBgn0027621
CG10098	FBgn0037472	yps	FBgn0022959	CG32698	FBgn0052698
NA	FBgn0262447	vri	FBgn0016076	dpr14	FBgn0029974
NA	FBgn0264439	msn	FBgn0010909	br	FBgn0283451
shn	FBgn0003396	RpLP2	FBgn0003274	Nup93-1	FBgn0027537
chic	FBgn0000308	CG34172	FBgn0085201	shn	FBgn0003396
cpx	FBgn0041605	chif	FBgn0000307	Vsp37A	FBgn0016038
mts	FBgn0004177	br	FBgn0283451	CG12581	FBgn0037213
NA	FBgn0265153	NA	FBgn0267201	Lcch3	FBgn0010240
14-3-3epsilon	FBgn0020238	svr	FBgn0004648	CG14234	FBgn0031065
NA	FBgn0267702	not	FBgn0013717	cib	FBgn0026084

NA	FBgn0052449	CG6785	FBgn0032399	su(sable)	FBgn0003575
Tet	FBgn0263392	Pka-C1	FBgn0000273	alpha-Man-Ia	FBgn0259170
jp	FBgn0032129	CG15465	FBgn0029746	BtbVII	FBgn0263108
Mpc1	FBgn0038662	dnc	FBgn0000479	sol	FBgn0003464
MEP-1	FBgn0035357	Usp2	FBgn0031187	spri	FBgn0085443
l(3)neo38	FBgn0265276	en	FBgn0000577	CG9413	FBgn0030574
Vha16-1	FBgn0262736	SrpRbeta	FBgn0011509	CG13323	FBgn0033788
NA	FBgn0012024	NA	FBgn0267559	Tlk	FBgn0283657
NA	FBgn0263486	en	FBgn0000577	chm	FBgn0028387
CycG	FBgn0039858	Rh5	FBgn0014019	CG5273	FBgn0040382
CG10082	FBgn0034644	RpS17	FBgn0005533	CG1677	FBgn0029941
NA	FBgn0265419	ras	FBgn0003204	CHES-1-like	FBgn0029504
Ext2	FBgn0029175	Ars2	FBgn0033062	fliI	FBgn0000709
fax	FBgn0014163	Daxx	FBgn0031820	Socs16D	FBgn0030869
Ald	FBgn0000064	NA	FBgn0011891	CG9413	FBgn0030574
Tango14	FBgn0031312	Faf2	FBgn0025608	CG43347	FBgn0263072
corto	FBgn0010313	THADA	FBgn0031077	CG9650	FBgn0029939
CG10019	FBgn0031568	CG12395	FBgn0030722	RpS3A	FBgn0017545
Eip74EF	FBgn0000567	crol	FBgn0020309	NA	FBgn0267100
NAT1	FBgn0010488	Sema1b	FBgn0016059	CG4078	FBgn0029798
mirr	FBgn0014343	hang	FBgn0026575	CG3842	FBgn0029866
vimar	FBgn0022960	NA	FBgn0275433	Ubr3	FBgn0260970
CG13323	FBgn0033788	ifc	FBgn0001941	HDAC4	FBgn0041210
CG6005	FBgn0038672	dnc	FBgn0000479	CG4766	FBgn0027546
fax	FBgn0014163	Zip99C	FBgn0039714	CG3775	FBgn0030425
CG6767	FBgn0036030	CanA-14F	FBgn0267912	CG32521	FBgn0052521
P5CDh1	FBgn0037138	dlg1	FBgn0001624	CG44774	FBgn0266000
CG43245	FBgn0262890	NA	FBgn0264702	IntS4	FBgn0026679
CCT5	FBgn0010621	slgA	FBgn0003423	stnB	FBgn0016975
trh	FBgn0262139	CG17124	FBgn0032297	Arp2	FBgn0011742
Bacc	FBgn0031453	NA	FBgn0027493	CG42580	FBgn0260870
NA	FBgn0051331	tup	FBgn0003896	CG12991	FBgn0030847
NA	FBgn0266819	Cerk	FBgn0037315	CG4661	FBgn0030429
plum	FBgn0039431	br	FBgn0283451	alpha-Man-Ia	FBgn0259170
CG9663	FBgn0031516	Srpk79D	FBgn0025702	NA	FBgn0047092
cbt	FBgn0043364	Pfk	FBgn0003071	dnc	FBgn0000479
pdm3	FBgn0261588	CG7326	FBgn0030970	CG6767	FBgn0036030
CG5380	FBgn0038951	NA	FBgn0065095	snz	FBgn0029976
chinmo	FBgn0086758	Sh	FBgn0003380	CG18508	FBgn0028746
Ppat-Dpck	FBgn0035632	NA	FBgn0065095	CG9784	FBgn0030761

Hr3	FBgn0000448	Raf	FBgn0003079	CG12643	FBgn0040942
CG18371	FBgn0033893	Mnt	FBgn0023215	ari-1	FBgn0017418
Msp300	FBgn0261836	CG43245	FBgn0262890	Mnt	FBgn0023215
put	FBgn0003169	Vsx2	FBgn0263512	CG9650	FBgn0029939
CG6163	FBgn0036155	FoxK	FBgn0036134	CG30020	FBgn0050020
cnk	FBgn0021818	CG43245	FBgn0262890	CG7556	FBgn0030990
PRAS40	FBgn0267824	CG3638	FBgn0261444	inaE	FBgn0261244
HnRNP-K	FBgn0267791	NA	FBgn0263345	CG34449	FBgn0085478
tara	FBgn0040071	corto	FBgn0010313	Appl	FBgn0000108
Reph	FBgn0021800	NA	FBgn0264826	CG11138	FBgn0030400
NA	FBgn0266209	Shc	FBgn0015296	CG30389	FBgn0050389
Stat92E	FBgn0016917	CG42700	FBgn0261611	Tango13	FBgn0086674
Syp	FBgn0038826	SH3PX1	FBgn0040475	ey	FBgn0005558
Inos	FBgn0025885	cdc14	FBgn0031952	Kap3	FBgn0028421
Lk6	FBgn0017581	Hr51	FBgn0034012	Cyp1	FBgn0004432
CG12054	FBgn0039831	CG1504	FBgn0031100	NA	FBgn0265454
CG7879	FBgn0035235	Corin	FBgn0033192	Scgdelta	FBgn0025391
simj	FBgn0010762	NA	FBgn0267962	CG15894	FBgn0029864
NTPase	FBgn0024947	NA	FBgn0264787	RunxA	FBgn0083981
NA	FBgn0267579	Pkn	FBgn0020621	muc	FBgn0283658
CadN	FBgn0015609	br	FBgn0283451	Usp2	FBgn0031187
Ssdp	FBgn0011481	CG12091	FBgn0035228	brk	FBgn0024250
NA	FBgn0052272	unc-119	FBgn0025549	bbx	FBgn0024251
Dys	FBgn0260003	CG3078	FBgn0023524	Pat1	FBgn0029878
CG11000	FBgn0263353	RpL28	FBgn0035422	CG42450	FBgn0259927
Ca-beta	FBgn0259822	disco-r	FBgn0285879	brk	FBgn0024250
Rh5	FBgn0014019	Mef2	FBgn0011656	CG11566	FBgn0031159
CG18371	FBgn0033893	sgg	FBgn0003371	CG2889	FBgn0030206
Pka-R2	FBgn0022382	Pp2C1	FBgn0022768	SkpA	FBgn0025637
NK7.1	FBgn0024321	velo	FBgn0035713	NA	FBgn0267741
CtBP	FBgn0020496	CG6201	FBgn0032343	nej	FBgn0261617
dos	FBgn0016794	sbb	FBgn0285917	CG43783	FBgn0264305
CG33203	FBgn0053203	e(y)3	FBgn0087008	lva	FBgn0029688
B4	FBgn0023407	lig	FBgn0020279	CrebB	FBgn0265784
MESR6	FBgn0036846	NA	FBgn0263039	rst	FBgn0003285
CG11000	FBgn0263353	CG6220	FBgn0033865	Rbp	FBgn0262483
alt	FBgn0038535	mib2	FBgn0086442	NA	FBgn0264678
Syx1A	FBgn0013343	Nf1	FBgn0015269	CG32813	FBgn0052813
CG31769	FBgn0051769	KrT95D	FBgn0020647	CG11138	FBgn0030400
CG45116	FBgn0266591	CG18265	FBgn0036725	CG12112	FBgn0030048
Sidpn	FBgn0032741	CG11658	FBgn0036196	CG6867	FBgn0030887

Rgl	FBgn0026376	CG13894	FBgn0035157	Mekk1	FBgn0024329
CG14505	FBgn0034327	CG7990	FBgn0030997	CkIIbeta	FBgn0000259
Syp	FBgn0038826	Tango5	FBgn0052675	tth	FBgn0030502
CG10082	FBgn0034644	CG16779	FBgn0037698	CG3842	FBgn0029866
mor	FBgn0002783	BTBD9	FBgn0030228	CG4496	FBgn0031894
Eip74EF	FBgn0000567	Taf4	FBgn0010280	unc-119	FBgn0025549
jumu	FBgn0015396	NA	FBgn0052748	Tis11	FBgn0011837
CG13321	FBgn0033787	Spt6	FBgn0028982	CG1718	FBgn0031170
CG13204	FBgn0033627	NA	FBgn0001079	CG14442	FBgn0029893
Akap200	FBgn0027932	Amun	FBgn0030328	mahe	FBgn0029979
NA	FBgn0086080	Raf	FBgn0003079	Gga	FBgn0030141
NA	FBgn0265153	bi	FBgn0000179	l(1)G0196	FBgn0027279
Hers	FBgn0052529	NetB	FBgn0015774	CHES-1-like	FBgn0029504
bor	FBgn0040237	Tlk	FBgn0283657	mamo	FBgn0267033
btsz	FBgn0266756	NA	FBgn0027493	MED22	FBgn0040339
brk	FBgn0024250	zfh2	FBgn0004607	Trf2	FBgn0261793
upSET	FBgn0036398	Stt3A	FBgn0031149	NA	FBgn0264678
salm	FBgn0261648	gw	FBgn0051992	br	FBgn0283451
NA	FBgn0267201	CG45071	FBgn0266441	CG14621	FBgn0031183
Cka	FBgn0044323	NA	FBgn0264439	dl	FBgn0260632
NA	FBgn0267634	SPoCk	FBgn0052451	NA	FBgn0265830
HmgZ	FBgn0010228	CG3703	FBgn0040348	CG12531	FBgn0031064
sm	FBgn0003435	CG9413	FBgn0030574	CG15373	FBgn0030889
CG11883	FBgn0033538	ND-SGDH	FBgn0011455	Hers	FBgn0052529
Dys	FBgn0260003	CanA-14F	FBgn0267912	sdt	FBgn0261873
smg	FBgn0016070	CG6424	FBgn0028494	CHES-1-like	FBgn0029504
NA	FBgn0011868	CG5953	FBgn0032587	NA	FBgn0264678
Trl	FBgn0013263	tou	FBgn0033636	fend	FBgn0030090
futsch	FBgn0259108	fs(1)h	FBgn0004656	Trxr-1	FBgn0020653
Socs36E	FBgn0041184	alpha-Man-IIb	FBgn0026616	rut	FBgn0003301
grp	FBgn0261278	lola	FBgn0283521	CG11151	FBgn0030519
CG11873	FBgn0039633	ey	FBgn0005558	CG14212	FBgn0031045
tara	FBgn0040071	Oaz	FBgn0284250	His3.3B	FBgn0004828
CG34347	FBgn0085376	X11Lbeta	FBgn0052677	CG15312	FBgn0030174
pk	FBgn0003090	Act5C	FBgn0000042	ph-d	FBgn0004860
Dpit47	FBgn0266518	rictor	FBgn0031006	CG11566	FBgn0031159
Atx2	FBgn0041188	srl	FBgn0037248	prage	FBgn0283741
CG42784	FBgn0263354	Nmdar2	FBgn0053513	Raf	FBgn0003079
bin3	FBgn0263144	VhaSFD	FBgn0027779	UBL3	FBgn0026076
NA	FBgn0266209	ERp60	FBgn0033663	DIP-alpha	FBgn0052791
mei-P26	FBgn0026206	Pp2C1	FBgn0022768	btd	FBgn0000233

eRF3	FBgn0020443	Appl	FBgn0000108	exd	FBgn0000611
CG2246	FBgn0039790	disco	FBgn0000459	CrebB	FBgn0265784
NA	FBgn0265419	Dlic	FBgn0030276	CG6961	FBgn0030959
SCAP	FBgn0033052	para	FBgn0285944	NA	FBgn0263334
FASN1	FBgn0283427	D19B	FBgn0022699	NA	FBgn0266350
CalpA	FBgn0012051	dac	FBgn0005677	vap	FBgn0003969
MESR6	FBgn0036846	CG15719	FBgn0030440	MFS10	FBgn0030452
Sox14	FBgn0005612	ome	FBgn0259175	pico	FBgn0261811
Sirt1	FBgn0024291	fzr	FBgn0262699	arm	FBgn0000117
TER94	FBgn0261014	bma	FBgn0085385	tup	FBgn0003896
CG16972	FBgn0032481	Cyp308a1	FBgn0030949	Hers	FBgn0052529
CG45071	FBgn0266441	mim	FBgn0053558	SkpD	FBgn0026174
l(3)neo38	FBgn0265276	Hsp22	FBgn0001223	psq	FBgn0263102
zfh2	FBgn0004607	vri	FBgn0016076	A16	FBgn0028965
Sh	FBgn0003380	CG32590	FBgn0052590	RSG7	FBgn0024941
Tet	FBgn0263392	CG42337	FBgn0259239	dpr8	FBgn0052600
Iris	FBgn0031305	Tpr2	FBgn0032586	NA	FBgn0265830
CG9084	FBgn0033582	shn	FBgn0003396	c11.1	FBgn0040236
dac	FBgn0005677	dsd	FBgn0039528	sd	FBgn0003345
mtd	FBgn0013576	not	FBgn0013717	Ahcy	FBgn0014455
sbb	FBgn0285917	rdgB	FBgn0003218	Shroom	FBgn0085408
hwt	FBgn0264542	CG18766	FBgn0042111	Drak	FBgn0052666
NA	FBgn0266835	CG9328	FBgn0032886	CG6481	FBgn0030936
NA	FBgn0267219	hwt	FBgn0264542	CG43347	FBgn0263072
NA	FBgn0262367	fal	FBgn0028380	shakB	FBgn0085387
dunk	FBgn0083973	CG3690	FBgn0040350	sesB	FBgn0003360
TER94	FBgn0261014	Eip74EF	FBgn0000567	CG1998	FBgn0030485
CG12054	FBgn0039831	Adar	FBgn0026086	CG12576	FBgn0031190
Hrb27C	FBgn0004838	Rbf	FBgn0015799	mam	FBgn0002643
RasGAP1	FBgn0004390	CBP	FBgn0026144	l(1)G0193	FBgn0027280
CG14762	FBgn0033250	sqz	FBgn0010768	CG1640	FBgn0030478
NA	FBgn0267203	Naa15-16	FBgn0031020	rdgA	FBgn0261549
CG12173	FBgn0037305	Tango14	FBgn0031312	RabX2	FBgn0030200
CG13204	FBgn0033627	CkIIbeta	FBgn0000259	CG14810	FBgn0029589
Dpit47	FBgn0266518	CanA-14F	FBgn0267912	CG33795	FBgn0053795
CG32547	FBgn0052547	glob1	FBgn0027657	unc	FBgn0003950
NA	FBgn0052826	NA	FBgn0053294	Tlk	FBgn0283657
cnn	FBgn0013765	tio	FBgn0028979	CG17598	FBgn0031194
NA	FBgn0265955	elav	FBgn0260400	Rip11	FBgn0027335
pros	FBgn0004595	CG10565	FBgn0037051	CG7332	FBgn0030973
Sin3A	FBgn0022764	tou	FBgn0033636	CG14408	FBgn0030581

Pka-C1	FBgn0000273	babo	FBgn0011300	nej	FBgn0261617
eIF3b	FBgn0034237	CG18467	FBgn0034218	CHES-1-like	FBgn0029504
east	FBgn0261954	NA	FBgn0053653	CG2918	FBgn0023529
metro	FBgn0050021	mlt	FBgn0265512	CG7058	FBgn0030961
Ih	FBgn0263397	NA	FBgn0267752	Syb	FBgn0003660
jumu	FBgn0015396	cac	FBgn0263111	NA	FBgn0264676
CG2865	FBgn0023526	NA	FBgn0086080	Cdc7	FBgn0028360
gem	FBgn0050011	CG8173	FBgn0030864	Rala	FBgn0015286
NA	FBgn0265924	BCL7-like	FBgn0026149	CG43902	FBgn0264503
msn	FBgn0010909	CG11448	FBgn0024985	CG16721	FBgn0029820
NA	FBgn0051331	ras	FBgn0003204	HDAC6	FBgn0026428
CG42788	FBgn0261859	disco-r	FBgn0285879	Fnta	FBgn0031633
NA	FBgn0265427	NA	FBgn0065095	CG8128	FBgn0030668
dikar	FBgn0261934	Ubqn	FBgn0031057	NA	FBgn0267162
CG7878	FBgn0037549	Mur2B	FBgn0025390	l(1)G0320	FBgn0028327
l(3)neo38	FBgn0265276	Cngl	FBgn0263257	mamo	FBgn0267033
hth	FBgn0001235	CG45603	FBgn0267163	CG15309	FBgn0030183
CG9328	FBgn0032886	EcR	FBgn0000546	Tak1	FBgn0026323
chif	FBgn0000307	nmo	FBgn0011817	l(1)1Bi	FBgn0001341
mrt	FBgn0039507	Pka-R1	FBgn0259243	NA	FBgn0267067
sax	FBgn0003317	sta	FBgn0003517	CG1582	FBgn0030246
CG5937	FBgn0029834	CG43736	FBgn0263993	Syx16	FBgn0031106
Syx1A	FBgn0013343	br	FBgn0283451	CG15891	FBgn0029860
sll	FBgn0038524	Sh	FBgn0003380	CG14810	FBgn0029589
RpS11	FBgn0033699	Tlk	FBgn0283657	bbx	FBgn0024251
CG3719	FBgn0024986	tou	FBgn0033636	hwt	FBgn0264542
NA	FBgn0267668	RpII215	FBgn0003277	Grip	FBgn0029830
mura	FBgn0037705	Shmt	FBgn0029823	CG12498	FBgn0040356
wapl	FBgn0004655	NA	FBgn0086037	dnc	FBgn0000479
tara	FBgn0040071	Dif	FBgn0011274	ph-p	FBgn0004861
14-3-3zeta	FBgn0004907	Rh5	FBgn0014019	psq	FBgn0263102
NA	FBgn0263483	CG2691	FBgn0030504	CG44422	FBgn0265595
px	FBgn0003175	Raf	FBgn0003079	CG9411	FBgn0030569
Taf4	FBgn0010280	CG15233	FBgn0033076	Pmp70	FBgn0031069
hrg	FBgn0015949	Ube3a	FBgn0061469	NA	FBgn0011951
Nep1	FBgn0029843	Raf	FBgn0003079	CG18508	FBgn0028746
CG42700	FBgn0261611	mamo	FBgn0267033	Ubr1	FBgn0030809
NA	FBgn0267782	Ten-a	FBgn0267001	UbcE2H	FBgn0029996
ATPsynC	FBgn0039830	amon	FBgn0023179	Rcd-1	FBgn0031047
CG6044	FBgn0034725	NA	FBgn0266892	CG6106	FBgn0030914
CG2924	FBgn0023528	Tob	FBgn0028397	SK	FBgn0029761

NA	FBgn0283558	Rab3-GEF	FBgn0030613	CG32806	FBgn0052806
hid	FBgn0003997	RhoGAP19D	FBgn0031118	B-H2	FBgn0004854
cg	FBgn0000289	Act5C	FBgn0000042	shakB	FBgn0085387
NA	FBgn0283426	NA	FBgn0263039	CG7378	FBgn0030976
pan	FBgn0085432	dnc	FBgn0000479	Yippee	FBgn0026749
Su(z)2	FBgn0265623	Wee1	FBgn0011737	pdgy	FBgn0027601
CG32085	FBgn0052085	ph-p	FBgn0004861	Roc1a	FBgn0025638
Rph	FBgn0030230	Ten-a	FBgn0267001	CG5004	FBgn0260748
CG1427	FBgn0037347	scramb1	FBgn0052056	CG14441	FBgn0029895
prtp	FBgn0030329	dpr8	FBgn0052600	CG15200	FBgn0030278
Pdi	FBgn0014002	NA	FBgn0086667	NA	FBgn0267068
CG17544	FBgn0032775	CG7231	FBgn0031968	betaNACtes3	FBgn0052601
Reph	FBgn0021800	NA	FBgn0052493	Pfrx	FBgn0027621
NA	FBgn0265427	CG5953	FBgn0032587	CG12155	FBgn0029957
tipE	FBgn0003710	CG6379	FBgn0029693	Ptpmeg2	FBgn0028341
CG9171	FBgn0031738	Gug	FBgn0010825	N	FBgn0004647
Gug	FBgn0010825	CG4660	FBgn0029839	l(1)G0334	FBgn0028325
Sxl	FBgn0264270	CG1722	FBgn0031168	RpL31	FBgn0285949
Uba1	FBgn0023143	NA	FBgn0264703	ben	FBgn0000173
sba	FBgn0016754	Hk	FBgn0263220	Tlk	FBgn0283657
cg	FBgn0000289	Awh	FBgn0013751	CG9380	FBgn0035094
Galphao	FBgn0001122	CG6481	FBgn0030936	NA	FBgn0265705
CG44838	FBgn0266101	NA	FBgn0267169	CG9380	FBgn0035094
CG6231	FBgn0038720	Raf	FBgn0003079	CG43759	FBgn0264090
VAChT	FBgn0270928	01-Sep	FBgn0011710	mamo	FBgn0267033
NA	FBgn0266830	Mur2B	FBgn0025390	Sap30	FBgn0030788
trv	FBgn0085391	Calr	FBgn0005585	NA	FBgn0058469
ps	FBgn0261552	pod1	FBgn0029903	NA	FBgn0263503
jim	FBgn0027339	Smox	FBgn0025800	RhoGAP19D	FBgn0031118
CG14434	FBgn0029915	Tomosyn	FBgn0030412	Tlk	FBgn0283657
NA	FBgn0267910	CG1578	FBgn0030336		
fne	FBgn0086675	Atf3	FBgn0028550		

Appendix F Candidate SWI/SNF targets in the larval MB

Candidate Snr1 Targets	Candidate E(y)3 Targets		
Flybase ID	**Gene Symbol**	**Flybase ID**	**Gene Symbol**
FBgn0036846	MESR6	FBgn0029095	aru
FBgn0264439	lncRNA:CR43857	FBgn0035427	ckd

FBgn0052626	AMPdeam	FBgn0036152	CG6175
FBgn0023526	CG2865	FBgn0036155	CG6163
FBgn0032587	CG5953	FBgn0039754	CG9747
FBgn0036196	CG11658	FBgn0085408	Shrm
FBgn0031516	CG9663	FBgn0261565	Lmpt
FBgn0013751	Awh	FBgn0262169	magu
FBgn0028387	chm	FBgn0266084	Fhos
FBgn0010488	NAT1		
FBgn0061469	Ube3a		
FBgn0029996	UbcE2H		
FBgn0026084	cib		
FBgn0266410	CG45050		
FBgn0000308	chic		
FBgn0000546	EcR		
FBgn0266696	Svil		
FBgn0263039	lncRNA:CR43334		
FBgn0030809	Ubr1		
FBgn0261014	TER4		
FBgn0001235	hth		

Appendix G Differentially expressed genes between Bap60-KD MBs and controls in juvenile and mature flies

Juvenile Bap60-KD MB compared to Juvenile control - Upregulated					
Gene Symbol	**Flybase ID**	**Gene Symbol**	**Flybase ID**	**Gene Symbol**	**Flybase ID**
Est-6	FBgn0000592	lncRNA:CR42862	FBgn0261808	Dic1	FBgn0027579
ppk22	FBgn0050052	dsx	FBgn0000504	Btk29A	FBgn0003502
nub	FBgn0082582	Su(var)3-3	FBgn0259736	CG7339	FBgn0035900
7B2	FBgn0040688	Myo81F	FBgn0266901	Uxs	FBgn0035425
CG42269	FBgn0086659	Iml1	FBgn0035041	CG17574	FBgn0033438
dnd	FBgn0038652	bs	FBgn0004028	14-3-3zeta	FBgn0004841
Inos	FBgn0023549	Cpn	FBgn0261549	Fhos	FBgn0265416
CG6665	FBgn0034075	CG17646	FBgn0263413	Vha68-1	FBgn0265002
CG4294	FBgn0034470	Snap24	FBgn0266084	Proc-R	FBgn0028993
CG14945	FBgn0032167	KdelR	FBgn0266666	CG1998	FBgn0030357
CG30158	FBgn0042174	Acn	FBgn0262855	up	FBgn0004117
CG13639	FBgn0265140	sev	FBgn0003366	CG9934	FBgn0032216

Doa	FBgn0265356	corn	FBgn0086690	jef	FBgn0033853
CG7778	FBgn0031913	app	FBgn0260462	Arc1	FBgn0033777
CG42319	FBgn0086906	CG32204	FBgn0051781	Mms19	FBgn0037164
CG45782	FBgn0266772	wupA	FBgn0267429	Rop	FBgn0004359
FMRFaR	FBgn0035144	tn	FBgn0265180	CG6145	FBgn0033504
Hip14	FBgn0259219	CG1213	FBgn0037292	Vha14-1	FBgn0261871
CG9686	FBgn0029831	Plp	FBgn0085638	Ran	FBgn0016696
His3.3B	FBgn0004795	tko	FBgn0003714	CG44245	FBgn0264562
LUBEL	FBgn0031692	MFS18	FBgn0023540	bmm	FBgn0036279
Atox1	FBgn0052121	zormin	FBgn0052112	salm	FBgn0261545
CG6695	FBgn0039114	Mmp1	FBgn0034959	CG32121	FBgn0051619
CG12081	FBgn0029723	Lim1	FBgn0026239	CG33521	FBgn0086604
Toll-7	FBgn0034137	CG4945	FBgn0034002	Gbeta76 C	FBgn0004587
su(w[a])	FBgn0003638	CG10562	FBgn0039215	fon	FBgn0032587
Arl6IP1	FBgn0038181	CG12483	FBgn0040397	CG31221	FBgn0050440
Kat60	FBgn0039897	CG43143	FBgn0261929	CG40485	FBgn0053143
IM4	FBgn0040383	Dop1R1	FBgn0011286	CG1208	FBgn0037171
CG6495	FBgn0026411	beat-IIa	FBgn0038197	gukh	FBgn0026181
CG4612	FBgn0034724	CG7781	FBgn0031869	CG17746	FBgn0035227
dnr1	FBgn0260397	knrl	FBgn0001323	mbf1	FBgn0262109
Mhc	FBgn0263997	Meltrin	FBgn0264494	rdgA	FBgn0261394
CG13067	FBgn0036449	CG42323	FBgn0250819	CG43861	FBgn0263395
Prosalpha3	FBgn0260866	Scgalpha	FBgn0031857	Hr38	FBgn0014396
CG42588	FBgn0260660	CG12945	FBgn0037448	dysf	FBgn0039229
T48	FBgn0004169	Hr4	FBgn0263659	CG7708	FBgn0038498
Mur18B	FBgn0030829	Shroom	FBgn0058470	Aef1	FBgn0005666
CG14883	FBgn0038147	side-VII	FBgn0037447	Prm	FBgn0003149
plh	FBgn0037146	RhoGAP18 B	FBgn0260941	CG5953	FBgn0032467
Mppe	FBgn0259678	tsh	FBgn0003866	RpS29	FBgn0261461
snoRNA:Psi1 8S-176	FBgn0085443	hec	FBgn0030208	jdp	FBgn0027598
srp	FBgn0003507	Mocs1	FBgn0262975	spri	FBgn0085408
Cen	FBgn0032683	CG41378	FBgn0085422	AGBE	FBgn0052549
CG33110	FBgn0052311	RyR	FBgn0010482	nkd	FBgn0002945
dpr2	FBgn0261641	igl	FBgn0013433	CG43219	FBgn0262617
Syngr	FBgn0033654	Vha26	FBgn0267431	h	FBgn0001168
CG32243	FBgn0052111	cher	FBgn0014135	Sem1	FBgn0265998
ush	FBgn0003963	CG13594	FBgn0034742	lncRNA:C R43459	FBgn0263198
CG11951	FBgn0039620	hoe2	FBgn0031251	sNPF	FBgn0032629

TpnC25D	FBgn0031313	ghi	FBgn0265595	lncRNA:CR45973	FBgn0267428
hppy	FBgn0263039	CG44247	FBgn0264695	CG18870	FBgn0040765

Juvenile Bap60-KD MB compared to Juvenile control - Downregulated					
Gene Symbol	**Flybase ID**	**Gene Symbol**	**Flybase ID**	**Gene Symbol**	**Flybase ID**
kek1	FBgn0015245	MtnA	FBgn0002868	awd	FBgn0000150
bt	FBgn0005586	CG7365	FBgn0036890	CG45781	FBgn0266720
Ctl2	FBgn0039483	klu	FBgn0013467	mt:ND5	FBgn0013678
Elal	FBgn0013726	CG10960	FBgn0036188	amon	FBgn0022097
Sytalpha	FBgn0260795	CG30440	FBgn0042180	CG14572	FBgn0036984
lncRNA:CR31781	FBgn0051191	sca	FBgn0003326	CG14459	FBgn0037129
rdgB	FBgn0003218	Obp44a	FBgn0033132	Rok	FBgn0025885
Kah	FBgn0035016	Hsp60A	FBgn0014859	JhI-21	FBgn0027844
eIF3l	FBgn0036032	CG11388	FBgn0034476	Zip71B	FBgn0036316
CG2938	FBgn0028665	CG13055	FBgn0036319	CG9372	FBgn0036880
ThrRS	FBgn0026409	Vha16-1	FBgn0262512	CG14024	FBgn0031649
Mct1	FBgn0023518	Appl	FBgn0000108	Act5C	FBgn0000042
Vha36-1	FBgn0019972	CG14565	FBgn0037026	NaPi-III	FBgn0259985
jus	FBgn0039562	Gapdh2	FBgn0001092	Irk2	FBgn0038839
CG1674	FBgn0039647	Syn2	FBgn0033958	CG42724	FBgn0261514
CG31191	FBgn0050158	lncRNA:CR31451	FBgn0051036	CG5273	FBgn0040074
CG13722	FBgn0035385	tim	FBgn0014141	TfIIS	FBgn0010380
CG33143	FBgn0052815	Aplip1	FBgn0039928	CG32815	FBgn0052243
sotv	FBgn0028662	CG14961	FBgn0035267	Tep2	FBgn0040653
ctp	FBgn0011695	CG43740	FBgn0263352	form3	FBgn0053116
CG9919	FBgn0030485	Mpcp2	FBgn0026206	beat-IIIc	FBgn0032482
CG7675	FBgn0038453	CG33116	FBgn0052446	nrv3	FBgn0032773
Pxn	FBgn0011760	CG15186	FBgn0037386	CG7166	FBgn0036939
Ent3	FBgn0036258	RpLP0	FBgn0000100	mt:CoI	FBgn0013469
Dgp-1	FBgn0027610	Scm	FBgn0003334	CG12531	FBgn0030955
foxo	FBgn0038143	CCHa2	FBgn0037758	nolo	FBgn0051105
inaD	FBgn0001263	Pka-R2	FBgn0020255	Cpr76Bd	FBgn0036589
Obp56d	FBgn0034135	CG14259	FBgn0039277	CG15784	FBgn0029175
retinin	FBgn0039688	Ggamma1	FBgn0004907	chp	FBgn0267330
cindr	FBgn0027550	PPP4R2r	FBgn0030053	Pect	FBgn0032336
comt	FBgn0000346	Ncc69	FBgn0036165	ZC3H3	FBgn0035553
Lsd-1	FBgn0038880	CG16711	FBgn0035848	CG9467	FBgn0037690

CG3625	FBgn0030997	EbpIII	FBgn0011693	CG42663	FBgn0261089
CG3655	FBgn0040281	CG44422	FBgn0265262	His4r	FBgn0013954
B52	FBgn0004574	Arr1	FBgn0000120	CG11438	FBgn0037128
CG13606	FBgn0039081	lncRNA:CR45237	FBgn0266124	CG5080	FBgn0031245
Daxx	FBgn0031673	trr	FBgn0022382	CG32549	FBgn0052204
CG40470	FBgn0053138	CG12998	FBgn0030742	CG44153	FBgn0264443
AP-1-2beta	FBgn0010105	CAH1	FBgn0027836	CG4645	FBgn0030158
GstD11	FBgn0037736	Tsp42Ej	FBgn0032876	Neto	FBgn0265182
CG43324	FBgn0262732	lncRNA:CR32111	FBgn0051221	CG6675	FBgn0032840
CG5958	FBgn0031820	pnut	FBgn0013725	Gabat	FBgn0036881
CG12163	FBgn0259824	CG34393	FBgn0069973	Kul	FBgn0039637
Drice	FBgn0016641	Pka-C1	FBgn0000273	CAH2	FBgn0027654
ND-20	FBgn0030437	Asph	FBgn0033926	RASSF8	FBgn0261714
CG11191	FBgn0032946	fend	FBgn0029766	CG5853	FBgn0032013
Sap130	FBgn0261986	CG3634	FBgn0036927	bnl	FBgn0013981
CG42390	FBgn0259173	scro	FBgn0028490	prt	FBgn0041182
CG8369	FBgn0040382	CG32112	FBgn0051451	Ppn	FBgn0003137
NimA	FBgn0260965	wat	FBgn0039411	CG31036	FBgn0043005
l(2)01289	FBgn0010452	Rab3	FBgn0004921	CG8079	FBgn0033876
CG9132	FBgn0030670	cysu	FBgn0038432	out	FBgn0259223
MFS3	FBgn0031064	sqh	FBgn0003514	side-VIII	FBgn0085431
TkR86C	FBgn0004828	lncRNA:CR43650	FBgn0263241	VhaPPA1-1	FBgn0028425
Hsp70Bb	FBgn0011828	Pgi	FBgn0003074	ImpL2	FBgn0001257
Cam	FBgn0000253	Mlc-c	FBgn0004623	Cpr76Bc	FBgn0036583
mt:Cyt-b	FBgn0013674	CAP	FBgn0033250	Ric	FBgn0265266
phyl	FBgn0013684	mino	FBgn0027081	CG9297	FBgn0038029
sls	FBgn0086367	SIFaR	FBgn0038641	CG13650	FBgn0039161
His2Av	FBgn0001197	kon	FBgn0032484	e	FBgn0000527
VhaAC39-1	FBgn0267435	CG9368	FBgn0036603	Fkbp12	FBgn0013949
lncRNA:CR45361	FBgn0266449	Mmp2	FBgn0033249	b	FBgn0000153
bic	FBgn0000181	trn	FBgn0010422	Task7	FBgn0037387
Saf-B	FBgn0039141	Pitslre	FBgn0015777	Act42A	FBgn0000043
Sclp	FBgn0030090	Cals	FBgn0039656	mei-P26	FBgn0026084
comm	FBgn0005694	CG31705	FBgn0028400	sqa	FBgn0259164
chrb	FBgn0035871	Pu	FBgn0003162	Tm2	FBgn0004101
CG34217	FBgn0053556	cu	FBgn0261599	CG4213	FBgn0030999
Glt	FBgn0001114	cib	FBgn0025684	tmod	FBgn0053294
CG13248	FBgn0036891	CG5254	FBgn0040208	5-HT2B	FBgn0261648

Sobp	FBgn0033268	retn	FBgn0004784	CR33294	FBgn0053110
Lis-1	FBgn0015324	ninaE	FBgn0002940	CG13062	FBgn0036461
CG5966	FBgn0029685	Ktl	FBgn0038610	Ldh	FBgn0001258
nrv2	FBgn0015399	babos	FBgn0034172	Gp93	FBgn0039326
CG7720	FBgn0038511	Unr	FBgn0263029	CG9813	FBgn0037755
Obp49a	FBgn0041707	Kr-h2	FBgn0265605	kek4	FBgn0032402
Neurochond rin	FBgn0037301	CG5162	FBgn0030718	spas	FBgn0038916
CG6891	FBgn0030791	CG7470	FBgn0037107	hpRNA:CR 18854	FBgn0267635
Pdh	FBgn0011582	luna	FBgn0040532	hid	FBgn0003997
CG13921	FBgn0035049	lncRNA:CR4 3334	FBgn0262736	CG31650	FBgn0031307
Cat	FBgn0000261	Pis	FBgn0030435	t	FBgn0085424
PTP-ER	FBgn0015754	Usp14	FBgn0032021	CG7990	FBgn0030828
CG3630	FBgn0023179	inaC	FBgn0004687	CG14762	FBgn0032973
cnc	FBgn0262714	CG18304	FBgn0031697	beat-Ia	FBgn0013278
ninaC	FBgn0002938	Dip-B	FBgn0000454	AstC	FBgn0032025
CG34402	FBgn0085246	al	FBgn0000061	BI-1	FBgn0035439
Syt4	FBgn0027843	Mp	FBgn0259834		

Mature Bap60-KD MB compared to Mature control - Upregulated					
Gene Symbol	**Flybase ID**	**Gene Symbol**	**Flybase ID**	**Gene Symbol**	**Flybase ID**
Crg-1	FBgn0021738	Gart	FBgn0000053	Nmdmc	FBgn0010222
fd3F	FBgn0264954	CG4752	FBgn0034733	AstA	FBgn0015591
Dot	FBgn0015663	CG17760	FBgn0033756	Cyp6a13	FBgn0033304
lncRNA:CR4 5627	FBgn0267187	Phk-3	FBgn0035089	lncRNA:CR 45223	FBgn0266750
Cyp6a14	FBgn0033302	Lgr3	FBgn0039354	GstE1	FBgn0034335
lncRNA:CR4 5625	FBgn0267185	CG10621	FBgn0032726	Loxl2	FBgn0034660
Bet3	FBgn0260859	CG11388	FBgn0034959	AstC	FBgn0032336
CG17290	FBgn0034201	atk	FBgn0036995	CG43448	FBgn0263402
IM23	FBgn0034328	CG7191	FBgn0031945	Tk	FBgn0037976
lncRNA:CR4 3428	FBgn0263376	CG9733	FBgn0039759		

Mature Bap60-KD MB compared to Mature control - Downregulated					
Gene Symbol	**Flybase ID**	**Gene Symbol**	**Flybase ID**	**Gene Symbol**	**Flybase ID**

CG13185	FBgn0033661	CG30285	FBgn0050285	CG13054	FBgn0036584
Cad96Cb	FBgn0039294	CG30438	FBgn0050438	CG12112	FBgn0030048
Hsp70Bb	FBgn0013278	Rif1	FBgn0050085	nub	FBgn0085424
SerRS	FBgn0031497	lncRNA:CR44644	FBgn0265855	ana2	FBgn0027513
lz	FBgn0002576	CG5535	FBgn0036764	CG30271	FBgn0050271
Spindly	FBgn0031549	CG4962	FBgn0036597	lncRNA:CR45717	FBgn0267281
NimA	FBgn0261514	exu	FBgn0000615	Ugt86Dh	FBgn0040252
CG14280	FBgn0038695	CG32436	FBgn0052436	dysf	FBgn0039411
CG14906	FBgn0015351	CG15784	FBgn0029766	Gadd45	FBgn0033153
Bdp1	FBgn0032512	CG14355	FBgn0038208	MFS3	FBgn0031307
Cap-D2	FBgn0039680	CG3014	FBgn0037519	CG31918	FBgn0031678
Dlish	FBgn0034264	Fdx1	FBgn0011769	Ldh	FBgn0001258
Cyt-c-d	FBgn0086907	lncRNA:CR44522	FBgn0265715	lncRNA:CR43753	FBgn0264084

Appendix H Differentially expressed genes between juvenile and mature flies in controls and Bap60-KD MBs

Juvenile control compared to Mature control - Upregulated					
Gene Symbol	**Flybase ID**	**Gene Symbol**	**Flybase ID**	**Gene Symbol**	**Flybase ID**
Orct2	FBgn0085424	Cpn	FBgn0261526	lncRNA:CR45717	FBgn0266361
CG4998	FBgn0036588	ap	FBgn0267233	CG13631	FBgn0040358
mRpS34	FBgn0267635	sona	FBgn0034844	ppk22	FBgn0051005
CG11425	FBgn0037123	dyl	FBgn0054038	Cyp6a16	FBgn0031571
CG40006	FBgn0053294	jhamt	FBgn0028516	CG8785	FBgn0033667
CG13722	FBgn0035439	CG30395	FBgn0047095	awd	FBgn0000099
Strica	FBgn0032878	Cc2d2a	FBgn0261990	ImpL2	FBgn0001253
Hml	FBgn0028789	PCNA2	FBgn0032707	spz5	FBgn0035103
Skp2	FBgn0037129	Dhc62B	FBgn0013469	CG13676	FBgn0035612
CG1850	FBgn0032973	Abd-B	FBgn0000015	CG5697	FBgn0038797
CG6592	FBgn0035553	CG14661	FBgn0037203	CG2861	FBgn0029167
Prip	FBgn0033520	ND-51	FBgn0031728	PCNA	FBgn0005592
Cpr72Ec	FBgn0036589	CG12239	FBgn0029507	Irk1	FBgn0263660
nub	FBgn0085234	Fmo-2	FBgn0032895	MsR2	FBgn0263019
CG13062	FBgn0036587	CG3635	FBgn0032850	CG17104	FBgn0040318
eEF1delta	FBgn0032025	CarT	FBgn0032836	Tsp42Ed	FBgn0028978
CG10899	FBgn0039161	DIP-epsilon	FBgn0259113	CG9759	FBgn0038073

reb	FBgn0033521	CG6512	FBgn0036603	mRF1	FBgn0032464
CG6040	FBgn0038468	neo	FBgn0039511	CG7470	FBgn0037115
CG8034	FBgn0030955	Orcokinin	FBgn0034859	lncRNA:CR44 498	FBgn0264488
salm	FBgn0261514	lncRNA:CR45 361	FBgn0265994	CG44014	FBgn0263239
CG43155	FBgn0261803	CG8728	FBgn0033051	Ddc	FBgn0000411
slif	FBgn0037127	CG14277	FBgn0031926	Oaz	FBgn0267435
al	FBgn0000061	CG18067	FBgn0034443	lncRNA:CR44 317	FBgn0264002
barc	FBgn0036939	Top2	FBgn0267433	stw	FBgn0267726
Ldh	FBgn0001257	wun2	FBgn0040794	CG42329	FBgn0259099
CG11131	FBgn0037128	yellow-g	FBgn0041156	Vdup1	FBgn0035050
eIF3c	FBgn0034085	CG17322	FBgn0026404	DCX-EMAP	FBgn0250746
Tsp	FBgn0031746	CG6429	FBgn0045852	p23	FBgn0037583
CG14229	FBgn0030999	IM1	FBgn0034157	Tsf1	FBgn0020372
CG4950	FBgn0036461	GstE2	FBgn0053978	CG7884	FBgn0030940
ValRS	FBgn0026702	mRpS18A	FBgn0051100	CG13067	FBgn0036520
Scox	FBgn0261648	H2.0	FBgn0001147	CG34347	FBgn0066365
lncRNA:CR 31044	FBgn0050471	CG5538	FBgn0037895	jtb	FBgn0033980
CG34398	FBgn0085277	Cda4	FBgn0052412	CG8642	FBgn0033154
CG31638	FBgn0051176	CG14565	FBgn0037085	CG5122	FBgn0032399
smt3	FBgn0263617	CG7131	FBgn0038447	CG40486	FBgn0262898
CG11852	FBgn0039235	CG6701	FBgn0033817	Fbxl7	FBgn0038201
CR33294	FBgn0053110	CCY	FBgn0266901	CG2680	FBgn0024222
slow	FBgn0035431	UGP	FBgn0035948	DNApol-alpha180	FBgn0250832
CG14232	FBgn0031001	CG34461	FBgn0086711	Desat1	FBgn0085482
Wnt2	FBgn0004101	CG31100	FBgn0051004	qua	FBgn0003162
qless	FBgn0050395	AANATL7	FBgn0040208	chp	FBgn0266900
boca	FBgn0003997	CG15445	FBgn0031031	CG12984	FBgn0036895
out	FBgn0259164	CG6910	FBgn0036101	nonA-l	FBgn0015035
eEF1alpha 2	FBgn0000527	Cyp305a1	FBgn0036880	Ppr-Y	FBgn0045495
Pvf1	FBgn0030828	CG7900	FBgn0037427	rib	FBgn0003187
CG5399	FBgn0038200	CG1941	FBgn0032981	meru	FBgn0052006
CG2736	FBgn0035049	lncRNA:CR45 360	FBgn0265691	CG14945	FBgn0032337
cysu	FBgn0038404	CG3902	FBgn0036742	Set	FBgn0013811
lsn	FBgn0259834	CG11249	FBgn0037042	Myo61F	FBgn0005655
Adgf-A	FBgn0036690	Npc2g	FBgn0039704	Lsp1beta	FBgn0002526
CG9701	FBgn0036595	pnr	FBgn0003011	CG42807	FBgn0261563

lncRNA:CR44468	FBgn0264462	AOX1	FBgn0266698	CG15923	FBgn0038720
CG18335	FBgn0033519	CG4461	FBgn0035952	mRpL19	FBgn0037538
Ppn	FBgn0003124	mRpL11	FBgn0038198	lncRNA:alphagamma-element:CR32865	FBgn0052572
Obp49a	FBgn0046697	ort	FBgn0002948	CG5644	FBgn0035845
IM23	FBgn0034143	CG1208	FBgn0037276	betaTub85D	FBgn0003513
sim	FBgn0004360	en	FBgn0000567	dmGlut	FBgn0010323
CG14696	FBgn0037755	CG9297	FBgn0038079	CG34166	FBgn0058006
lncRNA:CR43314	FBgn0261989	CG6067	FBgn0029573	Cyp6a22	FBgn0013278
CG13606	FBgn0039078	CG7214	FBgn0031906	CG5002	FBgn0034126
frm	FBgn0035539	Incenp	FBgn0259878	CG5397	FBgn0031161
CG11811	FBgn0035956	AstC-R2	FBgn0036727	Thor	FBgn0260745
PK1-R	FBgn0038180	ple	FBgn0005391	Dip-B	FBgn0000451
Crtp	FBgn0028841	Jheh3	FBgn0034275	VhaM9.7-a	FBgn0035379
Sdr	FBgn0038199	CG15211	FBgn0030114	CG14968	FBgn0035279
Nop60B	FBgn0259223	CG4306	FBgn0036717	eIF2beta	FBgn0004780
Dhc64C	FBgn0261534	CG4702	FBgn0037853	Gnmt	FBgn0037992
Act42A	FBgn0000043	CG32579	FBgn0052447	CG42749	FBgn0261560
yellow-e	FBgn0041182	CG3746	FBgn0034659	CG8630	FBgn0038052
to	FBgn0039237	Dic2	FBgn0038679	Prat2	FBgn0040817
CG13731	FBgn0036612	CG6013	FBgn0038460	CG9815	FBgn0034755
MFS9	FBgn0038695	CG14100	FBgn0036835	mfas	FBgn0259714
CG14182	FBgn0036881	CG15185	FBgn0037301	Cpr78Cc	FBgn0036922
dnd	FBgn0038846	Ude	FBgn0039130	Capa	FBgn0039656
Pxd	FBgn0004171	Prx2540-2	FBgn0033387	hbn	FBgn0005624
CG15201	FBgn0030158	aop	FBgn0000097	CG10932	FBgn0029728
eya	FBgn0000279	PIG-Q	FBgn0085427	Npc2b	FBgn0038105
CG2604	FBgn0037204	CG31809	FBgn0051189	CG10343	FBgn0032596
CG17048	FBgn0033733	MED8	FBgn0034408	GstE14	FBgn0033668
CG3009	FBgn0029147	CG1441	FBgn0033312	Mst98Cb	FBgn0004009
CG2970	FBgn0034861	e	FBgn0000454	CG31189	FBgn0051044
CG11313	FBgn0039686	Art7	FBgn0034709	cactin	FBgn0031012
CG3223	FBgn0037386	C15	FBgn0004777	ITP	FBgn0034903
Cyp301a1	FBgn0033635	CG30109	FBgn0046999	CG12730	FBgn0029501
CG14566	FBgn0037069	CG2650	FBgn0000092	bdl	FBgn0027843
Pu	FBgn0003141	Pect	FBgn0032405	Cyt-b5	FBgn0263113
CG34038	FBgn0053281	pr	FBgn0003137	ham	FBgn0042630
CG34054	FBgn0053286	CG8916	FBgn0030452	lncRNA:CR44772	FBgn0264894

CG4716	FBgn0033725	mre11	FBgn0016920	CG34453	FBgn0085400
kn	FBgn0001269	Ilp8	FBgn0036600	CG11407	FBgn0038598
sosie	FBgn0039131	CG42808	FBgn0261564	CG32447	FBgn0052260
CG9928	FBgn0032402	dtr	FBgn0020445	CG7497	FBgn0036659
CCHa1	FBgn0038130	Est-6	FBgn0000577	CG30427	FBgn0041711
ry	FBgn0003254	CG1273	FBgn0035398	CG13618	FBgn0039098
bs	FBgn0003975	klu	FBgn0011703	CG32816	FBgn0052499
CG10721	FBgn0032803	CG5160	FBgn0031849	tobi	FBgn0261341
Trpgamma	FBgn0032482	CG6055	FBgn0031850	Tsp29Fb	FBgn0032006
rdo	FBgn0086659	asRNA:CR45371	FBgn0265997	CG32457	FBgn0052365
CG31459	FBgn0051105	CG8745	FBgn0036225	Pex7	FBgn0035844
CG14892	FBgn0038353	CG33120	FBgn0052816	P5cr	FBgn0015282
wrapper	FBgn0025583	CG6231	FBgn0038577	Mlc1	FBgn0002576
CG5854	FBgn0038967	ms(3)76Cc	FBgn0036877	lncRNA:CR44833	FBgn0265042
Listericin	FBgn0033518	CAH1	FBgn0027562	mol	FBgn0085599
Bdp1	FBgn0032471	CecC	FBgn0000276	CG9016	FBgn0031726
lncRNA:CR45949	FBgn0266911	DIP-eta	FBgn0031542	CG32726	FBgn0052476
CG5862	FBgn0038814	Pisd	FBgn0026084	SmydA-5	FBgn0032879
Prosbeta4	FBgn0032483	Drice	FBgn0015904	Cyp6t2Psi	FBgn0041087
CG14280	FBgn0038511	CG13056	FBgn0040524	CG9411	FBgn0030234
CG43896	FBgn0263216	REG	FBgn0028573	Ir94e	FBgn0250844
Jheh1	FBgn0005626	btl	FBgn0267611	Doc1	FBgn0028482
exex	FBgn0040799	CG15414	FBgn0031375	CG13796	FBgn0031894
GstE3	FBgn0053556	RpS9	FBgn0008636	Phk-3	FBgn0035023
Echs1	FBgn0033760	CG46059	FBgn0267073	Galk	FBgn0262103
Ccp84Ag	FBgn0004577	CG32147	FBgn0046332	l(2)34Fc	FBgn0260653
CG42319	FBgn0250862	Cyp317a1	FBgn0033936	CG10178	FBgn0032587
lncRNA:CR32636	FBgn0052457	Pfdn4	FBgn0035522	Hsc70-1	FBgn0001170
ninaE	FBgn0002855	CG3823	FBgn0029720	CG6362	FBgn0028425
Dll	FBgn0000153	lncRNA:CR45517	FBgn0266096	erm	FBgn0031209
rtv	FBgn0259896	Ance-4	FBgn0033214	CG32260	FBgn0052072
pot	FBgn0243486	CecA1	FBgn0000251	CG3246	FBgn0031327
CG9452	FBgn0036778	CG9630	FBgn0037449	Pkg21D	FBgn0000422
asRNA:CR45330	FBgn0265661	Sox14	FBgn0004863	Rpt2	FBgn0015011
CG8051	FBgn0030964	CG10348	FBgn0032601	Obp99b	FBgn0039483
CG8303	FBgn0033982	CG13364	FBgn0026319	kl-5	FBgn0266869
GstO3	FBgn0035785	CG7910	FBgn0037387	GstE6	FBgn0053542

NimA	FBgn0259986	SmB	FBgn0261714	lncRNA:CR43253	FBgn0261834
CG4374	FBgn0038916	Gsc	FBgn0005696	Cyp6a20	FBgn0033889
FeCH	FBgn0265266	TpnC73F	FBgn0010246	CG30431	FBgn0047178
ZnT35C	FBgn0027844	ppk26	FBgn0035581	dbe	FBgn0020258
beag	FBgn0037547	CG32373	FBgn0052091	Pmm2	FBgn0036162
GstT2	FBgn0046687	CG43386	FBgn0262116	Obp99c	FBgn0039467
CG42766	FBgn0261561	CG5162	FBgn0030668	CG32086	FBgn0051809
ppk	FBgn0015946	CG5844	FBgn0037879	CG8046	FBgn0033268
CG5773	FBgn0034140	lncRNA:CR45425	FBgn0265998	IKKbeta	FBgn0023090
wb	FBgn0260991	Obp57a	FBgn0041336	Yp2	FBgn0004842
CG32039	FBgn0051459	asRNA:CR45009	FBgn0265376	LanA	FBgn0002023
CG11327	FBgn0031745	Desi	FBgn0037742	crn	FBgn0000320
LeuRS	FBgn0267592	CG1671	FBgn0033307	mthl14	FBgn0052373
La	FBgn0010497	CG5390	FBgn0032075	E23	FBgn0020294
CG14275	FBgn0031939	CG3862	FBgn0031097	mRpL41	FBgn0033949
polo	FBgn0003117	prc	FBgn0028406	CG5853	FBgn0032022
CG32982	FBgn0052579	lz	FBgn0002567	Cyp4d8	FBgn0014380
Ptp52F	FBgn0033979	blp	FBgn0038208	cN-IIIB	FBgn0034897
CG31176	FBgn0051036	sip1	FBgn0023001	sha	FBgn0003319
Cht7	FBgn0035255	NtR	FBgn0028740	lncRNA:CR44769	FBgn0264776
CG12945	FBgn0037678	Pkd2	FBgn0040827	CG13315	FBgn0040688
Zip71B	FBgn0036287	CG7227	FBgn0031918	Dhod	FBgn0000442
RNASEK	FBgn0261613	Iyd	FBgn0035977	Hsp70Bb	FBgn0011674
Tctp	FBgn0037772	NimB2	FBgn0028394	ReepA	FBgn0261277
CG10131	FBgn0033867	CG10562	FBgn0039239	CG41284	FBgn0085410
CG7299	FBgn0032167	CG14695	FBgn0037753	CG10747	FBgn0032773
CG11951	FBgn0039326	CG7135	FBgn0030715	CG14752	FBgn0033079
CG32365	FBgn0052086	CG14395	FBgn0037939	Sox21b	FBgn0041195
CG10663	FBgn0036125	Aatf	FBgn0031751	lncRNA:CR43651	FBgn0262685
CG13390	FBgn0031970	CG6723	FBgn0037832	Gli	FBgn0001981
fng	FBgn0010424	CG6356	FBgn0039084	Eip74EF	FBgn0000560
ND-MWFE	FBgn0085376	Ccp84Ad	FBgn0004666	Achl	FBgn0033828
CG33939	FBgn0046323	CG11825	FBgn0033388	mt:ND2	FBgn0011762
CG13675	FBgn0035669	Sesn	FBgn0034829	hid	FBgn0003889
rau	FBgn0031617	Cpr50Ca	FBgn0033753	Mms19	FBgn0037236
loco	FBgn0016930	ara	FBgn0015381	CG13640	FBgn0039178
ND-24	FBgn0030707	Ance-5	FBgn0034972	Dnah3	FBgn0035521

lncRNA:CR 43626	FBgn0262624	CG18622	FBgn0038385	CG12321	FBgn0038419
CG6638	FBgn0035797	CG9029	FBgn0031725	CG34424	FBgn0085370
ss	FBgn0003382	CG10559	FBgn0039238	Ttc19	FBgn0032684
CG8939	FBgn0030569	cad	FBgn0000157	dsf	FBgn0015033
DNApol-alpha50	FBgn0011591	CG42323	FBgn0250871	AhcyL2	FBgn0014343
CG3330	FBgn0039323	CG17387	FBgn0037167	lncRNA:CR45 188	FBgn0265457
NijC	FBgn0038017	obst-A	FBgn0031011	CG33978	FBgn0053126
CG9684	FBgn0037503	MFS10	FBgn0030160	CG14259	FBgn0039297
Fs	FBgn0259194	CG6891	FBgn0030799	CG4045	FBgn0025111
CG12483	FBgn0040496	CG15506	FBgn0039485	DNApol-alpha73	FBgn0005612
QC	FBgn0052150	CG33286	FBgn0053093	Cyp6a21	FBgn0033921
shams	FBgn0039232	CG14961	FBgn0035308	apolpp	FBgn0086448
exp	FBgn0033558	CG32091	FBgn0051869	CG6678	FBgn0038849
CG10333	FBgn0032593	pug	FBgn0020278	mRpS31	FBgn0036381
CG8834	FBgn0033610	CG33281	FBgn0052982	Lim3	FBgn0001987
CG10175	FBgn0038917	serp	FBgn0259247	Cpr76Bd	FBgn0036789
phu	FBgn0041709	ko	FBgn0019972	CG13255	FBgn0040491
CG9498	FBgn0031730	CG14625	FBgn0040091	CG7079	FBgn0038799
esg	FBgn0001319	CG42269	FBgn0250833	RYa-R	FBgn0004687

Juvenile control compared to Mature control - Downregulated					
Gene Symbol	**Flybase ID**	**Gene Symbol**	**Flybase ID**	**Gene Symbol**	**Flybase ID**
Cyp4d21	FBgn0031851	CG14109	FBgn0036183	yellow-b	FBgn0032486
CG6739	FBgn0031865	CG9279	FBgn0036824	Ahcy	FBgn0013773
lncRNA:CR 45673	FBgn0266268	lncRNA:CR44 357	FBgn0264294	Fum3	FBgn0035978
Nep4	FBgn0038733	CG15040	FBgn0030720	CG15432	FBgn0031489
antdh	FBgn0025629	CG7365	FBgn0036882	CG6686	FBgn0032282
dar1	FBgn0262467	Dup99B	FBgn0086687	PGRP-LF	FBgn0035922
ImpE1	FBgn0001248	AstCC	FBgn0032213	CG6870	FBgn0032512
CG13360	FBgn0024995	CG10680	FBgn0032744	CG17108	FBgn0032205
Kua	FBgn0032813	CG5280	FBgn0035854	CG44085	FBgn0263607
vito	FBgn0052187	CG13068	FBgn0036514	Amy-d	FBgn0000078
verm	FBgn0259937	CG10340	FBgn0020305	CG15661	FBgn0034474
Cyp12e1	FBgn0037728	CG13073	FBgn0036460	Kat60	FBgn0039802
CG9316	FBgn0032820	CG6675	FBgn0032846	Tre1	FBgn0043792
Mlc-c	FBgn0004403	Mat1	FBgn0023514	Or13a	FBgn0030558

Ir21a	FBgn0031059	vg	FBgn0003732	spd-2	FBgn0027081
melt	FBgn0020385	CG1774	FBgn0039798	CG31036	FBgn0050431
l(3)72Dp	FBgn0262601	RpLP0-like	FBgn0033366	Ugt58Fa	FBgn0039801
CG14253	FBgn0039273	Ant2	FBgn0024289	LManII	FBgn0027334
CG10345	FBgn0027094	CG2811	FBgn0034988	TyrRS	FBgn0026879
Tmhs	FBgn0261797	Acp26Aa	FBgn0002772	CG11200	FBgn0034406
Neu2	FBgn0036992	resilin	FBgn0034001	twit	FBgn0032845
Cyp4e3	FBgn0014455	trbl	FBgn0028543	CG12301	FBgn0036300
CG6083	FBgn0035982	CG9686	FBgn0029990	CG4872	FBgn0030631
b	FBgn0000150	CG5919	FBgn0038818	Hsp23	FBgn0001216
form3	FBgn0053123	CG8199	FBgn0037561	TrissinR	FBgn0085195
CG8008	FBgn0033235	Obp44a	FBgn0033061	Hsp68	FBgn0001226
CG15635	FBgn0031538	Nha1	FBgn0031771	NimC1	FBgn0259219
Cyp6a19	FBgn0033879	Dronc	FBgn0025878	CG9691	FBgn0030051
CG5778	FBgn0038868	JhI-21	FBgn0027783	Hsp26	FBgn0001224
CG5883	FBgn0036099	Cyt-b5-r	FBgn0000377	CG8925	FBgn0038234
dj-1beta	FBgn0039730	CG34248	FBgn0063497	CG17754	FBgn0029863
CG1427	FBgn0037255	CG15822	FBgn0035089	Iris	FBgn0031114
CG17834	FBgn0027571	NijA	FBgn0035964	Cyp6g1	FBgn0024956
Traf4	FBgn0025680	CG11447	FBgn0038675	insc	FBgn0011227
mesh	FBgn0050109	CG1354	FBgn0029969	CG7589	FBgn0036619
CG8128	FBgn0030272	Sb	FBgn0003308	CG13833	FBgn0038897
bark	FBgn0031452	nod	FBgn0002940	Swim	FBgn0034512
CG16749	FBgn0037548	Doc2	FBgn0035904	CG6503	FBgn0040376
Dhpr	FBgn0035911	CG14132	FBgn0040636	CG11796	FBgn0036889
CG14355	FBgn0038181	fbp	FBgn0032726	CG8549	FBgn0035578
RnrL	FBgn0011280	CG7296	FBgn0032198	wg	FBgn0267408
CG32006	FBgn0051450	l(1)G0004	FBgn0027079	Idh	FBgn0001230
Tep2	FBgn0040813	Cpr76Bc	FBgn0036787	CG14569	FBgn0037045
SiaT	FBgn0034936	CG30471	FBgn0050005	Obp19d	FBgn0010411
Cyp312a1	FBgn0036702	Pde11	FBgn0063498	Obp56h	FBgn0034405
CG2712	FBgn0024191	CG13639	FBgn0263830	Sodh-1	FBgn0023170
CG4021	FBgn0034503	ox	FBgn0010408	CG34205	FBgn0063494
Ugt86Da	FBgn0039828	Hsp60C	FBgn0031601	CG33110	FBgn0052726
CG13847	FBgn0038876	scpr-C	FBgn0037817	cer	FBgn0034328
CG15482	FBgn0032407	Psc	FBgn0004926	CG14805	FBgn0022355
Rpt3R	FBgn0037608	GILT3	FBgn0038930	CG2972	FBgn0030103
ThrRS	FBgn0027070	CG1542	FBgn0039754	Cpr65Au	FBgn0041194
CG42675	FBgn0260940	Hsp27	FBgn0001225	Osi17	FBgn0037298
NT1	FBgn0260460	Sik3	FBgn0261575	Rab32	FBgn0002565
CG12947	FBgn0037660	gskt	FBgn0043791	Npc2h	FBgn0039722

Obp56g	FBgn0034329	Drep4	FBgn0027611	CG7903	FBgn0039682
CG3520	FBgn0034748	CG4000	FBgn0038737	CG13449	FBgn0036364
CG7322	FBgn0030853	Prx2540-1	FBgn0033454	nab	FBgn0259229
Cyp6a17	FBgn0015075	CG7236	FBgn0031603	CG10584	FBgn0036910
Tspo	FBgn0031061	CG31075	FBgn0050493	CG31300	FBgn0051075
RpS14a	FBgn0004132	CG10307	FBgn0034500	mirr	FBgn0013680
upd3	FBgn0053120	Mmp1	FBgn0034935	CG6287	FBgn0032266
CG5225	FBgn0038387	Hsp70Ab	FBgn0011638	mt:ND4L	FBgn0013276
CG11052	FBgn0040321	CG10339	FBgn0034887	CG7778	FBgn0031940
CG4115	FBgn0037874	Ddx1	FBgn0014879	Pvr	FBgn0031925
CG13046	FBgn0036557	CG13707	FBgn0035515	Lsp2	FBgn0002563
CG14770	FBgn0029133	CG4302	FBgn0026576	Cht5	FBgn0038074
CG4957	FBgn0032031	ect	FBgn0000447	lncRNA:CR45973	FBgn0266974
Cwc25	FBgn0031263	CG1461	FBgn0030177	Vha68-3	FBgn0032394
CG11550	FBgn0039800	HGTX	FBgn0039856	GNBP3	FBgn0039864
CG17807	FBgn0034655	Dim1	FBgn0031459	CG1213	FBgn0037288
CG9861	FBgn0034735	ORY	FBgn0043535	Lst	FBgn0033981
Fip1	FBgn0037146	Cpr62Ba	FBgn0035082	CG14075	FBgn0036752
CG14879	FBgn0038279	CG33093	FBgn0052636	cry	FBgn0025454
Doa	FBgn0264922	CG32187	FBgn0052039	CG5114	FBgn0036262
Jheh2	FBgn0034258	fon	FBgn0032690	Obp8a	FBgn0029828
CG13051	FBgn0040600	CG13641	FBgn0039226	Gr28b	FBgn0042119
nompC	FBgn0015714	CG2862	FBgn0031286	CG12268	FBgn0039040
Pex19	FBgn0032388	CG14718	FBgn0037850	snoRNA:Psi18S-176	FBgn0085453
IM2	FBgn0024975	Dyrk2	FBgn0015781	CG13043	FBgn0036577
CG15202	FBgn0030151	Uhg5	FBgn0054054	RpS18	FBgn0010053
RpL39	FBgn0022344	l(1)G0045	FBgn0026268	D	FBgn0000406
CG12344	FBgn0033485	CG18302	FBgn0032076	Mur18B	FBgn0030895
eg	FBgn0000557	spirit	FBgn0029810	tej	FBgn0033820
St1	FBgn0034817	cib	FBgn0025620	CG14997	FBgn0035348
yellow-f2	FBgn0038049	snoRNA:Psi28S-3342	FBgn0085468	Cpr49Ac	FBgn0033593
CAH2	FBgn0027500	Buffy	FBgn0040259	gsb-n	FBgn0000592
Spn85F	FBgn0037709	firl	FBgn0032350	CG12896	FBgn0033464
CG9510	FBgn0032008	inv	FBgn0001258	CG7016	FBgn0039203
CG8005	FBgn0035714	CG10621	FBgn0032652	CG4610	FBgn0034638
CG2233	FBgn0029771	RhoL	FBgn0013683	Prosbeta7	FBgn0086667
CG14598	FBgn0037347	CG4218	FBgn0086712	Hacd1	FBgn0032283
CG9899	FBgn0034728	Egm	FBgn0086365	CG4496	FBgn0031801
CG14218	FBgn0030968	Elo68alpha	FBgn0051638	CG5953	FBgn0032472

CG9747	FBgn0039685	rad50	FBgn0034605	Nplp2	FBgn0040606
lncRNA:CR 43870	FBgn0263199	AlaRS	FBgn0027073	CG17224	FBgn0031305
FASN1	FBgn0267281	NLaz	FBgn0052865	CG6785	FBgn0032285
CG13082	FBgn0032703	CG31869	FBgn0051300	sano	FBgn0034290
grim	FBgn0015520	CG14837	FBgn0035603	CG42237	FBgn0087002
RabX5	FBgn0035076	CG14572	FBgn0037081	CG17189	FBgn0039298
CG16758	FBgn0035090	CG6227	FBgn0030271	CG10433	FBgn0034475
SMC2	FBgn0027375	CG30493	FBgn0050052	CG9920	FBgn0038160
side-V	FBgn0083123	RecQ5	FBgn0027080	CG5849	FBgn0038820
TM4SF	FBgn0020270	CG32572	FBgn0052418		

Juvenile Bap60-KD MB compared to Mature Bap60-KD MB - Upregulated					
Gene Symbol	**Flybase ID**	**Gene Symbol**	**Flybase ID**	**Gene Symbol**	**Flybase ID**
CG30395	FBgn0050395	Usp14	FBgn0032216	CG8927	FBgn0038405
snoRNA:Psi 18S-176	FBgn0086659	pr	FBgn0003141	CG12446	FBgn0031201
CG30471	FBgn0050471	SdhBL	FBgn0030975	elg1	FBgn0036574
CG12483	FBgn0040688	CG10559	FBgn0039323	Npc2f	FBgn0039154
lncRNA:CR 43626	FBgn0263617	CG5432	FBgn0039425	CG16904	FBgn0037763
CG9920	FBgn0038200	CG32260	FBgn0052260	CG13003	FBgn0030798
CG14355	FBgn0038208	Pkd2	FBgn0041195	sdk	FBgn0021764
nub	FBgn0085424	DNApol-alpha50	FBgn0011762	Cyp6a19	FBgn0033979
CG5697	FBgn0038846	CG9967	FBgn0031413	tej	FBgn0033921
CG9029	FBgn0031746	Pex7	FBgn0035922	Cad99C	FBgn0039709
Doc1	FBgn0028789	djl	FBgn0037463	CG13842	FBgn0039009
CG33281	FBgn0053281	sut1	FBgn0028563	CG4267	FBgn0264979
CG5853	FBgn0032167	lz	FBgn0002576	lncRNA:CR4 4768	FBgn0265993
CG8785	FBgn0033760	CG4741	FBgn0035040	Act42A	FBgn0000043
CG5225	FBgn0038468	NijC	FBgn0038079	ZC3H3	FBgn0035900
Mst98Cb	FBgn0004171	otu	FBgn0003023	CG42284	FBgn0259179
CG15024	FBgn0040699	Btk29A	FBgn0003502	vg	FBgn0003975
Cpr56F	FBgn0034499	CG7079	FBgn0038849	Tektin-C	FBgn0035638
CG42749	FBgn0261803	TrpA1	FBgn0035934	form3	FBgn0053556
CG13068	FBgn0036588	MsR2	FBgn0264002	CG7164	FBgn0031946
CG13606	FBgn0039161	Dyrk2	FBgn0016930	ken	FBgn0011236
lncRNA:CR 44468	FBgn0265661	nerfin-2	FBgn0041105	CG18568	FBgn0033888

slow	FBgn0035539	CG17834	FBgn0028394	CG14760	FBgn0033277
Prx2540-1	FBgn0033520	tsh	FBgn0003866	CG33978	FBgn0053978
CG13727	FBgn0036711	CG6040	FBgn0038679	CG12990	FBgn0030859
CG14565	FBgn0037129	Rpn5	FBgn0028690	hid	FBgn0003997
CG8925	FBgn0038404	Dlish	FBgn0034264	dnd	FBgn0038916
Mmp1	FBgn0035049	Pvf2	FBgn0031888	CG6071	FBgn0036186
CG7884	FBgn0031001	Sem1	FBgn0266666	CG30344	FBgn0050344
CG14569	FBgn0037123	CG10131	FBgn0033949	Rif1	FBgn0050085
lncRNA:CR 45949	FBgn0267611	Rpn1	FBgn0028695	Dl	FBgn0000463
CG10899	FBgn0039235	Npc2b	FBgn0038198	lncRNA:CR4 2862	FBgn0262109
CG14752	FBgn0033307	CR33294	FBgn0053294	Lsp1alpha	FBgn0002562
Abd-B	FBgn0000015	CG4218	FBgn0250844	CG12885	FBgn0039523
CG6891	FBgn0030955	Mur89F	FBgn0038492	RYa-R	FBgn0004842
CG14280	FBgn0038695	Dhc62B	FBgn0013811	grn	FBgn0001138
CG34248	FBgn0085277	CG17104	FBgn0040496	CG17048	FBgn0033828
CG4998	FBgn0036612	Zip71B	FBgn0036461	CycE	FBgn0010382
Cpr50Ca	FBgn0033867	out	FBgn0259834	Crtp	FBgn0029501
NimA	FBgn0261514	frm	FBgn0035612	prc	FBgn0028573
CG9316	FBgn0032878	CG30412	FBgn0050412	yuri	FBgn0045842
CG7886	FBgn0038248	CG15534	FBgn0039769	CG14034	FBgn0250847
Acp26Aa	FBgn0002855	CG10841	FBgn0038163	CG43646	FBgn0263655
CG12184	FBgn0025387	lncRNA:CR32 194	FBgn0052194	CG17387	FBgn0037276
CG13043	FBgn0036600	CG1942	FBgn0033215	Atg13	FBgn0261108
e	FBgn0000527	CG15040	FBgn0030940	BigH1	FBgn0038252
Tre1	FBgn0046687	Ppi1	FBgn0051025	lncRNA:CR4 5558	FBgn0267118
scpr-C	FBgn0037879	Mp	FBgn0260660	CG45050	FBgn0266410
lncRNA:CR 44769	FBgn0265994	RnrS	FBgn0011704	CG17377	FBgn0031859
Yp2	FBgn0005391	lint	FBgn0033359	ckd	FBgn0035427
CG9016	FBgn0031751	CG18659	FBgn0027561	Dhc36C	FBgn0013810
Cht5	FBgn0038180	mesh	FBgn0051004	Fum3	FBgn0036162
CG34205	FBgn0085234	CG15185	FBgn0037449	CG14082	FBgn0036851
Hsp60C	FBgn0031728	Ser	FBgn0004197	en	FBgn0000577
Cyp312a1	FBgn0036778	CG1773	FBgn0033439	CG31357	FBgn0051357
CG13640	FBgn0039237	thw	FBgn0037487	RhoGEF64C	FBgn0035574
CG12268	FBgn0039131	Prosalpha3	FBgn0261394	CG3829	FBgn0035091
eIF3d2	FBgn0037994	Asph	FBgn0034075	Neurochon drin	FBgn0037447
rib	FBgn0003254	CG8665	FBgn0032945	rdog	FBgn0039644

CG8303	FBgn0034143	CG13639	FBgn0265266	kl-2	FBgn0001313
Cpr49Ac	FBgn0033725	Neu2	FBgn0037085	mthl14	FBgn0052476
CG5953	FBgn0032587	CG12825	FBgn0033221	Ir21a	FBgn0031209
CG31176	FBgn0051176	exex	FBgn0041156	rha	FBgn0027376
CG14990	FBgn0035496	NT1	FBgn0261526	lncRNA:CR46075	FBgn0267744
CG15506	FBgn0039686	CG10345	FBgn0027562	CG15631	FBgn0031626
CG18335	FBgn0033610	CG32436	FBgn0052436	CG9593	FBgn0038365
CG34375	FBgn0085404	CG9861	FBgn0034844	H2.0	FBgn0001170
CG8630	FBgn0038130	CG14837	FBgn0035797	dila	FBgn0033447
CG32572	FBgn0052572	lncRNA:CR43253	FBgn0262898	CG17977	FBgn0040778
CG11825	FBgn0033519	Shroom	FBgn0085408	Mct1	FBgn0023549
Dronc	FBgn0026404	neb	FBgn0004374	NimC1	FBgn0259896
CG31459	FBgn0051459	CG13675	FBgn0035845	CG30392	FBgn0050392
ms(3)76Cc	FBgn0036895	inv	FBgn0001269	CR31427	FBgn0051427
CG6739	FBgn0031926	Klp59C	FBgn0034824	CG34461	FBgn0250833
AstCC	FBgn0032337	CG2556	FBgn0030396	Ugt37b1	FBgn0026755
abd-A	FBgn0000014	CG18641	FBgn0031426	FER	FBgn0000723
Ilp8	FBgn0036690	TpnC47D	FBgn0010423	Rab32	FBgn0002567
CG13046	FBgn0036595	Rpn2	FBgn0028692	timeout	FBgn0038118
al	FBgn0000061	Rpn13	FBgn0033886	Ets96B	FBgn0039225
CG6055	FBgn0031918	CG34107	FBgn0083943	ort	FBgn0003011
topi	FBgn0037751	Rpt3R	FBgn0037742	PK1-R	FBgn0038201
lncRNA:CR45973	FBgn0267635	lncRNA:CR45267	FBgn0266805	CG15128	FBgn0034467
CG5399	FBgn0038353	cad	FBgn0000251	CG33926	FBgn0053926
CCHa1	FBgn0038199	CG10014	FBgn0038000	CG44245	FBgn0265180
CG42323	FBgn0259223	CG11380	FBgn0040359	Acp53C14c	FBgn0053530
Ptp52F	FBgn0034085	ItgaPS4	FBgn0034005	Drep4	FBgn0028406
Meltrin	FBgn0265140	CG17189	FBgn0039485	comm2	FBgn0041160
gsb-n	FBgn0001147	CG10178	FBgn0032684	CG3770	FBgn0035085
Cht7	FBgn0035398	CCY	FBgn0267592	cnc	FBgn0262975
CG33939	FBgn0047095	CG8526	FBgn0037759	cep290	FBgn0035168
Prosbeta7	FBgn0250746	tx	FBgn0263118	CG15548	FBgn0039812
CG15564	FBgn0039833	TTLL6B	FBgn0039501	Gsc	FBgn0010323
CG14572	FBgn0037128	CG13071	FBgn0036585	CG14117	FBgn0036331
Pxd	FBgn0004577	CG7330	FBgn0036780	CG4213	FBgn0031251
CG10348	FBgn0032707	CG14457	FBgn0037174	wmd	FBgn0034876
Dnah3	FBgn0035581	bnl	FBgn0014135	Dhc93AB	FBgn0013812
CG42820	FBgn0262002	CG42237	FBgn0250862	Fili	FBgn0085397
lyd	FBgn0036125	ssp5	FBgn0037985	Vdup1	FBgn0035103

Prx2540-2	FBgn0033518	Kah	FBgn0035144	PK2-R2	FBgn0038139
CG11249	FBgn0037115	Hsp60B	FBgn0011244	IM2	FBgn0025583
CG5122	FBgn0032471	CG4945	FBgn0034137	SLC22A	FBgn0037140
CG7131	FBgn0038598	CG11449	FBgn0037162	Spn42Dc	FBgn0033113
CG3520	FBgn0034859	CG14566	FBgn0037127	CG9109	FBgn0031765
Fbxl7	FBgn0038385	CG15120	FBgn0034454	MFS14	FBgn0010651
CG33093	FBgn0053093	CG2861	FBgn0029728	tum	FBgn0086356
Doc2	FBgn0035956	lncRNA:CR43651	FBgn0263660	Cyp6d4	FBgn0039006
aop	FBgn0000097	CG46059	FBgn0267726	CG15923	FBgn0038814
Dup99B	FBgn0250832	Prosbeta4	FBgn0032596	CG31121	FBgn0051121
CG7589	FBgn0036727	Sclp	FBgn0030357	CG1806	FBgn0030360
lncRNA:CR45231	FBgn0266766	lncRNA:CR44779	FBgn0266005	swi2	FBgn0034262
CG18810	FBgn0042133	Trpgamma	FBgn0032593	CG44836	FBgn0266099
Rpt6R	FBgn0039788	dnr1	FBgn0260866	CG12009	FBgn0035430
Eip74EF	FBgn0000567	lncRNA:CR44830	FBgn0266088	PPO2	FBgn0033367
cu	FBgn0261808	lncRNA:CR45673	FBgn0267233	Prosalpha4	FBgn0004066
CG34038	FBgn0054038	CG11327	FBgn0031849	CG3009	FBgn0029720
lncRNA:CR43753	FBgn0264084	Psa	FBgn0261243	Traf4	FBgn0026319
Ran-like	FBgn0036497	ham	FBgn0045852	Prosbeta3	FBgn0026380
CG13847	FBgn0038967	CG42269	FBgn0259164	msi	FBgn0011666
mol	FBgn0086711	Nep5	FBgn0039478	CG2046	FBgn0037378
CG4681	FBgn0069913	Cpr78Cc	FBgn0037069	ninaD	FBgn0002939
cysu	FBgn0038511	Nox	FBgn0085428	CG43740	FBgn0263997
CG18622	FBgn0038460	spri	FBgn0085443	CG4462	FBgn0038752
CG3809	FBgn0037995	lncRNA:CR45115	FBgn0266590	CG8051	FBgn0031012
CG5080	FBgn0031313	Cpr76Bd	FBgn0036881	lncRNA:CR45430	FBgn0266979
CG12896	FBgn0033521	CG8483	FBgn0038126	CG6938	FBgn0036235
CG32086	FBgn0052086	CG12963	FBgn0034031	CG6723	FBgn0037895
CG13067	FBgn0036589	Prosbeta5	FBgn0029134	lncRNA:CR45360	FBgn0266900
CG12321	FBgn0038577	Rpn6	FBgn0028689	CG45782	FBgn0267429
NijA	FBgn0036101	CG14879	FBgn0038419	CG7069	FBgn0038952
serp	FBgn0260653	Ho	FBgn0037933	Sap-r	FBgn0000416
Doa	FBgn0265998	CG17669	FBgn0034352	Cyp316a1	FBgn0035790
ple	FBgn0005626	CG3259	FBgn0038221	Exn	FBgn0261547
CG14968	FBgn0035431	sim	FBgn0004666	rdhB	FBgn0038946

S-Lap1	FBgn0035915	fa2h	FBgn0050502	Cln7	FBgn0035767
CG4021	FBgn0034659	CG4115	FBgn0038017	CG14609	FBgn0037483
Cc2d2a	FBgn0263113	Rbp4	FBgn0010258	laza	FBgn0037163
lncRNA:CR 43724	FBgn0263970	polo	FBgn0003124	CG5172	FBgn0030830
CG14961	FBgn0035439	CG2444	FBgn0030326	Coop	FBgn0263240
Spn85F	FBgn0037772	CG33286	FBgn0053286	qless	FBgn0051005
CG7365	FBgn0036939	CG1791	FBgn0030163	CG13492	FBgn0034662
verm	FBgn0261341	qua	FBgn0003187	CG4455	FBgn0028506
Yp1	FBgn0004045	CG5958	FBgn0031913	shd	FBgn0003388
Prip	FBgn0033635	CG13641	FBgn0039239	CG18266	FBgn0031724
CG7910	FBgn0037547	stw	FBgn0259247	AdamTS-A	FBgn0038341
CG17754	FBgn0030114	CG3394	FBgn0034999	dpr2	FBgn0261871
sona	FBgn0034903	Prosalpha7	FBgn0023175	Ance-2	FBgn0032535
gskt	FBgn0046332	Nuf2	FBgn0031886	Ddr	FBgn0053531
pnr	FBgn0003117	rols	FBgn0041096	CG42534	FBgn0260487
CG13082	FBgn0032803	SiaT	FBgn0035050	TrissinR	FBgn0085410
Rpt2	FBgn0015282	TppII	FBgn0020370	CG5909	FBgn0039495
CG7848	FBgn0034127	babos	FBgn0034724	CG7236	FBgn0031730
CG34398	FBgn0085427	DIP-iota	FBgn0031837	CG11425	FBgn0037167
CG8642	FBgn0033312	CG30187	FBgn0050187	vn	FBgn0003984
DNApol-alpha180	FBgn0259113	CG18109	FBgn0028901	CG13088	FBgn0032047
tmod	FBgn0082582	CG12163	FBgn0260462	CG15822	FBgn0035308
stg	FBgn0003525	GATAe	FBgn0038391	CG14598	FBgn0037503
CG14892	FBgn0038447	Rpt4	FBgn0028685	CG7497	FBgn0036742
CG42675	FBgn0261561	CG6484	FBgn0034247	HisCl1	FBgn0037950
Cpr50Cb	FBgn0033869	CG10663	FBgn0036287	GstE14	FBgn0033817
CG4374	FBgn0039078	CG34256	FBgn0085285	IRSp53	FBgn0052082
CG3330	FBgn0039511	CG8034	FBgn0031011	CG5050	FBgn0032637
Ppr-Y	FBgn0046697	sas	FBgn0002306	Myo61F	FBgn0010246
Sans	FBgn0033785	sano	FBgn0034408	CG30377	FBgn0050377
Dhc16F	FBgn0013809	CG9899	FBgn0034829	CG9492	FBgn0037726
lncRNA:CR 45966	FBgn0267628	CG10919	FBgn0037514	Hmgcr	FBgn0263782
Rpn9	FBgn0028691	CG18130	FBgn0030359	CG12795	FBgn0031535
rdo	FBgn0243486	side-V	FBgn0085400	CG9684	FBgn0037583
CG13796	FBgn0031939	CG9626	FBgn0037565	OdsH	FBgn0026058
CG13705	FBgn0035582	jhamt	FBgn0028841	rdgA	FBgn0261549
nab	FBgn0259986	CG1273	FBgn0035522	Awh	FBgn0013751
slam	FBgn0043854	CG42807	FBgn0261989	cact	FBgn0000250
NtR	FBgn0029147	CG5397	FBgn0031327	CG3339	FBgn0039510

Prosalpha2	FBgn0086134	esg	FBgn0001981	CG43163	FBgn0262719
in	FBgn0001259	CG4950	FBgn0036587	lncRNA:CR45180	FBgn0266690
CG31100	FBgn0051100	Kua	FBgn0032850	CCAP-R	FBgn0039396
bark	FBgn0031571	CG32982	FBgn0052982	ara	FBgn0015904
Sox14	FBgn0005612	Whamy	FBgn0037750	thr	FBgn0003701
yellow-g	FBgn0041709	TkR86C	FBgn0004841	uif	FBgn0031879
CG5538	FBgn0038052	CG42663	FBgn0261545	CG10681	FBgn0036291
Cpr97Eb	FBgn0039481	CG31327	FBgn0051327	CG31324	FBgn0051324
Drat	FBgn0033188	CG6966	FBgn0038286	CG14459	FBgn0037171
CG6231	FBgn0038720	Np	FBgn0265011	Fmo-2	FBgn0033079
obst-A	FBgn0031097	Rpt4R	FBgn0036224	CG31690	FBgn0051690
Vha68-3	FBgn0032464	exp	FBgn0033668	CG43312	FBgn0263004
Rpn11	FBgn0028694	Fbp2	FBgn0000640	CG12861	FBgn0033953
CG8420	FBgn0037664	ACXC	FBgn0040508	CG15544	FBgn0039804
dar1	FBgn0263239	eg	FBgn0000560	CG9782	FBgn0030763
Cad74A	FBgn0036715	Ir94e	FBgn0259194	CG9003	FBgn0033639
lncRNA:CR45359	FBgn0266899	CG7227	FBgn0031970	sit	FBgn0038986
CG11345	FBgn0035546	lncRNA:CR44177	FBgn0265066	Psc	FBgn0005624
CG10252	FBgn0039104	lncRNA:CR44357	FBgn0265457	lncRNA:CR44957	FBgn0266262
CG12998	FBgn0030829	Lcp65Ac	FBgn0020642	CG8136	FBgn0037616
CG6059	FBgn0039491	CG9701	FBgn0036659	WDY	FBgn0267449
asp	FBgn0000140	obst-B	FBgn0027600	CG42494	FBgn0260026
Ubx	FBgn0003944	Ent1	FBgn0031250	scb	FBgn0003328
TpnC73F	FBgn0010424	arg	FBgn0023535	CG1208	FBgn0037386
CG6426	FBgn0034162	pot	FBgn0250871	S-Lap3	FBgn0045770
ZnT35C	FBgn0028516	CG10516	FBgn0036549	ft	FBgn0001075
spz5	FBgn0035379	pirk	FBgn0034647	Pvr	FBgn0032006
knk	FBgn0001321	MCPH1	FBgn0260959	pip	FBgn0003089
CG42808	FBgn0261990	CG12643	FBgn0040942	lncRNA:let7C	FBgn0263049
alpha-Est2	FBgn0015570	yellow-f2	FBgn0038105	T48	FBgn0004359
FASN2	FBgn0042627	salt	FBgn0039872	Indy	FBgn0036816
ImpL2	FBgn0001257	pk	FBgn0003090	blow	FBgn0004133
CG15482	FBgn0032483	Trxr-2	FBgn0037170	lncRNA:CR45312	FBgn0266851
Cpr11A	FBgn0030394	CG43331	FBgn0263036	CG8852	FBgn0031548
CG12607	FBgn0035545	CG33125	FBgn0053125	Ptx1	FBgn0020912
TTLL4B	FBgn0031574	CG15547	FBgn0039809	Pomp	FBgn0032884
CG31029	FBgn0051029	Cyp6a16	FBgn0031726	CG15478	FBgn0029955

Hsc70-2	FBgn0001217	yellow-e	FBgn0041711	CG8389	FBgn0034063
CG7720	FBgn0038652	CG32816	FBgn0052816	CG3838	FBgn0032130
CG9934	FBgn0032467	lncRNA:CR44498	FBgn0265691	CtsB1	FBgn0030521
CG14120	FBgn0036321	Yp3	FBgn0004047	CG11885	FBgn0031253
CG31178	FBgn0064912	Myd88	FBgn0033402	CREG	FBgn0025456
Prosalpha6	FBgn0250843	Sesn	FBgn0034897	raw	FBgn0003209
CG13722	FBgn0035553	sofe	FBgn0030242	btv	FBgn0023096
Cyp4e3	FBgn0015035	IP3K1	FBgn0032147	CG12947	FBgn0037753
resilin	FBgn0034157	AstC-R2	FBgn0036789	ds	FBgn0000497
CG15673	FBgn0034639	Porin2	FBgn0069354	lncRNA:CR45464	FBgn0267020
slif	FBgn0037203	ppk26	FBgn0035785	spz3	FBgn0031959
kkv	FBgn0001311	CG42366	FBgn0259712	CG34342	FBgn0085371
Gr43a	FBgn0041243	CG5644	FBgn0035948	Txl	FBgn0035631
Cyp317a1	FBgn0033982	CG32121	FBgn0052121	frac	FBgn0035798
CG17746	FBgn0035425	Peritrophin-A	FBgn0022770	d	FBgn0262029
loopin-1	FBgn0259795	drongo	FBgn0020304	CG11378	FBgn0040364
CG6675	FBgn0032973	CG32548	FBgn0052548	CG4168	FBgn0028888
Prosbeta2	FBgn0023174	ptc	FBgn0003892	spd-2	FBgn0027500
Gr66a	FBgn0035870	lncRNA:CR43314	FBgn0263019	asRNA:CR44894	FBgn0266199
CG14770	FBgn0029573	hmw	FBgn0038607	Cda5	FBgn0051973
sha	FBgn0003382	yl	FBgn0004649	Proc-R	FBgn0029723
kl-3	FBgn0267432	Rpn10	FBgn0015283	CG34367	FBgn0085396
Cda4	FBgn0052499	CG32365	FBgn0052365	vri	FBgn0016076
CG14395	FBgn0038073	CG32445	FBgn0052445	gukh	FBgn0026239
melt	FBgn0023001	Mal-A7	FBgn0033296	CG43329	FBgn0263034
CG6652	FBgn0036687	CG12766	FBgn0035476	Neto	FBgn0265416
CG32091	FBgn0052091	CG13258	FBgn0032582	CG10459	FBgn0033440
TTLL3B	FBgn0031853	hpRNA:CR18854	FBgn0042174	shf	FBgn0003390
Uch	FBgn0010288	Ccp84Ag	FBgn0004777	E23	FBgn0020445
exu	FBgn0000615	Mal-A8	FBgn0033297	CG11658	FBgn0036196
CG8128	FBgn0030668	CG7896	FBgn0039728	CG17931	FBgn0038421
CG10936	FBgn0034253	CanA1	FBgn0010015	CG6153	FBgn0032445
Lst	FBgn0034140	dmrt11E	FBgn0030477	CG10337	FBgn0032805
CG34347	FBgn0085376	bap	FBgn0004862	CG10175	FBgn0039084
Mur18B	FBgn0030999	Oseg5	FBgn0032891	CG12964	FBgn0034022
Rpt6	FBgn0020369	Cpr49Ah	FBgn0033731	Pect	FBgn0032482
lncRNA:CR45237	FBgn0266772	Ufd1-like	FBgn0036136	CG42266	FBgn0259151

CG14218	FBgn0031031	Jhe	FBgn0010052	CG6145	FBgn0033853
CG2650	FBgn0000092	CG4496	FBgn0031894	cindr	FBgn0027598
Elo68alpha	FBgn0052072	Desi	FBgn0037832	CG17279	FBgn0038850
CG13731	FBgn0036717	Axs	FBgn0000152	Obp83g	FBgn0046875
CG15414	FBgn0031542	RnrL	FBgn0011703	capu	FBgn0000256
RabX5	FBgn0035255	mirr	FBgn0014343	DIP-epsilon	FBgn0259714
CG15531	FBgn0039755	CG5254	FBgn0040383	CG34217	FBgn0085246
Spn38F	FBgn0028986	FASN3	FBgn0040001	CG32579	FBgn0052579
CG6592	FBgn0035669	CG8501	FBgn0033724	CG5160	FBgn0031906
tn	FBgn0265356	CG1288	FBgn0250845	QC	FBgn0052412
Tmhs	FBgn0262624	CG3630	FBgn0023540	CG14132	FBgn0040817
CG17574	FBgn0033777	Rcd2	FBgn0037012	Pde11	FBgn0085370
TrxT	FBgn0029752	CG14625	FBgn0040358	IKKbeta	FBgn0024222
Cpr62Bc	FBgn0035281	CG33494	FBgn0053494	CG6280	FBgn0033866
m	FBgn0002577	mud	FBgn0002873	CG12880	FBgn0046258
CG32447	FBgn0052447	lobo	FBgn0083946	Hs6st	FBgn0038755
CG13627	FBgn0039217	Fs	FBgn0259878	lncRNA:CR44317	FBgn0265376
edl	FBgn0023214	Rpn12	FBgn0028693	klhl10	FBgn0040038
CG1835	FBgn0031127	CG13073	FBgn0036577	Act87E	FBgn0000046
Rpn3	FBgn0261396	CG12984	FBgn0037042	Ets98B	FBgn0005659
CG9389	FBgn0037064	CG15530	FBgn0039752	CG42673	FBgn0261555
CG14877	FBgn0038380	S-Lap5	FBgn0033860	CG14259	FBgn0039483
CG8564	FBgn0035776	CG10339	FBgn0034972	sns	FBgn0024189
CG14540	FBgn0039398	FucTB	FBgn0032117	CG10311	FBgn0038420
CG43980	FBgn0264711	CG11069	FBgn0039244	spg	FBgn0264324
CG15445	FBgn0031161	CG14696	FBgn0037853	Gyc32E	FBgn0010197
cmet	FBgn0040232	CG15309	FBgn0030183	ClC-a	FBgn0051116
CG34457	FBgn0085486	Cp1	FBgn0013770	CG11791	FBgn0039266
Prosbeta6	FBgn0002284	trbl	FBgn0028978	Fem-1	FBgn0034542
CG13449	FBgn0036520	comm3	FBgn0259236	Cyp301a1	FBgn0033753
CG3119	FBgn0031466	Oaz	FBgn0261613	dmGlut	FBgn0010497
CG3223	FBgn0037538	red	FBgn0038220	Sox21b	FBgn0042630
Cpr100A	FBgn0039805	CG34124	FBgn0083960	CG13012	FBgn0030769
ppk22	FBgn0051105	yellow-f	FBgn0041710	CG45076	FBgn0266446
Uch-L5	FBgn0011327	CG5854	FBgn0039130	tup	FBgn0003896
CG15635	FBgn0031617	DIP-theta	FBgn0051646	CG33017	FBgn0053017
CG8736	FBgn0033308	CG7202	FBgn0037086	CG34393	FBgn0085422
Hr4	FBgn0264562	soti	FBgn0038225	CG8908	FBgn0034493
Lsp1gamma	FBgn0002564	ko	FBgn0020294	CG6051	FBgn0039492
Ccp84Ab	FBgn0004782	bmm	FBgn0036449	CG42747	FBgn0261801

Sb	FBgn0003319	ush	FBgn0003963	Oatp26F	FBgn0051634
CG30458	FBgn0050458	lncRNA:CR45916	FBgn0267576	Trim9	FBgn0051721
CG16786	FBgn0034974	NO66	FBgn0266570	Octbeta2R	FBgn0038063
Thor	FBgn0261560	CG3655	FBgn0040397	CG4678	FBgn0030778
CG14718	FBgn0037939	CG32280	FBgn0052280	erm	FBgn0031375
HGTX	FBgn0040318	CG13065	FBgn0036590	CG11404	FBgn0037169
kon	FBgn0032683	eIF4E7	FBgn0040368	ReepA	FBgn0261564
CG31189	FBgn0051189	Skeletor	FBgn0262717	unc-4	FBgn0024184
Wnt2	FBgn0004360	Swim	FBgn0034709	sqa	FBgn0259678
S-Lap2	FBgn0052351	CCHa1-R	FBgn0050106	CG7016	FBgn0039238
CG13154	FBgn0033736	Lim3	FBgn0002023	cdi	FBgn0004876
Ccp84Aa	FBgn0004783	lncRNA:CR44833	FBgn0266096	CG17806	FBgn0038548
CG42255	FBgn0259140	CG12914	FBgn0033499	Sh3beta	FBgn0035772
lncRNA:CR45361	FBgn0266901	CG11852	FBgn0039297	AstA-R1	FBgn0266429
CG9815	FBgn0034861	l(3)mbn	FBgn0002440	Ndc1	FBgn0039125
Rpn7	FBgn0028688	reb	FBgn0033667	Gasp	FBgn0026077
CG10680	FBgn0032836	CG43386	FBgn0263216	CG31778	FBgn0051778
Lsd-1	FBgn0039114	Cyp4d8	FBgn0015033	Hil	FBgn0050147
CG6429	FBgn0046999	lncRNA:CR43870	FBgn0264462	side-VIII	FBgn0086604
CG13062	FBgn0036603	CG17562	FBgn0038449	CG7744	FBgn0034447
CG34265	FBgn0085294	CG30050	FBgn0050050	Ugalt	FBgn0024994
CG4712	FBgn0033818	CG34251	FBgn0085280	Pino	FBgn0016926
CG4744	FBgn0033834	loco	FBgn0020278	CG5790	FBgn0032677
rau	FBgn0031745	ect	FBgn0000451	foxo	FBgn0038197
cas	FBgn0004878	betaTub85D	FBgn0003889	Irk1	FBgn0265042
CG43236	FBgn0262881	Mmp2	FBgn0033438	brv3	FBgn0040333
Cpr97Ea	FBgn0039480	CG30456	FBgn0050456	CG40160	FBgn0058160
ORY	FBgn0046323	Prosbeta1	FBgn0010590	CG1440	FBgn0030038
CG14275	FBgn0032022	ec	FBgn0000542	Drak	FBgn0052666
CG45062	FBgn0266432	CG30440	FBgn0050440	Grd	FBgn0001134
Dic2	FBgn0038797	lncRNA:CR32111	FBgn0052111	Root	FBgn0039152
AhcyL2	FBgn0015011	Cyp4s3	FBgn0030615	Cnb	FBgn0035295
ACXD	FBgn0040507	schuy	FBgn0036925	Lrt	FBgn0034540
CG13676	FBgn0035844	GlcT	FBgn0067102	ihog	FBgn0031872
Rpt5	FBgn0028684	CG10211	FBgn0032685		
l(2)34Fc	FBgn0261534	CG15196	FBgn0030296		

Juvenile Bap60-KD MB compared to Mature Bap60-KD MB - Downregulated					
Gene Symbol	**Flybase ID**	**Gene Symbol**	**Flybase ID**	**Gene Symbol**	**Flybase ID**
MrgBP	FBgn0033341	CG5466	FBgn0038815	CG15556	FBgn0039821
CG5819	FBgn0034717	Egm	FBgn0086712	Pgm	FBgn0003076
CG13868	FBgn0034501	HDAC1	FBgn0015805	eEF1alpha2	FBgn0000557
alpha-Est7	FBgn0015575	Mdh1	FBgn0262782	CG7506	FBgn0035805
Irp-1B	FBgn0024957	CG7246	FBgn0030081	Sdr	FBgn0038279
RpL10	FBgn0024733	xmas-2	FBgn0028974	DCTN3-p24	FBgn0010622
jim	FBgn0027339	CG14109	FBgn0036364	Gabat	FBgn0036927
SmD2	FBgn0261789	Calr	FBgn0005585	HP1b	FBgn0030082
ACC	FBgn0033246	KdelR	FBgn0267330	Obp99c	FBgn0039682
CG12605	FBgn0035481	CG34117	FBgn0083953	zye	FBgn0036985
Capa	FBgn0039722	Nup54	FBgn0033737	cry	FBgn0025680
fidipidine	FBgn0025519	CG11377	FBgn0031217	CG6180	FBgn0032453
sta	FBgn0003517	CG13630	FBgn0039219	Cen	FBgn0032876
Dhc64C	FBgn0261797	alphaSnap	FBgn0250791	CG9279	FBgn0036882
Arp8	FBgn0030877	FASN1	FBgn0027571	CG34424	FBgn0085453
CG15916	FBgn0030704	GPHR	FBgn0033995	Obp28a	FBgn0011283
Pal2	FBgn0262728	Rbp9	FBgn0010263	Nep4	FBgn0038818
Cdc2rk	FBgn0013435	Phk-3	FBgn0035089	La	FBgn0011638
pAbp	FBgn0265297	Ykt6	FBgn0260858	veli	FBgn0039269
Adi1	FBgn0052068	CG6443	FBgn0032290	CG17065	FBgn0031099
mahe	FBgn0029979	IA-2	FBgn0031294	e(y)1	FBgn0000617
CG7339	FBgn0036188	PIG-A	FBgn0034270	CG15202	FBgn0030271
CG15529	FBgn0039748	Rtc1	FBgn0020909	crn	FBgn0000377
cl	FBgn0000318	eIF3a	FBgn0037249	LManII	FBgn0027611
ear	FBgn0026441	Klp64D	FBgn0004380	CG11796	FBgn0036992
Argk	FBgn0000116	Prat2	FBgn0041194	Ance-5	FBgn0035076
Loxl2	FBgn0034660	Hlc	FBgn0001565	Ric	FBgn0265605
RpL15	FBgn0028697	mt:CoI	FBgn0013674	CG2233	FBgn0029990
Nup93-1	FBgn0027537	Ssadh	FBgn0039349	CG16978	FBgn0040972
CG5390	FBgn0032213	CG31638	FBgn0051638	mRpS7	FBgn0032236
CG6841	FBgn0036828	eIF3m	FBgn0033902	CG7299	FBgn0032282
CG11191	FBgn0033249	eIF3b	FBgn0034237	CG31549	FBgn0051549
CG5404	FBgn0038354	pont	FBgn0040078	CG31673	FBgn0051673
CG5844	FBgn0038049	CG11752	FBgn0030292	CG7214	FBgn0031940
r2d2	FBgn0031951	Asciz	FBgn0035407	CG31075	FBgn0051075
trp	FBgn0003861	CG18661	FBgn0040964	Cyt-b5	FBgn0264294
CG4849	FBgn0039566	D1	FBgn0000412	CG1544	FBgn0039827
CG8818	FBgn0033751	eys	FBgn0031414	Cyp6a22	FBgn0013773
mei-P26	FBgn0026206	alpha-	FBgn0030007	TyrRS	FBgn0027080

		PheRS			
CG17202	FBgn0038043	l(3)72Dp	FBgn0263607	REG	FBgn0029133
CG5955	FBgn0036997	Crz	FBgn0013767	Tspo	FBgn0031263
Snap24	FBgn0266720	CG33296	FBgn0053296	mRpL51	FBgn0032053
CG3634	FBgn0037026	inaC	FBgn0004784	CG10340	FBgn0022344
CG11137	FBgn0037199	Taldo	FBgn0023477	nonA-l	FBgn0015520
eIF2D	FBgn0041588	CG11089	FBgn0039241	CG2736	FBgn0035090
Paf-AHalpha	FBgn0025809	CG17765	FBgn0033529	CG10932	FBgn0029969
PIG-T	FBgn0030035	Echs1	FBgn0033879	Pdh	FBgn0011693
beta-Spec	FBgn0250788	Cyp1	FBgn0004432	atk	FBgn0036995
MFS3	FBgn0031307	eIF4B	FBgn0020660	Unr	FBgn0263352
U2af38	FBgn0017457	CG2862	FBgn0031459	RpS9	FBgn0010408
His3.3B	FBgn0004828	Bub3	FBgn0025457	CG10799	FBgn0033821
CG31650	FBgn0031673	Ctr9	FBgn0035205	mt:ND4L	FBgn0013683
CG12093	FBgn0035372	CG2918	FBgn0023529	RpS14a	FBgn0004403
Tsp42Ej	FBgn0033132	Rab21	FBgn0039966	ND-20	FBgn0030718
amon	FBgn0023179	7B2	FBgn0041707	RpII140	FBgn0262955
CG10565	FBgn0037051	AOX1	FBgn0267408	RpS5a	FBgn0002590
Xpac	FBgn0004832	CG3246	FBgn0031538	CG42329	FBgn0259229
CG1983	FBgn0039751	GNBP2	FBgn0040322	Dhpr	FBgn0035964
Sec22	FBgn0260855	mRpL23	FBgn0035335	CG18302	FBgn0032266
ND-51	FBgn0031771	mRpL2	FBgn0036135	Galk	FBgn0263199
Ccm3	FBgn0038331	CG34166	FBgn0085195	pug	FBgn0020385
Pgam5	FBgn0023517	CG10672	FBgn0035588	Npc2g	FBgn0039800
Cyp9f2	FBgn0038037	eIF2beta	FBgn0004926	GNBP-like3	FBgn0034511
lncRNA:CR31451	FBgn0051451	Mat1	FBgn0024956	GstE6	FBgn0063494
bsf	FBgn0032679	CR32745	FBgn0052745	Tctp	FBgn0037874
CG10226	FBgn0035695	CG5849	FBgn0038897	mt:ND2	FBgn0013680
Rnp4F	FBgn0014024	Hsp60A	FBgn0015245	CG8461	FBgn0038235
D2hgdh	FBgn0023507	CG14440	FBgn0029894	Ms	FBgn0011581
euc	FBgn0038665	Ugt35a	FBgn0026315	CG44247	FBgn0265182
CG18048	FBgn0037435	Idh	FBgn0001248	CG17928	FBgn0032603
MtnA	FBgn0002868	Parg	FBgn0023216	Dim1	FBgn0031601
CG16743	FBgn0032322	Bap111	FBgn0030093	Nplp2	FBgn0040813
trem	FBgn0038767	CG31918	FBgn0031678	CG7322	FBgn0030968
CG3792	FBgn0031662	ATPsynE	FBgn0038224	Gart	FBgn0000053
Gfat2	FBgn0039580	eIF3i	FBgn0015834	CG13364	FBgn0026879
CG9231	FBgn0036887	Rop	FBgn0004574	Arr1	FBgn0000120
Neos	FBgn0024542	phu	FBgn0043791	Ahcy	FBgn0014455
ltl	FBgn0052372	Obp19d	FBgn0011280	IscU	FBgn0037637

GstZ2	FBgn0037697	CG16711	FBgn0036032	Ptpa	FBgn0016698
GAA1	FBgn0029818	Cyp9b2	FBgn0015039	jdp	FBgn0027654
mRpL37	FBgn0261380	Ssb-c31a	FBgn0015299	Trissin	FBgn0038343
EbpIII	FBgn0011695	sPLA2	FBgn0033170	Cpr72Ec	FBgn0036619
RecQ5	FBgn0027375	Npc2h	FBgn0039801	eEF1delta	FBgn0032198
levy	FBgn0034877	ox	FBgn0011227	mt:ATPase6	FBgn0013672
ATPsynbet a	FBgn0010217	Psf3	FBgn0030196	CG32278	FBgn0052278
lncRNA:CR 44832	FBgn0266095	CG10333	FBgn0032690	IM23	FBgn0034328
Orcokinin	FBgn0034935	lost	FBgn0263594	Gnmt	FBgn0038074
betaggt-II	FBgn0028970	ecd	FBgn0000543	CG4598	FBgn0032160
Hsc70-1	FBgn0001216	Ance-4	FBgn0033366	Nup62	FBgn0034118
mRpL12	FBgn0011787	mago	FBgn0002736	CG10621	FBgn0032726
Cyt-c1	FBgn0035600	cactin	FBgn0031114	Hacd1	FBgn0032394
Nep1	FBgn0029843	RIOK2	FBgn0039306	CG30151	FBgn0050151
Lsp2	FBgn0002565	mRpS2	FBgn0031639	CG3902	FBgn0036824
CG13920	FBgn0025712	CG9391	FBgn0037063	Cpr65Au	FBgn0042119
CG12343	FBgn0033556	Rab18	FBgn0015794	CG14989	FBgn0035495
CG10444	FBgn0034494	ifc	FBgn0001941	Vhl	FBgn0041174
CG3704	FBgn0040346	Gapdh1	FBgn0001091	CG13055	FBgn0036583
CG4577	FBgn0031306	Pcyt2	FBgn0035231	CG2604	FBgn0037298
Fis1	FBgn0039969	CG6834	FBgn0037935	CG13631	FBgn0040600
beag	FBgn0037660	CG32075	FBgn0052075	CG6712	FBgn0032408
CG13404	FBgn0030559	CG3803	FBgn0034938	Desat1	FBgn0086687
CG9034	FBgn0040931	ND-75	FBgn0017566	boca	FBgn0004132
Ktl	FBgn0038839	mEFTs	FBgn0032646	Ugt86Da	FBgn0040259
CG9147	FBgn0031774	Gas41	FBgn0031873	CG7135	FBgn0030895
RpS23	FBgn0033912	CG13390	FBgn0032031	Obp57a	FBgn0043535
spidey	FBgn0029975	14-3-3zeta	FBgn0004907	CG11550	FBgn0039864
CG2680	FBgn0024995	CG9396	FBgn0037714	CG4278	FBgn0014092
CG2608	FBgn0032870	lsn	FBgn0260940	GstD11	FBgn0038029
Zw10	FBgn0004643	CG31548	FBgn0051548	CG7900	FBgn0037548
eIF3g1	FBgn0029629	CR43170	FBgn0262789	Cyp6a21	FBgn0033981
RpL26	FBgn0036825	Cyp6a13	FBgn0033304	CG7810	FBgn0032017
x16	FBgn0028554	JTBR	FBgn0025820	Cyp4d21	FBgn0031925
CG11601	FBgn0031244	Cyp311a1	FBgn0030367	CG6067	FBgn0029828
l(2)09851	FBgn0022288	CG18003	FBgn0061356	ThrRS	FBgn0027081
CG30431	FBgn0050431	PH4alphaN E1	FBgn0039780	CG9510	FBgn0032076
CG15695	FBgn0038832	Obp56g	FBgn0034474	CG4250	FBgn0034761
Pka-R2	FBgn0022382	mt:ND4	FBgn0262952	CG3823	FBgn0029863

JMJD7	FBgn0036366	RpS8	FBgn0039713	CG14661	FBgn0037288
Gba1b	FBgn0051414	CG5778	FBgn0038930	CG12239	FBgn0029810
CG14805	FBgn0023514	ND-24	FBgn0030853	CG9498	FBgn0031801
CG12895	FBgn0033523	CG3847	FBgn0029867	Iris	FBgn0031305
Gasz	FBgn0033273	Pfdn4	FBgn0035603	Cyp6g1	FBgn0025454
COX5A	FBgn0019624	RpL5	FBgn0064225	awd	FBgn0000150
Cyp305a1	FBgn0036910	Mip	FBgn0036713	ninaE	FBgn0002940
CG2004	FBgn0030060	rad50	FBgn0034728	CG14277	FBgn0032008
Dek	FBgn0026533	vig2	FBgn0046214	Tsf1	FBgn0022355
CG4612	FBgn0035016	bcn92	FBgn0013432	CG15201	FBgn0030272
CG5022	FBgn0032225	CG11349	FBgn0035550	NimB2	FBgn0028543
fbp	FBgn0032820	CG11200	FBgn0034500	Jheh2	FBgn0034405
RpL23	FBgn0010078	prt	FBgn0043005	AstC	FBgn0032336
Uba3	FBgn0263697	CG6693	FBgn0037878	Adgf-A	FBgn0036752
CG17549	FBgn0032774	GstE2	FBgn0063498	CG18067	FBgn0034512
comt	FBgn0000346	CG32726	FBgn0052726	Cyp9h1	FBgn0033775
Tep4	FBgn0041180	St1	FBgn0034887	CG7789	FBgn0039698
dnk	FBgn0022338	CG11417	FBgn0024364	CG32039	FBgn0052039
ringer	FBgn0266417	Eno	FBgn0000579	to	FBgn0039298
Elal	FBgn0013949	P5cr	FBgn0015781	Obp56h	FBgn0034475
CG6961	FBgn0030959	CG6178	FBgn0039156	CG13365	FBgn0029529
AP-2sigma	FBgn0043012	smt3	FBgn0264922	spirit	FBgn0030051
Arpc1	FBgn0001961	TfIIS	FBgn0010422	CG1441	FBgn0033464
Rh6	FBgn0019940	CG5114	FBgn0036460	CG1461	FBgn0030558
geminin	FBgn0033081	CG13397	FBgn0014417	His4r	FBgn0013981
CG8206	FBgn0030679	CCT6	FBgn0027329	Cyt-b5-r	FBgn0000406
CG12170	FBgn0037356	CG11407	FBgn0038733	Jheh1	FBgn0010053
Fkbp12	FBgn0013954	CG5377	FBgn0038974	CG4716	FBgn0033820
lncRNA:CR 45388	FBgn0266937	BEAF-32	FBgn0015602	GstE3	FBgn0063497
PCB	FBgn0027580	mt:ND5	FBgn0013684	CG13618	FBgn0039203
wrapper	FBgn0025878	CG14818	FBgn0026088	CG6910	FBgn0036262
Hr3	FBgn0000448	RpS18	FBgn0010411	Listericin	FBgn0033593
p23	FBgn0037728	Arc42	FBgn0038742	CG16758	FBgn0035348
Non1	FBgn0028473	ND-ASHI	FBgn0029888	CG7296	FBgn0032283
mRpL24	FBgn0031651	Pfdn1	FBgn0031776	CG9759	FBgn0038160
viaf	FBgn0036237	mRpS11	FBgn0038474	CG10433	FBgn0034638
CG13360	FBgn0025620	pnut	FBgn0013726	CG5773	FBgn0034290
RpL34a	FBgn0039406	bic	FBgn0000181	CG17108	FBgn0032285
CG43324	FBgn0263029	Cyp6a17	FBgn0015714	CG6503	FBgn0040606
yps	FBgn0022959	CG10747	FBgn0032845	CG13833	FBgn0039040
mRpS29	FBgn0034727	Top2	FBgn0003732	CG6870	FBgn0032652

CG12375	FBgn0031987	CG17324	FBgn0027074	CG9928	FBgn0032472
CG9577	FBgn0031092	IM1	FBgn0034329	CG4000	FBgn0038820
GCC88	FBgn0037881	Pfas	FBgn0000052	apolpp	FBgn0087002

Appendix I Differentially accessible genes between juvenile and mature flies in controls and Bap60-KD MBs

More accessible genes juvenile control compared to mature control					
Gene Symbol	Flybase ID	Gene Symbol	Flybase ID	Gene Symbol	Flybase ID
DAAM	FBgn0025641	Pfrx	FBgn0027621	nAChRbeta1	FBgn0000038
NA	FBgn0264914	mmd	FBgn0259110	Drep3	FBgn0028407
pdgy	FBgn0027601	CG14478	FBgn0028953	Bsg	FBgn0261822
NA	FBgn0262437	Dyrk2	FBgn0016930	CG34300	FBgn0085329
ninaB	FBgn0002937	wnd	FBgn0036896	Shroom	FBgn0085408
spir	FBgn0003475	Ars2	FBgn0033062	jumu	FBgn0015396
CG44774	FBgn0266000	Dop2R	FBgn0053517	CG9837	FBgn0037635
CG5254	FBgn0040383	croc	FBgn0014143	CG5789	FBgn0039207
NA	FBgn0265830	CG17574	FBgn0033777	Hr38	FBgn0014859
fs(1)h	FBgn0004656	dl	FBgn0260632	Rpb5	FBgn0033571
Proc-R	FBgn0029723	toc	FBgn0015600	CG11362	FBgn0034737
puc	FBgn0243512	SkpA	FBgn0025637	CG42671	FBgn0261553
NA	FBgn0264678	CG14234	FBgn0031065	trv	FBgn0085391
bru1	FBgn0000114	msi	FBgn0011666	CG9990	FBgn0039594
NA	FBgn0265866	alph	FBgn0086361	CG15529	FBgn0039748
Dys	FBgn0260003	shn	FBgn0003396	CG34357	FBgn0085386
oc	FBgn0004102	NA	FBgn0003374	psq	FBgn0263102
CG44815	FBgn0266050	Prat2	FBgn0041194	CG14186	FBgn0036935
CG12986	FBgn0030868	ph-p	FBgn0004861	nst	FBgn0036298
Myd88	FBgn0033402	brk	FBgn0024250	pigs	FBgn0029881
CG14441	FBgn0029895	CG8613	FBgn0033924	CG42748	FBgn0261802
CG11138	FBgn0030400	NA	FBgn0266155	puc	FBgn0243512
CG32698	FBgn0052698	NA	FBgn0052449	axo	FBgn0262870
CG42514	FBgn0260388	CG14491	FBgn0034284	HmgZ	FBgn0010228
NA	FBgn0266892	Liprin-gamma	FBgn0034720	Oaz	FBgn0284250
Strn-Mlck	FBgn0265045	ZnT63C	FBgn0035432	NA	FBgn0263539
NA	FBgn0263458	WASp	FBgn0024273	kis	FBgn0266557
Cyp6v1	FBgn0031126	modSP	FBgn0051217	AstC-R1	FBgn0036790
Syt12	FBgn0261085	Nna1	FBgn0265726	stai	FBgn0266521

inc	FBgn0025394	tara	FBgn0040071	Ktl	FBgn0038839
mgl	FBgn0261260	RhoGAPp190	FBgn0026375	RpS21	FBgn0015521
Lsd-2	FBgn0030608	NK7.1	FBgn0024321	NA	FBgn0265590
NA	FBgn0267314	CG8177	FBgn0036043	glec	FBgn0015229
MFS10	FBgn0030452	Wnt5	FBgn0010194	EndoB	FBgn0034433
hwt	FBgn0264542	NA	FBgn0263581	NA	FBgn0262993
brk	FBgn0024250	aralar1	FBgn0028646	PGRP-LA	FBgn0035975
Fas2	FBgn0000635	Eip63F-1	FBgn0004910	zfh2	FBgn0004607
NA	FBgn0267228	Sik3	FBgn0262103	mth	FBgn0023000
CG32407	FBgn0052407	Nmdar2	FBgn0053513	CdsA	FBgn0010350
dnc	FBgn0000479	chn	FBgn0015371	jeb	FBgn0086677
ct	FBgn0004198	Hs3st-B	FBgn0031005	CG44837	FBgn0266100
saturn	FBgn0052141	Usp2	FBgn0031187	NA	FBgn0265913
modSP	FBgn0051217	tou	FBgn0033636	CG8740	FBgn0027585
CG9650	FBgn0029939	CG42795	FBgn0261928	CG30377	FBgn0050377
CG13323	FBgn0033788	Sox102F	FBgn0039938	NA	FBgn0264470
Sp1	FBgn0020378	Ufd4	FBgn0032208	Shawl	FBgn0085395
CG44837	FBgn0266100	CG6059	FBgn0039491	bol	FBgn0011206
CG3632	FBgn0030735	kek5	FBgn0031016	REPTOR	FBgn0039209
moody	FBgn0025631	NA	FBgn0262400	NA	FBgn0265931
CG40485	FBgn0069973	CG9331	FBgn0032889	Eip93F	FBgn0264490
Hcf	FBgn0039904	Hr4	FBgn0264562	Acsl	FBgn0263120
unc-4	FBgn0024184	Act5C	FBgn0000042	CG44838	FBgn0266101
Ubi-p5E	FBgn0086558	for	FBgn0000721	akirin	FBgn0082598
CG8306	FBgn0034142	IntS6	FBgn0261383	Unc-115a	FBgn0051352
Rala	FBgn0015286	CG4502	FBgn0031896	CG5830	FBgn0036556
CG5160	FBgn0031906	CG32647	FBgn0052647	CG13255	FBgn0040636
NA	FBgn0051588	Men-b	FBgn0029155	dunk	FBgn0083973
CG10960	FBgn0036316	l(2)37Cg	FBgn0086447	fax	FBgn0014163
NA	FBgn0265691	CG15550	FBgn0039811	futsch	FBgn0259108
CG6870	FBgn0032652	caup	FBgn0015919	CG5890	FBgn0039380
bun	FBgn0259176	mRpS5	FBgn0044510	Eip74EF	FBgn0000567
ClC-a	FBgn0051116	inc	FBgn0025394	Syp	FBgn0038826
shakB	FBgn0085387	NA	FBgn0011879	CG34384	FBgn0085413
nAChRalpha7	FBgn0086778	Pkn	FBgn0020621	CG42750	FBgn0261804
Tango13	FBgn0086674	siz	FBgn0026179	tacc	FBgn0026620
CG9921	FBgn0030743	Pdi	FBgn0014002	Best2	FBgn0035696
NA	FBgn0266618	Ran	FBgn0020255	CG12605	FBgn0035481
Hers	FBgn0052529	Archease	FBgn0038893	Df31	FBgn0022893
Fur2	FBgn0004598	Got2	FBgn0001125	CG12262	FBgn0035811
NA	FBgn0051840	ci	FBgn0004859	NA	FBgn0263332

NA	FBgn0265924	NA	FBgn0263626	CG42674	FBgn0261556
NA	FBgn0267169	CG12402	FBgn0038202	TRAM	FBgn0040340
HmgZ	FBgn0010228	CG45075	FBgn0266445	NA	FBgn0284419
Ptpmeg	FBgn0261985	NA	FBgn0267729	wapl	FBgn0004655
CG6379	FBgn0029693	CG42663	FBgn0261545	EcR	FBgn0000546
Ten-a	FBgn0267001	CG32547	FBgn0052547	gem	FBgn0050011
gce	FBgn0261703	NA	FBgn0264787	Trl	FBgn0013263
dnc	FBgn0000479	Inos	FBgn0025885	Csp	FBgn0004179
CG5004	FBgn0260748	NA	FBgn0011934	Cirl	FBgn0033313
Act57B	FBgn0000044	NA	FBgn0267162	ChAT	FBgn0000303
NK7.1	FBgn0024321	beta-Spec	FBgn0250788	dunk	FBgn0083973
CkIalpha	FBgn0015024	ci	FBgn0004859	CG6163	FBgn0036155
CG18747	FBgn0042104	Prat2	FBgn0041194	Argk	FBgn0000116
cv	FBgn0000394	hiw	FBgn0030600	Mekk1	FBgn0024329
hth	FBgn0001235	CG32758	FBgn0052758	MESR6	FBgn0036846
CG6435	FBgn0034165	Vha16-1	FBgn0262736	CG13594	FBgn0035041
csw	FBgn0000382	kay	FBgn0001297	CG32052	FBgn0044328
ras	FBgn0003204	CG14006	FBgn0031733	bru3	FBgn0264001
NA	FBgn0265908	NA	FBgn0052690	corn	FBgn0259173
ct	FBgn0004198	gol	FBgn0004919	CG4050	FBgn0020312
bdl	FBgn0028482	CG42402	FBgn0259821	Ada2b	FBgn0037555
CG11448	FBgn0024985	Neb-cGP	FBgn0083167	Or67d	FBgn0036080
lawc	FBgn0262976	sbb	FBgn0285917	CG33169	FBgn0053169
btd	FBgn0000233	Trf4-1	FBgn0030049	fig	FBgn0039694
sd	FBgn0003345	Lnk	FBgn0028717	Snoo	FBgn0085450
cpo	FBgn0263995	rho	FBgn0004635	CG4729	FBgn0036623
Tlk	FBgn0283657	mub	FBgn0262737	spab	FBgn0033358
nej	FBgn0261617	bbx	FBgn0024251	mura	FBgn0037705
CG1124	FBgn0037290	Nedd4	FBgn0259174	CG10283	FBgn0032681
tsh	FBgn0003866	beat-Va	FBgn0038087	GlcAT-P	FBgn0036144
fend	FBgn0030090	CG14153	FBgn0036094	uzip	FBgn0004055
AMPdeam	FBgn0052626	GlyP	FBgn0004507	eg	FBgn0000560
oc	FBgn0004102	smt3	FBgn0264922	Kdm2	FBgn0037659
mGluR	FBgn0019985	CG32767	FBgn0052767	mspo	FBgn0020269
ct	FBgn0004198	Ca-alpha1T	FBgn0264386	CG8180	FBgn0034021
rst	FBgn0003285	CG43245	FBgn0262890	Teh1	FBgn0037766
Ubx	FBgn0003944	Syn2	FBgn0034135	aru	FBgn0029095
Pp2C1	FBgn0022768	NA	FBgn0052285	MFS14	FBgn0010651
sgg	FBgn0003371	NA	FBgn0052207	sol	FBgn0003464
su(sable)	FBgn0003575	Amun	FBgn0030328	CG1648	FBgn0033446
CG1791	FBgn0030163	Ptp99A	FBgn0004369	Atg1	FBgn0260945

bab2	FBgn0025525	Eip63F-1	FBgn0004910	Octbeta1R	FBgn0038980
santa-maria	FBgn0025697	ATP8B	FBgn0037989	rdx	FBgn0264493
cib	FBgn0026084	SPoCk	FBgn0052451	bark	FBgn0031571
Clk	FBgn0023076	NA	FBgn0004190	Ih	FBgn0263397
Ubr1	FBgn0030809	Hipk	FBgn0035142	mib1	FBgn0263601
CG7763	FBgn0040503	CG32017	FBgn0052017	NA	FBgn0265444
CG8180	FBgn0034021	CG10651	FBgn0032853	unc-13-4A	FBgn0035756
CG5778	FBgn0038930	CG11122	FBgn0030266	Rph	FBgn0030230
CG12065	FBgn0030052	Eip74EF	FBgn0000567	cl	FBgn0000318
sd	FBgn0003345	RhoGAP71E	FBgn0036518	Rfx	FBgn0020379
CG9413	FBgn0030574	CG44439	FBgn0265632	bun	FBgn0259176
sens-2	FBgn0051632	NA	FBgn0266831	NA	FBgn0052218
SCOT	FBgn0035298	DOR	FBgn0035542	nub	FBgn0085424
NA	FBgn0264678	CG2201	FBgn0032955	CG4538	FBgn0038745
rudhira	FBgn0266019	CG9164	FBgn0030634	HGTX	FBgn0040318
His3.3B	FBgn0004828	nudC	FBgn0021768	Gel	FBgn0010225
sr	FBgn0003499	futsch	FBgn0259108	NA	FBgn0051143
NA	FBgn0263532	capu	FBgn0000256	sano	FBgn0034408
Mnt	FBgn0023215	Unc-76	FBgn0040395	Top3beta	FBgn0026015
disco	FBgn0000459	NA	FBgn0263345	IA-2	FBgn0031294
CG44774	FBgn0266000	CG12054	FBgn0039831	Swip-1	FBgn0032731
Mnt	FBgn0023215	Pdk1	FBgn0020386	THADA	FBgn0031077
Pino	FBgn0016926	Zasp52	FBgn0265991	NA	FBgn0052330
NA	FBgn0040569	NA	FBgn0267672	CG42321	FBgn0259221
Cyp6t1	FBgn0031182	Ubqn	FBgn0031057	Irc	FBgn0038465
NFAT	FBgn0030505	Src42A	FBgn0264959	jdp	FBgn0027654
CHES-1-like	FBgn0029504	NA	FBgn0265692	NA	FBgn0264505
dnc	FBgn0000479	CG13168	FBgn0033705	CG5674	FBgn0032656
trh	FBgn0262139	cbt	FBgn0043364	sif	FBgn0085447
Rpn13R	FBgn0029745	CG6023	FBgn0030912	nAChRalpha6	FBgn0032151
Nipsnap	FBgn0030724	Rab9Db	FBgn0030221	CG31038	FBgn0051038
CG18622	FBgn0038460	Rdh	FBgn0064227	Sox21a	FBgn0036411
sim	FBgn0004666	Bx	FBgn0265598	CaMKII	FBgn0264607
nod	FBgn0002948	Eip93F	FBgn0264490	CngA	FBgn0261612
Rbcn-3B	FBgn0023510	Pde8	FBgn0266377	cg	FBgn0000289
su(f)	FBgn0003559	wdb	FBgn0027492	Ars2	FBgn0033062
CG11630	FBgn0032964	Xrp1	FBgn0261113	NA	FBgn0267155
Inx2	FBgn0027108	Pdh	FBgn0011693	CG32264	FBgn0052264
CCHa2-R	FBgn0033058	CG10038	FBgn0038013	CG43347	FBgn0263072
noc	FBgn0005771	Sesn	FBgn0034897	tara	FBgn0040071
RhoGAP19D	FBgn0031118	CG10651	FBgn0032853	Sdc	FBgn0010415

Klp98A	FBgn0004387	zfh2	FBgn0004607	NA	FBgn0266851
CG9932	FBgn0262160	NA	FBgn0264787	Lk6	FBgn0017581
CG5445	FBgn0030838	CG17839	FBgn0036454	CG3918	FBgn0029873
CG32066	FBgn0052066	CG43231	FBgn0262876	CG10734	FBgn0034082
Syt12	FBgn0261085	CG18472	FBgn0039463	NA	FBgn0265470
NA	FBgn0264390	CG43901	FBgn0264502	CG34398	FBgn0085427
NA	FBgn0011848	psq	FBgn0263102	Ank2	FBgn0261788
CG7280	FBgn0030966	fok	FBgn0263773	Hr4	FBgn0264562
ric8a	FBgn0028292	lace	FBgn0002524	BCL7-like	FBgn0026149
nub	FBgn0085424	sdk	FBgn0021764	NA	FBgn0262898
NA	FBgn0267154	gw	FBgn0051992	NA	FBgn0011890
rut	FBgn0003301	CG43427	FBgn0263346	CG9328	FBgn0032886
l(1)G0469	FBgn0040153	crp	FBgn0001994	Sox14	FBgn0005612
CG17572	FBgn0032753	CG11825	FBgn0033519	nub	FBgn0085424
B-H2	FBgn0004854	RpL38	FBgn0040007	CG42394	FBgn0259740
CG15312	FBgn0030174	EcR	FBgn0000546	trv	FBgn0085391
hth	FBgn0001235	NA	FBgn0267600	CG43102	FBgn0262562
toy	FBgn0019650	Top1	FBgn0004924	SNF4Agamma	FBgn0264357
NA	FBgn0264787	Pde8	FBgn0266377	CG43236	FBgn0262881
en	FBgn0000577	CG18265	FBgn0036725	mei-W68	FBgn0002716
NA	FBgn0267744	CG6218	FBgn0038321	ref(2)P	FBgn0003231
DIP1	FBgn0024807	mAChR-A	FBgn0000037	pst	FBgn0035770
CG32196	FBgn0052196	Mnt	FBgn0023215	CG11873	FBgn0039633
CG34039	FBgn0054039	vri	FBgn0016076	Svil	FBgn0266696
pum	FBgn0003165	CG11883	FBgn0033538	msn	FBgn0010909
CG4678	FBgn0030778	Slob	FBgn0264087	Ace	FBgn0000024
NA	FBgn0265830	NA	FBgn0266844	CG10960	FBgn0036316
bor	FBgn0040237	CG5830	FBgn0036556	NA	FBgn0267131
sgg	FBgn0003371	CG14212	FBgn0031045	beat-VII	FBgn0250908
Sxl	FBgn0264270	NA	FBgn0027493	Fas1	FBgn0285925
sns	FBgn0024189	r-cup	FBgn0031142	Raf	FBgn0003079
CG16721	FBgn0029820	spen	FBgn0016977	CG6966	FBgn0038286
gol	FBgn0004919	AspRS-m	FBgn0051739	dsf	FBgn0015381
nej	FBgn0261617	corto	FBgn0010313	NA	FBgn0011974
PGRP-LE	FBgn0030695	Dll	FBgn0000157	HmgD	FBgn0004362
NA	FBgn0263379	bel	FBgn0263231	CG10924	FBgn0034356
NA	FBgn0265830	NA	FBgn0264857	CG31108	FBgn0051108
Tlk	FBgn0283657	CG4679	FBgn0033816	CG42878	FBgn0262170
RyR	FBgn0011286	Tlk	FBgn0283657	DNApol-iota	FBgn0037554
NA	FBgn0011954	Dhit	FBgn0028743	CG15233	FBgn0033076
fs(1)h	FBgn0004656	Spn28Db	FBgn0053121	Calx	FBgn0013995

CG17027	FBgn0036553	NA	FBgn0267099	plum	FBgn0039431
chrb	FBgn0036165	Hnf4	FBgn0004914	CG8788	FBgn0028955
CG46301	FBgn0283651	Cyp6a13	FBgn0033304	CG5946	FBgn0036211
AP-2alpha	FBgn0264855	ATPsynbeta	FBgn0010217	MEP-1	FBgn0035357
Sh	FBgn0003380	NA	FBgn0262315	NA	FBgn0052218
N	FBgn0004647	CG14810	FBgn0029589	Pi3K21B	FBgn0020622
sdt	FBgn0261873	drongo	FBgn0020304	CG10019	FBgn0031568
bin3	FBgn0263144	Ten-m	FBgn0004449	CG1607	FBgn0039844
Neu2	FBgn0037085	Pkg21D	FBgn0000442	CG41099	FBgn0039955
NA	FBgn0266355	CG32137	FBgn0052137	CG42524	FBgn0260429
fs(1)h	FBgn0004656	CG4199	FBgn0025628	Ptx1	FBgn0020912
CBP	FBgn0026144	Socs16D	FBgn0030869	nvy	FBgn0005636
CG31997	FBgn0051997	NA	FBgn0051331	Egfr	FBgn0003731
CG12576	FBgn0031190	rad	FBgn0265597	CG10098	FBgn0037472
CG42594	FBgn0260971	NA	FBgn0266835	CG31145	FBgn0051145
how	FBgn0264491	fz	FBgn0001085	Pdp1	FBgn0016694
mamo	FBgn0267033	CG5355	FBgn0032242	sea	FBgn0037912
CG4927	FBgn0034139	Nfl	FBgn0042696	CG14082	FBgn0036851
NA	FBgn0266389	Cdc42	FBgn0010341	Gfrl	FBgn0262869
bi	FBgn0000179	Syn1	FBgn0037130	sas	FBgn0002306
NA	FBgn0265830	tio	FBgn0028979	Picot	FBgn0024315
vn	FBgn0003984	nvy	FBgn0005636	NA	FBgn0011849
pnt	FBgn0003118	chinmo	FBgn0086758	CG5973	FBgn0031914
Imp	FBgn0285926	tx	FBgn0263118	per	FBgn0003068
Mnt	FBgn0023215	Ars2	FBgn0033062	NA	FBgn0267668
CG32521	FBgn0052521	CG33262	FBgn0053262	simj	FBgn0010762
Psc	FBgn0005624	bru3	FBgn0264001	Snoo	FBgn0085450
Ac13E	FBgn0022710	NA	FBgn0267159	chn	FBgn0015371
spen	FBgn0016977	NA	FBgn0266805	CG18467	FBgn0034218
Pfrx	FBgn0027621	Tip60	FBgn0026080	CG42544	FBgn0260713
CG42389	FBgn0259735	CG15096	FBgn0034394	spir	FBgn0003475
elav	FBgn0260400	NA	FBgn0266308	jim	FBgn0027339
IM3	FBgn0040736	larp	FBgn0261618	Oatp58Dc	FBgn0034716
Tlk	FBgn0283657	gro	FBgn0001139	RasGAP1	FBgn0004390
slgA	FBgn0003423	Fer1	FBgn0037475	Glut4EF	FBgn0267336
NA	FBgn0267820	alpha-Est7	FBgn0015575	KrT95D	FBgn0020647
CG43736	FBgn0263993	Sur-8	FBgn0038504	Diap1	FBgn0260635
NA	FBgn0266679	Tob	FBgn0028397	hwt	FBgn0264542
Trf2	FBgn0261793	obst-B	FBgn0027600	mrj	FBgn0034091
klu	FBgn0013469	NA	FBgn0259996	CG10600	FBgn0032717
Rab32	FBgn0002567	NA	FBgn0086659	alphaKap4	FBgn0035657

CG7378	FBgn0030976	Eaat1	FBgn0026439	Sap130	FBgn0262714
CG4842	FBgn0036620	Hers	FBgn0052529	GlyT	FBgn0034911
Sh	FBgn0003380	CG2082	FBgn0027608	CG18371	FBgn0033893
CG32832	FBgn0052832	Dlic	FBgn0030276	mub	FBgn0262737
Dyrk2	FBgn0016930	Cngl	FBgn0263257	Hus1-like	FBgn0026417
ph-d	FBgn0004860	CG15630	FBgn0031627	CG7971	FBgn0035253
mnb	FBgn0259168	KCNQ	FBgn0033494	Clc	FBgn0024814
CG42637	FBgn0261360	NA	FBgn0262440	CG8321	FBgn0033677
bi	FBgn0000179	CG12896	FBgn0033521	CG43351	FBgn0263083
salm	FBgn0261648	CG11023	FBgn0031208	cmpy	FBgn0037015
tou	FBgn0033636	Slob	FBgn0264087	Rdh	FBgn0064227
shakB	FBgn0085387	alpha-Est10	FBgn0015569	CG10055	FBgn0037482
Pkc53E	FBgn0003091	Abd-B	FBgn0000015	Cnx99A	FBgn0015622
NA	FBgn0267259	NA	FBgn0011881	Ptp61F	FBgn0267487
pb	FBgn0051481	CG14823	FBgn0035734	soti	FBgn0038225
Klc	FBgn0010235	Adar	FBgn0026086	Rtnl1	FBgn0053113
RhoGAP18B	FBgn0261461	CG42540	FBgn0260657	sala	FBgn0003313
ctrip	FBgn0260794	mahe	FBgn0029979	JIL-1	FBgn0020412
CG14810	FBgn0029589	NA	FBgn0267579	RpS11	FBgn0033699
fus	FBgn0023441	CG33798	FBgn0053798	CG45093	FBgn0266526
CG31998	FBgn0051998	NA	FBgn0266414	brat	FBgn0010300
CG17778	FBgn0023534	NA	FBgn0264703	dati	FBgn0262636
NA	FBgn0264678	chic	FBgn0000308	smal	FBgn0085409
Top1	FBgn0004924	Ids	FBgn0035445	CG17974	FBgn0034624
kirre	FBgn0028369	NA	FBgn0265792	Atet	FBgn0020762
Appl	FBgn0000108	DCP2	FBgn0036534	NLaz	FBgn0053126
nudC	FBgn0021768	CG42238	FBgn0250867	CG31688	FBgn0263355
Usp2	FBgn0031187	Sox102F	FBgn0039938	CG43335	FBgn0263040
NA	FBgn0011927	futsch	FBgn0259108	CG33640	FBgn0053640
NA	FBgn0051331	otp	FBgn0015524	NA	FBgn0028910
anne	FBgn0052000	CG12547	FBgn0250830	CG30389	FBgn0050389
nAChRalpha5	FBgn0028875	CG13526	FBgn0034774	NA	FBgn0267201
CG9932	FBgn0262160	CG6540	FBgn0030943	HnRNP-K	FBgn0267791
NA	FBgn0266750	CG5853	FBgn0032167	Ir56a	FBgn0050125
salm	FBgn0261648	CG31694	FBgn0051694	ZnT63C	FBgn0035432
bbx	FBgn0024251	ey	FBgn0005558	NA	FBgn0264438
ppk8	FBgn0052792	alpha-Est9	FBgn0015577	CG33640	FBgn0053640
CG18547	FBgn0037973	GC	FBgn0035245	Su(z)2	FBgn0265623
Ald	FBgn0000064	beat-Vb	FBgn0038092	spi	FBgn0005672
sw	FBgn0003654	pyx	FBgn0035113	NA	FBgn0267571
mol	FBgn0086711	CG5758	FBgn0032666	ATPsynG	FBgn0010612

kermit	FBgn0010504	l(3)neo38	FBgn0265276	Scgdelta	FBgn0025391
CG8034	FBgn0031011	Eip74EF	FBgn0000567	ST6Gal	FBgn0035050
car	FBgn0000257	sgl	FBgn0261445	CG44837	FBgn0266100
Adk3	FBgn0042094	Bx	FBgn0265598	fng	FBgn0011591
mirr	FBgn0014343	tara	FBgn0040071	CG11961	FBgn0034436
stnB	FBgn0016975	CG14434	FBgn0029915	Mef2	FBgn0011656
lawc	FBgn0262976	cic	FBgn0262582	sv	FBgn0005561
CG42673	FBgn0261555	Dp1	FBgn0027835	robl37BC	FBgn0028569
Takl2	FBgn0039015	B4	FBgn0023407	PRAS40	FBgn0267824
Mur2B	FBgn0025390	rdgC	FBgn0265959	Galphao	FBgn0001122
Spn77Ba	FBgn0262057	ths	FBgn0033652	Ssdp	FBgn0011481
CG11674	FBgn0030551	NA	FBgn0265591	hb	FBgn0001180
Nrg	FBgn0264975	NA	FBgn0264941	CG46301	FBgn0283651
NA	FBgn0267322	PlexB	FBgn0025740	CG30371	FBgn0050371
NA	FBgn0020556	vn	FBgn0003984	cpo	FBgn0263995
CG2865	FBgn0023526	Eip63E	FBgn0005640	ACC	FBgn0033246
nocte	FBgn0261710	CG14024	FBgn0031697	CG10510	FBgn0037059
esg	FBgn0001981	NA	FBgn0086080	Eip75B	FBgn0000568
RapGAP1	FBgn0264895	NA	FBgn0012018	CG1142	FBgn0037504
Nost	FBgn0259734	Mnt	FBgn0023215	CG7956	FBgn0038890
CG42741	FBgn0261705	Eph	FBgn0025936	Droj2	FBgn0038145
IM14	FBgn0067905	CG42831	FBgn0262020	CG5909	FBgn0039495
dac	FBgn0005677	fs(1)h	FBgn0004656	Pdp1	FBgn0016694
CrebB	FBgn0265784	KP78b	FBgn0026063	red	FBgn0285913
NA	FBgn0086667	Pp2C1	FBgn0022768	CG31191	FBgn0051191
Dys	FBgn0260003	NA	FBgn0265839	CG16791	FBgn0038881
Nplp1	FBgn0035092	bi	FBgn0000179	CG3394	FBgn0034999
Usp7	FBgn0030366	Cyp49a1	FBgn0033524	Hs3st-A	FBgn0053147
Rab3-GEF	FBgn0030613	Sap-r	FBgn0000416	pHCl-1	FBgn0264908
NA	FBgn0267781	trx	FBgn0003862	NA	FBgn0050298
bbx	FBgn0024251	CG12605	FBgn0035481	NA	FBgn0266768
fz4	FBgn0027342	NA	FBgn0261638	Rpn12R	FBgn0036465
NA	FBgn0265982	CG7971	FBgn0035253	NA	FBgn0263336
NA	FBgn0262290	bsk	FBgn0000229	CG13252	FBgn0037016
IM4	FBgn0040653	Drat	FBgn0033188	CG34114	FBgn0083950
tay	FBgn0260938	AhcyL2	FBgn0015011	drm	FBgn0024244
hid	FBgn0003997	brat	FBgn0010300	CASK	FBgn0013759
CG5937	FBgn0029834	NA	FBgn0261709	NUCB1	FBgn0052190
CG9380	FBgn0035094	beat-IIa	FBgn0038498	wdp	FBgn0034718
Tlk	FBgn0283657	Cad96Ca	FBgn0022800	Lac	FBgn0010238
CHES-1-like	FBgn0029504	Sema1b	FBgn0016059	Oseg2	FBgn0035317

shi	FBgn0003392	CG12484	FBgn0086604	NA	FBgn0262391
conu	FBgn0039994	REPTOR	FBgn0039209	RpL18A	FBgn0010409
mbt	FBgn0025743	dan	FBgn0039286	Pkc98E	FBgn0003093
sdt	FBgn0261873	Pdp1	FBgn0016694	CG42402	FBgn0259821
Eaf6	FBgn0035624	CG32982	FBgn0052982	lola	FBgn0283521
NA	FBgn0263492	CG40045	FBgn0058045	Strn-Mlck	FBgn0265045
Skeletor	FBgn0262717	CG15136	FBgn0032625	lig	FBgn0020279
alpha-Est8	FBgn0015576	CG4629	FBgn0031299	CG30497	FBgn0050497
CG9932	FBgn0262160	Rgl	FBgn0026376	CG17744	FBgn0035730
CG12772	FBgn0030055	fru	FBgn0004652	klar	FBgn0001316
nuf	FBgn0013718	NA	FBgn0263543	CG6225	FBgn0038072
CG18467	FBgn0034218	Fatp	FBgn0267828	CG7029	FBgn0039026
Lar	FBgn0000464	dunk	FBgn0083973	RhoGEF3	FBgn0264707
CG4230	FBgn0031683	Fur1	FBgn0004509	Tsp39D	FBgn0032943
NA	FBgn0266964	Mad	FBgn0011648	CG13894	FBgn0035157
ush	FBgn0003963	NA	FBgn0266822	oys	FBgn0033476
GlcAT-S	FBgn0032135	Rdl	FBgn0004244	east	FBgn0261954
CG9413	FBgn0030574	CG3638	FBgn0261444	sba	FBgn0016754
CG11294	FBgn0030058	tna	FBgn0026160	cv-c	FBgn0285955
CG12643	FBgn0040942	CG11145	FBgn0033168	NA	FBgn0052123
CG1998	FBgn0030485	zfh2	FBgn0004607	hdc	FBgn0010113
sim	FBgn0004666	mago	FBgn0002736	CG11357	FBgn0035558
CG6123	FBgn0030913	RluA-1	FBgn0051719	CG13723	FBgn0036705
Amun	FBgn0030328	chinmo	FBgn0086758	CG42637	FBgn0261360
CG12769	FBgn0033252	Exn	FBgn0261547	l(2)k14710	FBgn0021847
CG15894	FBgn0029864	CG9005	FBgn0033638	bwa	FBgn0045064
klu	FBgn0013469	Sh	FBgn0003380	tok	FBgn0004885
shep	FBgn0052423	Ets98B	FBgn0005659	pan	FBgn0085432
NA	FBgn0019661	Fbl6	FBgn0033609	Naa15-16	FBgn0031020
NA	FBgn0262897	Clk	FBgn0023076	Rbp	FBgn0262483
lawc	FBgn0262976	Swip-1	FBgn0032731	CG42523	FBgn0260428
Tlk	FBgn0283657	H15	FBgn0016660	bab1	FBgn0004870
CG42680	FBgn0261566	CG13639	FBgn0265266	da	FBgn0267821
CG1718	FBgn0031170	NA	FBgn0265586	Pi3K68D	FBgn0015278
raw	FBgn0003209	dpr13	FBgn0034286	GstE12	FBgn0027590
CG7530	FBgn0038256	fwe	FBgn0261722	CG14137	FBgn0036178
CG14441	FBgn0029895	NA	FBgn0263533	mor	FBgn0002783
opa	FBgn0003002	CG13653	FBgn0039288	CG43795	FBgn0264339
RhoGEF64C	FBgn0035574	psq	FBgn0263102	ASPP	FBgn0034606
NA	FBgn0019661	ctrip	FBgn0260794	CG6495	FBgn0027550
BTBD9	FBgn0030228	Gapdh2	FBgn0001092	bun	FBgn0259176

CG43897	FBgn0264489	Ets65A	FBgn0005658	CG42337	FBgn0259239
Svil	FBgn0266696	grp	FBgn0261278	CG30389	FBgn0050389
l(1)G0193	FBgn0027280	sim	FBgn0004666	Eaat2	FBgn0026438
Ih	FBgn0263397	CG4622	FBgn0035021	NA	FBgn0262331
NA	FBgn0266209	Teh3	FBgn0040697	mam	FBgn0002643
pnr	FBgn0003117	CG14434	FBgn0029915	crb	FBgn0259685
Smox	FBgn0025800	NA	FBgn0001079	Pep	FBgn0004401
esg	FBgn0001981	CG9649	FBgn0038211	Mctp	FBgn0034389
tim	FBgn0014396	CG7365	FBgn0036939	NA	FBgn0267203
rdhB	FBgn0038946	CG31689	FBgn0031449	CG15019	FBgn0035541
CG14411	FBgn0030582	ftz-f1	FBgn0001078	mei-S332	FBgn0002715
Octbeta2R	FBgn0038063	larp	FBgn0261618	mts	FBgn0004177
mthl10	FBgn0035132	BI-1	FBgn0035871	sqd	FBgn0263396
Svil	FBgn0266696	Corin	FBgn0033192	jeb	FBgn0086677
CG7120	FBgn0035888	CG6024	FBgn0036202	Dh31-R	FBgn0052843
CG34136	FBgn0083972	Den1	FBgn0033716	CG4036	FBgn0032149
CG32369	FBgn0052369	14-3-3zeta	FBgn0004907	Pax	FBgn0041789
Act5C	FBgn0000042	Vha100-2	FBgn0028670	chrb	FBgn0036165
luna	FBgn0040765	ari-2	FBgn0025186	CG6701	FBgn0033889
NA	FBgn0267559	Oatp74D	FBgn0036732	l(3)neo38	FBgn0265276
mrt	FBgn0039507	chinmo	FBgn0086758	Cam	FBgn0000253
UbcE2H	FBgn0029996	Trpgamma	FBgn0032593	par-1	FBgn0260934
NA	FBgn0259996	CG42492	FBgn0259994	Dop1R1	FBgn0011582
Rcd2	FBgn0037012	dop	FBgn0267390	CG17075	FBgn0031239
RpL37a	FBgn0030616	NA	FBgn0262447	dysc	FBgn0264006
CG2519	FBgn0037336	GPHR	FBgn0033995	Galphaq	FBgn0004435
NA	FBgn0263039	CG42492	FBgn0259994	pros	FBgn0004595
CG3655	FBgn0040397	X11Lbeta	FBgn0052677	beat-Vc	FBgn0038084
Su(z)2	FBgn0265623	Tab2	FBgn0086358	Galphao	FBgn0001122
CadN	FBgn0015609	NA	FBgn0000055	cnk	FBgn0021818
CG34253	FBgn0085282	Rab5	FBgn0014010	CG6191	FBgn0027581
SoxN	FBgn0029123	dpr16	FBgn0037295	Atpalpha	FBgn0002921
Bx	FBgn0265598	CG42389	FBgn0259735	Snoo	FBgn0085450
alpha-Est9	FBgn0015577	Snoo	FBgn0085450	Cdep	FBgn0265082
tj	FBgn0000964	CG12950	FBgn0037736	Gp150	FBgn0013272
nAChRalpha3	FBgn0015519	NA	FBgn0283547	Pak	FBgn0267698
CG1492	FBgn0030361	apt	FBgn0015903	CG11151	FBgn0030519
CG40178	FBgn0058178	NA	FBgn0086661	aop	FBgn0000097
CCKLR-17D3	FBgn0030954	NA	FBgn0050198	dpr19	FBgn0032233
CkIIbeta	FBgn0000259	hrg	FBgn0015949	NA	FBgn0263557
Eip75B	FBgn0000568	NA	FBgn0283551	l(1)G0156	FBgn0027291

CG1578	FBgn0030336	ru	FBgn0003295	Diap1	FBgn0260635
rudhira	FBgn0266019	CG42748	FBgn0261802	CG34429	FBgn0085458
CG9413	FBgn0030574	CG18467	FBgn0034218	Pka-R1	FBgn0259243
Reph	FBgn0021800	NA	FBgn0266991	lute	FBgn0262871
CG14275	FBgn0032022	RpLP2	FBgn0003274	tutl	FBgn0010473
PGRP-SC2	FBgn0043575	pdm3	FBgn0261588	CG11000	FBgn0263353
NA	FBgn0052218	CG32369	FBgn0052369	NA	FBgn0264880
bowl	FBgn0004893	Pde11	FBgn0085370	CG43066	FBgn0262476
srp	FBgn0003507	Ddr	FBgn0053531	fne	FBgn0086675
CG10924	FBgn0034356	NA	FBgn0264915	Dmtn	FBgn0037443
trn	FBgn0010452	Pde8	FBgn0266377	EcR	FBgn0000546
CG3703	FBgn0040348	ara	FBgn0015904	CG10384	FBgn0034731
5-HT2A	FBgn0087012	CAH2	FBgn0027843	NA	FBgn0262368
Cngl	FBgn0263257	Rbp6	FBgn0260943	tow	FBgn0035719
CG42700	FBgn0261611	lolal	FBgn0022238	CG18812	FBgn0042135
grn	FBgn0001138	CG9003	FBgn0033639	roq	FBgn0036621
hwt	FBgn0264542	Dif	FBgn0011274	numb	FBgn0002973
Eglp2	FBgn0034883	jing	FBgn0086655	Skadu	FBgn0259922
beta-Spec	FBgn0250788	sbb	FBgn0285917	arr	FBgn0000119
elav	FBgn0260400	betaTub56D	FBgn0284243	CG17508	FBgn0039970
mam	FBgn0002643	CG16771	FBgn0032779	Cul3	FBgn0261268
CG5708	FBgn0032196	CG6908	FBgn0037936	CG10413	FBgn0032689
spin	FBgn0086676	robo2	FBgn0002543	HnRNP-K	FBgn0267791
CG11138	FBgn0030400	qsm	FBgn0028622	Iris	FBgn0031305
PhKgamma	FBgn0011754	para	FBgn0285944	pros	FBgn0004595
pdm3	FBgn0261588	NA	FBgn0027493	Tsp42Ej	FBgn0033132
mlt	FBgn0265512	NA	FBgn0264857	NA	FBgn0265525
Cyp317a1	FBgn0033982	Frq1	FBgn0030897	TAF1B	FBgn0037792
CG9170	FBgn0030716	siz	FBgn0026179	CG7368	FBgn0036179
NA	FBgn0052127	sr	FBgn0003499	wun	FBgn0016078
CG34347	FBgn0085376	CG43231	FBgn0262876	CG11505	FBgn0035424
CG12395	FBgn0030722	NA	FBgn0265853	CG44098	FBgn0264907
Exn	FBgn0261547	Gug	FBgn0010825	NA	FBgn0284415
CG14810	FBgn0029589	Pka-R1	FBgn0259243	CG11486	FBgn0035397
Tsp66E	FBgn0035936	cib	FBgn0026084	Lpin	FBgn0263593
mRpL33	FBgn0040907	Swim	FBgn0034709	AspRS	FBgn0002069
Eaf6	FBgn0035624	ey	FBgn0005558	Daxx	FBgn0031820
CG10481	FBgn0032827	Nprl3	FBgn0036397	Acsl	FBgn0263120
ctp	FBgn0011760	Tsp	FBgn0031850	ftz-f1	FBgn0001078
CG9380	FBgn0035094	CG16716	FBgn0034459	l(3)04053	FBgn0010830
Fife	FBgn0264606	CG1695	FBgn0031116	CG3529	FBgn0035995

kek3	FBgn0028370	nrv1	FBgn0015776	NA	FBgn0262378
Mp	FBgn0260660	Eip75B	FBgn0000568	NA	FBgn0263413
DIP-zeta	FBgn0051708	Pdp1	FBgn0016694	CG9005	FBgn0033638
tal-2A	FBgn0259730	shep	FBgn0052423	btsz	FBgn0266756
CG31522	FBgn0051522	CG13794	FBgn0031936	Glut1	FBgn0264574
CG1677	FBgn0029941	Cpr	FBgn0015623	salr	FBgn0000287
CG45263	FBgn0266801	tio	FBgn0028979	NA	FBgn0267746
CG32806	FBgn0052806	fru	FBgn0004652	CG2747	FBgn0037541
CG9331	FBgn0032889	CG9281	FBgn0030672	CG5535	FBgn0036764
CG34383	FBgn0085412	hth	FBgn0001235	CG6145	FBgn0033853
PGRP-LC	FBgn0035976	CG11191	FBgn0033249	CG17544	FBgn0032775
TfAP-2	FBgn0261953	CG43245	FBgn0262890	Galphas	FBgn0001123
NA	FBgn0266251	Lamp1	FBgn0032949	m-cup	FBgn0038488
Sin1	FBgn0033935	Kdm4B	FBgn0053182	Hnf4	FBgn0004914
prominin-like	FBgn0026189	NA	FBgn0086037	NA	FBgn0267199
NA	FBgn0267729	nrv3	FBgn0032946	c(3)G	FBgn0000246
mamo	FBgn0267033	CG13321	FBgn0033787	CG12684	FBgn0029717
CG32700	FBgn0267253	LRP1	FBgn0053087	CG13506	FBgn0034723
para	FBgn0285944	NA	FBgn0052826	Rbbp5	FBgn0036973
disco-r	FBgn0285879	aop	FBgn0000097	D	FBgn0000411
snky	FBgn0086916	NA	FBgn0266819	CG16972	FBgn0032481
Fatp	FBgn0267828	CG6231	FBgn0038720	CG4297	FBgn0031258
spi	FBgn0005672	CG10631	FBgn0032817	cdi	FBgn0004876
dpr8	FBgn0052600	CG16894	FBgn0034483	Rbp6	FBgn0260943
Tgi	FBgn0036373	Blimp-1	FBgn0035625	cdc14	FBgn0031952
dar1	FBgn0263239	CenG1A	FBgn0028509	yps	FBgn0022959
Rh5	FBgn0014019	ey	FBgn0005558	CG12581	FBgn0037213
cu	FBgn0261808	Tao	FBgn0031030	CG7458	FBgn0037144
Rbp1-like	FBgn0030479	Pde1c	FBgn0264815	l(2)dtl	FBgn0013548
app	FBgn0260941	for	FBgn0000721	Nf1	FBgn0015269
Top1	FBgn0004924	CG7326	FBgn0030970	klg	FBgn0017590
Syp	FBgn0038826	CG6225	FBgn0038072	wmd	FBgn0034876
CG11566	FBgn0031159	sima	FBgn0266411	CG31221	FBgn0051221
betaCOP	FBgn0008635	NimC3	FBgn0001967	CG16974	FBgn0032479
gish	FBgn0250823	CG32532	FBgn0052532	CG2889	FBgn0030206
Mrp4	FBgn0263316	UQCR-11	FBgn0260008	mtd	FBgn0013576
CG10311	FBgn0038420	scny	FBgn0260936	CG13300	FBgn0035699
NA	FBgn0026197	Rac2	FBgn0014011	sif	FBgn0085447
Gyf	FBgn0039936	NA	FBgn0262397	Sytbeta	FBgn0261090
Cyp12e1	FBgn0037817	Abd-B	FBgn0000015	CG12818	FBgn0037809
Gr98d	FBgn0046885	A16	FBgn0028965	Idgf3	FBgn0020414

bru2	FBgn0262475	SKIP	FBgn0051163	Cdk12	FBgn0037093
tty	FBgn0015558	SPoCk	FBgn0052451	Vha100-2	FBgn0028670
Sh	FBgn0003380	stv	FBgn0086708	kay	FBgn0001297
Octbeta2R	FBgn0038063	tna	FBgn0026160	NA	FBgn0267753
Blimp-1	FBgn0035625	Pde6	FBgn0038237	fray	FBgn0023083
Gli	FBgn0001987	ZnT41F	FBgn0025693	Akap200	FBgn0027932
CrebB	FBgn0265784	CG10960	FBgn0036316	miple2	FBgn0029002
CG4404	FBgn0030432	CG42828	FBgn0262010	Alk	FBgn0040505
Fili	FBgn0085397	mam	FBgn0002643	dsx	FBgn0000504
l(3)72Dr	FBgn0263608	cmet	FBgn0040232	heph	FBgn0011224
BCL7-like	FBgn0026149	CG43778	FBgn0264308	ssp3	FBgn0032723
Pde9	FBgn0259171	dpr2	FBgn0261871	CG13471	FBgn0036443
CG14853	FBgn0038246	Sar1	FBgn0038947	bru2	FBgn0262475
NA	FBgn0267672	Eglp4	FBgn0034885	CG7139	FBgn0027532
Dfd	FBgn0000439	Orct2	FBgn0086365	CG10910	FBgn0034289
CG12531	FBgn0031064	CG4230	FBgn0031683	CG8301	FBgn0037717
inc	FBgn0025394	Treh	FBgn0003748	dally	FBgn0263930
fuss	FBgn0039932	alpha-Man-Ia	FBgn0259170	hng3	FBgn0035160
CG34172	FBgn0085201	haf	FBgn0261509	zf30C	FBgn0270924
jigr1	FBgn0039350	cry	FBgn0025680	CG43312	FBgn0263004
mtSSB	FBgn0010438	NA	FBgn0266898	l(3)05822	FBgn0010877
NA	FBgn0265427	scrib	FBgn0263289	CG7879	FBgn0035235
Loxl1	FBgn0039848	CG13323	FBgn0033788	Diap1	FBgn0260635
ctrip	FBgn0260794	NA	FBgn0267249	CG43066	FBgn0262476
Trxr-2	FBgn0037170	elB	FBgn0004858	dve	FBgn0020307
Fbxl7	FBgn0038385	CG10082	FBgn0034644	h-cup	FBgn0038334
pAbp	FBgn0265297	Ir47a	FBgn0033515	unc80	FBgn0039536
CG17598	FBgn0031194	CG6614	FBgn0032369	CG9663	FBgn0031516
sty	FBgn0014388	CCHa2-R	FBgn0033058	CG11658	FBgn0036196
SP2637	FBgn0034371	bun	FBgn0259176	trx	FBgn0003862
lz	FBgn0002576	CG18135	FBgn0036837	Dop1R2	FBgn0266137
Drak	FBgn0052666	Syx13	FBgn0036341	CG5968	FBgn0032588
CHES-1-like	FBgn0029504	CG2162	FBgn0035388	ine	FBgn0011603
CG14073	FBgn0036814	NA	FBgn0261453	CG10543	FBgn0034570
eyg	FBgn0000625	Bili	FBgn0039282	Clamp	FBgn0032979
NA	FBgn0265147	NA	FBgn0266405	Sar1	FBgn0038947
NA	FBgn0083994	CG13743	FBgn0033368	NA	FBgn0266628
Tlk	FBgn0283657	CG7378	FBgn0030976	dpp	FBgn0000490
MRP	FBgn0032456	NA	FBgn0267708	msn	FBgn0010909
Spt6	FBgn0028982	CG12289	FBgn0036160	cpx	FBgn0041605
Atet	FBgn0020762	NA	FBgn0265588	Ubc6	FBgn0004436

CG1504	FBgn0031100	sm	FBgn0003435	CG2182	FBgn0037360
NA	FBgn0264821	Uba1	FBgn0023143	nudC	FBgn0021768
NA	FBgn0052546	Cyt-c1L	FBgn0039651	CG3764	FBgn0036684
Lim1	FBgn0026411	ome	FBgn0259175	par-1	FBgn0260934
mod(mdg4)	FBgn0002781	fne	FBgn0086675	nAChRalpha5	FBgn0028875
CG34351	FBgn0085380	Elk	FBgn0011589	CG42402	FBgn0259821
eyg	FBgn0000625	px	FBgn0003175	mim	FBgn0053558
mtd	FBgn0013576	CG17364	FBgn0036391	Nc73EF	FBgn0010352
NA	FBgn0082959	NA	FBgn0004185	CG14669	FBgn0037326
cic	FBgn0262582	CG8745	FBgn0036381	miple1	FBgn0027111
wcy	FBgn0030812	CG11438	FBgn0037164	Lar	FBgn0000464
mid	FBgn0261963	CG11825	FBgn0033519	Eip74EF	FBgn0000567
RpL7A	FBgn0014026	CG12355	FBgn0040805	CG33299	FBgn0053299
Hers	FBgn0052529	CG13676	FBgn0035844	Teh1	FBgn0037766
Sin3A	FBgn0022764	dve	FBgn0020307	klar	FBgn0001316
CG45050	FBgn0266410	Fim	FBgn0024238	ebd2	FBgn0037076
CG6767	FBgn0036030	Unc-76	FBgn0040395	Eip93F	FBgn0264490
CG11594	FBgn0035484	CG17834	FBgn0028394	CG17270	FBgn0038828
grh	FBgn0259211	mam	FBgn0002643	CG13982	FBgn0031811
Scr	FBgn0003339	grim	FBgn0015946	tmod	FBgn0082582
CG2162	FBgn0035388	lqf	FBgn0028582	fru	FBgn0004652
HP5	FBgn0030301	CG5455	FBgn0039430	crc	FBgn0000370
Hr4	FBgn0264562	CG13581	FBgn0035014	NA	FBgn0266830
tai	FBgn0041092	Rab27	FBgn0025382	yem	FBgn0005596
Clic	FBgn0030529	Pmp70	FBgn0031069	Chd64	FBgn0035499
ben	FBgn0000173	CG32333	FBgn0052333	CG34370	FBgn0085399
Syngr	FBgn0033876	CG34354	FBgn0085383	fru	FBgn0004652
CG11138	FBgn0030400	pdm3	FBgn0261588	E(spl)m3-HLH	FBgn0002609
elav	FBgn0260400	Tsp42Ee	FBgn0029506	sax	FBgn0003317
CG11791	FBgn0039266	CG34353	FBgn0085382	jef	FBgn0033958
mam	FBgn0002643	CG32085	FBgn0052085	Dpit47	FBgn0266518
NA	FBgn0051162	CG14442	FBgn0029893	02-Sep	FBgn0014029
NA	FBgn0011944	Adhr	FBgn0000056	Sfxn1-3	FBgn0037239
CG4935	FBgn0028897	dnc	FBgn0000479	NA	FBgn0265076
CG42668	FBgn0261550	Gga	FBgn0030141	tou	FBgn0033636
ham	FBgn0045852	CG42392	FBgn0259738	mod	FBgn0002780
CG1695	FBgn0031116	NA	FBgn0267702	slo	FBgn0003429
scaf	FBgn0033033	CG10365	FBgn0039109	flfl	FBgn0024555
CkIalpha	FBgn0015024	inaE	FBgn0261244	dsd	FBgn0039528
CG9920	FBgn0038200	CG6036	FBgn0039421	NA	FBgn0266046
trv	FBgn0085391	Hr39	FBgn0261239	CG15803	FBgn0038606

Scr	FBgn0003339	mtd	FBgn0013576	CG1358	FBgn0033196
PRL-1	FBgn0024734	CG6424	FBgn0028494	CG14292	FBgn0038658
CG10428	FBgn0032724	sbb	FBgn0285917	CtBP	FBgn0020496
wda	FBgn0039067	aralar1	FBgn0028646	Abd-B	FBgn0000015
sens	FBgn0002573	Fur1	FBgn0004509	CG14905	FBgn0038452
CG9328	FBgn0032886	ko	FBgn0020294	lbl	FBgn0008651
NA	FBgn0047092	Slc45-1	FBgn0035968	CG5382	FBgn0038950
Smr	FBgn0265523	Socs36E	FBgn0041184	Axn	FBgn0026597
CG42450	FBgn0259927	E2f1	FBgn0011766	Dr	FBgn0000492
slgA	FBgn0003423	prage	FBgn0283741	CG17378	FBgn0031858
NA	FBgn0267087	NA	FBgn0266895	Dek	FBgn0026533
betaTub97EF	FBgn0003890	CG9990	FBgn0039594	Mef2	FBgn0011656
NA	FBgn0052200	CG14795	FBgn0025393	Sidpn	FBgn0032741
nAChRalpha7	FBgn0086778	NA	FBgn0265636	raw	FBgn0003209
px	FBgn0003175	a5	FBgn0011294	CG12158	FBgn0040775
NA	FBgn0004168	Clk	FBgn0023076	mfrn	FBgn0039561
PNPase	FBgn0039846	CG42788	FBgn0261859	Dys	FBgn0260003
sens-2	FBgn0051632	GCS2alpha	FBgn0027588	Vha55	FBgn0005671
caps	FBgn0023095	LpR2	FBgn0051092	CG9084	FBgn0033582
ptc	FBgn0003892	Su(dx)	FBgn0003557	Zip99C	FBgn0039714
CG31760	FBgn0051760	Hr4	FBgn0264562	NA	FBgn0263664
sea	FBgn0037912	ro	FBgn0003267	laza	FBgn0037163
mAChR-B	FBgn0037546	CG32264	FBgn0052264	Argk	FBgn0000116
NA	FBgn0001234	RpL34b	FBgn0037686	Corin	FBgn0033192
acj6	FBgn0000028	Yeti	FBgn0267398	GstD11	FBgn0038029
CG7332	FBgn0030973	stj	FBgn0261041	NAT1	FBgn0010488
CG12531	FBgn0031064	NA	FBgn0262319	CG6424	FBgn0028494
olf413	FBgn0037153	nrm	FBgn0262509	CG4502	FBgn0031896
rdgA	FBgn0261549	CG6044	FBgn0034725	CG42831	FBgn0262020
lectin-46Cb	FBgn0040092	Fkbp14	FBgn0010470	subdued	FBgn0038721
Mob2	FBgn0259481	east	FBgn0261954	sick	FBgn0263873
CG11977	FBgn0037650	CG10011	FBgn0039590	ND-SGDH	FBgn0011455
Awh	FBgn0013751	Nrt	FBgn0004108	shep	FBgn0052423
CG9413	FBgn0030574	NFAT	FBgn0030505	CG13577	FBgn0034998
CG6006	FBgn0063649	CG42514	FBgn0260388	Glut1	FBgn0264574
grh	FBgn0259211	CG31729	FBgn0051729	Trl	FBgn0013263
tkv	FBgn0003716	tup	FBgn0003896	Argk	FBgn0000116
ctrip	FBgn0260794	CG6330	FBgn0039464	CG13921	FBgn0035267
NA	FBgn0264510	Rbp9	FBgn0010263	danr	FBgn0039283
MFS18	FBgn0025684	shn	FBgn0003396	CNMaR	FBgn0053696
CG9717	FBgn0039789	Fer2LCH	FBgn0015221	kcc	FBgn0261794

stwl	FBgn0003459	CG2104	FBgn0037365	Aps	FBgn0036111
Rme-8	FBgn0015477	metro	FBgn0050021	NA	FBgn0285940
NA	FBgn0265422	CG43188	FBgn0262817	CG11486	FBgn0035397
shot	FBgn0013733	CG6497	FBgn0036704	Oda	FBgn0014184
CG15771	FBgn0029801	NA	FBgn0263554	Hr51	FBgn0034012
NA	FBgn0263385	MYPT-75D	FBgn0036801	amon	FBgn0023179
S6KL	FBgn0283473	DIP-theta	FBgn0051646	CG2993	FBgn0037521
brk	FBgn0024250	CG7029	FBgn0039026	psq	FBgn0263102
foxo	FBgn0038197	GstD1	FBgn0001149	Pglym78	FBgn0014869
NA	FBgn0265926	NA	FBgn0012024	Apc	FBgn0015589
fzr	FBgn0262699	Rip11	FBgn0027335	NA	FBgn0266908
PDZ-GEF	FBgn0265778	sty	FBgn0014388	CG5377	FBgn0038974
LRP1	FBgn0053087	Bacc	FBgn0031453	Cyt-c-p	FBgn0284248
dpr11	FBgn0053202	CG7737	FBgn0033584	CG15561	FBgn0039829
mamo	FBgn0267033	CG2224	FBgn0039773	tutl	FBgn0010473
RabX2	FBgn0030200	CG15673	FBgn0034639	Nckx30C	FBgn0028704
cpx	FBgn0041605	tou	FBgn0033636	Obp28a	FBgn0011283
msi	FBgn0011666	CG13408	FBgn0038929	CG34384	FBgn0085413
CanA-14F	FBgn0267912	CG12913	FBgn0033500	ap	FBgn0267978
Rm62	FBgn0003261	NA	FBgn0028981	gish	FBgn0250823
bin3	FBgn0263144	SP1173	FBgn0035710	stmA	FBgn0086784
CG16721	FBgn0029820	CG17364	FBgn0036391	atms	FBgn0010750
Utx	FBgn0260749	zormin	FBgn0052311	jumu	FBgn0015396
norpA	FBgn0262738	Rdh	FBgn0064227	CG18012	FBgn0038552
tmod	FBgn0082582	NA	FBgn0267629	Taf4	FBgn0010280
sn	FBgn0003447	arm	FBgn0000117	Kr-h1	FBgn0266450
grnd	FBgn0032682	mRpL53	FBgn0050481	Kul	FBgn0039688
CG11486	FBgn0035397	glob1	FBgn0027657	scramb1	FBgn0052056
CG13917	FBgn0035237	CG2246	FBgn0039790	CG5726	FBgn0034313
P58IPK	FBgn0037718	Dscam4	FBgn0263219	Cow	FBgn0039054
mgl	FBgn0261260	Optix	FBgn0025360	Arf79F	FBgn0010348
CG7031	FBgn0039027	Eno	FBgn0000579	Treh	FBgn0003748
CG32772	FBgn0052772	emc	FBgn0000575	CG2225	FBgn0032957
CG42747	FBgn0261801	pyd	FBgn0262614	RanBPM	FBgn0262114
Scamp	FBgn0040285	Rgk3	FBgn0085426	ari-2	FBgn0025186
CG42784	FBgn0263354	NA	FBgn0082922	Smg5	FBgn0019890
eIF4H1	FBgn0262734	NA	FBgn0050235	gprs	FBgn0024232
pum	FBgn0003165	CG13712	FBgn0035570	CG9815	FBgn0034861
Hex-A	FBgn0001186	NA	FBgn0264857	CG9801	FBgn0037623
eya	FBgn0000320	Dscam3	FBgn0261046	CenG1A	FBgn0028509
CG5953	FBgn0032587	NA	FBgn0265058	CG31808	FBgn0062978

Hr3	FBgn0000448	vari	FBgn0250785	tipE	FBgn0003710
Vsx2	FBgn0263512	insc	FBgn0011674	PIG-Z	FBgn0266438
Pur-alpha	FBgn0022361	CG42674	FBgn0261556	Glut4EF	FBgn0267336
NA	FBgn0262388	Ptpmeg2	FBgn0028341	CG11399	FBgn0037021
CG31717	FBgn0051717	CG42747	FBgn0261801	CG12163	FBgn0260462
Gpo-1	FBgn0022160	CG17716	FBgn0000633	Uev1A	FBgn0035601
HDAC4	FBgn0041210	CG7991	FBgn0035260	CG1927	FBgn0027547
galectin	FBgn0031213	CG31075	FBgn0051075	cact	FBgn0000250
NA	FBgn0264787	pod1	FBgn0029903	NA	FBgn0267794
NA	FBgn0262447	CG2017	FBgn0037391	Ald	FBgn0000064
dsx	FBgn0000504	Smurf	FBgn0029006	CG8498	FBgn0031992
CG9444	FBgn0037730	Eip78C	FBgn0004865	Sln	FBgn0033657
Dl	FBgn0000463	NA	FBgn0264883	NA	FBgn0265149
crol	FBgn0020309	Sox21b	FBgn0042630	NA	FBgn0267460
Ten-a	FBgn0267001	CG15309	FBgn0030183	Rab26	FBgn0086913
NA	FBgn0264438	Gycalpha99B	FBgn0013972	NA	FBgn0011861
Sh	FBgn0003380	Pde11	FBgn0085370	UQCR-Q	FBgn0036728
ph-p	FBgn0004861	NA	FBgn0262388	jim	FBgn0027339
neur	FBgn0002932	NA	FBgn0262378	lov	FBgn0266129
ari-1	FBgn0017418	hang	FBgn0026575	jumu	FBgn0015396
skd	FBgn0003415	CG7029	FBgn0039026	ps	FBgn0261552
dpr8	FBgn0052600	Ace	FBgn0000024	CG9945	FBgn0034527
ras	FBgn0003204	Dscam4	FBgn0263219	CG7781	FBgn0032021
Ptp99A	FBgn0004369	CG6465	FBgn0037818	CG4374	FBgn0039078
toe	FBgn0036285	chn	FBgn0015371	NA	FBgn0261700
bdl	FBgn0028482	l(2)k14505	FBgn0021856	trio	FBgn0024277
bip1	FBgn0026263	jing	FBgn0086655	Lk6	FBgn0017581
Ets98B	FBgn0005659	Mad	FBgn0011648	CG7168	FBgn0038586
NA	FBgn0263532	CG10139	FBgn0033951	CG42337	FBgn0259239
CG43707	FBgn0263846	NA	FBgn0026162	CG16896	FBgn0035073
CG42492	FBgn0259994	NA	FBgn0265889	NA	FBgn0011915
rdx	FBgn0264493	NA	FBgn0266161	CG10182	FBgn0039091
CG11221	FBgn0031855	CASK	FBgn0013759	seq	FBgn0028991
sll	FBgn0038524	btsz	FBgn0266756	Hrb98DE	FBgn0001215
Trf4-1	FBgn0030049	Ir56d	FBgn0034458	NA	FBgn0265067
CG1737	FBgn0030293	Sema2a	FBgn0011260	h	FBgn0001168
Ca-beta	FBgn0259822	CG9821	FBgn0037636	Hrb27C	FBgn0004838
Dad	FBgn0020493	CG10713	FBgn0036360	CG13920	FBgn0025712
Rdl	FBgn0004244	Baldspot	FBgn0260960	CG6785	FBgn0032399
UbcE2H	FBgn0029996	NA	FBgn0020617	NA	FBgn0265149
CG9413	FBgn0030574	NA	FBgn0266953	eRF3	FBgn0020443

CG18766	FBgn0042111	CG3638	FBgn0261444	Blimp-1	FBgn0035625
Wdr62	FBgn0031374	br	FBgn0283451	Syx1A	FBgn0013343
CG5381	FBgn0032218	CG43231	FBgn0262876	Acsl	FBgn0263120
CG13204	FBgn0033627	dtn	FBgn0262730	NA	FBgn0264704
CG7990	FBgn0030997	dikar	FBgn0261934	Syx1A	FBgn0013343
CG9377	FBgn0032507	CG5644	FBgn0035948	ced-6	FBgn0029092
RapGAP1	FBgn0264895	toe	FBgn0036285	Cap-H2	FBgn0037831
CG6959	FBgn0037956	tara	FBgn0040071	Cp1	FBgn0013770
NA	FBgn0050212	CG30197	FBgn0050197	smg	FBgn0016070
rdgB	FBgn0003218	ths	FBgn0033652	Men	FBgn0002719
CCAP-R	FBgn0039396	NA	FBgn0266238	Fas3	FBgn0000636
GATAd	FBgn0032223	CG6465	FBgn0037818	retm	FBgn0031814
jp	FBgn0032129	tau	FBgn0266579	en	FBgn0000577
CG6767	FBgn0036030	rgn	FBgn0261258	NA	FBgn0266782
Ddc	FBgn0000422	CAP	FBgn0033504	put	FBgn0003169
Pdp1	FBgn0016694	Mkp3	FBgn0036844	Rab30	FBgn0031882
NA	FBgn0031778	kek1	FBgn0015399	Pal2	FBgn0262728
Cyp12b2	FBgn0034387	CtBP	FBgn0020496	CG10863	FBgn0027552
CG13898	FBgn0035161	Shaw	FBgn0003386	CG7920	FBgn0039737
CG42684	FBgn0261570	Gpdh	FBgn0001128	CG1265	FBgn0035517
ptc	FBgn0003892	Ppa	FBgn0020257	CG31523	FBgn0051523
AstC-R2	FBgn0036789	NA	FBgn0266786	CG12769	FBgn0033252
CG43867	FBgn0264449	ps	FBgn0261552	CG31140	FBgn0051140
so	FBgn0003460	CG3505	FBgn0038250	fdl	FBgn0045063
homer	FBgn0025777	Oatp30B	FBgn0032123	CG3061	FBgn0038195
NA	FBgn0265679	CG2269	FBgn0033484	Hmx	FBgn0264005
CG1090	FBgn0037238	eIF2beta	FBgn0004926	CG33111	FBgn0053111
nolo	FBgn0051619	CG5059	FBgn0037007	Atx2	FBgn0041188
hbs	FBgn0029082	CG33203	FBgn0053203	dati	FBgn0262636
e(y)3	FBgn0087008	CG10512	FBgn0037057	MED19	FBgn0036761
CG30472	FBgn0050472	RhoGEF3	FBgn0264707	alphaTub84B	FBgn0003884
CG34300	FBgn0085329	sta	FBgn0003517	ATPsynF	FBgn0035032
Appl	FBgn0000108	CG31221	FBgn0051221	CG43783	FBgn0264305
CG3638	FBgn0261444	Nup205	FBgn0031078	NA	FBgn0011868
CG32850	FBgn0052850	PKD	FBgn0038603	Mpc1	FBgn0038662
CG16753	FBgn0035393	dco	FBgn0002413	Mbs	FBgn0005536
Atf3	FBgn0028550	CG13739	FBgn0033403	slim	FBgn0261477
sea	FBgn0037912	Dab	FBgn0000414	unk	FBgn0004395
CG17896	FBgn0023537	CG45071	FBgn0266441	Arl5	FBgn0035866
CG42784	FBgn0263354	chico	FBgn0024248	Ufl1	FBgn0037467
Tob	FBgn0028397	PsGEF	FBgn0264598	Sap47	FBgn0013334

CG34172	FBgn0085201	CG30089	FBgn0050089	CG14762	FBgn0033250
CG13323	FBgn0033788	CG11629	FBgn0032965	CG6115	FBgn0040985
NA	FBgn0053294	Faa	FBgn0016013	Rab14	FBgn0015791
2mit	FBgn0260793	AGO2	FBgn0087035	Tm1	FBgn0003721
CG32432	FBgn0052432	DOR	FBgn0035542	CG15172	FBgn0032740
MsR2	FBgn0264002	NA	FBgn0267928	cue	FBgn0011204
CG14147	FBgn0036112	Tollo	FBgn0029114	CG13850	FBgn0038961
mbl	FBgn0265487	CG13654	FBgn0039290	SCAP	FBgn0033052
NA	FBgn0265508	IA-2	FBgn0031294	Kdm2	FBgn0037659
bchs	FBgn0043362	gcl	FBgn0005695	Sin3A	FBgn0022764
disco-r	FBgn0285879	NA	FBgn0267145	pgant5	FBgn0031681
Tomosyn	FBgn0030412	beat-IIIb	FBgn0053179	dsd	FBgn0039528
CG6163	FBgn0036155	CG10924	FBgn0034356	l(3)02640	FBgn0010786
Toll-4	FBgn0032095	dati	FBgn0262636	CG15431	FBgn0031602
CG9005	FBgn0033638	kat-60L1	FBgn0037375	CG3434	FBgn0036000
Kap3	FBgn0028421	Poc1	FBgn0036354	CG3793	FBgn0028507
CG14810	FBgn0029589	CG10348	FBgn0032707	CalpA	FBgn0012051
CG15233	FBgn0033076	CG9760	FBgn0036259	Tnpo	FBgn0024921
NA	FBgn0263330	CG3961	FBgn0036821	GstZ2	FBgn0037697
SLO2	FBgn0261698	CG11768	FBgn0037625	Cka	FBgn0044323
MAPk-Ak2	FBgn0013987	CG3764	FBgn0036684	wech	FBgn0259745
Tlk	FBgn0283657	CG13894	FBgn0035157	mrt	FBgn0039507
NA	FBgn0267119	Dscam1	FBgn0033159	CG5361	FBgn0037786
CG7990	FBgn0030997	milt	FBgn0262872	Syp	FBgn0038826
tws	FBgn0004889	Ac3	FBgn0023416	GlyRS	FBgn0027088
X11Lbeta	FBgn0052677	CG13917	FBgn0035237	Asph	FBgn0034075
futsch	FBgn0259108	NA	FBgn0266764	Lis-1	FBgn0015754
shakB	FBgn0085387	NA	FBgn0052420	CG1427	FBgn0037347
jar	FBgn0011225	CG7368	FBgn0036179	Dat	FBgn0019643
rad	FBgn0265597	Eip93F	FBgn0264490	Akt1	FBgn0010379
Vav	FBgn0040068	CG13323	FBgn0033788	dup	FBgn0000996
CG10508	FBgn0037060	NA	FBgn0263049	CG12071	FBgn0039808
CG3788	FBgn0034800	CG41378	FBgn0085638	NA	FBgn0265419
Tet	FBgn0263392	vvl	FBgn0086680	pnut	FBgn0013726
CG42580	FBgn0260870	NA	FBgn0263019	Alh	FBgn0261238
CycG	FBgn0039858	sty	FBgn0014388	cry	FBgn0025680
svr	FBgn0004648	C1GalTA	FBgn0032078	NA	FBgn0263838
shn	FBgn0003396	CG14877	FBgn0038380	Xe7	FBgn0010772
tou	FBgn0033636	MsR1	FBgn0035331	Strip	FBgn0035437
18w	FBgn0004364	Sema1a	FBgn0011259	eff	FBgn0011217
Ubx	FBgn0003944	CG10311	FBgn0038420	Dak1	FBgn0028833

NA	FBgn0086053	CG14696	FBgn0037853	SCCRO4	FBgn0036967
cpx	FBgn0041605	CadN	FBgn0015609	BEAF-32	FBgn0015602
Pfrx	FBgn0027621	Keap1	FBgn0038475	RpS9	FBgn0010408
CadN2	FBgn0262018	CG31098	FBgn0051098	NA	FBgn0267703
DNaseII	FBgn0000477	Prosap	FBgn0040752	crp	FBgn0001994
Msp300	FBgn0261836	spen	FBgn0016977	CG4360	FBgn0038787
pnt	FBgn0003118	l(2)09851	FBgn0022288	14-3-3epsilon	FBgn0020238
Wdr62	FBgn0031374	Snap25	FBgn0011288		

Less accessible genes juvenile control compared to mature control					
Gene Symbol	**Flybase ID**	**Gene Symbol**	**Flybase ID**	**Gene Symbol**	**Flybase ID**
NA	FBgn0065083	CG31678	FBgn0051678	NA	FBgn0267430
CG10170	FBgn0039085	CG31550	FBgn0051550	CG43116	FBgn0262576
CG31051	FBgn0051051	CG15167	FBgn0032709	CG43366	FBgn0263109
Msp300	FBgn0261836	CG14089	FBgn0036861	Optix	FBgn0025360
NA	FBgn0267133	htt	FBgn0027655	vvl	FBgn0086680
slam	FBgn0043854	Clk	FBgn0023076	lig	FBgn0020279
Nlp	FBgn0016685	CG31523	FBgn0051523	CG43102	FBgn0262562
CG2127	FBgn0033286	CG5478	FBgn0038386	CG14650	FBgn0037252
w-cup	FBgn0032269	CG31051	FBgn0051051	NA	FBgn0266390
NA	FBgn0266909	ths	FBgn0033652	Rbp6	FBgn0260943
Shroom	FBgn0085408	mEFTs	FBgn0032646	sna	FBgn0003448
CG31191	FBgn0051191	pk	FBgn0003090	CG3267	FBgn0042083
CG15005	FBgn0035508	NA	FBgn0011858	NA	FBgn0266969
robo3	FBgn0041097	tnc	FBgn0039257	NA	FBgn0262616
RpL38	FBgn0040007	CG8379	FBgn0037638	CG32238	FBgn0052238
CG13705	FBgn0035582	NA	FBgn0262107	CG6686	FBgn0032388
NA	FBgn0053653	NA	FBgn0283428	CG5065	FBgn0034145
NA	FBgn0267606	CG16908	FBgn0037741	pip	FBgn0003089
NA	FBgn0086032	NA	FBgn0052480	NA	FBgn0267399
Pglym87	FBgn0011270	CG7311	FBgn0028848	CG31522	FBgn0051522
CG42534	FBgn0260487	CG16772	FBgn0032835	TBCB	FBgn0034451
NA	FBgn0266222	CG17883	FBgn0040005	CG17698	FBgn0040056
CG8219	FBgn0035693	CG9596	FBgn0031832	CG6094	FBgn0032261
Dhc98D	FBgn0013813	CG10748	FBgn0036327	CG5003	FBgn0039554
CG8562	FBgn0035779	CG9664	FBgn0031515	NA	FBgn0263328
AstA-R2	FBgn0039595	fkh	FBgn0000659	ninaC	FBgn0002938
CG11333	FBgn0039850	Glt	FBgn0001114	Scp2	FBgn0020907
Gld2	FBgn0038934	Nelf-E	FBgn0017430	rpr	FBgn0011706

NA	FBgn0284412	CG3714	FBgn0031589	Sfp65A	FBgn0259969
CG31007	FBgn0051007	NA	FBgn0266390	ValRS	FBgn0027079
CG44290	FBgn0265317	CG31693	FBgn0051693	mtsh	FBgn0262598
psd	FBgn0086265	NA	FBgn0267642	CG7084	FBgn0038938
hth	FBgn0001235	NA	FBgn0267775	NA	FBgn0267774
CG8620	FBgn0040837	retn	FBgn0004795	alpha-Est10	FBgn0015569
NA	FBgn0267277	sona	FBgn0034903	NA	FBgn0267800
CG8745	FBgn0036381	CG12147	FBgn0037325	Cyp6g1	FBgn0025454
Klp59C	FBgn0034824	Cda9	FBgn0034197	NA	FBgn0262432
BigH1	FBgn0038252	Dscam3	FBgn0261046	Acn	FBgn0263198
CG6688	FBgn0039038	Acam	FBgn0011273	CG7714	FBgn0038645
CG10749	FBgn0036328	CG45546	FBgn0267106	NA	FBgn0266824
bond	FBgn0260942	NA	FBgn0265646	NA	FBgn0262382
bdl	FBgn0028482	Alk	FBgn0040505	ppk31	FBgn0051065
px	FBgn0003175	CG13561	FBgn0034906	CG33301	FBgn0053301
CG8086	FBgn0032010	CG9928	FBgn0032472	Ccp84Af	FBgn0004778
NA	FBgn0086200	msps	FBgn0027948	croc	FBgn0014143
ohgt	FBgn0037780	Prat2	FBgn0041194	CG9422	FBgn0033092
NA	FBgn0266831	Cap-D2	FBgn0039680	NA	FBgn0264506
CG5867	FBgn0027586	CG31677	FBgn0051677	Cpr66D	FBgn0052029
mad2	FBgn0035640	CG15160	FBgn0032688	CG5292	FBgn0038491
CG15167	FBgn0032709	CG42355	FBgn0259701	Bruce	FBgn0266717
shg	FBgn0003391	CG3773	FBgn0038692	NA	FBgn0267571
CG10182	FBgn0039091	Irk3	FBgn0032706	MCU	FBgn0042185
CG6688	FBgn0039038	fz2	FBgn0016797	CG42826	FBgn0262008
nAChRalpha4	FBgn0266347	CG7492	FBgn0035807	CG7200	FBgn0032671
CG12320	FBgn0038590	CG8272	FBgn0033337	Ppn	FBgn0003137
Adk3	FBgn0042094	Sec23	FBgn0262125	NA	FBgn0267114
Tdc2	FBgn0050446	Tim17b2	FBgn0020371	CG6511	FBgn0035923
Cyp6a8	FBgn0013772	NA	FBgn0267993	CG6142	FBgn0039415
Plp	FBgn0086690	CG10463	FBgn0032819	Rcd2	FBgn0037012
SPE	FBgn0039102	NA	FBgn0264723	NA	FBgn0267668
Toll-6	FBgn0036494	CG30369	FBgn0050369	CG3358	FBgn0033117
Phk-3	FBgn0035089	robo1	FBgn0005631	NA	FBgn0086060
NA	FBgn0265065	Or22c	FBgn0026396	CG14011	FBgn0031722
BBS8	FBgn0031255	CG6271	FBgn0039476	Ino80	FBgn0086613
CG11997	FBgn0037662	NA	FBgn0267724	NA	FBgn0266869
CG13133	FBgn0032181	cN-IIIB	FBgn0034988	CG4161	FBgn0028892
Gbp3	FBgn0039031	NA	FBgn0262689	Cyp4aa1	FBgn0034053
CG33191	FBgn0053191	NA	FBgn0267653		

More accessible genes juvenile Bap60-KD MB compared to mature Bap60-KD MB					
Gene Symbol	**Flybase ID**	**Gene Symbol**	**Flybase ID**	**Gene Symbol**	**Flybase ID**
RhoGEF64C	FBgn0035574	NA	FBgn0267798	Osi12	FBgn0037419
reb	FBgn0033667	AGO3	FBgn0250816	CG10910	FBgn0034289
CG18622	FBgn0038460	NA	FBgn0267430	NA	FBgn0039987
Mst87F	FBgn0002862	CG40439	FBgn0284080	CG8301	FBgn0037717
NA	FBgn0264914	CG43098	FBgn0262544	NA	FBgn0267798
NA	FBgn0267797	NA	FBgn0085570	dally	FBgn0263930
NA	FBgn0267983	NA	FBgn0267983	hng3	FBgn0035160
NA	FBgn0085734	NA	FBgn0267797	ato	FBgn0010433
tll	FBgn0003720	NA	FBgn0085804	NA	FBgn0266323
NA	FBgn0266684	MFS17	FBgn0058263	zf30C	FBgn0270924
NA	FBgn0267798	NA	FBgn0284410	CG43312	FBgn0263004
ptc	FBgn0003892	CG40178	FBgn0058178	l(3)05822	FBgn0010877
shd	FBgn0003388	CG16716	FBgn0034459	Mdr65	FBgn0004513
CG6435	FBgn0034165	NA	FBgn0267797	NA	FBgn0265951
saturn	FBgn0052141	NA	FBgn0058182	NA	FBgn0085734
DptA	FBgn0004240	Ncc69	FBgn0036279	NA	FBgn0264835
CG14301	FBgn0038632	NA	FBgn0085734	CG13747	FBgn0033364
CG14316	FBgn0038567	NA	FBgn0265931	CG7879	FBgn0035235
CG5002	FBgn0034275	NA	FBgn0058182	Diap1	FBgn0260635
NA	FBgn0267524	NA	FBgn0264570	CG43066	FBgn0262476
Myd88	FBgn0033402	NA	FBgn0039987	dve	FBgn0020307
CG11966	FBgn0037645	CG15167	FBgn0032709	h-cup	FBgn0038334
Ppr-Y	FBgn0046697	NA	FBgn0267798	NA	FBgn0263495
bbg	FBgn0087007	CG15800	FBgn0034904	NA	FBgn0266747
NA	FBgn0266747	NA	FBgn0263107	unc80	FBgn0039536
Gr28b	FBgn0045495	NA	FBgn0085612	CG9663	FBgn0031516
CG32447	FBgn0052447	CG40228	FBgn0063670	CG11658	FBgn0036196
AhcyL2	FBgn0015011	NA	FBgn0267883	trx	FBgn0003862
ND-MLRQ	FBgn0052230	NA	FBgn0058182	Dop1R2	FBgn0266137
NA	FBgn0263495	NA	FBgn0267797	CG5968	FBgn0032588
NA	FBgn0267797	NA	FBgn0058182	CG7514	FBgn0035567
NA	FBgn0267798	pnt	FBgn0003118	nvd	FBgn0259697
AGO3	FBgn0250816	CG1299	FBgn0035501	NA	FBgn0267798
NA	FBgn0058182	Mhc	FBgn0264695	NA	FBgn0267132
SCOT	FBgn0035298	CG6675	FBgn0032973	ine	FBgn0011603
NA	FBgn0264835	exp	FBgn0033668	CG41284	FBgn0085599
NA	FBgn0260469	Cyt-b5-r	FBgn0000406	CG10543	FBgn0034570
NA	FBgn0267598	NA	FBgn0266747	Clamp	FBgn0032979
NA	FBgn0267797	kni	FBgn0001320	Sar1	FBgn0038947

LManI	FBgn0032253	NA	FBgn0267133	NA	FBgn0266628
CG34398	FBgn0085427	CG14621	FBgn0031183	NA	FBgn0267862
beta4GalT7	FBgn0039258	CG40228	FBgn0063670	CG17684	FBgn0263780
NA	FBgn0267524	CG43106	FBgn0262566	NA	FBgn0085582
UQCR-11	FBgn0260008	AGO3	FBgn0250816	NA	FBgn0267798
NA	FBgn0267797	NA	FBgn0058461	dpp	FBgn0000490
NA	FBgn0267430	wg	FBgn0284084	msn	FBgn0010909
ttm3	FBgn0032971	CG30440	FBgn0050440	cpx	FBgn0041605
AGO3	FBgn0250816	NA	FBgn0264914	CG32081	FBgn0052081
ND-MLRQ	FBgn0052230	Ir94e	FBgn0259194	Ubc6	FBgn0004436
CG8630	FBgn0038130	NA	FBgn0058354	CG2182	FBgn0037360
CG14362	FBgn0038186	NA	FBgn0266222	CG4374	FBgn0039078
CG43102	FBgn0262562	CG13720	FBgn0035555	nudC	FBgn0021768
CG13639	FBgn0265266	ham	FBgn0045852	NA	FBgn0266747
bnl	FBgn0014135	NA	FBgn0263019	CG3764	FBgn0036684
CG14960	FBgn0035428	NA	FBgn0266747	par-1	FBgn0260934
NA	FBgn0267797	NA	FBgn0263019	NA	FBgn0266747
CG40439	FBgn0284080	CG32447	FBgn0052447	nAChRalpha5	FBgn0028875
CG30114	FBgn0050114	jim	FBgn0027339	NA	FBgn0267798
CG40470	FBgn0058470	Oatp58Dc	FBgn0034716	CG34433	FBgn0085462
NA	FBgn0267797	NA	FBgn0266747	CG42402	FBgn0259821
NA	FBgn0266796	CG7017	FBgn0036951	mim	FBgn0053558
Cpr47Ed	FBgn0033601	RasGAP1	FBgn0004390	Nc73EF	FBgn0010352
CG30103	FBgn0050103	CG17018	FBgn0039972	CG14669	FBgn0037326
CG30440	FBgn0050440	Glut4EF	FBgn0267336	miple1	FBgn0027111
NA	FBgn0267798	KrT95D	FBgn0020647	CG43441	FBgn0263389
NA	FBgn0263617	Diap1	FBgn0260635	Lar	FBgn0000464
Pkg21D	FBgn0000442	hwt	FBgn0264542	NA	FBgn0266747
CG16884	FBgn0028544	NA	FBgn0085612	CG33217	FBgn0053217
MFS17	FBgn0058263	Cpr97Ea	FBgn0039480	Eip74EF	FBgn0000567
how	FBgn0264491	mrj	FBgn0034091	CG33299	FBgn0053299
CG7695	FBgn0038631	CG10600	FBgn0032717	Teh1	FBgn0037766
CG2003	FBgn0039886	NA	FBgn0266747	NA	FBgn0039987
uif	FBgn0031879	alphaKap4	FBgn0035657	klar	FBgn0001316
NA	FBgn0267797	NA	FBgn0265047	Myo81F	FBgn0267431
NA	FBgn0260435	Sap130	FBgn0262714	ebd2	FBgn0037076
Tsp	FBgn0031850	GlyT	FBgn0034911	NA	FBgn0267798
Lsp1gamma	FBgn0002564	CG18371	FBgn0033893	CG17018	FBgn0039972
CG7675	FBgn0038610	mub	FBgn0262737	CG6793	FBgn0036242
CG40498	FBgn0069969	Hus1-like	FBgn0026417	NA	FBgn0264914
Myo81F	FBgn0267431	CG7971	FBgn0035253	CG30103	FBgn0050103

NA	FBgn0266747	Clc	FBgn0024814	Eip93F	FBgn0264490
CG41099	FBgn0039955	CG8321	FBgn0033677	CG17270	FBgn0038828
NA	FBgn0265047	CG45782	FBgn0267429	CG13982	FBgn0031811
CG42598	FBgn0260997	NA	FBgn0267430	tmod	FBgn0082582
CG10570	FBgn0040992	NA	FBgn0267430	fru	FBgn0004652
Myo81F	FBgn0267431	Clk	FBgn0023076	CG40228	FBgn0063670
Naa20B	FBgn0051851	kni	FBgn0001320	NA	FBgn0058182
Cht10	FBgn0250907	CG43351	FBgn0263083	NA	FBgn0039987
NA	FBgn0267793	cmpy	FBgn0037015	Maf1	FBgn0267861
Myo81F	FBgn0267431	ND-MLRQ	FBgn0052230	crc	FBgn0000370
NA	FBgn0058182	CG40228	FBgn0063670	NA	FBgn0266830
nub	FBgn0085424	CG42598	FBgn0260997	NA	FBgn0039987
NA	FBgn0085784	Rdh	FBgn0064227	NA	FBgn0284412
NA	FBgn0085612	CG10055	FBgn0037482	yem	FBgn0005596
ninaB	FBgn0002937	Cnx99A	FBgn0015622	Myo81F	FBgn0267431
NA	FBgn0265951	Ptp61F	FBgn0267487	Chd64	FBgn0035499
Maf1	FBgn0267861	soti	FBgn0038225	NA	FBgn0265371
CG2003	FBgn0039886	NA	FBgn0267132	CG34370	FBgn0085399
CG42598	FBgn0260997	Rtnl1	FBgn0053113	NA	FBgn0266323
CG43968	FBgn0264699	NA	FBgn0262368	NA	FBgn0260469
Ctr1C	FBgn0062411	sala	FBgn0003313	AGO3	FBgn0250816
Or49a	FBgn0033727	JIL-1	FBgn0020412	fru	FBgn0004652
NA	FBgn0085664	verm	FBgn0261341	CG13315	FBgn0040827
CG43168	FBgn0262787	NA	FBgn0085804	E(spl)m3-HLH	FBgn0002609
NA	FBgn0058182	NA	FBgn0267798	sax	FBgn0003317
Spn77Bc	FBgn0036970	RpS11	FBgn0033699	ND-AGGG	FBgn0085736
Thor	FBgn0261560	CG45093	FBgn0266526	CG30440	FBgn0050440
Cht10	FBgn0250907	brat	FBgn0010300	jef	FBgn0033958
grh	FBgn0259211	dati	FBgn0262636	NA	FBgn0039987
CG5160	FBgn0031906	smal	FBgn0085409	CG9483	FBgn0032072
NA	FBgn0265508	CG17974	FBgn0034624	NimA	FBgn0261514
en	FBgn0000577	NA	FBgn0267797	NA	FBgn0264914
NA	FBgn0266747	Atet	FBgn0020762	Dpit47	FBgn0266518
NA	FBgn0267987	Ir94h	FBgn0039080	Ir41a	FBgn0040849
Ir40a	FBgn0259683	NLaz	FBgn0053126	NA	FBgn0267797
Lmpt	FBgn0261565	CG31688	FBgn0263355	CG42674	FBgn0261556
srp	FBgn0003507	CG4374	FBgn0039078	NA	FBgn0039987
ClC-a	FBgn0051116	CG13028	FBgn0036676	02-Sep	FBgn0014029
bnl	FBgn0014135	CG43335	FBgn0263040	Sfxn1-3	FBgn0037239
NA	FBgn0267704	CG33640	FBgn0053640	NA	FBgn0265076
NA	FBgn0267798	NA	FBgn0267798	NA	FBgn0267430

NA	FBgn0058182	NA	FBgn0028910	tou	FBgn0033636
NA	FBgn0058182	AGO3	FBgn0250816	mod	FBgn0002780
CG41284	FBgn0085599	CG30389	FBgn0050389	slo	FBgn0003429
Fatp	FBgn0267828	NA	FBgn0085804	NA	FBgn0267798
CG10000	FBgn0039596	eg	FBgn0000560	NA	FBgn0085804
Takl2	FBgn0039015	NA	FBgn0267201	Ir41a	FBgn0040849
Prat2	FBgn0041194	NA	FBgn0039987	flfl	FBgn0024555
NA	FBgn0040045	HnRNP-K	FBgn0267791	dsd	FBgn0039528
NA	FBgn0267797	ND-MLRQ	FBgn0052230	NA	FBgn0264548
Maf1	FBgn0267861	NA	FBgn0267797	CG41099	FBgn0039955
NA	FBgn0058182	Ir56a	FBgn0050125	NA	FBgn0266046
CG14607	FBgn0037488	NA	FBgn0260469	CG15803	FBgn0038606
msi	FBgn0011666	NA	FBgn0265896	CG1358	FBgn0033196
NA	FBgn0039987	ZnT63C	FBgn0035432	CG14292	FBgn0038658
NA	FBgn0263496	NA	FBgn0264438	CtBP	FBgn0020496
NA	FBgn0267430	AGO3	FBgn0250816	Abd-B	FBgn0000015
NA	FBgn0265792	CG33640	FBgn0053640	CG42598	FBgn0260997
NA	FBgn0058182	ND-AGGG	FBgn0085736	NA	FBgn0267430
CG40439	FBgn0284080	Su(z)2	FBgn0265623	CG14905	FBgn0038452
Ir41a	FBgn0040849	spi	FBgn0005672	CG17514	FBgn0039959
NA	FBgn0266727	CG17018	FBgn0039972	CG41242	FBgn0085569
AGO3	FBgn0250816	NA	FBgn0267571	AGO3	FBgn0250816
NA	FBgn0265676	ATPsynG	FBgn0010612	lbl	FBgn0008651
NA	FBgn0267744	Set1	FBgn0040022	CG5382	FBgn0038950
ND-MLRQ	FBgn0052230	Scgdelta	FBgn0025391	Axn	FBgn0026597
NA	FBgn0267797	ST6Gal	FBgn0035050	CG42402	FBgn0259821
Set1	FBgn0040022	CG44837	FBgn0266100	NA	FBgn0058461
Tsp	FBgn0031850	Ir41a	FBgn0040849	Dr	FBgn0000492
NA	FBgn0264371	fng	FBgn0011591	NA	FBgn0058182
NA	FBgn0267524	CG14506	FBgn0039659	NA	FBgn0058182
NA	FBgn0267798	CG11961	FBgn0034436	CG30048	FBgn0050048
Cht10	FBgn0250907	Mef2	FBgn0011656	NA	FBgn0266762
CG42402	FBgn0259821	sv	FBgn0005561	CG17378	FBgn0031858
CG4374	FBgn0039078	NA	FBgn0085804	CG42598	FBgn0260997
NA	FBgn0267864	NA	FBgn0266153	Dek	FBgn0026533
NA	FBgn0266850	robl37BC	FBgn0028569	nyo	FBgn0039852
NA	FBgn0266842	CG4374	FBgn0039078	ND-AGGG	FBgn0085736
NA	FBgn0058182	NA	FBgn0051840	Mef2	FBgn0011656
CG44174	FBgn0265063	Sfp78E	FBgn0261059	Sidpn	FBgn0032741
ND-MLRQ	FBgn0052230	PRAS40	FBgn0267824	raw	FBgn0003209
NA	FBgn0267133	Galphao	FBgn0001122	CG12158	FBgn0040775

NA	FBgn0039987	Ser	FBgn0004197	NA	FBgn0260469
mdy	FBgn0004797	Ssdp	FBgn0011481	NA	FBgn0264370
CG42238	FBgn0250867	hb	FBgn0001180	Set1	FBgn0040022
NA	FBgn0085784	CG46301	FBgn0283651	mfrn	FBgn0039561
santa-maria	FBgn0025697	NA	FBgn0267798	Dys	FBgn0260003
ORY	FBgn0046323	CG30371	FBgn0050371	NA	FBgn0267798
reb	FBgn0033667	cpo	FBgn0263995	Vha55	FBgn0005671
NA	FBgn0267430	ACC	FBgn0033246	NA	FBgn0002526
CG32248	FBgn0052248	CG10510	FBgn0037059	NA	FBgn0085734
Myo81F	FBgn0267431	Eip75B	FBgn0000568	CG9084	FBgn0033582
CG40813	FBgn0085521	CG1142	FBgn0037504	Zip99C	FBgn0039714
NA	FBgn0266747	CG13160	FBgn0033720	NA	FBgn0264548
RYa	FBgn0085512	CG14506	FBgn0039659	NA	FBgn0263664
NA	FBgn0265994	NA	FBgn0267798	NA	FBgn0267519
CG44102	FBgn0264911	NA	FBgn0266747	laza	FBgn0037163
CG43203	FBgn0262839	CG7956	FBgn0038890	CG14259	FBgn0039483
NA	FBgn0266032	Droj2	FBgn0038145	Argk	FBgn0000116
NA	FBgn0267987	CG5909	FBgn0039495	Cht10	FBgn0250907
CG43098	FBgn0262544	Pdp1	FBgn0016694	Cpr47Ee	FBgn0033602
NA	FBgn0058182	red	FBgn0285913	Corin	FBgn0033192
CG42598	FBgn0260997	CG31191	FBgn0051191	CG42598	FBgn0260997
bdl	FBgn0028482	CG16791	FBgn0038881	GstD11	FBgn0038029
CG15800	FBgn0034904	CG3394	FBgn0034999	NAT1	FBgn0010488
CG17018	FBgn0039972	Hs3st-A	FBgn0053147	NA	FBgn0267798
Ref2	FBgn0032439	pHCl-1	FBgn0264908	NA	FBgn0267430
kni	FBgn0001320	NA	FBgn0050298	CG6424	FBgn0028494
CG5532	FBgn0034902	serp	FBgn0260653	NA	FBgn0085784
NA	FBgn0265719	NA	FBgn0266768	CG4502	FBgn0031896
NA	FBgn0266153	FASN3	FBgn0040001	Ir21a	FBgn0031209
CG43203	FBgn0262839	NA	FBgn0266323	CG42831	FBgn0262020
NA	FBgn0266842	Rpn12R	FBgn0036465	subdued	FBgn0038721
MFS17	FBgn0058263	NA	FBgn0263336	sick	FBgn0263873
NA	FBgn0267708	tnc	FBgn0039257	ND-SGDH	FBgn0011455
CG7365	FBgn0036939	CG13252	FBgn0037016	Slmap	FBgn0040011
NA	FBgn0266842	wg	FBgn0284084	CG17684	FBgn0263780
dpy	FBgn0053196	CG34114	FBgn0083950	shep	FBgn0052423
frac	FBgn0035798	drm	FBgn0024244	CG13577	FBgn0034998
NA	FBgn0266590	CASK	FBgn0013759	Glut1	FBgn0264574
CG40228	FBgn0063670	CG43294	FBgn0262986	Trl	FBgn0013263
NA	FBgn0266953	NUCB1	FBgn0052190	Argk	FBgn0000116
CG6225	FBgn0038072	wdp	FBgn0034718	NA	FBgn0264835

thw	FBgn0037487	Lac	FBgn0010238	CG13921	FBgn0035267
Ncc69	FBgn0036279	Naa20B	FBgn0051851	danr	FBgn0039283
NA	FBgn0266747	Oseg2	FBgn0035317	inv	FBgn0001269
NA	FBgn0266590	scro	FBgn0028993	NA	FBgn0266747
NA	FBgn0266909	NA	FBgn0262391	CNMaR	FBgn0053696
NA	FBgn0266747	RpL18A	FBgn0010409	kcc	FBgn0261794
CG13676	FBgn0035844	Or22a	FBgn0026398	CG44102	FBgn0264911
spir	FBgn0003475	Pkc98E	FBgn0003093	Aps	FBgn0036111
PRY	FBgn0267489	Yeti	FBgn0267398	ND-AGGG	FBgn0058002
NA	FBgn0085804	NA	FBgn0266825	CG40228	FBgn0063670
CG44085	FBgn0264894	CG42402	FBgn0259821	NA	FBgn0285940
NA	FBgn0264835	CG17018	FBgn0039972	Ir94g	FBgn0039079
NA	FBgn0264569	LManIII	FBgn0032066	CG11486	FBgn0035397
NA	FBgn0266684	lola	FBgn0283521	NA	FBgn0266747
NA	FBgn0267430	CG3092	FBgn0034835	Oda	FBgn0014184
NA	FBgn0267430	Strn-Mlck	FBgn0265045	Hr51	FBgn0034012
exp	FBgn0033668	lig	FBgn0020279	amon	FBgn0023179
NA	FBgn0266251	CG30497	FBgn0050497	NA	FBgn0264914
NA	FBgn0262437	scro	FBgn0028993	CG2993	FBgn0037521
Strn-Mlck	FBgn0265045	CG7255	FBgn0036493	CG17684	FBgn0263780
vvl	FBgn0086680	CG17744	FBgn0035730	psq	FBgn0263102
Gr28a	FBgn0041247	NA	FBgn0002526	Pglym78	FBgn0014869
NA	FBgn0266747	NA	FBgn0085612	Apc	FBgn0015589
NA	FBgn0266632	NA	FBgn0267430	NA	FBgn0266908
Myo81F	FBgn0267431	klar	FBgn0001316	IntS3	FBgn0262117
CG34398	FBgn0085427	NA	FBgn0085784	CG5377	FBgn0038974
NA	FBgn0267983	CG6225	FBgn0038072	Cyt-c-p	FBgn0284248
CG40178	FBgn0058178	CG7029	FBgn0039026	CG15561	FBgn0039829
CG43203	FBgn0262839	eya	FBgn0000320	tutl	FBgn0010473
NA	FBgn0267132	CG13155	FBgn0033723	NA	FBgn0267797
CG8180	FBgn0034021	RhoGEF3	FBgn0264707	Nckx30C	FBgn0028704
CG43203	FBgn0262839	Tsp39D	FBgn0032943	CG43098	FBgn0262544
CG17514	FBgn0039959	NA	FBgn0058182	Obp28a	FBgn0011283
NA	FBgn0039987	CG13721	FBgn0035554	CG34384	FBgn0085413
nolo	FBgn0051619	CG13894	FBgn0035157	ap	FBgn0267978
exp	FBgn0033668	oys	FBgn0033476	gish	FBgn0250823
NA	FBgn0085664	east	FBgn0261954	CG40470	FBgn0058470
TpnC4	FBgn0033027	NA	FBgn0267797	stmA	FBgn0086784
NA	FBgn0267301	sba	FBgn0016754	CG40439	FBgn0284080
Fad2	FBgn0029172	cv-c	FBgn0285955	atms	FBgn0010750
NA	FBgn0260469	NA	FBgn0052123	NA	FBgn0267797

NA	FBgn0266905	NA	FBgn0266684	jumu	FBgn0015396
ImpE1	FBgn0001253	FASN3	FBgn0040001	CG18012	FBgn0038552
NA	FBgn0040569	hdc	FBgn0010113	Taf4	FBgn0010280
NA	FBgn0267797	AGO3	FBgn0250816	Kr-h1	FBgn0266450
Swim	FBgn0034709	CG11357	FBgn0035558	Kul	FBgn0039688
NA	FBgn0085804	Slmap	FBgn0040011	scramb1	FBgn0052056
ND-AGGG	FBgn0058002	AGO3	FBgn0250816	NA	FBgn0267798
Nipped-A	FBgn0053554	CG13723	FBgn0036705	CG5726	FBgn0034313
NA	FBgn0267798	Lsp1gamma	FBgn0002564	NA	FBgn0265896
IntS3	FBgn0262117	NA	FBgn0039987	CG31343	FBgn0051343
CG31750	FBgn0046888	NA	FBgn0267519	CG41099	FBgn0039955
NA	FBgn0267797	CG42637	FBgn0261360	CG10845	FBgn0039246
CG13492	FBgn0034662	CG17974	FBgn0034624	Cow	FBgn0039054
NA	FBgn0266153	Cht10	FBgn0250907	NA	FBgn0266747
CG5853	FBgn0032167	NA	FBgn0058182	Arf79F	FBgn0010348
NA	FBgn0267144	l(2)k14710	FBgn0021847	NA	FBgn0058182
NA	FBgn0267524	bwa	FBgn0045064	ImpL2	FBgn0001257
spok	FBgn0086917	tok	FBgn0004885	Treh	FBgn0003748
CG45781	FBgn0267428	pan	FBgn0085432	CG2225	FBgn0032957
NA	FBgn0085771	Naa15-16	FBgn0031020	RanBPM	FBgn0262114
NA	FBgn0051228	Rbp	FBgn0262483	ari-2	FBgn0025186
NA	FBgn0266842	CG42523	FBgn0260428	Smg5	FBgn0019890
CG45781	FBgn0267428	bab1	FBgn0004870	gprs	FBgn0024232
NA	FBgn0267798	da	FBgn0267821	nyo	FBgn0039852
CG18622	FBgn0038460	Pi3K68D	FBgn0015278	CG43742	FBgn0263999
CG17514	FBgn0039959	scro	FBgn0028993	CG9815	FBgn0034861
NA	FBgn0039987	GstE12	FBgn0027590	CG9801	FBgn0037623
NA	FBgn0267797	CG14137	FBgn0036178	CenG1A	FBgn0028509
Cyp6d4	FBgn0039006	mor	FBgn0002783	CG11349	FBgn0035550
Cpr49Ag	FBgn0033730	CG43795	FBgn0264339	NA	FBgn0266747
CG42598	FBgn0260997	knrl	FBgn0001323	NA	FBgn0260435
ems	FBgn0000576	NA	FBgn0267430	MFS17	FBgn0058263
htl	FBgn0010389	ASPP	FBgn0034606	CG31808	FBgn0062978
CG42402	FBgn0259821	CG6495	FBgn0027550	NA	FBgn0267797
NA	FBgn0039987	kni	FBgn0001320	nyo	FBgn0039852
l(2)k05911	FBgn0284244	bun	FBgn0259176	tipE	FBgn0003710
NA	FBgn0267797	CG42337	FBgn0259239	CG45781	FBgn0267428
NA	FBgn0264569	CG30438	FBgn0050438	PIG-Z	FBgn0266438
NA	FBgn0267797	CG43203	FBgn0262839	Glut4EF	FBgn0267336
CG41099	FBgn0039955	CG30389	FBgn0050389	CG11399	FBgn0037021
NA	FBgn0085804	NA	FBgn0267797	CG12163	FBgn0260462

NA	FBgn0265255	Eaat2	FBgn0026438	NA	FBgn0266684
NA	FBgn0058182	CG17018	FBgn0039972	Uev1A	FBgn0035601
Eaf6	FBgn0035624	NA	FBgn0262331	CG1927	FBgn0027547
NA	FBgn0039987	mam	FBgn0002643	NA	FBgn0267133
NA	FBgn0085804	crb	FBgn0259685	cact	FBgn0000250
NA	FBgn0263588	NA	FBgn0082980	CG33012	FBgn0053012
Jheh3	FBgn0034406	Pep	FBgn0004401	knrl	FBgn0001323
NA	FBgn0040045	CG10428	FBgn0032724	NA	FBgn0267794
dsx-c73A	FBgn0261799	CG6793	FBgn0036242	wntD	FBgn0038134
Doc2	FBgn0035956	NA	FBgn0085804	Myo81F	FBgn0267431
NA	FBgn0267798	Mctp	FBgn0034389	Ald	FBgn0000064
CG41284	FBgn0085599	NA	FBgn0267203	CG8498	FBgn0031992
NA	FBgn0085570	CG42598	FBgn0260997	CG18666	FBgn0040967
CG14838	FBgn0035799	NA	FBgn0267733	CG13023	FBgn0036677
CG40228	FBgn0063670	NA	FBgn0264914	Sln	FBgn0033657
NA	FBgn0264914	CG15019	FBgn0035541	NA	FBgn0266747
NA	FBgn0267798	mei-S332	FBgn0002715	mey	FBgn0039851
thw	FBgn0037487	mts	FBgn0004177	NA	FBgn0265149
Myo81F	FBgn0267431	sqd	FBgn0263396	CG11570	FBgn0036230
CG32447	FBgn0052447	jeb	FBgn0086677	NA	FBgn0267460
NA	FBgn0058182	CG41099	FBgn0039955	Rab26	FBgn0086913
NA	FBgn0267797	NA	FBgn0266747	NA	FBgn0266690
IM14	FBgn0067905	NA	FBgn0266747	NA	FBgn0011861
NA	FBgn0085804	Dh31-R	FBgn0052843	UQCR-Q	FBgn0036728
CG17684	FBgn0263780	CG4036	FBgn0032149	jim	FBgn0027339
NA	FBgn0267430	Pax	FBgn0041789	lov	FBgn0266129
CG40228	FBgn0063670	chrb	FBgn0036165	jumu	FBgn0015396
spok	FBgn0086917	NA	FBgn0085804	ps	FBgn0261552
CG18417	FBgn0035780	CG6701	FBgn0033889	CG9945	FBgn0034527
CG45781	FBgn0267428	l(3)neo38	FBgn0265276	CG7781	FBgn0032021
axo	FBgn0262870	CG44174	FBgn0265063	Myo81F	FBgn0267431
NA	FBgn0058182	Cam	FBgn0000253	CG4374	FBgn0039078
NA	FBgn0051432	par-1	FBgn0260934	Mhc	FBgn0264695
NA	FBgn0267133	NA	FBgn0085784	NA	FBgn0261700
Sb	FBgn0003319	Dop1R1	FBgn0011582	trio	FBgn0024277
NA	FBgn0261453	CG17075	FBgn0031239	NA	FBgn0085734
CG41242	FBgn0085569	dysc	FBgn0264006	Lk6	FBgn0017581
NA	FBgn0267798	Galphaq	FBgn0004435	NA	FBgn0039987
NA	FBgn0039987	Np	FBgn0265011	CG43441	FBgn0263389
CG4622	FBgn0035021	Ir41a	FBgn0040849	CG7168	FBgn0038586
ITP	FBgn0035023	NA	FBgn0085804	CG18666	FBgn0040967

CG16886	FBgn0028938	pros	FBgn0004595	ppk26	FBgn0035785
AGO3	FBgn0250816	beat-Vc	FBgn0038084	nvd	FBgn0259697
CG15800	FBgn0034904	NA	FBgn0263091	CG42337	FBgn0259239
CG17018	FBgn0039972	Galphao	FBgn0001122	NA	FBgn0039987
NA	FBgn0267797	NA	FBgn0265719	CG16896	FBgn0035073
NA	FBgn0085582	NA	FBgn0266969	ND-MLRQ	FBgn0052230
Oatp58Dc	FBgn0034716	cnk	FBgn0021818	NA	FBgn0011915
spok	FBgn0086917	CG6191	FBgn0027581	NA	FBgn0085786
NA	FBgn0085804	CG40160	FBgn0058160	NA	FBgn0265896
CG14621	FBgn0031183	CG40228	FBgn0063670	NA	FBgn0085784
CG15800	FBgn0034904	NA	FBgn0267797	CG10182	FBgn0039091
NA	FBgn0267797	Atpalpha	FBgn0002921	CG43694	FBgn0263777
CG43203	FBgn0262839	Snoo	FBgn0085450	seq	FBgn0028991
eg	FBgn0000560	Cdep	FBgn0265082	NA	FBgn0266747
NA	FBgn0085784	Gp150	FBgn0013272	Hrb98DE	FBgn0001215
Myo81F	FBgn0267431	CG14606	FBgn0037485	NA	FBgn0265067
NA	FBgn0266747	CG17018	FBgn0039972	h	FBgn0001168
NA	FBgn0085664	Pak	FBgn0267698	Ir41a	FBgn0040849
AGO3	FBgn0250816	CG11151	FBgn0030519	Hrb27C	FBgn0004838
Best2	FBgn0035696	Myo81F	FBgn0267431	CG32447	FBgn0052447
NA	FBgn0266944	NA	FBgn0266747	CG13920	FBgn0025712
Eig71Eh	FBgn0014848	salr	FBgn0000287	CG6785	FBgn0032399
Slmap	FBgn0040011	aop	FBgn0000097	NA	FBgn0266909
NA	FBgn0265951	NA	FBgn0267939	NA	FBgn0265149
CG42598	FBgn0260997	dpr19	FBgn0032233	eRF3	FBgn0020443
NA	FBgn0265371	NA	FBgn0263557	Cyt-b5-r	FBgn0000406
CG40228	FBgn0063670	NA	FBgn0264914	Blimp-1	FBgn0035625
NA	FBgn0267524	CG13049	FBgn0036592	Syx1A	FBgn0013343
CG13047	FBgn0036594	l(1)G0156	FBgn0027291	Acsl	FBgn0263120
NA	FBgn0267524	CG17684	FBgn0263780	NA	FBgn0264704
NA	FBgn0267797	NA	FBgn0266909	Syx1A	FBgn0013343
Myo81F	FBgn0267431	Diap1	FBgn0260635	NA	FBgn0266892
NA	FBgn0058182	CG34429	FBgn0085458	NA	FBgn0267460
NA	FBgn0058182	Samuel	FBgn0032330	ced-6	FBgn0029092
ds	FBgn0284247	ND-20L	FBgn0039669	Cap-H2	FBgn0037831
NA	FBgn0266703	Pka-R1	FBgn0259243	Cp1	FBgn0013770
sit	FBgn0038986	lute	FBgn0262871	smg	FBgn0016070
NA	FBgn0267797	tutl	FBgn0010473	Men	FBgn0002719
NA	FBgn0267797	CG11000	FBgn0263353	Slmap	FBgn0040011
CG17154	FBgn0036246	NA	FBgn0265593	Fas3	FBgn0000636
spok	FBgn0086917	NA	FBgn0260469	retm	FBgn0031814

CG17683	FBgn0262115	NA	FBgn0267608	en	FBgn0000577
CG32407	FBgn0052407	NA	FBgn0264880	NA	FBgn0085734
CG34289	FBgn0085318	sob	FBgn0004892	NA	FBgn0266782
Duox	FBgn0283531	NA	FBgn0058182	put	FBgn0003169
CG10348	FBgn0032707	CG43066	FBgn0262476	CG45782	FBgn0267429
CG31176	FBgn0051176	fne	FBgn0086675	Rab30	FBgn0031882
CG34289	FBgn0085318	NA	FBgn0039987	Tsp29Fa	FBgn0032074
CG6793	FBgn0036242	Dmtn	FBgn0037443	CG40228	FBgn0063670
CG45781	FBgn0267428	EcR	FBgn0000546	NA	FBgn0085804
Ir56d	FBgn0034458	CG5945	FBgn0032494	Pal2	FBgn0262728
AGO3	FBgn0250816	CG10384	FBgn0034731	CG10863	FBgn0027552
CG13722	FBgn0035553	NA	FBgn0262368	eIF4B	FBgn0020660
NA	FBgn0264569	tow	FBgn0035719	CG7920	FBgn0039737
NA	FBgn0085804	CG18812	FBgn0042135	CG1265	FBgn0035517
for	FBgn0000721	roq	FBgn0036621	CG31523	FBgn0051523
NA	FBgn0263495	cv-c	FBgn0285955	CG12769	FBgn0033252
Cyp4ad1	FBgn0033292	NA	FBgn0085804	CG31140	FBgn0051140
NA	FBgn0260435	numb	FBgn0002973	CG30440	FBgn0050440
CG15167	FBgn0032709	NA	FBgn0267133	fdl	FBgn0045063
NA	FBgn0264914	NA	FBgn0085612	CG3061	FBgn0038195
NA	FBgn0265371	RhoGEF64C	FBgn0035574	Hmx	FBgn0264005
Fatp	FBgn0267828	Skadu	FBgn0259922	CG33111	FBgn0053111
NA	FBgn0012016	arr	FBgn0000119	Atx2	FBgn0041188
Lcp65Ad	FBgn0020641	NA	FBgn0265896	dati	FBgn0262636
en	FBgn0000577	exp	FBgn0033668	MED19	FBgn0036761
CG11438	FBgn0037164	CG17508	FBgn0039970	LManV	FBgn0032068
CG4374	FBgn0039078	Cul3	FBgn0261268	alphaTub 84B	FBgn0003884
Scp1	FBgn0020908	CG10413	FBgn0032689	CG17018	FBgn0039972
NA	FBgn0267797	HnRNP-K	FBgn0267791	CG45781	FBgn0267428
RluA-1	FBgn0051719	Iris	FBgn0031305	ATPsynF	FBgn0035032
CG13040	FBgn0036608	NA	FBgn0058182	NA	FBgn0058182
NA	FBgn0085734	pros	FBgn0004595	CG11069	FBgn0039244
NA	FBgn0266690	Tsp42Ej	FBgn0033132	NA	FBgn0267430
uif	FBgn0031879	wg	FBgn0284084	CG43783	FBgn0264305
NA	FBgn0267798	NA	FBgn0265525	NA	FBgn0085804
CG34038	FBgn0054038	TAF1B	FBgn0037792	NA	FBgn0011868
NA	FBgn0052127	CG7368	FBgn0036179	Slmap	FBgn0040011
NA	FBgn0085784	wun	FBgn0016078	Mpc1	FBgn0038662
Ser	FBgn0004197	CG11505	FBgn0035424	Mbs	FBgn0005536
CG44102	FBgn0264911	CG44098	FBgn0264907	NA	FBgn0266747
CG40006	FBgn0058006	NA	FBgn0284415	slim	FBgn0261477

CG17475	FBgn0038481	CG11486	FBgn0035397	NA	FBgn0266762
DNApol-alpha180	FBgn0259113	Lpin	FBgn0263593	NA	FBgn0263764
NA	FBgn0266747	AspRS	FBgn0002069	unk	FBgn0004395
NA	FBgn0264835	NA	FBgn0266747	NA	FBgn0085734
NA	FBgn0259859	Daxx	FBgn0031820	Arl5	FBgn0035866
salm	FBgn0261648	Acsl	FBgn0263120	Ufl1	FBgn0037467
NA	FBgn0267430	NA	FBgn0085784	Sap47	FBgn0013334
NA	FBgn0265546	ftz-f1	FBgn0001078	CG14762	FBgn0033250
NA	FBgn0267798	CG4374	FBgn0039078	Myo81F	FBgn0267431
CG17018	FBgn0039972	l(3)04053	FBgn0010830	CG6115	FBgn0040985
NA	FBgn0265062	CG3529	FBgn0035995	NA	FBgn0264548
NA	FBgn0267797	NA	FBgn0262378	Rab14	FBgn0015791
NA	FBgn0267446	NA	FBgn0263413	Tsp29Fa	FBgn0032074
CG40439	FBgn0284080	CG9005	FBgn0033638	Tm1	FBgn0003721
knrl	FBgn0001323	vvl	FBgn0086680	CG11313	FBgn0039798
NA	FBgn0267797	NA	FBgn0266640	CG15172	FBgn0032740
CG15544	FBgn0039804	cic	FBgn0262582	cue	FBgn0011204
NA	FBgn0260469	NA	FBgn0266849	CG13850	FBgn0038961
AGO3	FBgn0250816	btsz	FBgn0266756	SCAP	FBgn0033052
Ir41a	FBgn0040849	NA	FBgn0267008	NA	FBgn0264548
NA	FBgn0267797	Glut1	FBgn0264574	Kdm2	FBgn0037659
NA	FBgn0259855	salr	FBgn0000287	dpp	FBgn0000490
NA	FBgn0266747	NA	FBgn0267746	Sin3A	FBgn0022764
NimA	FBgn0261514	CG2747	FBgn0037541	pgant5	FBgn0031681
ITP	FBgn0035023	CG31343	FBgn0051343	NA	FBgn0266747
UQCR-11	FBgn0260008	CG5535	FBgn0036764	RYa	FBgn0085512
Strn-Mlck	FBgn0265045	CG6145	FBgn0033853	CG43694	FBgn0263777
NA	FBgn0267798	CG17544	FBgn0032775	dsd	FBgn0039528
NA	FBgn0085734	Galphas	FBgn0001123	l(3)02640	FBgn0010786
CG40178	FBgn0058178	PRY	FBgn0267489	CG15431	FBgn0031602
NA	FBgn0284412	m-cup	FBgn0038488	MFS17	FBgn0058263
Nplp3	FBgn0042201	Myo81F	FBgn0267431	NA	FBgn0266323
CG41242	FBgn0085569	Hnf4	FBgn0004914	CG17739	FBgn0033710
NA	FBgn0266825	NA	FBgn0267199	CG3434	FBgn0036000
CG17104	FBgn0040496	Myo81F	FBgn0267431	CG3793	FBgn0028507
CG13280	FBgn0032609	c(3)G	FBgn0000246	CalpA	FBgn0012051
dpy	FBgn0053196	CG12684	FBgn0029717	CG3650	FBgn0035070
Maf1	FBgn0267861	Cpr49Af	FBgn0033729	NA	FBgn0085664
eIF4B	FBgn0020660	CG13506	FBgn0034723	NA	FBgn0085734
NA	FBgn0266747	Rbbp5	FBgn0036973	Tnpo	FBgn0024921
NA	FBgn0266747	MFS17	FBgn0058263	GstZ2	FBgn0037697

CG43968	FBgn0264699	D	FBgn0000411	Cka	FBgn0044323
wg	FBgn0284084	mey	FBgn0039851	wech	FBgn0259745
CG14605	FBgn0037486	CG16972	FBgn0032481	NA	FBgn0085582
ND-20L	FBgn0039669	NA	FBgn0266747	mrt	FBgn0039507
CG15167	FBgn0032709	CG4297	FBgn0031258	CG4374	FBgn0039078
NA	FBgn0267430	cdi	FBgn0004876	CG18666	FBgn0040967
CG41378	FBgn0085638	Gasp	FBgn0026077	NA	FBgn0264548
CG8172	FBgn0033362	nyo	FBgn0039852	CG10226	FBgn0035695
NA	FBgn0267798	NA	FBgn0266842	NA	FBgn0267146
NA	FBgn0264835	ttk	FBgn0003870	CG31013	FBgn0051013
NA	FBgn0266909	CG41099	FBgn0039955	laf	FBgn0020280
Tsp	FBgn0031850	Rbp6	FBgn0260943	CG5361	FBgn0037786
AGO3	FBgn0250816	CG43203	FBgn0262839	spok	FBgn0086917
CG41520	FBgn0087011	cdc14	FBgn0031952	NA	FBgn0085582
CG30048	FBgn0050048	CG41284	FBgn0085599	Ser	FBgn0004197
CG40228	FBgn0063670	NA	FBgn0265594	NA	FBgn0266323
CG43098	FBgn0262544	yps	FBgn0022959	NA	FBgn0266909
NA	FBgn0058182	CG12581	FBgn0037213	Syp	FBgn0038826
CG43203	FBgn0262839	CG7458	FBgn0037144	GlyRS	FBgn0027088
NA	FBgn0039987	cv-c	FBgn0285955	CG13492	FBgn0034662
NA	FBgn0058182	l(2)dtl	FBgn0013548	Asph	FBgn0034075
ine	FBgn0011603	NA	FBgn0267620	NA	FBgn0085734
NA	FBgn0263496	CG40498	FBgn0069969	Lis-1	FBgn0015754
NA	FBgn0267798	Nf1	FBgn0015269	CG1427	FBgn0037347
NA	FBgn0058182	klg	FBgn0017590	Dat	FBgn0019643
NA	FBgn0265896	wmd	FBgn0034876	Akt1	FBgn0010379
NA	FBgn0267797	CG31221	FBgn0051221	dup	FBgn0000996
NA	FBgn0267798	CG16974	FBgn0032479	NA	FBgn0266747
scro	FBgn0028993	NA	FBgn0011865	CG12071	FBgn0039808
NA	FBgn0085804	CG9205	FBgn0035181	NA	FBgn0265419
grh	FBgn0259211	NA	FBgn0267430	NA	FBgn0267986
NA	FBgn0267133	CG2889	FBgn0030206	pnut	FBgn0013726
CG13251	FBgn0037014	mtd	FBgn0013576	Alh	FBgn0261238
CG32241	FBgn0052241	CG13300	FBgn0035699	CG13312	FBgn0035931
NA	FBgn0267798	sif	FBgn0085447	CG9507	FBgn0031808
CG15167	FBgn0032709	Sytbeta	FBgn0261090	NA	FBgn0266909
CG42402	FBgn0259821	CG12818	FBgn0037809	emp	FBgn0010435
NA	FBgn0264569	Idgf3	FBgn0020414	cry	FBgn0025680
CG17684	FBgn0263780	NA	FBgn0264914	NA	FBgn0264835
NA	FBgn0267473	Cdk12	FBgn0037093	NA	FBgn0263838
NA	FBgn0039987	NA	FBgn0264835	Pka-C2	FBgn0000274

NA	FBgn0264914	NA	FBgn0266747	Xe7	FBgn0010772
CG17018	FBgn0039972	Vha100-2	FBgn0028670	Strip	FBgn0035437
NA	FBgn0266747	Sb	FBgn0003319	spok	FBgn0086917
NA	FBgn0058182	NA	FBgn0267704	E(spl)m3-HLH	FBgn0002609
CG40178	FBgn0058178	kay	FBgn0001297	eff	FBgn0011217
CG30048	FBgn0050048	NA	FBgn0263869	Dak1	FBgn0028833
CG17018	FBgn0039972	ND-MLRQ	FBgn0052230	NA	FBgn0264569
CG41099	FBgn0039955	NA	FBgn0267753	cv-c	FBgn0285955
NA	FBgn0267430	fray	FBgn0023083	NA	FBgn0266747
NA	FBgn0267744	Akap200	FBgn0027932	SCCRO4	FBgn0036967
CG42284	FBgn0259179	miple2	FBgn0029002	fj	FBgn0000658
NA	FBgn0085734	Alk	FBgn0040505	NA	FBgn0264548
NA	FBgn0266747	dsx	FBgn0000504	NA	FBgn0266208
NA	FBgn0058182	NA	FBgn0085570	BEAF-32	FBgn0015602
nvd	FBgn0259697	CG31869	FBgn0051869	RpS9	FBgn0010408
eIF4B	FBgn0020660	heph	FBgn0011224	NA	FBgn0267703
NA	FBgn0267128	CG42598	FBgn0260997	crp	FBgn0001994
AGO3	FBgn0250816	ssp3	FBgn0032723	eIF4H2	FBgn0039797
knrl	FBgn0001323	Maf1	FBgn0267861	CG4360	FBgn0038787
Myo81F	FBgn0267431	CG13471	FBgn0036443	14-3-3epsilon	FBgn0020238
CG14305	FBgn0038630	bru2	FBgn0262475	Parp	FBgn0010247
NA	FBgn0266747	NA	FBgn0267798	CG11106	FBgn0030280
CG30043	FBgn0050043	CG7139	FBgn0027532		

Less accessible genes juvenile Bap60-KD MB compared to mature Bap60-KD MB					
Gene Symbol	**Flybase ID**	**Gene Symbol**	**Flybase ID**	**Gene Symbol**	**Flybase ID**
Atpalpha	FBgn0002921	CG4596	FBgn0037849	plx	FBgn0261261
Tpi	FBgn0086355	coro	FBgn0265935	NA	FBgn0011858
DUBAI	FBgn0033738	Glut4EF	FBgn0267336	Pcl	FBgn0003044
CG5590	FBgn0039537	CG31522	FBgn0051522	CG42809	FBgn0261991
NA	FBgn0065083	CG12589	FBgn0040684	Stip1	FBgn0024352
CG10947	FBgn0032857	Rrp4	FBgn0034879	tnc	FBgn0039257
CG18135	FBgn0036837	Sry-delta	FBgn0003512	Kap-alpha3	FBgn0027338
CG10170	FBgn0039085	Rtnl1	FBgn0053113	bma	FBgn0085385
Vps52	FBgn0031710	CG1688	FBgn0027589	NA	FBgn0263463
Tsp97E	FBgn0039465	Dpck	FBgn0037469	lilli	FBgn0041111
fwd	FBgn0004373	CG30076	FBgn0050076	NA	FBgn0263329

CG42389	FBgn0259735	XNP	FBgn0039338	NA	FBgn0266635
Uch-L5	FBgn0011327	Hsc70-4	FBgn0266599	NA	FBgn0266415
CG6791	FBgn0037918	NA	FBgn0284412	tex	FBgn0037569
CG9175	FBgn0031779	MED15	FBgn0027592	CG5290	FBgn0036772
U4-U6-60K	FBgn0036733	CG31007	FBgn0051007	NA	FBgn0262373
Tsp86D	FBgn0037848	CG7031	FBgn0039027	CG8379	FBgn0037638
trx	FBgn0003862	CG44290	FBgn0265317	NA	FBgn0262107
NA	FBgn0265419	Ccm3	FBgn0038331	NA	FBgn0283428
RpL32	FBgn0002626	neb	FBgn0004374	CG11857	FBgn0039303
COX5A	FBgn0019624	NA	FBgn0263049	CG16908	FBgn0037741
Hex-A	FBgn0001186	Hus1-like	FBgn0026417	NA	FBgn0052480
Sin3A	FBgn0022764	Diap1	FBgn0260635	NA	FBgn0267643
Pka-C1	FBgn0000273	beat-VII	FBgn0250908	Cyt-c1	FBgn0035600
Elp1	FBgn0037926	NA	FBgn0263413	CG7311	FBgn0028848
CG8314	FBgn0034057	Pp1alpha-96A	FBgn0003134	CG16772	FBgn0032835
NA	FBgn0263579	tHMG2	FBgn0038979	CG10737	FBgn0034420
NA	FBgn0266781	Pgk	FBgn0250906	CG32485	FBgn0052485
Pka-R2	FBgn0022382	CG14883	FBgn0038432	lectin-30A	FBgn0040097
CG17734	FBgn0037890	Abl	FBgn0000017	CG14864	FBgn0038311
CG5065	FBgn0034145	CG34172	FBgn0085201	NA	FBgn0266648
wde	FBgn0027499	psd	FBgn0086265	CG9773	FBgn0037609
NA	FBgn0264702	CG13766	FBgn0031834	CG34117	FBgn0083953
Art4	FBgn0037770	CheB53b	FBgn0261293	Pcyt2	FBgn0035231
CG31051	FBgn0051051	RpL26	FBgn0036825	DCTN6-p27	FBgn0086446
Ntf-2r	FBgn0032680	hth	FBgn0001235	Pka-R1	FBgn0259243
CG10949	FBgn0032858	CG34188	FBgn0085217	CG17883	FBgn0040005
Miro	FBgn0039140	CG17698	FBgn0040056	CG9596	FBgn0031832
sfl	FBgn0020251	bru2	FBgn0262475	Mob2	FBgn0259481
CG15561	FBgn0039829	CHMP2B	FBgn0035589	CG34045	FBgn0054045
Fmr1	FBgn0028734	CG8620	FBgn0040837	CG10853	FBgn0035478
psq	FBgn0263102	CG7461	FBgn0034432	Brf	FBgn0038499
Msp300	FBgn0261836	FASN1	FBgn0283427	NC2beta	FBgn0028926
nSyb	FBgn0013342	dpr5	FBgn0037908	lola	FBgn0283521
Arpc1	FBgn0001961	angel	FBgn0016762	NA	FBgn0262419
Abp1	FBgn0036372	NA	FBgn0266415	CG10748	FBgn0036327
CG31688	FBgn0263355	NA	FBgn0262391	CG46339	FBgn0285963
chb	FBgn0021760	CG11722	FBgn0037777	CG9664	FBgn0031515
NA	FBgn0262378	hppy	FBgn0263395	TfIIEalpha	FBgn0015828
gukh	FBgn0026239	NA	FBgn0267277	fkh	FBgn0000659
Drice	FBgn0019972	Mtp	FBgn0266369	Glt	FBgn0001114

mld	FBgn0263490	NA	FBgn0263579	Pfdn2	FBgn0010741
Bin1	FBgn0024491	CG33233	FBgn0053233	CG11263	FBgn0036330
Pp1-87B	FBgn0004103	tipE	FBgn0003710	Nelf-E	FBgn0017430
NA	FBgn0267133	CG14340	FBgn0031302	bma	FBgn0085385
dsd	FBgn0039528	CG10268	FBgn0032811	CG3714	FBgn0031589
slam	FBgn0043854	CG1607	FBgn0039844	Cam	FBgn0000253
GstD1	FBgn0001149	Cam	FBgn0000253	beta4GalNAcTA	FBgn0027538
dom	FBgn0020306	Tfb4	FBgn0031309	NA	FBgn0266390
FASN1	FBgn0283427	CG30463	FBgn0050463	Hasp	FBgn0032797
Atg13	FBgn0261108	DCAF12	FBgn0037980	CG31693	FBgn0051693
Nlp	FBgn0016685	Gug	FBgn0010825	NA	FBgn0265874
CG18812	FBgn0042135	spir	FBgn0003475	CG11200	FBgn0034500
alt	FBgn0038535	CG1236	FBgn0037370	NA	FBgn0267642
ms(3)K81	FBgn0002838	CG33143	FBgn0053143	NA	FBgn0267775
tamo	FBgn0041582	NA	FBgn0267626	CG14160	FBgn0036066
dpr5	FBgn0037908	NA	FBgn0267643	M1BP	FBgn0037621
Snap29	FBgn0034913	Sap47	FBgn0013334	retn	FBgn0004795
colt	FBgn0019830	CG8745	FBgn0036381	sona	FBgn0034903
AspRS	FBgn0002069	CG7069	FBgn0038952	CG12147	FBgn0037325
Sirt1	FBgn0024291	Klp54D	FBgn0263076	sbb	FBgn0285917
uri	FBgn0035025	CG8888	FBgn0033679	Nplp1	FBgn0035092
Hmu	FBgn0015737	CG15812	FBgn0035405	Cda9	FBgn0034197
Ncoa6	FBgn0031698	CG11576	FBgn0039882	CG43739	FBgn0263996
IntS12	FBgn0039459	CG4266	FBgn0034598	NimC4	FBgn0260011
beag	FBgn0037660	Klp59C	FBgn0034824	dgt3	FBgn0034569
Ddx1	FBgn0015075	14-3-3zeta	FBgn0004907	wrd	FBgn0042693
tws	FBgn0004889	CG31029	FBgn0051029	Dscam3	FBgn0261046
CG9960	FBgn0031454	CG4294	FBgn0034742	Hrb87F	FBgn0004237
CG6420	FBgn0039451	CG14100	FBgn0036889	Acam	FBgn0011273
fdl	FBgn0045063	bor	FBgn0040237	Rs1	FBgn0021995
CG45075	FBgn0266445	CG7705	FBgn0038639	CG45546	FBgn0267106
Eip74EF	FBgn0000567	mld	FBgn0263490	toc	FBgn0015600
Rdl	FBgn0004244	Drep2	FBgn0028408	Pdp1	FBgn0016694
mRpS18A	FBgn0051450	RpII18	FBgn0003275	Gfrl	FBgn0262869
P5cr	FBgn0015781	CG6726	FBgn0039049	NA	FBgn0265646
Capr	FBgn0042134	CG9467	FBgn0037758	CG11539	FBgn0039859
PSR	FBgn0038948	Scsalpha	FBgn0004888	Alk	FBgn0040505
CG2127	FBgn0033286	NA	FBgn0265444	Nup358	FBgn0039302
dpr4	FBgn0053512	Liprin-gamma	FBgn0034720	NA	FBgn0264266
jing	FBgn0086655	sll	FBgn0038524	sns	FBgn0024189

NA	FBgn0267742	CG9135	FBgn0031769	NA	FBgn0267774
CG12007	FBgn0037293	Not10	FBgn0260444	Pka-C1	FBgn0000273
Ube3a	FBgn0061469	Glut4EF	FBgn0267336	CG13561	FBgn0034906
DNApol-eta	FBgn0037141	AQP	FBgn0033807	CG42268	FBgn0259163
CG8027	FBgn0033392	BigH1	FBgn0038252	CG9928	FBgn0032472
CG31917	FBgn0031668	NA	FBgn0041721	CG43219	FBgn0262855
amon	FBgn0023179	Wdr33	FBgn0046222	CG7168	FBgn0038586
CG9425	FBgn0036451	CG13409	FBgn0038926	CG14661	FBgn0037288
BicD	FBgn0000183	CG6688	FBgn0039038	msps	FBgn0027948
NTPase	FBgn0024947	CG10749	FBgn0036328	spg	FBgn0264324
Glut4EF	FBgn0267336	NA	FBgn0262370	Prat2	FBgn0041194
NA	FBgn0267937	NA	FBgn0263338	CaBP1	FBgn0025678
CG31200	FBgn0051200	Spt-I	FBgn0086532	CG1907	FBgn0039674
Usp10	FBgn0052479	bond	FBgn0260942	CalpA	FBgn0012051
Atpalpha	FBgn0002921	CG3797	FBgn0036842	Cap-D2	FBgn0039680
Hexim	FBgn0038251	Slh	FBgn0264978	NA	FBgn0262391
Mtpalpha	FBgn0028479	hb	FBgn0001180	porin	FBgn0004363
spir	FBgn0003475	NA	FBgn0263626	l(2)35Be	FBgn0261881
CG3634	FBgn0037026	Dys	FBgn0260003	dpr12	FBgn0085414
Non2	FBgn0035370	CG3358	FBgn0033117	CG31677	FBgn0051677
CG7484	FBgn0036745	bdl	FBgn0028482	CG15160	FBgn0032688
NA	FBgn0266416	CG9986	FBgn0039589	RpS15	FBgn0034138
CG3822	FBgn0038837	px	FBgn0003175	CG42355	FBgn0259701
CG2614	FBgn0032873	Desat1	FBgn0086687	CG3773	FBgn0038692
CG14591	FBgn0033054	Nrk	FBgn0020391	CG42489	FBgn0259992
NA	FBgn0065096	ND-ACP	FBgn0011361	loqs	FBgn0032515
pins	FBgn0040080	CG8086	FBgn0032010	Eip75B	FBgn0000568
Argk	FBgn0000116	Pfdn5	FBgn0038976	Irk3	FBgn0032706
Fbw5	FBgn0031773	CG16753	FBgn0035393	fz2	FBgn0016797
Hrb98DE	FBgn0001215	Sin3A	FBgn0022764	NA	FBgn0266771
CCDC53	FBgn0031979	fz	FBgn0001085	CG8746	FBgn0033330
w-cup	FBgn0032269	beag	FBgn0037660	CG7492	FBgn0035807
Eip74EF	FBgn0000567	NA	FBgn0263539	CG11396	FBgn0037022
dpr12	FBgn0085414	NA	FBgn0086200	NA	FBgn0266985
noi	FBgn0014366	ohgt	FBgn0037780	CG8272	FBgn0033337
NA	FBgn0266909	CG43445	FBgn0263399	CG30015	FBgn0050015
Acp33A	FBgn0267327	CG9253	FBgn0032919	jing	FBgn0086655
CCT7	FBgn0037632	CG8003	FBgn0036096	NA	FBgn0262331
NA	FBgn0266414	NA	FBgn0262378	Nup44A	FBgn0033247
bru1	FBgn0000114	CG10914	FBgn0034307	NA	FBgn0266942
VepD	FBgn0053200	NA	FBgn0264508	Xpc	FBgn0004698

Rpn2	FBgn0028692	Oseg2	FBgn0035317	NA	FBgn0264470
CG5361	FBgn0037786	TTLL3A	FBgn0031854	Sry-alpha	FBgn0003510
bic	FBgn0000181	Sfp79B	FBgn0259973	CG8321	FBgn0033677
CG14352	FBgn0031351	Gfrl	FBgn0262869	Sec23	FBgn0262125
Edc3	FBgn0036735	CG34377	FBgn0263117	Tim17b2	FBgn0020371
mbc	FBgn0015513	CG10383	FBgn0032699	CG31769	FBgn0051769
PNPase	FBgn0039846	NA	FBgn0266831	NA	FBgn0267993
NA	FBgn0086039	DNApol-gamma35	FBgn0004407	CG10463	FBgn0032819
CG4022	FBgn0035986	grau	FBgn0001133	CG7137	FBgn0034422
ebi	FBgn0263933	CG5867	FBgn0027586	NA	FBgn0264723
CG11137	FBgn0037199	Cks85A	FBgn0037613	bru3	FBgn0264001
Gp93	FBgn0039562	CG1890	FBgn0039869	CG4497	FBgn0031895
COX4	FBgn0032833	mad2	FBgn0035640	NA	FBgn0263442
REPTOR	FBgn0039209	NA	FBgn0264470	LysRS	FBgn0027084
Shroom	FBgn0085408	coro	FBgn0265935	NA	FBgn0263577
elm	FBgn0037358	CG43192	FBgn0262821	CG15432	FBgn0031603
CG6695	FBgn0039215	CG5608	FBgn0038058	CG30369	FBgn0050369
CG31191	FBgn0051191	mtSSB	FBgn0010438	Xrp1	FBgn0261113
CG15005	FBgn0035508	CG3792	FBgn0031662	CG4537	FBgn0032153
Calx	FBgn0013995	HP1c	FBgn0039019	aru	FBgn0029095
Glut4EF	FBgn0267336	fray	FBgn0023083	Ars2	FBgn0033062
robo3	FBgn0041097	NA	FBgn0266895	Hmg-2	FBgn0026582
RpL38	FBgn0040007	CG15167	FBgn0032709	pasi1	FBgn0038545
ND-B12	FBgn0034645	NA	FBgn0267799	robo1	FBgn0005631
CG18549	FBgn0038053	CG5065	FBgn0034145	oaf	FBgn0011818
Arfip	FBgn0037884	shg	FBgn0003391	Trs31	FBgn0266723
beat-VI	FBgn0039584	NA	FBgn0267249	Or22c	FBgn0026396
CG9257	FBgn0032916	Sce	FBgn0003330	CG6271	FBgn0039476
Gfrl	FBgn0262869	NA	FBgn0264378	chinmo	FBgn0086758
CG2911	FBgn0037350	MtnE	FBgn0262146	NA	FBgn0263664
CG14967	FBgn0035420	Tm1	FBgn0003721	NA	FBgn0266800
Src42A	FBgn0264959	CG14650	FBgn0037252	CG9988	FBgn0039591
Rac1	FBgn0010333	Aldh-III	FBgn0010548	CG6115	FBgn0040985
NA	FBgn0065098	Eip75B	FBgn0000568	Rbp6	FBgn0260943
ATPsyngamma	FBgn0020235	CG12502	FBgn0035171	CG32202	FBgn0052202
Ag5r	FBgn0015010	HipHop	FBgn0036815	CG15394	FBgn0250835
RpLP1	FBgn0002593	Taf13	FBgn0032847	Vps25	FBgn0022027
Pde8	FBgn0266377	CG1688	FBgn0027589	NA	FBgn0267724
Tet	FBgn0263392	CG10182	FBgn0039091	cN-IIIB	FBgn0034988
Golgin245	FBgn0034854	PNPase	FBgn0039846	NA	FBgn0262689
CG13705	FBgn0035582	NA	FBgn0267581	NA	FBgn0052480

CG6425	FBgn0039449	corto	FBgn0010313	NA	FBgn0267653
14-3-3zeta	FBgn0004907	sqz	FBgn0010768	l(2)37Cc	FBgn0002031
RpL3	FBgn0020910	Itp-r83A	FBgn0010051	Plod	FBgn0036147
NA	FBgn0053653	Mkk4	FBgn0024326	CG31191	FBgn0051191
CG6966	FBgn0038286	Sfp79B	FBgn0259973	NA	FBgn0267430
ics	FBgn0028546	qkr58E-3	FBgn0022984	CG43116	FBgn0262576
Pka-R1	FBgn0259243	CG14252	FBgn0039462	Sry-alpha	FBgn0003510
CG42837	FBgn0262026	CG6688	FBgn0039038	NA	FBgn0266416
CG14710	FBgn0037920	CG31808	FBgn0062978	Ktl	FBgn0038839
olf413	FBgn0037153	hook	FBgn0001202	CG6044	FBgn0034725
dpr12	FBgn0085414	PpD3	FBgn0005777	CG43366	FBgn0263109
sea	FBgn0037912	RpIII128	FBgn0004463	olf413	FBgn0037153
trio	FBgn0024277	NA	FBgn0039357	Optix	FBgn0025360
CG10747	FBgn0032845	CG34113	FBgn0083949	NA	FBgn0267753
CG10376	FBgn0032702	thr	FBgn0003701	Pino	FBgn0016926
Hydr1	FBgn0033382	CG42784	FBgn0263354	msn	FBgn0010909
NA	FBgn0267606	alpha-Catr	FBgn0029105	vvl	FBgn0086680
Epac	FBgn0085421	NA	FBgn0264703	lig	FBgn0020279
NA	FBgn0086032	CG14711	FBgn0037922	Pi3K92E	FBgn0015279
Sugb	FBgn0036191	Rgk3	FBgn0085426	hd	FBgn0086695
wrd	FBgn0042693	VAChT	FBgn0270928	Trl	FBgn0013263
CG8032	FBgn0037606	Rm62	FBgn0003261	Fen1	FBgn0025832
Pglym87	FBgn0011270	D1	FBgn0000412	ncm	FBgn0086707
CG6567	FBgn0037842	NA	FBgn0267198	CG15456	FBgn0040650
CG5913	FBgn0039385	nito	FBgn0027548	CG43102	FBgn0262562
CG42534	FBgn0260487	ProRS-m	FBgn0027082	shep	FBgn0052423
Rcd1	FBgn0033897	CG42817	FBgn0261999	MCU	FBgn0042185
NA	FBgn0264470	nAChRalpha 4	FBgn0266347	CG16791	FBgn0038881
GstD11	FBgn0038029	CG13625	FBgn0039210	CG14650	FBgn0037252
NA	FBgn0267219	CG8888	FBgn0033679	NA	FBgn0266390
Kdm4B	FBgn0053182	sns	FBgn0024189	LpR2	FBgn0051092
Oli	FBgn0032651	NA	FBgn0266414	Rbp6	FBgn0260943
NA	FBgn0267578	CG43245	FBgn0262890	sna	FBgn0003448
Tnks	FBgn0027508	CG12320	FBgn0038590	Phk-3	FBgn0035089
NA	FBgn0267748	Ssdp	FBgn0011481	CG3267	FBgn0042083
Mst85C	FBgn0028708	Ccs	FBgn0010531	NA	FBgn0266969
RpS10a	FBgn0027494	CG14314	FBgn0038581	NA	FBgn0262616
CG8331	FBgn0033906	Ppox	FBgn0020018	tara	FBgn0040071
GCS2beta	FBgn0032643	CG10602	FBgn0032721	NA	FBgn0267668
CG14044	FBgn0031650	Vps37B	FBgn0037299	NA	FBgn0266392
cora	FBgn0010434	CG14671	FBgn0037340	CG5290	FBgn0036772

CG6674	FBgn0036063	Fife	FBgn0264606	Galphaq	FBgn0004435
Neos	FBgn0024542	Adk3	FBgn0042094	Rcd1	FBgn0033897
CG10384	FBgn0034731	fne	FBgn0086675	CG11873	FBgn0039633
RpS20	FBgn0019936	CG4238	FBgn0031384	NA	FBgn0086601
Kr-h2	FBgn0266449	Mlc2	FBgn0002773	CG7339	FBgn0036188
CG8516	FBgn0037757	Lar	FBgn0000464	CG32238	FBgn0052238
Su(var)3-7	FBgn0003598	CG1598	FBgn0033191	Plc21C	FBgn0004611
NA	FBgn0266222	CG10424	FBgn0036848	Ady43A	FBgn0026602
adp	FBgn0000057	ps	FBgn0261552	Nab2	FBgn0028471
Ctf4	FBgn0033890	CG6329	FBgn0033872	CG6686	FBgn0032388
Vta1	FBgn0035251	RpL18A	FBgn0010409	CG34435	FBgn0085464
Cyt-c1	FBgn0035600	stops	FBgn0086704	CG5065	FBgn0034145
NA	FBgn0262415	CG8617	FBgn0033925	pip	FBgn0003089
CG4820	FBgn0037876	bol	FBgn0011206	CG5065	FBgn0034145
Art4	FBgn0037770	NA	FBgn0086039	NA	FBgn0267399
CG4390	FBgn0038771	CG12863	FBgn0033948	Hs3st-A	FBgn0053147
RpL27	FBgn0039359	CG14339	FBgn0031301	CG31522	FBgn0051522
Tet	FBgn0263392	CG42496	FBgn0260222	NA	FBgn0264883
Svil	FBgn0266696	Opa1	FBgn0261276	Tango11	FBgn0050404
poly	FBgn0086371	Tdc2	FBgn0050446	GluRIB	FBgn0264000
NA	FBgn0266395	Cyp6a8	FBgn0013772	otk	FBgn0004839
CG3358	FBgn0033117	Pym	FBgn0034918	Ace	FBgn0000024
Mitofilin	FBgn0019960	Plp	FBgn0086690	TBCB	FBgn0034451
CG12316	FBgn0036483	Idh3b	FBgn0038922	CG17698	FBgn0040056
ND-51	FBgn0031771	NA	FBgn0052370	CG6094	FBgn0032261
Xbp1	FBgn0021872	CG14079	FBgn0036849	NA	FBgn0265997
Hip14	FBgn0259824	NA	FBgn0004186	CG6495	FBgn0027550
Eip75B	FBgn0000568	CG12241	FBgn0038304	CG5003	FBgn0039554
NA	FBgn0265982	Taf11	FBgn0011291	Cyp4aa1	FBgn0034053
CG30334	FBgn0050334	Tet	FBgn0263392	NA	FBgn0263328
Gfat2	FBgn0039580	NA	FBgn0051614	Ubc6	FBgn0004436
eEF1gamma	FBgn0029176	CG34384	FBgn0085413	ninaC	FBgn0002938
NA	FBgn0267763	SPE	FBgn0039102	Syx1A	FBgn0013343
NSD	FBgn0039559	kat-60L1	FBgn0037375	CG15130	FBgn0032860
Rpn12	FBgn0028693	Nab2	FBgn0028471	CG2931	FBgn0037342
CG8219	FBgn0035693	Ndc1	FBgn0039125	Scp2	FBgn0020907
CG14966	FBgn0035415	Sod2	FBgn0010213	CG6495	FBgn0027550
qkr58E-2	FBgn0022985	Toll-6	FBgn0036494	NA	FBgn0011891
NA	FBgn0267702	Syp	FBgn0038826	NA	FBgn0266205
Jra	FBgn0001291	pigeon	FBgn0010309	p	FBgn0086679
COX4	FBgn0032833	sns	FBgn0024189	rpr	FBgn0011706

CG3061	FBgn0038195	Phk-3	FBgn0035089	Sfp65A	FBgn0259969
CG11523	FBgn0037156	CG15803	FBgn0038606	CG5641	FBgn0038046
CG10151	FBgn0033960	NA	FBgn0265065	ValRS	FBgn0027079
NA	FBgn0264439	BBS8	FBgn0031255	Art4	FBgn0037770
Cirl	FBgn0033313	CG12347	FBgn0038558	mtsh	FBgn0262598
spin	FBgn0086676	CG42304	FBgn0259200	CG7084	FBgn0038938
Drl-2	FBgn0033791	Hr4	FBgn0264562	NA	FBgn0267774
Gdi	FBgn0004868	mRpL4	FBgn0001995	alpha-Est10	FBgn0015569
CG30158	FBgn0050158	NA	FBgn0266986	corto	FBgn0010313
CycT	FBgn0025455	tadr	FBgn0032911	a	FBgn0000008
borr	FBgn0032105	Rpn3	FBgn0261396	NA	FBgn0267800
TBCD	FBgn0027509	CG11997	FBgn0037662	Cerk	FBgn0037315
NA	FBgn0262182	Gycbeta100B	FBgn0013973	Rdh	FBgn0064227
Su(P)	FBgn0004465	CG13133	FBgn0032181	Cyp6g1	FBgn0025454
CG4797	FBgn0034909	Gbp3	FBgn0039031	NA	FBgn0262432
bocks	FBgn0037719	CG6403	FBgn0039453	CG11835	FBgn0031264
CG13171	FBgn0033701	Klp64D	FBgn0004380	CG31388	FBgn0051388
Dys	FBgn0260003	Nlp	FBgn0016685	FRG1	FBgn0036964
siz	FBgn0026179	mino	FBgn0027579	CG8027	FBgn0033392
Dhc98D	FBgn0013813	eIF3j	FBgn0027619	rho-6	FBgn0032415
Trl	FBgn0013263	Dat	FBgn0019643	Acn	FBgn0263198
CG16935	FBgn0033883	lilli	FBgn0041111	raw	FBgn0003209
NA	FBgn0266820	phu	FBgn0043791	lilli	FBgn0041111
RpS4	FBgn0011284	Rad23	FBgn0026777	NA	FBgn0011891
stck	FBgn0020249	CG3795	FBgn0025378	CG7714	FBgn0038645
CG3662	FBgn0031285	CG4553	FBgn0039336	CG4960	FBgn0039371
Taf5	FBgn0010356	Toll-7	FBgn0034476	NA	FBgn0266824
dany	FBgn0050401	CG8036	FBgn0037607	NA	FBgn0262382
NA	FBgn0265929	CG43125	FBgn0262588	ppk31	FBgn0051065
CG45428	FBgn0266977	fuss	FBgn0039932	NA	FBgn0267621
Tango8	FBgn0040737	can	FBgn0011569	CG13025	FBgn0036660
NA	FBgn0265073	HEATR2	FBgn0051320	CG33301	FBgn0053301
NA	FBgn0267702	dnk	FBgn0022338	SmB	FBgn0262601
CG43188	FBgn0262817	CG31140	FBgn0051140	NA	FBgn0086080
MFS9	FBgn0038799	dpr12	FBgn0085414	Rbp6	FBgn0260943
CG12516	FBgn0039577	CG33191	FBgn0053191	CG1126	FBgn0037280
CG5021	FBgn0035944	Der-1	FBgn0267972	Adk3	FBgn0042094
NA	FBgn0263582	eIF2Bdelta	FBgn0034858	Ccp84Af	FBgn0004778
mus304	FBgn0002901	CG31678	FBgn0051678	croc	FBgn0014143
CG4741	FBgn0035040	CG31550	FBgn0051550	CG9422	FBgn0033092

l(2)35Bd	FBgn0001974	Nprl3	FBgn0036397	Kcmf1	FBgn0037655
Ktl	FBgn0038839	spn-A	FBgn0003479	NA	FBgn0264506
Pkn	FBgn0020621	CG15167	FBgn0032709	Cpr66D	FBgn0052029
MFS9	FBgn0038799	betaNACtes3	FBgn0052601	CG5292	FBgn0038491
CG7265	FBgn0038272	Itp-r83A	FBgn0010051	Bruce	FBgn0266717
CG42389	FBgn0259735	Tsp96F	FBgn0027865	fkh	FBgn0000659
MCU	FBgn0042185	CG11999	FBgn0037312	CG31523	FBgn0051523
Nca	FBgn0013303	br	FBgn0283451	NA	FBgn0267571
CG42817	FBgn0261999	tmod	FBgn0082582	axed	FBgn0035708
NA	FBgn0266876	SLO2	FBgn0261698	MCU	FBgn0042185
sca	FBgn0003326	beat-VII	FBgn0250908	Bsg	FBgn0261822
CG5114	FBgn0036460	CG9547	FBgn0031824	CG30497	FBgn0050497
CG8485	FBgn0033915	Rsf1	FBgn0011305	CG42826	FBgn0262008
Atg1	FBgn0260945	CG14089	FBgn0036861	Or85f	FBgn0037685
Eno	FBgn0000579	ps	FBgn0261552	CG7218	FBgn0038569
ftz-f1	FBgn0001078	htt	FBgn0027655	CG7200	FBgn0032671
NA	FBgn0264883	CG31522	FBgn0051522	Ppn	FBgn0003137
GstE1	FBgn0034335	NA	FBgn0267710	NA	FBgn0267114
amon	FBgn0023179	Clk	FBgn0023076	CG6511	FBgn0035923
CG8562	FBgn0035779	CG12321	FBgn0038577	CG18812	FBgn0042135
CG7985	FBgn0028499	NA	FBgn0267800	CG6142	FBgn0039415
CG3570	FBgn0035035	CG31523	FBgn0051523	CG9799	FBgn0038146
NA	FBgn0267582	CG5478	FBgn0038386	Rcd2	FBgn0037012
SdhC	FBgn0037873	NA	FBgn0262446	NA	FBgn0267668
NA	FBgn0265645	CG31140	FBgn0051140	CG31522	FBgn0051522
Rcc1	FBgn0002638	CG31051	FBgn0051051	CG3358	FBgn0033117
AstA-R2	FBgn0039595	CG10864	FBgn0038621	NA	FBgn0086060
NA	FBgn0267742	Acsl	FBgn0263120	CG14011	FBgn0031722
Prosbeta7	FBgn0250746	nkd	FBgn0002945	NA	FBgn0267621
Chmp1	FBgn0036805	Wwox	FBgn0031972	Ino80	FBgn0086613
CG11333	FBgn0039850	CG31248	FBgn0051248	NA	FBgn0266869
Gld2	FBgn0038934	ths	FBgn0033652	CG4161	FBgn0028892
CG13605	FBgn0039150	mEFTs	FBgn0032646	Fmr1	FBgn0028734
NA	FBgn0263664	pk	FBgn0003090	Cyp4aa1	FBgn0034053
TwdlQ	FBgn0039448	Kr-h1	FBgn0266450		

Appendix J Candidate Bap60 target genes in the juvenile adult MB

Candidate Bap60 targets in the juvenile MB					
Gene	**Flybase ID**	**Gene**	**Flybase ID**	**Gene**	**Flybase ID**

Symbol		Symbol		Symbol	
MFS18	FBgn0025684	ctp	FBgn0011760	jef	FBgn0033958
CG13921	FBgn0035267	Act5C	FBgn0000042	Lis-1	FBgn0015754
corn	FBgn0259173	fend	FBgn0030090	Syn2	FBgn0034135
BI-1	FBgn0035871	His3.3B	FBgn0004828	IM4	FBgn0040653
chrb	FBgn0036165	Ran	FBgn0020255	Dll	FBgn0000157
CG14024	FBgn0031697	CG1998	FBgn0030485	CG8745	FBgn0036381
Sap130	FBgn0262714	rdgB	FBgn0003218	D	FBgn0000411
CG10960	FBgn0036316	Gapdh2	FBgn0001092	grim	FBgn0015946
trn	FBgn0010452	CG7990	FBgn0030997	dsf	FBgn0015381
Pdh	FBgn0011693	CG12531	FBgn0031064	fng	FBgn0011591
hid	FBgn0003997	CG40485	FBgn0069973	nod	FBgn0002948
Daxx	FBgn0031820	CG6495	FBgn0027550	MFS10	FBgn0030452
CR33294	FBgn0053294	kek1	FBgn0015399	CG6785	FBgn0032399
side-VII	FBgn0037736	Hr38	FBgn0014859	NLaz	FBgn0053126
GstD11	FBgn0038029	nrv3	FBgn0032946	Gli	FBgn0001987
Dop1R1	FBgn0011582	Vha16-1	FBgn0262736	Ddc	FBgn0000422
CG7781	FBgn0032021	Tsp42Ej	FBgn0033132	CG6701	FBgn0033889
CG31221	FBgn0051221	Inos	FBgn0025885	Sik3	FBgn0262103
Ktl	FBgn0038839	CG11191	FBgn0033249	insc	FBgn0011674
CG31191	FBgn0051191	CG14762	FBgn0033250	klu	FBgn0013469
amon	FBgn0023179	pnut	FBgn0013726	CAH2	FBgn0027843
Kul	FBgn0039688	14-3-3zeta	FBgn0004907	cib	FBgn0026084
jdp	FBgn0027654	Cam	FBgn0000253		
Appl	FBgn0000108	Syngr	FBgn0033876		

Appendix K Supplementary figure

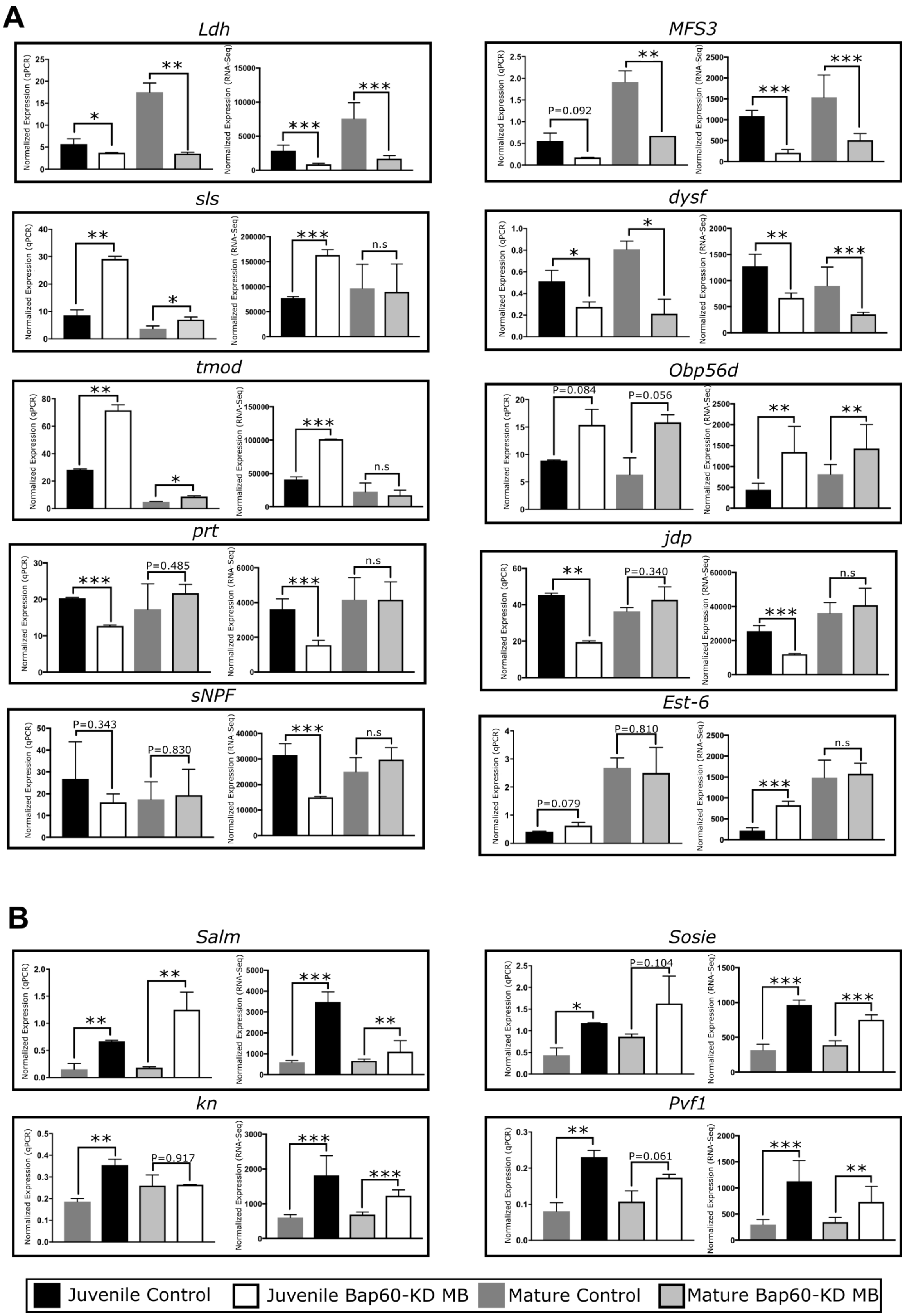

Figure S1: qPCR validation of RNAseq gene expression changes. Average normalized gene expression ± SD of genes as measured through RT-qPCR (left panel) and RNA-Seq (right panel) in Bap60-KD MB and control mushroom body (MB) samples. RT-qPCR gene expression is normalized to the housekeeping genes *eIF2β* and *βCOP* and RNA-Seq gene expression is normalized by DESeq2. (A) Validation of overall gene expression trends for *Ldh, MFS3, sls, dysf, tmod, Obp56d, prt, jdp, sNPF*, and *Est-6*. Comparisons were made between juvenile control and juvenile Bap60-KD MB and between mature control and mature Bap60-KD MB. Genes validated by RT-qPCR were: *Ldh*, *sls*, *dysf*, *tmod*, *prt*, and *jdp*. Genes that were showing similar trends between RTqPCR and RNA-Seq were: *MFS3*, *Obp56d*, and *Est-6*. *sNPF* could not be validated by RT-qPCR due to variation between biological replicates. (B) Validation of gene expression trends of developmental genes: *Salm*, *Sosie*, *kn*, and *Pvf1* that were induced in juvenile control flies, but not juvenile Bap60-KD MB. Comparisons were made between mature control and juvenile control and between mature Bap60-KD MB and juvenile Bap60-KD MB. Genes validated were: *kn* and *Pvf1*. *Sosie* is validated despite variability of the data. *Salm* is not validated. Significance for RT-qPCR is determined by Student's t-test; significance for RNA-Seq is determined by binomial Wald test (DESeq2); **P*<0.05, ***P*<0.01, ****P*<0.001.

Curriculum Vitae

Name:	Kevin Cedric John Nixon
Post-secondary Education and Degrees:	The University of Western Ontario London, Ontario, Canada 2010-2014 B.Sc.
	The University of Guelph Guelph, Ontario, Canada 2014-2015 M.Binf.
	The University of Western Ontario London, Ontario, Canada 2016-2020 Ph.D.
Honours and Awards:	Ontario Graduate Scholarship 2016-2017, 2017-2018, 2018-2019
Related Work Experience	Graduate Teaching Assistant The University of Western Ontario 2016-2019

Publications:

Vanderboor, CMG, Thibeaulty, PE, **Nixon, KCJ**, Gros, R, Kramer, JM, and Ramachandran, R. (2019) Proteinase-Activated Receptor 4 (PAR4) Activation Triggers Cell Membrane Blebbing through RhoA and β-arrestin. *Molecular Pharmacology*. (*Submitted*) BioRxiv: 746677.

Nixon KCJ, Rousseau J, Stone MH, Sarikahya M, Ehresmann S, Mizuno S, Matsumoto N, Miyake N, DDD Study, Baralle D, McKee S, Izumi K, Ritter AL, Heide S, Héron D, Depienne C, Titheradge H, Kramer JM, Campeau PM. (2019) A Syndromic Neurodevelopmental Disorder Caused by Mutations in SMARCD1, a Core SWI/SNF Subunit Needed for Context-Dependent Neuronal Gene Regulation in Flies. American Journal of Human Genetics. 104: 595-610.

Chubak, MC, **Nixon KCJ**, Stone MH, Raun N, Rice SL, Sarikahya M, Jones SG, Lyons TA, Jakub TE, Mainland RLM, Knip MJ, Edwards TN, and Kramer JM. (2019) Individual Components of the SWI/SNF Chromatin Remodeling Complex have Distinct Roles in Memory Neurons of the Drosophila Mushroom Body. Disease Models and Mechanisms. 12: dmm037325.

Jones, SJ, **Nixon, KCJ**, Chubak, MC, and Kramer, JM. (2018) Mushroom body specific transcriptome analysis reveals dynamic regulation of learning and memory genes after acquisition of long-term courtship memory in *Drosophila*. *G3*. doi: 10.1534/g3.118.200560.

Farhan, SMK, **Nixon, KCJ**, Everest, M, Edwards, T, Long, S, Segal, D, Knip, MJ, Arts HH, Chakrabarti, R, Wang J, Robinson, JF, Rupar, CA, Siu, VM, Poulter, MO, FORGE Canada Consortium, Hegele, RA, and Kramer, JM. (2017) Identification of a novel synaptic protein, TMTC3, involved in periventricular nodular heterotopia with intellectual disability and epilepsy. *Human Molecular Genetics*. **26:** 4278-4289.

Conference Presentations:

Nixon, KCJ and Kramer, JM. (2019, June). Mushroom body-specific gene regulation by the SWI/SNF chromatin remodeling complex. Oral presentation at the Canadian *Drosophila* Research Conference (CanFly), Toronto, Canada.

Farhan, SMK, **Nixon, KCJ**, Everest, M, Edwards, T, Long, S, Segal, D, Knip, MJ, Arts HH, Chakrabarti, R, Wang J, Robinson, JF, Rupar, CA, Siu, VM, Poulter, MO, FORGE Canada Consortium, Hegele, RA, and Kramer, JM. (2017, May) Identification of a novel synaptic protein, TMTC3, involved in periventricular nodular heterotopia with intellectual disability and epilepsy. Oral presentation at the Canadian Society for Molecular Biosciences annual meeting, Ottawa, Canada.

Nixon, KCJ and Kramer, JM. (2017, June). SWI/SNF-dependent gene regulation in the *Drosophila* mushroom body. Poster session at the Canadian *Drosophila* Research Conference (CanFly), Banff, Canada.

Nixon, KCJ, Stone, MH, and Kramer, JM. (2017, November). SWI/SNF-dependent gene regulation in the *Drosophila* mushroom body. Poster session at the Physiology and Pharmacology Research Day, London, Canada.

Nixon, KCJ, Stone, MH, and Kramer, JM. (2018, March). SWI/SNF-dependent gene regulation in the *Drosophila* mushroom body. Poster session at the Western University Health and Research Conference, London, Canada.

Nixon, KCJ, Stone, MH, and Kramer, JM. (2018, May). SWI/SNF-dependent gene regulation in the *Drosophila* mushroom body. Poster session at the London Health Research Day, London, Canada.

Nixon, KCJ and Kramer, JM. (2018, September). SWI/SNF-dependent gene regulation in the *Drosophila* mushroom body. Poster session at the EMBL ATAC-Seq training course, Heidelberg, Germany.